Methylhydropolysiloxanes from Cohydrolysis of Methylhydrochlorosilanes and Methylchlorosilanes

By Rokuro ŌKAWARA and Minoru SAKIYAMA

(Received January 23, 1956)

Recently, we reported[1] on the presence of tetramethylsilane (I′) (b. p. 26.5°C), dimethylchlorosilane (II′) (b. p. 36°C), hydrocarbon by-product (b. p. 33°–37°C) and methyldichlorosilane (III′) (b. p. 41°C) in the low boiling product of silicon-methylchloride reaction. We wish now to report on the lower members of copolymer which were obtained by hydrolyzing these two methylhydrochlorosilanes with three kinds of methylchlorosilane.

In this experiment, for the source of **M′***, industrial low boiling fraction (b. p. 35°–36°C) was used without further purification. Because of the result of the preceding paper, it was considered to be difficult to obtain pure (II′) by conventional fractionation through an ordinary laboratory column. Also the hydrolyzate of the low boiling fraction used in this experiment was found to be composed of mainly methylhydropolysiloxanes and a small amount of (I′) and the hydrocarbon by-product. The percentage composition of the lower members of the methylhydropolysiloxanes based on the amount of the hydrolyzate is given in Table I (Expt. 1). It was considered that $\mathbf{M}'_2$ was formed from (II′) and the succeeding linear polymers, $\mathbf{M'D'_nM'}$ from (II′) and (III′).

In the preceding paper, a small amount of linear polysiloxanes, **M′DM′**, **M′D′DM′** and $\mathbf{M'D_2M'}$, were found to be present in the hydrolyzate of the low boiling product, but among them only **M′DM′** could be characterized. In that case, **D** unit was supposed to be formed from (II′) by the fission of Si-H bond during the hydrolysis reaction. In order to obtain sufficient amounts of **M′D′DM′** and $\mathbf{M'D_2M'}$, various amounts of dimethyldichlorosilane (II), as a source of **D** unit, were added to the low boiling fraction. It succeeded to characterize these two compounds from the hydrolyzate which were obtained by mixing a relatively small amount of (II).

The polysiloxane which could be accurately characterized from the cohydrolyzate of trimethylchlorosilane (I) with the low boiling fraction was **MM′**.

The trisiloxanes which were supposed to be formed, such as **M′DM′**, **M′D′M**, **M′DM** and **MD′M** could not be separated.

Since the linear polysiloxanes were formed from the low boiling fraction itself, it was not easy to separate the branched chain polysiloxanes from the isomeric linear polymers when the low boiling fraction was cohydrolyzed with methyltrichlorosilane (III). Two branched chain polymers, $\mathbf{M'_3T}$ and $\mathbf{M'_2TD'M'}$, could be characterized in this experiment.

Further, a series of copolymer $\mathbf{MD'_nM}$ ($n=1-6$), some of which have already been characterized by Sauer[2], were obtained by cohydrolysis of (I) and (III′).

Properties of copolymers obtained in this experiment are summarized in Table II.

Experimental

Starting Materials.—The low boiling fraction (b. p. 35°–36°C, specific gravity : 0.873, chlorine content: 38.5%) and methylchlorosilanes used in this experiment were supplied from Shin-etsu Chem. Ind. Co. Methyltrichlorosilane and methyldichlorosilane were redistilled through a Stedman column of about 30 theoretical plates and the fraction having the calculated chlorine content was used for the experiments.

Cohydrolysis.—In all cases, cohydrolysis was performed by the same method described in the preceding paper. The fractionation of the hydrolyzate was carried out by a semi-micro Stedman column of about 50 theoretical plates throughout this experiment.

Analysis of Active Hydrogen.—Active hydrogen content was measured by decomposing the sample with aqueous ethanolic sodium hydroxide in a Zerewitinoff's apparatus.

Cohydrolyzate with Dimethyldichlorosilane (II), (Expt. 2–5).—The results of the cohydrolysis are given in Table I. In Expt. 2, 3 and 4, the amounts of (II) mixed were 90, 65 and 51% of the low boiling fraction respectively. In each case, the distribution of the fraction boiling below 150°C was determined. Then the residues of

1) R. Ōkawara and M. Sakiyama, This Bulletin, **29**, 236 (1956).

* In this paper, the shorthand notation will be used which was indicated in the preceding paper[1].

$\mathbf{M'}=H(CH_3)_2SiO_{1/2}$ $\quad$ $\mathbf{M}=(CH_3)_3SiO_{1/2}$

$\mathbf{D'}=HCH_3SiO$ $\quad$ $\mathbf{D}=(CH_3)_2SiO$

$\mathbf{T}=CH_3SiO_{3/2}$

2) R. O. Sauer, W. J. Scheiber and S. D. Brewer, *J. Am. Chem. Soc.*, **68**, 962 (1946).

CHEMISTRY HALL LIBRARY

TABLE I

Expt. No.	Mixture of chlorosilanes		Hydrolyzate yield		Composition of the hydrolyzate (%) Disiloxanes			Trisiloxanes			Tetrasiloxanes	Higher siloxanes
		(g.)	(g.)	(%)theory**	M'_2	MM′	M_2	M′D′M′	M′DM′	MD′M		
1	(L)*	2200	1120	73	44	—	—	15	1	—	10	19
2	(L)	95	86	74	5	—	—	5	17	—	(69)	
	(II)	86										
3	(L)	113	88	71	7	—	—	5	17	—	(68)	
	(II)	77										
4	(L)	113	84	75	10	—	—	7	21	—	(60)	
	(II)	58										
5	(L)	435	250	72	21	—	—	9	19	—	10	28
	(II)	75										
6	(L)	350	390	65	4	24	38	3	(5)		(19)	
	(I)	400										
7	(L)	380	224	75	12	—	—	7	2	—	26	37
	(III)	75										
8	(III′)	200	345	89	—	—	46	—	—	10	8	30
	(I)											

* (L): The low boiling fraction, (I): $(CH_3)_3SiCl$, (II): $(CH_3)_2SiCl_2$, (III): CH_3SiCl_3, (III′): CH_3SiHCl_2

** Calculated from the chlorine content of the mixture of chlorosilanes.

TABLE II

METHYLHYDROPOLYSILOXANES

Polysiloxanes	Boiling point °C/mmHg	Refractive index n_D^{20}	Density d_4^{20}	Molar refraction	Molecular weight	%H(-Si)
	((Reported))[2]	Found ((Reported))	Found ((Reported))	Found (Calcd.)*	Found** (Calcd.)	Found (Calcd.)
MD′M	141.5/760	1.3818	0.8193	63.18	—	0.45
		((1.3818))	((0.8194))	(63.19)	(222.52)	(0.45)
MD′₂M	81/28	1.3862	0.8556	77.63	—	0.70
		((1.3854))	((0.8559))	(77.46)	(282.66)	(0.71)
MD′₃M	105/28	1.3880	0.8798	91.94	—	0.87
	((85.6/10))	((1.3878))	((0.8806))	(91.73)	(342.79)	(0.88)
MD′₄M	77/2	1.3904	0.8966	106.6	—	1.00
	((107/10))	((1.3895))	((0.8991))	(106.0)	(402.92)	(1.00)
MD′₅M	94/2	1.3920	0.9136	120.7	—	1.08
				(120.3)	(463.06)	(1.09)
MD′₇M	104/2	1.3925	—	—	—	1.11
					(523.19)	(1.16)
MM′	85/760	1.3740	0.7578	44.71	145	0.68
				(44.55)	(148.36)	(0.68)
M′D′DM′	71/26	1.3862	0.8623	73.21	272	1.13
				(73.09)	(268.63)	(1.13)
M′D₂M′	77/25	1.3875	0.8632	77.18	285	0.72
				(77.46)	(282.66)	(0.71)
M′₂T	60/19	1.3852	0.8612	73.13	270	1.14
				(73.09)	(268.63)	(1.13)
M′₂TD′M′	100/38	1.3882	0.8891	87.29	329	1.22
				(87.36)	(328.76)	(1.23)

* Calculated from bond refractivities by E. L. Warrick, *J. Am. Chem. Soc.*, **68**, 2455 (1946).

** Cryoscopic measurements in benzene.

these three runs were gathered and rigorously fractionated. A small plateau (ca. 10 cc.) of **M′D′DM′**, though not so pure (Found: H(−Si), 1.15. Calcd. for **M′D′DM′**: H(−Si), 1.13%.) and a succeeding large plateau (ca. 45 cc.) of gradually rising temperature (80°–85°C/31 mm.) were obtained.

As the refractive index (n_D^{20}) of this incomplete plateau changed from 1.3911 to 1.3935 and the active hydrogen content of the distillate showed a lower value than that of $M'D_2M'$, it may be natural to suppose that $M'D_2M'$ was contaminated with cyclic polysiloxanes having **D** (reported[3]: D_4, n_D^{20} 1.3968), or **D** and **D'** units in this plateau.

In Expt. 5, the low boiling fraction was cohydrolyzed with a relatively small amount (17% of the low boiling fraction) of (II) to avoid the formation of cyclic polysiloxanes as far as possible. By redistillation, $M'D'DM'$ and $M'D_2M'$ were obtained as the complete plateaus and were accurately characterized.

Cohydrolyzate with Trimethylchlorosilane (I), (Expt. 6).—The low boiling fraction was cohydrolyzed with (I). The succeeding plateaus of M_2' (b. p. 70.5°C), **MM'** (b. p. 85°C) and M_2 (b. p. 100°C) were obtained. Above $M'D'M'$ (b. p. 117°C), two main plateaus having a gradually changing refractive index were observed until 141°C. One centering around 130°C was supposed to contain a pair of isomers $M'DM'$ and $M'D'M$ (Found: H(−Si), 0.95. Calcd. for $M'DM'$ or $M'D'M$: H(−Si), 0.97%.), the other from 137° to 141°C, $M'DM$ and $MD'M$ (Found: H(−Si), 0.53. Calcd. for $M'DM$ or $MD'M$: H(−Si), 0.45%.). Owing to the close boiling points of isomers in a pair, neither was accurately separated. The distribution of the components in the hydrolyzate is given in Table I.

Cohydrolyzate with Methyltrichlorosilane (III), (Expt. 7).—After $M'D_2'M'$ has been distilled out, a large plateau (ca. 50 cc.) was obtained between 73°C to 77°C at 38 mm. The first 30 cc. of this plateau had the value of refractive index (n_D^{20}) of 1.3850 to 1.3853 and then it gradually increased to 1.3860. Since the branched chain polysiloxane (M_3T) has been reported[3] to have a slightly lower boiling point and refractive index than the isomeric linear polysiloxane (MD_2M), it was supposed naturally in this experiment that the fore part of this plateau is that of $M_3'T$ and at the back part of the plateau, $M_3'T$ is gradually contaminated with accompanying isomeric linear $M'D'DM'$ (n_D^{20} 1.3862) which was produced inevitably from the hydrolysis of the starting material. By redistilling the portion having the refractive index 1.3850 to 1.3853, the plateau having the constant refractive index was obtained, and this was assigned to $M_3'T$.

3) W. Patnode and D. Wilcock, *J. Am. Chem. Soc.*, **68**, 358 (1946).

The succeeding five small plateaus were obtained until 115°C/0.4 mm. Among them only the plateau (100°C/38 mm., n_D^{20} 1.3882), which was found next to the linear $M'D_3'M'$, had its active hydrogen content and molecular weight consistent with the calculated value for the branched chain pentasiloxane, $M_2'TD'M'$. But the purity of this compound would not be insisted upon merely because of its hydrogen content and molecular weight, for there is a possibility of contamination of a small amount, if any, of isomeric linear pentasiloxane.

Cohydrolyzate of Methyldichlorosilane (III') and Trimethylchlorosilane (I), (Expt. 8).—A series of methylhydropolysiloxanes indicated by $MD_n'M$ ($n=1-4$) was first synthesized by Sauer[2], but the boiling points of trisiloxane and tetrasiloxane were not reported. We synthesized a series of these compounds by cohydrolysis of (I) and (III'). As no equilibration by concentrated sulfuric acid was performed to avoid the fission of Si-H by this reagent, trisiloxane was much contaminated with cyclic tetrasiloxane, D_4' (b.p. 134.5°C) and it was necessary to repeat rigorous fractionation until the distillate gave a satisfactory active hydrogen content. Tetrasiloxane and pentasiloxane were also redistilled once. Octasiloxane was supposed to be not so pure as other compounds referring to its active hydrogen content.

Summary

1) The low boiling fraction of silicon-methylchloride reaction was cohydrolyzed with the three kinds of methylchlorosilane and the methylhydropolysiloxanes, **MM'**, $M'D'DM'$, $M'D_2M'$, $M_3'T$ and $M_2'TD'M'$, have been prepared and characterized.

2) A complete series of linear methylhydropolysiloxanes, $MD_n'M$ having three to eight silicon atoms have been prepared and characterized from the cohydrolyzate of methyldichlorosilane and trimethylchlorosilane.

We wish to express our hearty thanks to Shin-etsu Chem. Ind. Co. for giving us precious samples.

Department of Applied Chemistry
Faculty of Engineering, Osaka University, Osaka

Über die heterogene Acetylierung der ebenen Cellulose

Von Toshikazu FUJIMURA

(Eingegangen am 9. Januar 1956)

Einleitung

Um die Grundlage der chemischen Veredlung der Kunstseide und der Zellwolle aufzuklären, ist es interessant, die Reaktionsgeschwindigkeit der heterogenen Acetylierung der Cellulose, den Reaktionsmechanismus und die Beziehung mit der inneren Struktur zu untersuchen. Darüber hat der Autor die verkürzten Formel auf der zyliderischen Form unter der Annahme des quasistationären Zustandes vorgestellt[1]. Diesmal wird die Methode auf die unendliche Ebene angewandt und wird die Gültigkeit über mehreren aufeinandergestellten Schichten der Cellophane geprüft, die ungeachtet der inneren heterogenen Struktur im ganzen als einheitlich betrachtet werden kann. Der Haufen wurde mit dem Gemisch, das aus Benzol, Essigsäureanhydrid und Sulfoessigsäure besteht, von einer Seite ab durchgesetzt und die acetylierten Schichten wurden mittels der Anfärbung unterschieden. Dabei wurde der Einfluss der Zusammensetzung des Gemisches, des Verhältnisses des Gemisches zur Folien (nämlich des statischen Druks), der Temperatur und der Weise der Vorbehandlung untersucht.

Ableitung der theoretischen Gleichung

Wird der quasi-stationäre Zustand und die gleichen Hinüberwanderngeschwindigkeiten des Acetylierungsmittels an allen Orten angenommen, so ergibt die Differentialgleichung:

$$dm'/dt=dm/dt=dm''/dt=a(dX/dt) \quad (1)$$

Wenn die Reaktion der ersten Ordnung gilt, so ergibt man die Gleichung:

$$dm''/dt=k''(C''-C''') \quad (2)$$

Für das Stoffüberwndern an der Oberfläche erhält man;

$$dm'/dt=k'(C^*-C') \quad (3)$$

Als Zusammenhang der innen Diffusion ergibt die Ficksche Gesetze:

$$dm/dt=D(dC/dx) \quad (4)$$

Hierbei:

C^*, C', C, C'', C''': Konzentration des Acetylierungsmittels im aussen Acetylierungsmittel, an der Oberfläche, in acetylierten Schicht, an der Reaktionsgrenze unter Gleichgewicht.

dm'/dt: Stoffübergangsgeschwindigkeit an der Oberfläche.

dm/dt: Diffusionsgeschwindigkeit in der acetylierten Schicht.

dm''/dt: Reaktionsgeschwindigkeit.

X: Dicke der acetylierten Schicht.

a: Die Gewicht des ein Längseinheit der Cellophane von einer Flächenraumeinheit acetylierenden Acetylierungsmittels.

D: Diffusionskonstante.

k': Stoffübergangskonstante an der Oberfläche.

k'': Reaktionskonstante.

Durch Einsetzen von (1) in (4) ergibt sich:

$$Ddc=a(dX/dt)dx.$$

Mit der Integration auf x von 0 bis X gewinnt man:

$$D(C'-C'')=aX(dX/dt). \quad (5)$$

Aus (1) und (2) folgt:

$$C''=C'''+a(dX/dt)/k''. \quad (6)$$

Aus (1) und (3) erhält man:

$$C'=C^*-a(dX/dt)/k'. \quad (7)$$

Durch Elimination von C' und C'' ergeben (5), (6) und (7):

$$D\{C^*-C'''-a(dX/dt)/k'-a(dX/dt)/k''\}=aX(dX/dt). \quad (8)$$

Für das Integral auf t von 0 bis t und auf X von 0 bis X folgt:

$$(C^*-C'')t=a(X^2/2D+X/k'+X/k''). \quad (9)$$

(a) Für den mit der Diffusion bestimmten Fall:

$$D\ll k',\ k'';\ X^2=2D(C^*-C'')t/a. \quad (10)$$

(b) Für den mit dem Oberflächewiederstand bestimmten Fall:

$$k'\ll D,\ k'';\ X=k'(C^*-C'')t/a. \quad (11)$$

(c) Für den mit der chemischen Reaktion bestimmten Fall:

$$k''\ll D,\ k';\ X=k''(C^*-C'')t/a. \quad (12)$$

Material und Methode

Cellophane (0.02 mm dick, 2–3 mg/cm²) wurde in 2 cm×23 cm geschinitten und in 10 Schichten gefaltet und diese 6–10 Haufen wurde aufeinandergesetzt. Falls keine besondere Bemerkung, wurden diese Haufen zwei Tage lang in Wasser getaucht, auf dem Verhältnis des Gewichts von 1:2.4 abgepresst, und dann in zwölffachen Teile Essigsäure zu Cellophane eingesetzt. Diese Vorbehandlung wurde zehnmal wiederholt. Dann wurde die Folien zwischen der Flanschen der in

1) T. Fujimura, Dieses Bulletin, 28, 248 (1955).

Abb. 1 gezeigten Apparat geklemmt und in den

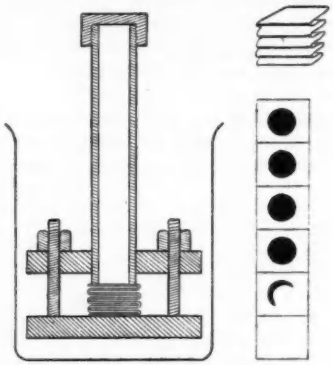

Abb. 1. Acetylierungsapparat.

Vorbehandlungsmittel enthaltenden Becherglas eingetaucht und der Gemisch, der zwei Stunden lang bei 75°C zwecks der Umwandlung der Schwefelsäure in die Sulfoessigsäure erwärmt geworden war, wurde in der oberen Röhre eingegossen.

Nach bestimmten Dauer wurde die Folien weggenommen, dann mit Alkohol und Wasser nacheinander gewäscht und mit dem Gemisch von Celliton-Farbstoff und Substantiv-Farbstoff anfärbt, um die Zahl der acetylierten Schichten zu erkennen. Die Fraktion einer Schicht wurde auf den Flächenraum des angefärbten Teils bezogen.

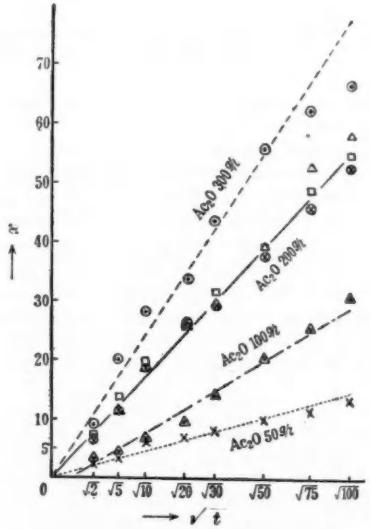

H_2SO_4 6.75 g/l H_2SO_4 4.5 g/l
H_2SO_4 2.25 g/l

Abb. 2. Der Einfluss von der Zusammensetzung des Acetylierungsmittels.
t: Zeit (Stunden),
x: Anzahl der acetylierten Schichten.

Ergebnisse und Diskussion

Zusammensetzung des Acetylierungsmittels.—Wie aus Abb. 2 hervorgeht, ist die Zahl der acetylierten Schichten ungefähr in Verhältnis zur Quadratwurzel der Zeit, so dass die von der innen Diffusion abhängige Gleichung (10) gelten muss. Aber, nach der langen Reaktionszeit eintritt die Abweichung aus der Gleichung. Es kann davon herrühren, dass die acetylierte Schicht allmählich quillt, dass der kleinere Durchmesser des acetylierten Teils in der tieferen Schichten mit der Annahme der Diffusion in einen Richtung im Widerspruch steht und dass der Verbrauch der Essigsäureanhydrid zufolge der Reaktion die Konzentration um 10% abnimmt.

Am ersten geraden Teil der Kurve wird die Regression-Analyse nach der Gleichung:

$$X=a+bt^{1/2} \tag{13}$$

ausgeführt und die Ergebnisse in der Tabelle I wiedergegeben.

TABELLE I

REGRESSION-ANALYSE

(EINFLUSS DER KONZENTRATION VON ESSIGSÄUREANHYDRID)

Essigsäureanhydrid (g/l)	50	100	200	300
Konstant b	1.39	2.97	5.43	7.65
Konstant a	0.66	−2.13	1.01	1.28
Streung der a: S_a	2.62	27.2	6.12	9.85
Streung der Fehler: S_f	0.40	1.26	1.22	5.18
$F_0=S_a/S_f$	6.5	21.6	5.0	1.9

Hierbei: $S_a=n(a-0)^2$
$S_f\sum(X-a-bt)^2/(n-2)$
n: Anzahl der Punkte.

Abgesehen von der Konzentration 100 g/l, kann die Annahme nicht aufgegeben wurden, dass die Konstant a als Null betrachtet wird. Daraus ergibt sich:

$$X=bt^{1/2} \tag{14}$$

Daher passiert die gerade Linie durch die Anfangspunkt. Aus (10) und (14) folgt:

$$b^2=2D(C^*-C'')/a \tag{15}$$

Wie aus Abb. 3 ersichtlich, ist die Beziehung zwischen b^2 und C^* zwar in Hauptteil geradlinig, aber an der Bereich der niedrigen Konzentration gebogen. Es kann auf die Veränderung der Quellungszustandes beruhen.

Da die Konzentration der Sulfoessigsäure wenigen Einfluss ausübt, kann die Hinüberwanderngeschwindigkeit nicht von der Reaktion, auf die die Sulfoessigsäure katalytisch auswirkt, sondern von Diffusion bestimmt werden.

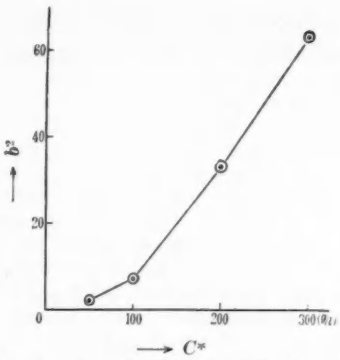

Abb. 3. Die Beziehung zwischen der Regression-Koefizient (b) und der Konzentration von Essigsäureanhydrid (C).

Volumenverhältnis.—Das Verhältnis der Acetylierungsmittels zur Folien, d.h. die Höhe des Acetylierungsmittels in der Röhre, ist von kleine Bedeutung auf der Zahl der acetylierten Schichten, wie in Abb. 4 gezeigt. Deshalb muss das hydrodynamischen Fliessen zufolge des statischen Drucks keine Rolle spielen.

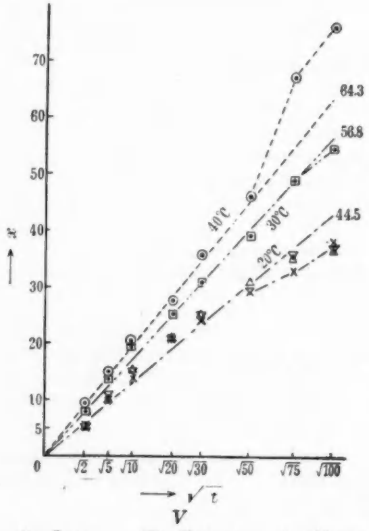

△ 5 ccm ▽ 10 ccm × 15 ccm

Abb. 4. Der Einfluss von Temperatur und von Volumen des Acetylierungsmittels (V).
t: Zeit (Stunden),
x: Anzahl der acetylierten Schichten.

Temperatur der Reaktion.—Es ist in Abb. 4 dargestellt. Bei 20°C und 30°C, gilt ungefähr die geradlinige Beziehung von der Gleichung (10), bei 40°C nicht. Es kann davon herrühren, dass die Folien verdorben werden und die Diffusion gefördert wird.

Die gemäss der Gleichung (15) berechnete Diffusionskonstant nimmt bei höher Temperatur zu, aber die Veränderung ist so klein dass die Vorgang nicht von der chemischen Reaktion sondern von der Diffusion entschieden werden mag.

Vorbehandlungsweise.—Der Einfluss der Vorbehandlung wurde in Abb. 5 verglichen. Je grösser die Quellung nach der Vorbe-

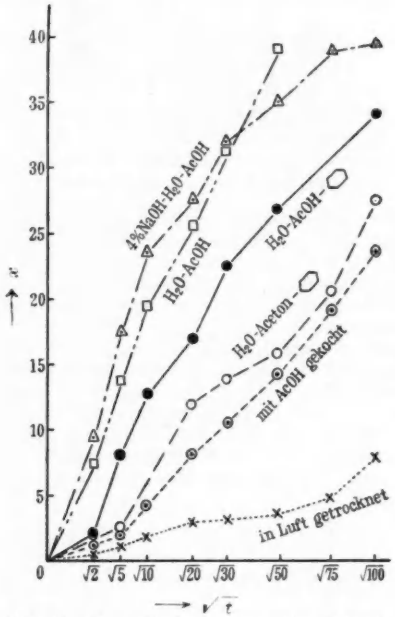

Abb. 5. Der Einfluss von Vorbehandlungsweise.
t: Zeit (Stunden),
x: Anzahl der acetylierten Schichten.

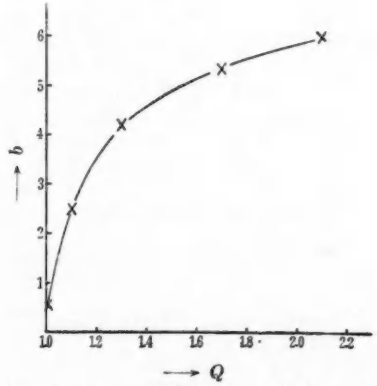

Abb. 6. Die Beziehung zwischen der Regression-Koeffizient (b) und des Quellungs grads (Q).

handlung, desto schneller die Acetylierung, wie in Abb. 6 ersichtlich. Die Beziehung von der Gleichung (10) besteht nicht mehr bei der geringen Quellung, abgesehen vom nicht vorbehandelten Fall. Es kann darauf beruhen, dass der stationäre Zustand nicht in Anfang erreicht wird. Die mit der Alkali-Lauge vorbehandelten Folien ist so schwach, dass die Zahl zufolge Verderben nicht sicher gezählt wird.

Zusammenfassung

Um den Mechanismus der heterogen Acetylierung der Cellulose in eine Dimmension aufzuklären, wurde mehreren aufeinandergesetzten Schichten der Cellophane von einer Seite mit Acetylierungsmittel aus Essigsäureanhydrid—Benzol—Sulfoessigsäure behandelt und der acetylierte Teil wurde mit Anfärbung unterschieden. Das Ergebnis wurde mit der Gleichung verglichen, die unter der Annahme des quasi-stationären Zustand abgeleitet wird.

1. Die Beziehung zwischen der Anzahl der acetylierten Schichten und der Zeit entspricht ungefähr von Diffusion bestimmten Gleichung, nach welcher die Zahl in Verhältnis zum Quadratwurzel der Zeit ist.
2. Je höher die Konzentration der Essigsäureanhydrid, desto schneller das Hinüberwandern der acetylierten Grenze.
3. Da die Konzentration der Sulfossigsäure oder der statische Druck wenigen Einfluss hat und die Abhängigkeit von der Temperatur nicht bedeutend ist, kann der von Diffusion bestimmte Mechanismus unterstützt werden.
4. Die die höhere Quellung ergebende Vorbehandlungsweise übt den grösseren Einfluss aus.

Kokoku Reyon und Zellstoff G.m.b.H.,
Yatsushiro-Fabrik, Yatsushiro-shi,
Kumamoto-ken

The Electronic Structures of Azine Compounds. II. The General Considerations on the Electronic Structures of Azine and Dihydroazine Compounds

By Yûmi Akimoto

(Received January 28, 1956)

Introduction

In the preceding paper[1], the semi-empirical LCAO molecular orbital calculations were made on some azine and dihydroazine compounds. In this paper, for the purpose of generalizing the above conclusions, the scope of the discussions is extended to ten odd azine, dihydroazine, and aza compounds. The results are arranged and investigated systematically from several viewpoints: electronic states, molecular structures, stabilities, etc.

Experimental

With the object of replenishing the spectra data for the sphere of azine compounds, the electronic absorption spectrum was taken on quinoxaline (1, 4-diaza-naphthalene). The sample used was synthesized by the members of Kawai Laboratory of Tokyo University of Education. For the solvent, anhydrous methanol was always employed. The other experimental conditions were similar to that previously described. The result is shown in Fig. 1.

From the standpoint of the transition intensity and the correspondency with the absorption curves of phenazine or quinoline, the strong absorption maximum near 32000 cm^{-1}, may be considered as the π–π transition.

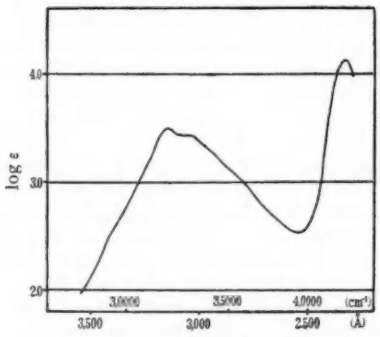

Fig. 1. The absorption spectrum of 1:4-diaza-naphthalene (quinoxaline) (in anhydrous methanol).

1) Y. Akimoto, This Bulletin 29, 460 (1956).

MO Calculation

MO calculations have been carried out for all the molecules shown in Fig. 2. The same calculations were extended to several aza compounds. The π-electron energies of the molecules in the heavy line frames, were calculated by the simplest variation method, and the others by the second order perturbation method, taking as the parent molecules the corresponding molecules which are in the heavy line frames, and for the perturbation term the changes of Coulomb integral values affected by the replacements by N atoms or the introductions of meso-H atoms[2]. According to the conclusions of the previous paper[1], Coulomb integral values are taken as follows:

for every N atom, $\alpha_c+0.6\beta$
for every N_H atom, $\alpha_c+1.2\beta$
for every adjacent atom of
N or N_H atoms (r), $\alpha_c+\frac{1}{8}\sum(\alpha_r-\alpha_c)$

Regarding the other conditions and the detailed explanations of the calculations, the previous paper[1] is to be quoted.

The results of the calculations are summarized in Table I-II, and Fig. 3. Table I shows the results of the variation method calculations applied to the "parent molecules" of the following perturbation calculations. Fig. 3 indicates the π-electron energy states of all molecules referred to above. The underlined column shows the results obtained by the variation method calculations, and the others by the perturbation calculations. In Table II, two calculation methods: variation and perturbation methods, are compared in regard to the numerical results. The first column indicates the electron energies cal-

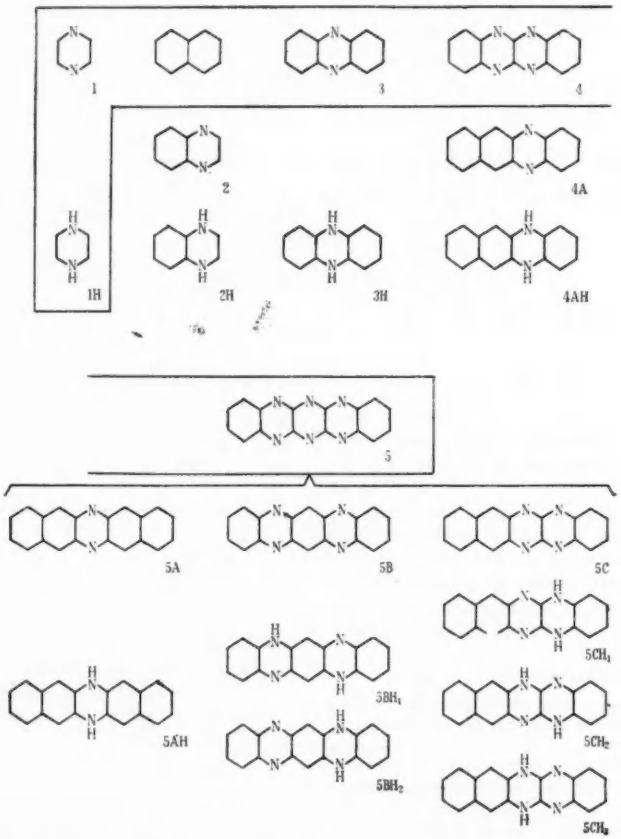

Fig. 2. The model numbers of azine and dihydroazine compounds quoted for the calculations.

2) Per-Olov Löwdin, *J. Chem. Phys.*, **21**, 496 (1953).

culated by the second order perturbation method taking anthracene as the parent molecule, and the second column by the simplest variation method. The result is in a satisfactory agreement.

TABLE I

THE ORBITAL ENERGIES OF "PARENT MOLECULES" CALCULATED BY THE SIMPLE VARIATION METHOD

$x=(\varepsilon-\alpha)/\beta$

Pyrazine (x)		Naphthalene (x)		Phenazine (x)	
				B_{3g}	-2.2834
				A_{1u}	-1.9760
		B_{3g}	-2.0000	B_{3g}	-1.3384
		B_{1u}	-1.6180	B_{1u}	-1.2493
B_{3g}	-1.5716	A_{1u}	-1.6180	B_{2g}	-0.9878
A_{1u}	-0.8500	B_{3g}	-0.6180	A_{1u}	-0.9618
B_{1u}	-0.2394	B_{2g}	-0.6180	B_{1u}	-0.1565
B_{2g}	1.1500	A_{1u}	0.6180	B_{3g}	0.6132
B_{3g}	1.9216	B_{1u}	0.6180	A_{1u}	1.0129
B_{1u}	2.5894	B_{2g}	1.6180	B_{2g}	1.0368
		B_{3g}	1.6180	B_{1u}	1.4908
		B_{1u}	2.0000	B_{3g}	1.6836
				B_{2g}	2.0261
				B_{1u}	2.5900

On 5, 6, 11 12-tetraaza-naphtacene, and 5, 6, 7, 12, 13, 14-hexaaza-pentacene, cf. ref. (1).

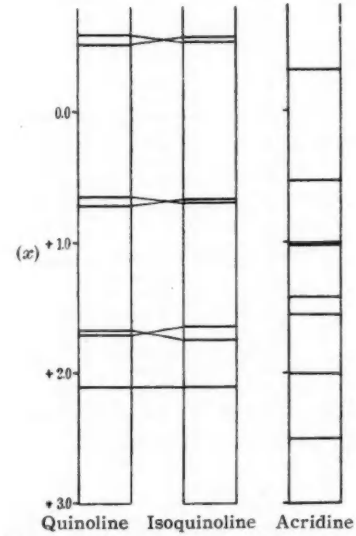

Quinoline Isoquinoline Acridine

Fig. 3a. The electronic states of some aza compounds.

$x=\frac{\varepsilon-\alpha}{\beta}$ (Calculated by the perturbation method).

TABLE II

THE COMPARISON OF TWO CALCULATION METHODS ON THE ORBITAL ENERGIES OF ANTHRACENE

	Calculated by perturbation method (A)	Calculated by variation method (B)	Differences (A)–(B)
B_{3g}	0.415	0.414	+0.01
A_{1u}	1.000	1.000	0
B_{2g}	1.000	1.000	0
B_{1u}	1.414	1.414	0
B_{3g}	1.412	1.414	−0.02
B_{2g}	2.000	2.000	0
B_{1u}	2.416	2.414	−0.02

Discussion

1) **Delocalization Energy**.—In consideration of the previous paper's results[1], the positions of meso–N atoms are determined in comparing the vertical delocalization energy values (vertical delocalization energy $\Delta\varepsilon$ is defined as follows:

$$\Delta\varepsilon=\varepsilon(L)-\varepsilon(D)$$

cf. ref. (1))

over all isomers of each compound (see Table III). Underlined isomers are the most stable ones.

Through the considerations continued from the preceeding paper[1], as far as dihydroazines are concerned, the following practical principle may be established. *The stabilities of dihydroazine isomers increase according to the following order of molecular symmetry:* $C_{2v}\rightarrow C_{2h}\rightarrow V_h$. In Table IV, the vertical delocalization energy of the most stable isomer of each dihydroazine compound is compared with that of its parent azine compound.

In general, the reactivities and the stabilities of meso dihydro derivatives increase rapidly with the increase of the number of rings of azine compounds[3]: It is impossible to oxidize fluoflavine to parent azine compound[4], while quinoxaline has not any stable dihydroazine derivatives. Table IV shows that delocalization energies of all dihydroazine compounds are smaller than those of the corresponding azine compounds, nevertheless on account of the differences which the number of atoms or π-electrons make, the direct comparisons can not provide the conclusion that all dihydroazine compounds are less stable than the corresponding azine compounds. However, the tendency to contract the difference of both energies according to the increase of molecular sizes, enables

3) G.M. Badger and R. Pettit, *J. Chem. Soc.*, 1951, 3211.

4) S. Kawai and S. Noguchi, private communication.

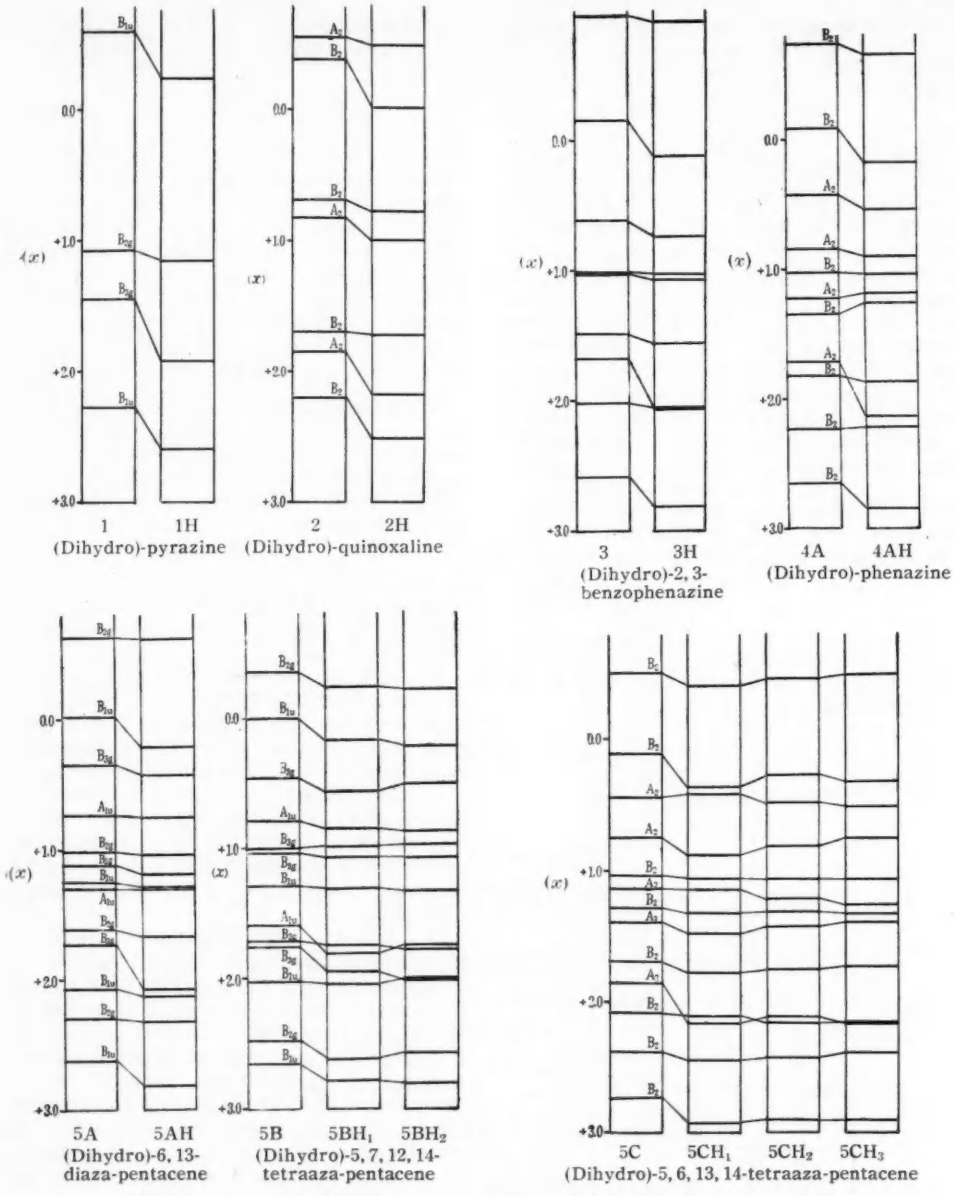

Fig. 3b. The electronic states of some azine and dihydroazine compounds.

$$x=\frac{\varepsilon-\alpha}{\beta}$$

us to predict the stabilities from the ground of the vertical delocalization energies. The reduction rates of the energies, shown in the last column of Table IV, seem to give us some criteria. None of the molecules which have the reduction rates over 17% have any stable dihydroazine derivatives, and less than 6% of any azine compounds. About 9% of the rate seems to correspond to the equal stability between azine and dihydroazine compounds.

In 1926, Dutt reported on his accomplishment of synthesis of 5, 7, 12, 14-tetraza-pentacene[5]. But the result of the re-examination which was followed by Badger et al.[3] was negative. On 5, 6, 11, 12-tetraza-naphtacene, since Hinsberg had reported on his success of the syntheses in 1896[6], no report has been presented, while, the recent result of the re-examination performed by Kawai and Noguchi is negative[4]. Such being the case, the prediction of the stability based on the reduction rates of the delocalization energies, may, though it has not any close theoretical backing, be put to the practical uses.

TABLE III

THE COMPARISONS OF THE DELOCALIZATION ENERGIES ON DIHYDROAZINE ISOMERS

Compounds	Position of meso-H atoms (Model number)	Delocalization energy (β)
Dihydro-5, 7, 12, 14-tetraaza-pentacene	5, 14 ($5BH_2$)	28.920
	5, 12 ($5BH_1$)	28.979
Dihydro-5, 6, 13, 14-tetraaza-pentacene	5, 14 ($5CH_1$)	29.296
	5, 13 ($5CH_2$)	29.205
	6, 13 ($5CH_2$)	29.201

2) The position of the Longest Wave-length Absorption.—Supposing that only the most stable isomer exists on each molecule, the longest wave-length π-π absorption is calculated. In Table V, these values are compared with the observed ones. The conversion rates are chosen so that the calculated transition energies of the corresponding polyacene molecules, agree with the observed absorptions[7] (see ref. (1)). In Fig. 4, these

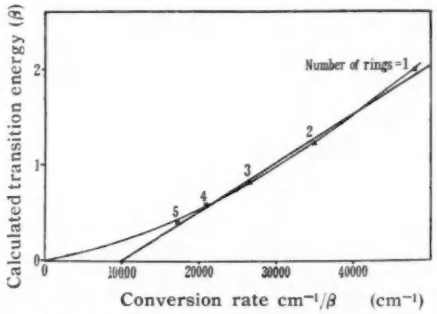

Fig. 4. The conversion rates for the absorption wave number calculations.

TABLE IV

THE DELOCALIZATION ENERGIES OF AZINE AND DIHYDROAZINE COMPOUNDS

Group model number	Molecular structure	Delocalization energy (β) Azine (A)	Dihydroazine (B)	A–B	$\frac{A-B}{A}$
1		8.081	(5.743)	2.338	28.9
2		13.060	(10.807)	2.253	17.25
3	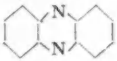	19.407 >	17.482	1.924	9.91
4A	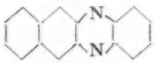	25.084 <	23.103	1.981	7.89
4	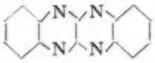	/25.097/	23.614	1.483	5.91
5A	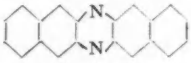	(30.808)	29.126	1.682	5.46
5B		/30.677/	28.979	1.698	5.54
5C	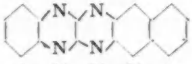	(30.723)	29.296	1.427	4.64
5	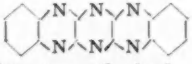	(30.775)	29.353	1.422	4.62

( ) Not yet synthesized.
/ / Accomplishment of synthesis was reported, but negotiated by the re-examination.
> The stability tendency.

5) O. Dutt, *J. Chem. Soc.*, **1926**, 1178.
6) O. Hinsberg and J. Pollak, *Ber.*, **29**, 784 (1896).
7) E. Clar, *Ber.*, **69**, 607 (1936).

rates are shown: The smooth relations are observed between them.

The lack of the spectra data in this sphere, obstructs the overall examinations, while the presented observed values show almost perfect agreements with the calculated ones.

TABLE V

THE COMPARISONS OF THE CALCULATED LONGEST WAVE-LENGTH ABSORPTION POSITIONS WITH THE OBSERVED ONES

Group model number	Molecular skeleton	Conversion rate	Azine compounds				Dihydroazine compound				Reference
			calcd.		obs.	calcd. −obs.	calcd.		obs.	calcd. −obs.	
		(cm^{-1}/β)	(β)	(cm^{-1})	(cm^{-1})	(cm^{-1})	(β)	(cm^{-1})	(cm^{-1})	(cm^{-1})	
1		24,000	1.672	40100	38000	+2100	0.511	12300			(8)
		28,500	1.156	32900	31900	+1000	—	—			(9)
		28,500	1.198	34100	31300	+3000	—	—			(9)
2		28,500	1.070	30500	31700	−1200	0.490	14000			Present paper
	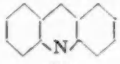	32,500	0.840	27300	28000	− 700	—	—			(10)
3	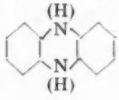	32,500	0.770	25000	27800	−2800	1.047	34000			(10)
4A	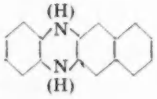	35,500	0.520	18500			0.825	29300			
4	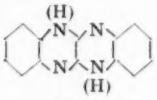	35,500	0.542	19200			0.723	25700	22500	+3200	(1)
5A	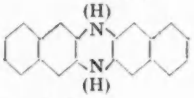	39,000	0.377	14700			0.826	32200			
5B	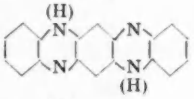	39,000	0.409	16000			0.409	16000	17700	−1700	(3)
5C	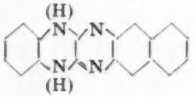	39,000	0.542	21100			0.706	27500			
5	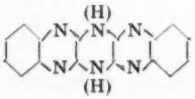	39,000	0.406	15800			0.707	27600	23000	+4600	(1)

8) W.K. Miller, S.B. Knight and A. Roe, *J. Am. Chem. Soc.*, **72**, 1629 (1950).
9) G.W. Ewing and E.A. Steck, *J. Am. Chem. Soc.*, **68**, 2181 (1946).
10) G.M. Badger, R.S. Pearce and R. Pettit, *J. Chem. Soc.*, **1951** 3198.

3) **Molecular Diagram.**—On several molecules, the charge densities and the bond orders are calculated (see Fig. 5). Except 6, 13-dihydro-5, 6, 7, 12, 13, 14-hexaaza-pentacene, all diagrams are calculated by the simplest variation method. On the former molecule, perturbation method is used in applying the following relations[1,2].

$$q_\mu^j = q_\mu^{j(0)} + \sum_\kappa V_\kappa \pi_{\mu\mu,\nu\kappa}^{jj(0)}$$

$$p_{\mu\nu}^j = p_{\mu\nu}^{j(0)} + \sum_\kappa V_\kappa \pi_{\mu\nu,\nu\kappa}^{jj(0)}$$

$$\pi_{\mu\nu,\nu\kappa}^{jj} = \sum_{j \neq \alpha} \frac{d_{\mu\nu}^{j\alpha} d_{\kappa\kappa}^{\alpha j} + d_{\kappa\kappa}^{j\alpha} d_{\mu\nu}^{\alpha j}}{(j\alpha)}$$

$$d_{\mu\nu}^{j\alpha} = C_\mu^j C_\nu^\alpha$$

where q indicates the charge density, p, bond order, V, perturbation terms, C, orbital coefficient, and π, mutability. Upper indices j, α,……indicate the molecular orbitals, lower indices μ, ν, κ,……the atomic orbitals, (0) the quantities belonging to the original system, and $(j\alpha)$ the energy difference between j-th and α-th orbitals.

The unification of the exchange integral to 1β, takes away the significance of bond order considerably[11], while the tendency to prejudicing the orders according to the increase of azine molecule size, and to compensate the prejudice in introducing the meso–H atoms explains the above mentioned tendency which is observed on the reactivities or the stabilities of azine compound series. This tendency will support the conclusions deduced from the former vertical delocalization energy discussions. In any way, the MO recalculation based on the above diagrams, will make more reliable the conclusions stated above.

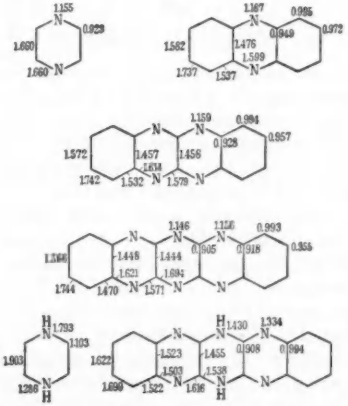

Fig. 5. The molecular diagrams of several azine and dihydroazine compounds.

11) C. A. Coulson, J. de Heer, *J. Chem. Soc.*, **1952** 482.

Summary and Conclusions

1) The absorption spectrum of quinoxaline was observed in anhydrous methanol solution.

2) The longest wave-length π-π transition was observed near 31000–33000 cm^{-1}.

3) The MO calculations were made on ten odd aza, azine, and dihydroazine compounds.

4) Comparing the vertical delocalization energies, the most stable isomer was decided as follows.

molecules	positions of meso–H atoms
dihydro-5, 7, 12, 14-tetraaza-pentacene	5, 14
dihydro-5, 6, 12, 13-tetraaza-pentacene	5, 12.

5) Concerning the stabilities of each dihydroazine isomers, the following tendency was observed. *The stabilities of dihydroazine isomers, increase according to the certain order of molecular symmetry:* $C_{2v} \rightarrow C_{2h} \rightarrow V_h$.

6) The reduction rates of the delocalization energies, azine to dihydroazine compounds, could be a criterion to predict the stabilities of dihydroazine compound as compared with the corresponding azine compounds. When the rate was less than 6%, only the dihydroazine form could exist steadily; more than 17%, the only stable form was the azine form; and between 6–17%, both forms could exist, while the stability of the azine form was surpassed by that of the dihydroazine form near the rate of 9%.

7) The positions of the longest wavelength absorption were predicted or compared with the observed ones. Agreements were satisfactory in the permissible ranges.

8) The molecular diagrams were drawn on several azine and dihydroazine molecules, which could possibly explain the higher stabilities of dihydroazines, the larger skeletons of molecules.

The author wishes to express his sincere thanks to Prof. A. Kotera and Assist. Prof. K. Suzuki for their continued encouragement and valuable advice for this study. The kindness of Prof. S. Kawai who gave us the sample is gratefully acknowledged. Thanks are also due to Mr. S. Noguchi and Mr. K. Ihaya for their helpful discussions.

A part of the cost of this research has been defrayed from the Scientific Research Encouragement Grant from the Ministry of Education, to which the author's thanks are due.

*Chemical Laboratory Tokyo Bunrika University, Tokyo**

* Author's present adress: *Hosokura Smelter and Refinery, Mitsubishi Metal Mining Co. Ltd., Miyagi-ken.*

The Effect of the Segment Size upon Thermodynamic Properties of Polymer Solutions

By Tōru KAWAI

(Received February 16, 1956)

Introduction

The statistical mechanical theories of polymer solutions currently in use do not entirely conform with observed thermodynamic data. Recently it has become apparent from the extensive measurements on the polymer-solvent systems, that the entropy of dilution differs widely for a given polymer in different solvents, and that, moreover, these entropy values are many times lower than can be accounted for by current theories[1,2].

The crucial point in all these theories lies in the expression for the second virial coefficient A_2. Various theories based on the idealized lattice model are essentially equivalent[3], and may be written uniquely as

$$A_2=(1/V_1\rho^2)\left\{\frac{1}{2}-\left(\frac{1}{Z}\right)\left(1-\frac{1}{m}\right)\right\} \qquad (1)$$

where V_1 is the molar volume of the solvent, ρ, density of the polymer, Z, the coordination number of the lattice sites, and m, the number of submolecules in a polymer molecule. (Hereafter we shall designate the degree of the approximation in these theories as the first order approximation.) A number of osmotic measurements, however, give evidence that the observed values of A_2, in general, are much less than is predicted by Eq. (1).

Various attempts have been made to eliminate this lack of conformity; however, none of them seems to have successfully removed it. Accounting for the influence of a bending back of the polymer chain on to itself (long-range interference), Flory and Krigbaum[4] derived an expression for the second virial coefficient. When the polymer is homogeneous, their expression may be written

$$A_2=(1/V_1\rho^2)(\varphi_1-\kappa_1)F(\chi) \qquad (2)$$

$$\chi=2(\alpha^2-1) \qquad (3)$$

where φ_1 and κ_1 are the entropy and energy parameters respectively. The function $F(\chi)$ is a definite integral the evaluation of which is discussed in reference (4). The quantity α is a factor by which the spatial distribution of segments is expanded due to the long-range interference. Thus, the effect of the long-range interference (designated, for convenience, as the "long-range excluded volume effect") upon A_2 appears only through the function $F(\chi)$. Actually, Eq. (2), in combinaton with Eq. (3), well interprets the dependency of the molecular weight of the polymer on A_2, which has been borne out by experiments. As an example, the A_2 values were cited in Table I from the osmotic data

TABLE I

EXAMINATION OF THE DEPENDENCY OF A^2 UPON MOLECULAR WEIGHTS (M: NUMBER AVERAGE MOLECULAR WEIGHT) BY THE THEORY OF FLORY ET AL. (POLYSTYRENE-TOLUENE)

At 25°C

$M\times10^{-4}$	$A_2\times10^4$ g^{-2} cc	α	$F(\chi)$	$A_2/F(\chi)$
158	2.89	1.52	0.82	3.52
87	3.01	1.44	0.87	3.46
32	3.28	1.32	0.89_5	3.66
28.8	3.09	1.31	0.90	3.43
24.8	3.32	1.30	0.90_5	3.67
16.2	3.36	1.25	0.91_5	3.67
9.4	3.89	1.21	0.93_5	4.16

of Bawn et al. for various molecular weights of polystyrene in toluene[5]. The values of $F(\chi)$ are calculated for the corresponding molecular weights, employing the α values evaluated from the data of intrinsic viscosities[2,6]. The ratio $A_2/F(\chi)$ may be regarded as constant in a wide range of molecular weights (M).

However, the question how the abnormally low values of $(\varphi_1-\kappa_1)$ should be explained remains unsolved; since the value of $F(\chi)$ is seldom far from unity (the α values are smaller than 2 apparently including all practical cases for any polymer-solvent pair so far investigated), the "long-range excluded

1) M.J. Schick, P. Doty and B.H. Zimm, *J. Am. Chem. Soc.*, **72**, 530 (1950).
2) T.G. Fox, Jr., and P.J. Flory, *J. Am. Chem. Soc.*, **73**, 1909; 1915 (1951).
3) T. Kawai, This Bulletin, **26**, 409 (1953); **25**, 336 (1952).
4) P.J. Flory and W.R. Krigbaum, *J. Chem. Phys.*, **18**, 1086 (1950).
5) C.E.H. Bawn and M.A. Wajid, *J. Polymer Sci.*, **12**, 109 (1954).
6) P.J. Flory and T.G. Fox, Jr., *J. Am. Chem. Soc.*, **73**, 1904 (1951).

volume effect" cannot eliminate the above lack of conformity between theory and experiment. Moreover, the definition of the parameters φ_1 and κ_1 still lacks precision; a more careful analysis of the meaning of these parameters is desirable.

At first, we must consider the problem of the preferential ordering induced in the solution by difference in the interaction energies, when the heat of dilution is not zero. However, it was shown that Eq. (I) did not conform with observed thermodynamic data for several systems which can be regarded as more or less athermal[7].

Another possible reason for this nonconformity may exist in neglecting the excluded volume effect in a short range scale, which will be discussed in the next section together with the segment size effect; the excluded volume for a segment in a polymer chain (not for a polymer molecule as the whole) would have to be taken into account, beside the effect in a long-range scale mentioned above.

It may be remarked here that existing theories of polymer solutions fail to take into account the specific geometrical character of the solvent in relation to the polymer segment. Considering the widely different entropies of dilution exhibited by different solutions of the same polymer at the same concentration, it is obvious that this is a serious deficiency which must be made up. In order to establish a unique explanation of these thermodynamic data in terms of molecular concept, an attempt will be made in this paper by proceeding with the idea of the segment size effect, which was already discussed briefly in the previous paper[3].

Athermal Solutions

Most of the existing theories involve an over-simplified assumption which usually has escaped notice; it was assumed that the solvent molecule and segment are the same in size and shape. Some investigators arrived within crude approximations, at the conclusion that the choice of any length of the submolecule along the polymer chain as a segment has no appreciable effect on the resultant formula for the entropy of dilution[8,9]. However, no one has taken into account the dependence of the entropy of dilution and of other related quantities on the relative dimensions of the solvent molecules and the solute molecule cross sections. As was shown in the treatment of rod-like molecules[10], this might play an important role on the explanation of unreasonably low values of φ_1. Zimm[11] also has shown an analogous effect for athermal solutions of various infinite chains in an artificial cubic lattice.

Here, the modification of the entropy expression by Flory[12], who first introduced the effect of the segment size, may be recalled, although his definition of the segment was somewhat ambiguous. In our treatment the segment in a thermodynamical sense will be redefined as a purely stereometric one in character. The essential feature of it is that it has to satisfy the condition that it is isotropic and spherical. The effect of anisotropy in the force fields around the segment can be ignored in athermal solutions; however, the geometrical anisotropy, i.e. its shape factor, must be taken into account. If the segment is assumed as a section of the polymer chain which occupies a volume equal to that of the solvent molecule, the resultant expression of the entropy must fail its validity, since it is quite different from the solvent molecule in shape when the dimensions of the polymer cross sections differ extremely from those of the solvent molecule. Therefore, we must construct a more realistic model with regard to the molecular constructions of the solvent and solute. The restriction of the lattice model, which arise from its artificiality, may possibly be removed by choosing a suitable size and shape of the segment as well as by introducing the coordination number characterizing the type of the lattice.

Let us consider four cases; (a) both the polymer and solvent are "aliphatic" (The term "aliphatic" used here means, for convenience, the "effectively" small dimensions of the solvent molecule and the polymer molecule cross sections. The solutions of the polymer consisting of a linear sequence of carbon atoms without any bulky side chains or branches in the open chain solvents belong to this case.) (b) the polymer consists of a sequence of rings[13] (the polymers in

7) H. Stuart, "Das Makromolekül in Lösungen", Berlin (1953).
8) M.L. Huggins, *Ann. N.Y. Acad. Sci.*, 43, 1 (1942).
9) B.H. Zimm, *J. Chem. Phys.*, 14, 164 (1946).
10) Exactly the same expression was derived for the solutions of large rigid rod-like molecules as Eq. (1). Even for these solutions, where both the excluded volume effect and ordering effect mentioned above need not be considered, Eq. (1) does not coincide with the formula obtained by methods using molecular distribution function, without considering the segment size effect (This Bulletin, 24, 269 (1951)).
11) B.H. Zimm, ref. (20), p. 364.
12) P.J. Flory, *J. Chem. Phys.*, 10, 51 (1942).
13) These rings may be contained not only in the main chain but in the side chains; the bulky nature of the effective cross sections of such polymer chain is speculated here.

this class are designated by "aromatic polymer"), and the solvent is "aliphatic". (c) the polymer is "aliphatic", and the solvent is "aromatic" (of course, all rigid cyclic compounds such as cyclohexane or dioxane are also involved). (d) both the polymer and solvent are "aromatic". These are hypothetically illustrated in Fig. 1.

Thus, the segment is defined by the steric factor only, and is characteristic of the polymer without regard to the type of the solvent.

To the case (c) our equation derived previously[3] is also applicable;

$$A_2=(1/V_1\rho^2)\{1/2-(V_1/V_2)(1/2-\varphi_1^*)\}. \quad (6)$$

In arriving at this equation, the probability

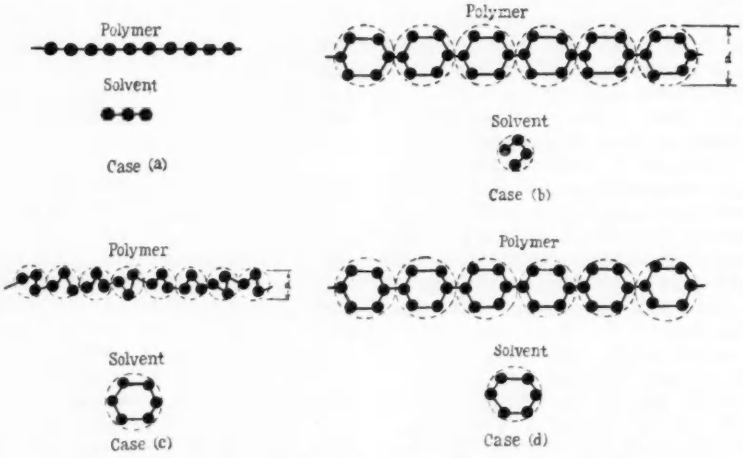

Fig. 1. Hypothetical models of polymer and solvent molecules.

For the case (a) Guggenheim obtained, within a crude approximation, an expression of entropy of dilution, which does not much differ from the results (for instance, Eq. (1)) deduced from the usual assumption that the solvent molecule and segment are the same in size and shape[14]. Here, considering the effect of the flexibility of the polymer chain[15,16], it would be preferable to write

$$A_2=(1/V_1\rho^2)\varphi_1^*. \quad (4)$$

The parameter φ_1^* is characteristic to the polymer chain, irrespective of the solvent, and the effect of flexibility of the chain, if it gives rise to some alteration in the expression of A_2, may be involved into this parameter[15,16].

For the case (b) the author derived[3]

$$A_2=(1/V_1\rho^2)(V_1/V_2)\varphi_1^* \quad (5)$$

which is formally analogous to the Flory's formula in reference (12). In our derivation of Eq. (5), however, the segment was assumed to be a sphere of radius $d/2$ (d is the diameter of the cross section of the polymer chain), the "molar" volume of which is V_2. that V_1/V_2 sites must be in one group was calculated to an approximation which corresponds to that employed usually for the mixing of substances of low molecular weight[3], leading to the expression of the entropy of mixing;

$$\Delta S=-R[N_1\ln v_1+N_2\ln v_2]$$

(the N's are the numbers of the molecules and the v's, the volume fractions of the two components).

To the case (d) Eqs. (5) and (6) may be applicable again, according to the respective cases when $V_1>V_2$ and when $V_1<V_2$.

The above simplified models would not be able to provide the comprehensive picture of actual polymer solutions. It seems difficult, however, to take into account the molecular structure of the two components in more detail, because of the complicated character including the effect of the side chains, the non-uniformity of the cross sections along the polymer chain, and the spatial factors of the solvent molecule (our treatment of copolymer solutions may be suggestive in this point[17]).

Therefore, it seems to be rather preferable

14) E. A. Guggenheim, "Mixture", Oxford Univ. Press, London (1952), p. 197.
15) M. Kurata, M. Tamura and T. Watari, *J. Chem. Phys.*, **23**, 991 (1955).
16) M. L. Huggins, *J. Polymer Sci.*, **16**, 209 (1955).
17) T. Kawai, Meeting of Soc. of High Polymer, Japan, IIth Dec., 1954.

to introduce effective volumes of the solvent molecule and segment, V_1^* and V_2^*, involving all the complicated factors mentioned above, instead of V_1 and V_2, and use Eq. (5) when $V_1^* < V_2^*$ and Eq. (6) when $V_1^* > V_2^*$.

Furthermore, as was pointed out by Rushbrook et al.[18], even small molecules such as trimer or tetramer (in their terms) provide some difference in the entropy of mixing between rigid and flexible chains. This difference may be considered to arise from such effect of the excluded volume in a short-range scale as was mentioned previously. Zimm[9] showed an analogous effect on polymer solutions in somewhat different way; in his expression of A_2, the higher segment interaction integrals cannot be ignored in some cases. These integrals describe the effect of the interaction of the neighbouring segments on the probability of a meeting between a segment of one polymer molecule and that of the other molecule at a particular place. Thus, this effect depends on the local structure of the chain molecule and is more or less appreciable, except in the case where the segments are many times longer than their width (such long segments may be inadequate from our viewpoint in this treatment).

Here, the effect of the higher segment interaction, in Zimm's term, upon A_2 has been separated into two factors; the segment size effect (represented by V_1^*/V_2^*) and the effect of the chain flexibility (expressed by the parameter φ_1^*). The flexibility parameter φ_1^*, in other words, represents the just mentioned excluded volume effect in a short-range scale, and, if necessary, the expression of Kurata et al.[15] for A_2 may be utilized:

$$\varphi_1^* = 1/3 - (1/24)\{6\tau + (1-\tau)^2\} \qquad (7)$$

where τ is a parameter adjustable between zero and one, which increases with increasing flexibility of the polymer chain and reaches unity when polymer chains coil up tightly.

Taking account of the "long-range excluded volume effect", the final formulas may be written:

when $V_1^* < V_2^*$

$$A_2 = (1/V_1\rho^2)(V_1^*/V_2^*)\varphi_1^* F(\chi) \qquad (8)$$

when $V_1 > {}^*V_2^*$

$$A_2 = (1/V_1\rho^2)\{1/2 - (V_1^*/V_2^*)(1/2 - \varphi_1^*)\}F(\chi). \qquad (9)$$

Since the segment in this treatment is characteristic of the polymer chain regardless of the solvent, Eqs. (8) and (9) would be very useful especially when we inquire into the effect of the solvent type on the thermodynamic properties of polymer solutions[3]. However, unless the spatial character of the solvent molecule (including the average configurations of its flexible carbon chains) may be represented by the "effective sphere" of volume V_1^*, the validity of this treatment fails[19]. The theoretical limitations for further analysis of this spatial factor would be apparent.

Solutions not Athermal

In this section, we shall consider the segments and solvent molecules of different sizes, each being approximated by an effective sphere in shape as was considered in the previous section, and we shall discuss the case when mixing of them is not athermal. Let us assume Z_{11} unit sites around the solvent molecule, and similarly Z_{22} unit sites around the segment; i.e., Z_{11} or Z_{22} corresponds to the surface area of each molecule and approximately, to its volume (in the latter case, this procedure is analogous to the usual treatment employing the cohesive energy density[20]). In their pure state, both the solvent molecule and segment may be assumed to have Z nearest neighbor contacts, and then, each one contact occupies Z_{11}/Z and Z_{22}/Z unit sites, respectively (Z is determined by the steric character of the segment and solvent molecule. When both

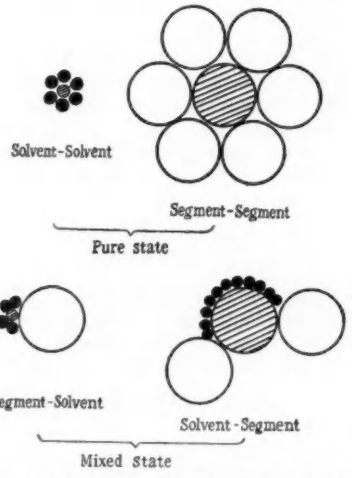

Fig. 2. Illustration of kinds of contacts.

18) G.S. Rushbrook, H.I. Scoins and A.J. Wakefield, *Trans. Faraday Soc., Discussion*, **15**, 57 (1953).

19) The value of V_1^* is to be determined by the spatial character of the solvent. When the solvent molecule consists of a long flexible carbon chain, "the flexibility entropy" of the solvent molecule contributes to the partial molal entropy of the solvent (see reference (16)).

20) J.H. Hildebrand and R.L. Scott, "The Solubility of Nonelectrolyes", 3rd edition, Reinhold Publ. Co., New York (1950).

are effectively spherical, we can assume $Z=12$ for the closely compacted state).

When the two kinds of elements are mixed, we can suppose that, of the $Z_{11}n_1/2$ sites around the solvent molecule, X'_{12} sites come from the segments (n_1: the total number of the solvent molecules), and that, similarly, of the $Z_{22}n_2/2$ sites around the segment, X'_{12} sites come from the solvent molecules (n_2: the total number of the segments). (see Fig. 2).

One solvent molecule occupies Z_{11}/Z unit sites both around the solvent molecule and segment, and, similarly, one segment occupies Z_{22}/Z unit sites. Therefore the number of each contact in the mixture may be written as follows:

kinds of contacts	number of contacts expressed by that of the unit sites	actual number of contacts
solvent-solvent	$\frac{Z_{11}n_1}{2}-X'_{12}$	$X_{11}=a\left(\frac{Z_{11}n_1}{2}-X'_{12}\right)$
solvent-segment	X'_{12}	aX'_{12}
segment-solvent	X'_{12}	bX'_{12}
segment-segment	$\frac{Z_{22}n_2}{2}-X'_{12}$	$X_{22}=b\left(\frac{Z_{22}n_2}{2}-X'_{12}\right)$

$(a=Z/Z_{11}, \quad b=Z/Z_{22}).$

Here, we have distinguished between the solvent-segment contacts (solvent molecules around a segment) and the segment-solvent contacts (segments around a solvent molecule).

Introducing the combinatory method developed by Guggenheim[14], the above assumptions lead to

$$g=g^*\times\frac{X_{11}^*!\,(aX'^*_{12})!\,(bX'^*_{12})!\,X_{22}^*!}{X_{11}!\,(aX'_{12})!\,(bX'_{12})!\,X_{22}!} \tag{10}$$

where g^* is the number of configurations for the athermal mixing of the two kinds of the elements, which was discussed in the previous section, and g, that for specified n_1, n_2 and X'_{12} (the asterisk means the athermal mixing).

For a given value of X'_{12} the configurational energy is given by

$$E_c=X_{11}w_{11}+X_{22}w_{22}+(a+b)X'_{12}w_{12} \tag{11}$$

where the w's denote the energies of the respective contacts. Consequently the configurational partition function Ω may be written

$$\Omega=\sum_{X'_{12}} g(n_1, n_2, X'_{12})\exp\{E_c(n_1, n_2, X'_{12})\}. \tag{12}$$

By replacing the sum of g on all X'_{12} values by its maximum term,

$$\Omega=g(n_1, n_2, X'_{12})\exp\{X_{11}w_{11}+X_{22}w_{22}+(a+b)X'_{12}w_{12}\}. \tag{13}$$

Now, X'_{12} should have the value determined by

$$\partial \ln \Omega/\partial X'_{12}=0.$$

From this condition the following relationship is obtained;

$$(u-y)^a(v-y)^b=Ay^{(a+b)} \tag{14}$$

where $A=e^{W/kT}$,

with $W=(a+b)w_{12}-aw_{11}-bw_{22}$.

In arriving at Eq. (14) we have introduced such abbreviations as Guggenheim[14] did:

$$u=\frac{Z_{11}n_1}{Z_{11}n_1+Z_{22}n_2}, \qquad v=\frac{Z_{22}n_2}{Z_{11}n_1+Z_{22}n_2}$$

$$y=\frac{X'_{12}}{Z_{11}n_1+Z_{22}n_2}. \tag{15}$$

Similarly, since X'^*_{12} denotes the values of X'_{12} which maximizes the expression, $X_{11}!\,(aX'_{12})!\,(bX'_{12})!\,X_{22}!$, there is obtained

$$(u-y^*)^a(v-y^*)^b=y^{*(a+b)}\left(y^*=\frac{X'^*_{12}}{Z_{11}n_1+Z_{22}n_2}\right). \tag{16}$$

Eqs. (14) and (16) cannot be solved straightforwardly; however, writing $y=y^*+\Delta y$, we can evaluate y in spite of the crude approximation involved in its calculation[21]. The resultant equation is given by

$$y\fallingdotseq Kuv+(1-A^{1/b})(v-Kuv). \tag{17}$$[21]

We thus obtain the energy of mixing ΔE:

21) Expanding Eq. (14) into the binomial series with respect to Δy, we may write

$$A^{\frac{1}{b}}\left\{y^*\frac{\frac{a+b}{b}}{(u-y^*)}-\frac{a}{b}+\left[\left(\frac{a+b}{b}\right)y^*\frac{\left(\frac{a+b}{b}\right)-1}{}\right.\right.$$

$$\left.\left.\times(u-y^*)^{-\frac{a}{b}}-\left(\frac{a}{b}\right)y^*\frac{\frac{a+b}{b}}{(u-y^*)}-\left(\frac{a+b}{b}\right)\right]\Delta y+\cdots\right\}$$

$$=v-y^*-\Delta y.$$

Since we can neglect safely the coefficient of Δy in the left hand side of this equation in comparison to that in the right (i.e. $(-1)\times\Delta y$) when $y^*<v\ll 1$ (for dilute solutions), except the case when $a\ll b$, the relation, $y=y^*+(1-A^{1/b})(v-y^*)$ is obtained to a satisfactory approximation provided that $\Delta y<y^*$. Next, Eq. (16) can be solved approximately as follows: when $a=b$, $y^*=uv$, and at infinite dilution, $y^*=uv$ when $a\gg b$ and $y^*=uv/2$ when $a\ll b$. So long as the extremely dilute region (say, 0-2% polymer) is concerned, it is possible to show that y^* may be written approximately as Kuv, where K is about unity when $a>b$ and decreases with the decreasing values of a/b when $a<b$.

$$\Delta E=(Z_{11}n_1+Z_{22}n_2)Wy=(Z_{11}n_1+Z_{22}n_2)W\{Kuv+(1-A^{1/2})(v-Kuv)\}. \quad (18)$$

From this we may obtain the Helmholtz free energy of mixing, ΔF, by integration, assuming W independent of temperature T;

$$-\frac{\Delta F}{T}=\int\frac{\Delta E}{T^2}\mathrm{d}T+C. \quad (19)$$

The temperature independent term C is of course the athermal entropy of mixing (ΔS^*). The integration yields ΔF, and the partial molal quantities may be written as follows;

$$\Delta\bar{F}_1=\Delta\bar{S}_1{}^*+KZ_{11}W[1+(1/2)\{W/(bkT)\}+(1/6)\{W/(bkT)\}^2+\cdots\cdots]v^2+\cdots\cdots \quad (20)$$

$$\Delta\bar{E}_1=KZ_{11}W[1+W/(bkT)+(1/2)\{W/(bkT)\}^2+\cdots\cdots]v^2+\cdots\cdots \quad (21)$$

$$\Delta\bar{S}_1=\Delta\bar{S}_1{}^*+KZ_{11}W[(1/2)\{W/(bkT)\}+(1/3)\{W/(bkT)\}^2+\cdots\cdots]v^2+\cdots\cdots. \quad (22)$$

In the above treatment the connection between the segments in the chain molecule is not essentially taken into account. So far as the second virial coefficient is concerned, however, it was shown[4,9] that the neglect of it does not bring out any serious difference in the resultant formula. Evidently from the theory of Flory and Krigbaum[4], only interaction between pairs of the segments belonging to two different polymer molecules was considered in the introduction of the parameters φ_1 and κ_1. Therefore, the treatment in this section may be available to discuss the parameters φ_1 and κ_1, and the second virial coefficient may be written

$$A_2=(1/V_1\rho^2)(\varphi_1-\kappa_1)F(\chi),$$

with

$$\varphi_1=\varphi_1{}^{**}+KZ_{11}(V_1Z_{22}/V_2Z_{11})^2W[(1/2)\times\{W/(bkT)\}+(1/3)\{W/(bkT)\}^2+\cdots\cdots] \quad (23)$$

where $\varphi_1{}^{**}=(V_1{}^*/V_2{}^*)\varphi_1{}^*$ when $V_1{}^*<V_2{}^*$, and $\varphi_1{}^{**}=1/2-(V_1{}^*/V_2{}^*)(1/2-\varphi_1{}^*)$ when $V_1{}^*>V_2{}^*$.

And

$$\kappa_1=KZ_{11}(V_1Z_{22}/V_2Z_{11})^2W[1+W/(bkT)+(1/2)\{W/(bkT)\}^2+\cdots\cdots] \quad (24)$$

Comparison with Experiment

Unfortunately, there are very few polymer-solvent systems which have been investigated accurately enough either with respect to the temperature dependency of osmotic pressure or to (the direct measurements of) the heat of dilution to permit anything but a rough estimate of the adequacy of the treatment developed here for calculating $\Delta\bar{S}_1$ (or φ_1) and $\Delta\bar{E}_1$ (or κ_1). The treatment of intrinsic viscosities presented by Flory and Fox[5] affords very good agreement with the experiment as was pointed out elsewhere[22], and fortunately, the $(\varphi_1-\kappa_1)$ values deduced from intrinsic viscosity measurements[2] well coincide with those from osmotic data[1,5,23], at least for the polymer solutions investigated here. This is illustrated in Table II (for polyisobutyrene solutions) and in Table III (for polystyrene solutions). These values of φ_1 and κ_1 may be available for the present purpose.

TABLE II

COMPARISON BETWEEN THEORY AND EXPERIMENT FOR POLYISOBUTYRENE SOLUTIONS

At 25°C

Solvent	$(\varphi_1-\kappa_1)$ from $[\eta]$[2]	$(\varphi_1-\kappa_1)$ from osmotic data	$(\varphi_1)_{exp.}$	κ_1	$\varphi_1{}^{**}$	V_1 cc.
Benzene	0	0[23]	0.15	0.15	0.21_8	89.4_7
Cyclohexane	0.081	0.074_2[23]	0.14	0.059	0.15_7	108.7
Toluene	0.02		0.14	0.12	0.16_3	106.8
Ethylbenzene	0.023		0.14	0.117	0.11_4	122.4
75:25 E.B.:P.E.	0		0.17	0.17	(0.10_1)	126.3
50:50 E.B.:P.E.	−0.03		0.21	0.24	(0.07_7)	133.9_5
Diisobutyrene	0.040		0.056	0.016	0.04_7	156.9
n-Hexadecane	0.039		0.094	0.055	(−0.42)	291.9_2
n-Heptane	0.035		0.035	0	0.03_5	147.3_2
Triptane	0.047		0.047	0	—	—

TABLE III

COMPARISON BETWEEN THEORY AND EXPERIMENT FOR POLYSTYRENE SOLUTIONS

At 25°C

Solvent	$(\varphi_1-\kappa_1)$ From $[\eta]$[2]	$(\varphi_1-\kappa_1)$ From osmotic data	$(\varphi_1)_{exp.}$	κ_1	V_1 cc
Cyclohexane	0	0.003_7[1]	0.13	0.13	108.7
Toluene	0.05	0.050_2[1]	0.11	0.06	106.8
Benzene	0.06	—	0.09	0.03	89.4_7
Dichloroethane	0.022	—	0.06	0.038	84.3
Methyl ethyl ketone	0.006	0.005_8[5]	0.006	0	90.1_2

22) T. Kawai and R. Kashiwagi, Annual Meeting of Chem. Soc. Japan, April 1955.

23) P.J. Flory, *J. Am. Chem. Soc.*, **65**, 372 (1943).

All these φ_1 values are much smaller than those predicted from Eq. (1). Furthermore, it has become apparent that the entropy of dilution differs widely for a given polymer in different solvents. For athermal mixing, the φ_1 values are predicted from Eqs. (8) and (9) to decrease with the increasing V_1^* values when $V_1^* > V_2^*$ and with the decreasing V_1^* when $V_1^* < V_2^*$.

To polyisobutyrene solutions Eq. (9) may be applicable, since it seems reasonable to choose the isobutene unit as the segment, which is considered to be smaller than the solvents used. Assuming $\varphi_1^* = 0.2$[24], for convenience, the ratio V_1^*/V_2^* has been calculated from the $(\varphi_1)_{exp.}$ value (experimental values of φ_1) for heptane solution, which can be regarded as athermal. This ratio is 1.55 for heptane and then, assuming $V_1^* = V_1$, $V_2^* = 95$ cc. This value of the segment volume V_2^* corresponds approximately to the isobutene unit. Regardless of these values of V_2^* and φ_1^*, we can evaluate the φ_1^{**} values for the solvents used from Eq. (9), regarding the heptane solution as a standard. Also these values are given in Table II (by employing the approximation, $V_1^* = V_1$ again), together with the molar volumes of the solvents. Except the two mixed solvents (ethylbenzene (E. B.)-phenyl ether (P. E.)) and *n*-hexadecane, the agreement between the $(\varphi_1)_{exp.}$ and φ_1^{**} values is rather satisfactory, considering the crudity of the assumptions on the one hand and the uncertainty of absolute magnitude of $(\varphi_1)_{exp.}$ on the other[25]. There appears to be no correlation between $(\varphi)_{exp.}$ and κ_1. In the systems having great κ_1 values such as the two mixed solvent solutions, however, there might be some contribution of the heat of mixing to φ_1. For *n*-hexadecane, the long asymmetrical solvent capable of assuming a number of different configurations, the assumption $V_1^* = V_1$ could no longer hold its validity[19].

The situation is entirely different for polystyrene solutions. For methyl ethyl ketone, in which $\kappa_1 = 0$, the $(\varphi_1)_{exp.}$ value is unexpectedly small. Considering the bulky nature of the aromatic side chain of polysyrene, we are inclined to apply Eq. (8) to these solutions. However, Eq. (8) leads us to an unreasonably large value of V_2^*; from this φ_1^{**} value we obtain $V_1^*/V_2^* = 0.02$ and $V_2^* = 7370$ cc. (assuming $\varphi_1^* = 0.3$ and $V_1^* = V_1$)[26]. The reason for this is not known, and probably, this might be partly due to the same reason as was mentioned in reference (25). Nevertheless, it may be easily supposed from the chemical structure of the polystyrene chain that the value of V_2^* is fairly great, and the values of φ_1^{**} would not exceed, at the greatest, 0.1 for all the solvents cited in Table III (see the V_1 values given in the same table)[27]. The apparent discrepancy between thus estimated value of φ_1^{**} and the $(\varphi_1)_{exp.}$ values cannot be interpreted until Eq. (23) is introduced for the expression of φ_1. We can find semiqantitatively good correspondence between $(\varphi)_{exp.}$ and κ_1 values in Table III. This, of course, may be expected from Eqs. (23) and (24).

It must be emphasized that the preferential ordering induced by the difference in the interaction energies gives rise to a notable contribution to φ_1 for polystyrene solutions, whereas it does not appear to bring out so much influence for polyisobutyrene solutions. This result is in good agreement with Eq. (23), since the value of $(1/b)$ may be supposed to be much larger for polystyrene than for polyisobutyrene. It is an important conclusion in our theory that the above ordering effect is governed to a large extent by the size of the segment (strictly speaking, by its surface area, and approximately by V_2^*) as well as by the value of κ_1. At this point it is of interest to note that in an osmotic investigation of dilute polyvinylchloride solutions the highest entropy values were obtained in the solvents capable of the least specific interaction with the polymer[28].

In view of the simplicity of the concepts involved and of the paucity of available data, the good agreement between our theory and the experiments such as mentioned above may be to some extent fortuitous, and further improvement of the present theory and more extensive measurements would be necessary to establish the unique explanation of experimental data in terms of more detailed molecular concept. It may be said, however,

24) According to Eq. (7) the value of φ_1^* decreases from 0.292 to 0.083 with increasing flexibility (γ) of the chain. Here, for convenience, we adopt $\varphi_1^* = 0.2$, obtained with $\gamma = 0.5$ for polyisobutyrene.

25) The free energy is fairly insensitive to the errors introduced in any over-simplified treatment, but the entropy and heat are not. Therefore, even if the $(\varphi_1 - \kappa_1)$ values coincide with those obtained from osmotic data, we cannot conclude that the precise values of φ_1 and κ_1 have been obtained. Especially in the case of the good solvent, estimated uncertainties in φ_1 and κ_1 amount to 20-30%, whereas they are very little (0-5%) for the bad solvent.

26) We have assumed $\varphi_1^* = 0.3$, with $\gamma = 0$ for polystyrene (see Eq. (7)).

27) It may be remarked that the $(\varphi_1)_{exp.}$ value is larger for the polyisobutyrene-*n*-heptane system (a fairly flexible chain) than for the polystyrene-methyl ethyl ketone (a less flexible chain). This is approved by our treatment, but is in contradiction with the theories in which only the flexibility of the chain was taken into account.

28) P. Doty and E. Mishuck, *J. Am. Chem. Soc.*, **69**, 1631 (1947).

that the widely different entropies of dilution exhibited by different solutions of the same polymer and abnormally low values of them have been semiquantitatively interpreted by the above treatment.

This paper was read at the Special Symposium on Polymer Solutions, held by Chem. Soc., Japan, Phys. Soc., Japan, and the Soc. of High Polymer, Japan, in Tokyo, on 9th Oct., 1955.

Laboratory of Textile Chemistry,
Tokyo Institute of Technology, Tokyo

Mikroanalyse mit Hilfe von Ionenaustauschharzen. III. Über den Nachweis geringer Menge des Sulfides mit p-Aminodimethylanilin oder p-Phenylendiamin*[1]

Von Masatoshi FUJIMOTO

(Eingegangen am 27. Januar 1956)

Einleitung

Durch mikroanalytische Anwendung der Ionenaustauschharze zur Tüpfelmethode wird die Empfindlichkeit oder die Selektivität der Nachweisreaktionen häufig auffallend erhöht[1,2,3,4]. Diese Erhöhung der Empfindlichkeit oder Selektivität beruht hauptsächlich auf dem selektiven Austausch sowie der bemerkenswerten Konzentrierung der Ionen in die Harzphase und manchmal auf besonderen Zuständen von den in sie adsorbierten Ionen[1,2,5]. Um diese Bedingungen befriedigend zu realisieren, untersucht man spezifische Reaktionen mit bemerkenswürdigen Zustandsänderung der Probe, z. B. Färbung, Entfärbung, Gasenentwicklung, Niederschlagbildung usw. Als ein Beispiel von diesen Reaktionen hat der Verfasser die Bildung von kationischen[6] Thiazinfarbstoffe wie Methylenblau oder Lauthschem Violett (Thionin), die in die farblosen starksauren Kationenaustauschharze stark adsorbiert werden und diese entschieden deutlich grün bzw. blau färben, zum Nachweis des Sulfides angewendet[7].

Wenn *p*-Aminodimethylanilin (I) oder *p*-Phenylendiamin (III) bei Gegenwart von Salzsäure und Eisen(III)chlorid mit Schwefelwasserstoffsäure oder Sulfide reagiert, entsteht Methylenblau (II) oder Lauthsches Violett (IV) gemäss den folgenden Reaktionen:

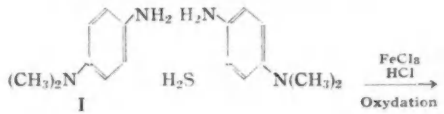

I
farblos

II
blau

oder

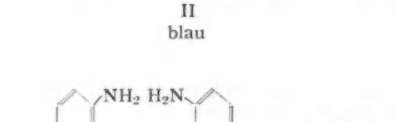

III
farblos

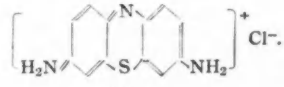

IV
violett

* Statt des Ausdrucks „ionenaustauschendes Harz." der in den vorhergehenden Mitteilungen als geeignete Übersetzung vom Englisch „ion-exchange resin" gebraucht wurde, wird hier die gegenwärtige Terminologie „Ionenaustauschharz." die heute gewöhnlicher angewendet wird, folgerichtig angewendet.

1) Zweite Mitteilung: M. Fujimoto, Dieses Bulletin **27**, 347 (1954).

2) M. Fujimoto, Dieses Bulletin **27**, 48 (1954).

3) H. Kakihana und T. Murase, *J. Chem. Soc. Japan (Pure Chem. Sect.)*, **75**, 907 (1954).

4) H. Kakihana, Y. Mori und K. Yamasaki, *ibid.* **76**, 215 (1955).

5) M. Fujimoto, Dieses Bulletin **29**, 285 (1956).

6) Die freie Base von diesen Farbstoffen sind sehr starkbasisch; d. h. pKo (negativer gemeiner Logarithmus von Dissoziationskonstante als die freie Base, Ko) sind weniger als 1 (Methylenblau) und 2.73 (Lauthsches Violett): Vgl. O. Tomiček, „Chemical Indicators", übersetzt von A.R. Weir, 1. Aufl., London (1951), S. 150.

7) Vgl. E. Fischer, *Ber.* **16**, 2234 (1883), sowie F. Feigl, „Spot Tests. I. Inorganic Applications," übersetzt von R. E. Oesper, 4. engl. Aufl., Amsterdam (1954), S. 283.

Die so gebildeten chinoiden Farbstoffkationen werden ins hellgelbe starksaure Kationenaustauschharz adsorbiert, und geben der Harzphase eine grüne oder blaue Färbung, die entschieden deutlicher im Vergleich mit der von Lösungsphase ist. Z. B.:

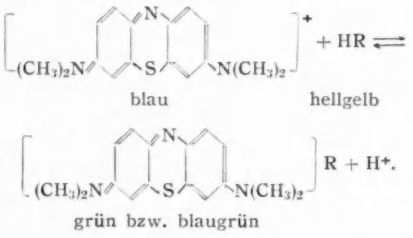

HR bedeutet ein starksaures Kationenaustauschharz von freier Säureform.

Dass das obige Ionenaustauschgleichgewicht wegen des grösseren Ionengewichts des Farbstoffkations beträchtlich auf der rechten Seite liege, trotzdem dieses Gleichgewicht verhältnismässig langsam erreicht werde, ist vor allem für den Nachweis des Sulfides sehr günstig[8].

Das in dieser Untersuchung benutzte Kationenaustauschharz

Dowex 50W-X8[9]: Ein farbloses aus Styrol und Divinylbenzol dargestelltes starksaures Harz von Sulfonsäuretypus, das vor dem Gebrauch durch zweimaliges Durchlaufen der 2 N Salzsäure oder 2 N Lösung von Natriumchlorid und destilliertes Wassers in die HR- oder NaR-Form übergeführt wurde. Die Korngrösse ist 50 bis 100 Maschen von Tylerschem Normalsieb.

Versuchsanordnung

Auf einer weissen Tüpfelplatte[2] versetzt man zuerst kleinste Menge vom festen Reagens mit einem Tropfen (0.04 ccm[10]) mit Kapillarpipette) der Salzsäurelösung des Eisen(III)chlorides. Nach einige Minuten lang stehen gelassen, fügt man dazu einige Körnchen von Kationenaustauschharz, schüttelt danach um, und versetzt man mit einem Tropfen der Probelösung. Von einigen Minuten bis einer Stunde nach, je nach der Sulfidmenge der Probelösung, entsteht am Rande oder über das Ganze der Harzkörnchen eine grüne bzw. blaugrüne Färbung, welche mit einer Lupe von etwa zwanzigfacher Vergrösserung wohl nachweisbar ist.

Bestimmung der Bedingungen höchster Empfindlichkeit

1. Massflüssigkeit.—Eine Reihe der Massflüssigkeiten wurde aus der wässerigen Lösung des extrareinen Natriumsulfides dargestellt, deren 1 ccm 7.85 mg von Sulfide (als S^{2-}) enthielt[11]. Alle folgende Vergleichungen der Experimentalbedingungen wurden mit einer Lösung ausgeführt, deren ein Tropfen (0.04 ccm) 3.14 γ von Sulfide enthielt.

2. Schematische Darstellung von der scheinbaren Intensität der Färbung[1].—Um die Versuchsergebnisse halbquantitativ zu bestimmen, stellte der Verfasser die scheinbare Intensität der Färbung durch eine Reihe der Zahlen, d. h., die Zeichen, −, ±, (+), + usw.[12] durch 0, 1, 1.5, 2 usw. dar, und betrachtete die Gesamtsumme dieser Zahlen an allen für die Reaktion benutzten Vertiefungen von der Platte, die durch die Zahl der Vertiefungen geteilt wurde, als die scheinbare Durchschnittsintensität der Färbung. Nach diesem Verfahren kann man beispielsweise die Erfassungsgrenze der Reaktion durch die Durchschnittszahl „2" deutlich bezeichnen.

3. Die Bedingungen höchster Empfindlichkeit.—Die Resultate der Vergleichung der Empfindlichkeiten unter verschiedenen Bedingungen ausgeführter Reaktionen werden in Abb. I und Tabelle I kurz gefasst:

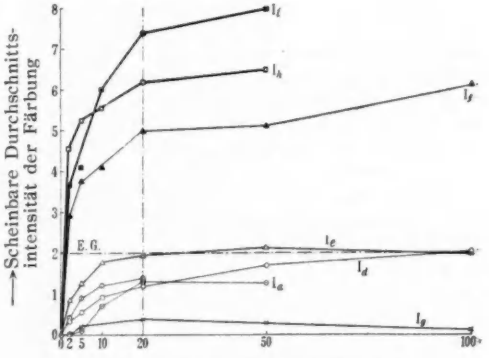

Abb. 1. Vergleichung verschiedener Bedingungen.

8) Vgl. z. B. R. W. Richardson, *Nature*, **164**, 916 (1949) sowie M. Honda, „Ionenaustausch (Ion-kôkan)" 1. Aufl. (japanisch), Tokyo (1954), S. 59.

9) Dowex 50 von verschiedenem Divinylbenzolgehalt, sowie Amberlite IR-120 und IR-112, die durch gelindes Erwärmen mit verdünnter Natronlauge und ungefähr zehnprozentiger Lösung des Wasserstoffperoxyds fast völlig entfärbt werden, wurden gleichfalls benutzt, wobei befriedigende Ergebnisse erhalten wurden. In Bezug auf die Entfärbung der gefärbten starksauren Kationenaustauschharze, vergleiche M. Honda, H. Kakihana und Y. Yoshino, „Ionenaustauschharze (Ion-kôkan Jushi)" 1. Aufl. (japanisch), Tokyo (1955), S. 48.

10) Da 0.02 ccm, der in den vorhergehenden Mitteilungen als ein Tropfen der Mikropipette verwendet wurde, für gewöhnliches mikroanalytisches Verfahren allzu klein ist, wählt der Verfasser von nun an „0.04 ccm" als ein Tropfenmenge der Mikropipette aus.

11) Die Menge von Sulfide wurde folgenderweise einfach bestimmt: Nach der Oxydation der Probelösung mit bestimmtem Überschusse der 0.1 N Massflüssigkeit des Jodes, wurde deren Überschuss mit einer Massflüssigkeit des 0.1 N Natriumthiosulfats umgekehrt titriert.

12) In Bezug auf die Zeichen, −, ±, (+) ±, ∓, ∓ usw., vergleiche Tabelle II von Fussnote 1).

TABELLE I

VERSCHIEDENE REAKTIONSBEDINGUNGEN VON ABB. I

Nr. des Expts.	Zeichen	Ordnung der Versetzung von Reagenzien und Probelösung 1.	2.	3.	4.	Anmerkungen über die Resultate*
I_a	⊖	Probelsg.**	1proz. Lsg. (3 N HCl) des *p*-Phenylendiamins	0.05 M Lsg. (6 N HCl) des Eisen-(III)chlorids	NaR	*a*
I_b	◐	Probelsg.	ungefähr 2 mg vom festen *p*-Phenylen-diamin	0.05 M Lsg. (6 N HCl) des Eisen-(III)chlorids	NaR	*a*
I_d	○	Probelsg.	ungefähr 1 mg vom festen *p*-Phenylen-diamin	0.1 M Lsg. (12 N HCl) des Eisen-(III)chlorids	NaR	*a*
I_e***	△	ungefähr 1 mg vom festen *p*-Phenylen-diamin	0.1 M Lsg. (12 N HCl) des Eisen(III)chlorids	NaR	Probelsg.	*a*
I_f***	▲	Nadelspitzmenge**** vom festen *p*-Phenyl-endiamin	0.1 M Lsg. (12 N HCl) des Eisen(III)chlorids	NaR	Probelsg.	*b*
I_g***	×	Nadelspitzmenge vom festen *p*-Phenyl-endiamin	0.03 M Lsg. (12 N HCl) des Eisen(III)chlorids	NaR	Probelsg.	—
I_h***	□	Nadelspitzmenge vom festen *p*-Phenyl-endiamin	0.1 M Lsg. (12 N HCl) des Eisen(III)chlorids	HR	Probelsg.	*b*
I_i***	■	Nadelspitzmenge vom festen *p*-Amino-dimethylanilin	0.1 M Lsg. (12 N HCl) des Eisen(III)chlorids	HR	Probelsg.	*c*

a: mit sehr merklichem Unterschied
b: mit grösserem Unterschied
c: ohne Unterschied
} der Färbungsintensität zwischen den verschiedenen Vertiefungen der Platte.

** Die hier benutzte Probelösung enthält 3.14 γ Sulfid (78.5 γ/ccm).

*** Etwa 5 Min nach dem Zusatz von NaR oder HR wird die Probelösung vorsichtig beigefügt.

**** Ungefähr 30 γ.

TABELLE II

EINFLÜSSE DER BEGLEITIONEN

Begleitionen	benutzter Verbindungstypus	Menge der Begleitionen	Nachweisbare Sulfidmenge	Grenzverhältnis	Anmerkungen
SO_3^{2-}	Na_2SO_3	Völlig hemmt die Reaktion.		——	Die oben erörterte Trennungsmethode ist gar nicht anwendbar
$S_2O_4^{2-}$	$Na_2S_2O_4$	〃	〃	——	〃 〃 〃
$S_2O_3^{2-}$	$Na_2S_2O_3$	〃	〃	——	〃 〃 〃
F^-*	KF	130 γ	0.16 γ	$1:4.2\times10^2$	Nur wenn die Konzentration des Fluorides weniger ist, ist dieses Verhältnis nutzbar.
$PO_4^{3-}(H_2PO_4^-)$*	H_3PO_4	1.0 mg	1.6 γ	$1:6.5\times10^2$	——
〃*	〃	8.0 mg	0.31 γ	$1:2.6\times10^5$	Nach der Trennung von S^{2-} als H_2S.
NO_3^-	KNO_3	2.1 mg	0.25 γ	$1:8.3\times10^4$	——
Fe^{2+}	Mohrsches Salz	Völlig hemmt die Reaktion.		——	Die obige Trennungsmethode ist wohl anwendbar.
〃	〃 〃	2.3 mg	0.31 γ	$1:7.4\times10^4$	Nach der Trennung von S^{2-} als H_2S.

* Zwei bzw. drei Tropfen der Eisen(III)chloridlösung werden angewendet.

Betrachtet man von diesen Ergebnissen und sorgsamen Beobachtungen der Färbungen aus, wird das folgende Verfahren als ein am besten geeignetes festgestellt:

„Man versetzt auf einer Tüpfelplatte eine Nadelspitzmenge vom festen *p*-Aminodimethylanilin mit einem Tropfen in die 12 N Salzsäure gelöster 0.1 M Lösung des Eisen(III)chlorids, und lässt sie etwa fünf Minuten lang stehen. Man fügt dann dazu einige Körnchen vom starksauren Kationenaustauschharz von HR-Form, rührt sie völlig mit einem kleinen Glasstab um. Nach einigen Minuten, versetzt man mit einem Tropfen der Probelösung, und beobachtet man die Grünfärbung, die die Harzphase nach zwanzig Minuten beinahe vollends liefert."

Hier muss man besonders das entbehrende Überschuss des *p*-Aminodimethylanilins (ebenso wie des *p*-Phenylendiamins) und die niedrige Konzentration der Salzsäure sowie des Eisen(III)-chlorids vermeiden, da diese beide die Reaktionsempfindlichkeit beträchtlich beschädigen.

Wie man aus der obigen Abbildung und dem folgenden Abschnitt ersieht, ist das *p*-Aminodimethylanilin als das Reagens für den Nachweis des Sulfides in mancher Hinsicht, z. B. grösserer Empfindlichkeit und bedeutend grösserer Sicherheit der Reaktionen, dem *p*-Phenylendiamin entschieden überlegen.

Bestimmung der Erfassungsgrenze[13]

Die Resultate der Experimente werden nach gleichem Verfahren mit dem vorhergehendes Abschnitts in Abb. 2 kurz zusammengestellt:

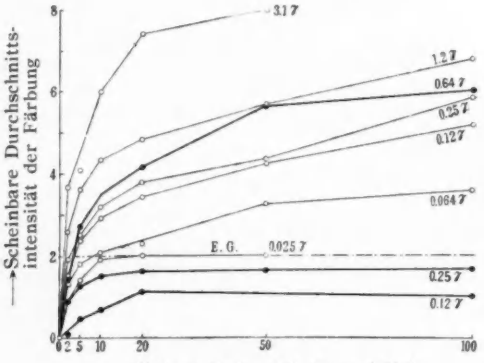

Abb. 2. Bestimmung der Erfassungsgrenze.
—○—: mit p-Aminodimethylanilin,
—●—: mit p-Phenylendiamin.

An diesen Reaktionen für den Nachweis des Sulfides (S^{2-}) wurden die Erfassungsgrenze 0.05 γ unter Grenzkonzentration $1:0.8\times10^5$, wenn man als Reagens *p*-Aminodimethylanilin verwendet, sowie dieselbe 0.3 γ unter Grenzkonzentration $1:1.3\times10^5$, wenn man *p*-Phenylendiamin verwendet, festgestellt.

13) Hinsichtlich der Bedeutung der Erfassungsgrenze, vergleiche Fussnote 2).

Trennung des Sulfides als Schwefelwasserstoff von den Begleitstoffen

Wenn die Probelösung fremde Ionen, die die Reaktion stören, enthält, ist es oft nötig die Sulfide in der Form von Schwefelwasserstoff von diesen Begleitionen zu trennen. Zu diesem Zwecke, stellte der Verfasser einen einfachen Apparat (Abb. 3) auf[14], worin Schwefelwasserstoff, der durch gelindes Erhitzen der Probelösung mit verdünnter (1 bis 4 N) Schwefelsäure über Mikrobrenner[15] sich entwickelt, in 0.01 bis 0.02 ccm von 1 N Natronlauge aufgesogen, und danach in gleicher Weise wie die obige ohne Störung der Begleitstoffe geprüft wird.

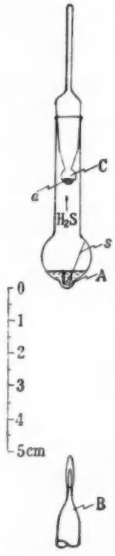

A: Gefäss von der Probelösung und verdünnter Schwefelsäure.
B: Mikrobrenner.
C: Glasknopf mit dem Absorptionsmittel (a), d. h., 0.01 bis 0.02 ccm von 1 N Natronlauge.
s: Mikrosiedestein.

Abb. 3. Apparat zur Trennung und aufsaugung des Schwefelwasserstoffs.

Die kleinste Sulfidmenge, die auf solche Weise deutlich nachgewiesen wird, ist doch 0.3 γ unter Grenzkonzentration $1:1.3\times10^5$, wenn man als Reagens *p*-Aminodimethylanilin verwendet.

Einflüsse der Begleitionen

Die Resultate der mit *p*-Aminodimethylanilin als der Vertreter dieser Art der Reagenzien ausgeführten Versuche werden in Tabelle II (S. 569) kurz gefasst:

Zusammenfassung

1. Durch einfache Anwendung von der farblosen starksauren Kationenaustauschharze wird die Empfindlichkeit der Nach-

14) Vgl. F. Feigl, „Spot Tests. I. Inorganic Applications," übersetzt von R. E. Oesper, 4. engl. Aufl., Amsterdam (1954), S. 46.

15) A. A. Benedetti-Pichler, „Introduction to the Microtechnique of Inorganic Analysis," 1. Aufl., New York (1942), S. 8.

weisreaktion von Sulfide mit *p*-Aminodimethylanilin oder *p*-Phenylendiamin bemerkenswerterweise erhöht, wobei als Reagens *p*-Aminodimethylanilin in vieler Hinsicht weit überlegen ist.

2. Die Bedingungen höchster Empfindlichkeit werden durch genaue Untersuchungen vollkommen festgestellt, und die Einflüsse der Begleitionen werden ausführlich untersucht.

3. Durch schematische Darstellung von der scheinbaren Intensität der Färbung wird eine neue halbquantitative Methode zur Bestimmung der Erfassungsgrenze sowie der Experimentalbedingungen vorgeschlagen und erfolgreich angewendet.

Zum Schluss möchte der Verfasser Herrn Prof. Dr. E. Minami für seine wertvolle Ratschläge über diese Untersuchung seinen herzlichen Dank aussprechen.

Laboratorium der analytischen Chemie, Chemisches Institut der wissenschaftlichen Fakultät, Tokyo Universität, Tokyo

---

Mikroanalyse mit Hilfe von Ionenaustauschharzen. IV. Über den Nachweis geringer Menge des Bromides mit Schiffschem Reagens[1]

Von Masatoshi FUJIMOTO

(Eingegangen am 17. Februar 1956)

Einleitung

Wegen der bedeutend selektiven Austauschbarkeit der Farbstoffionen in die Harzphase sowie der charakteristischen starken Färbung dieser Phase, bietet die mikroanalytische Anwendung der Farbstoffionenbildungsreaktionen zur Tüpfelanalyse mit Ionenaustauschharzen eine sehr geeignte Nachweismethode[1]. Bei gegenwärtigem Versuche, wurde eine violette Färbung[2], die bei Anwesenheit von Brom mit Schiffschem Reagens in der farblosen Kationenaustauschharzphase entsteht, auf den Nachweis geringer Menge des Bromides sowie Broms wohl angewandt.

Die in dieser Untersuchung benutzten Ionenaustauschharze

Dowex 50 W-X8: Ein farbloses aus Styrol und Divinylbenzol dargestelltes starksaures Kationenaustauschharz von Sulfonsäuretypus, das vor Gebrauch durch zweimaliges Durchlaufen der 2 N Salzsäure oder 2 N Lösung von Natriumchlorid und destilliertes Wassers in die HR- oder NaR-Form übergeführt wurde. Die Korngrösse ist 50 bis 100 Maschen von Tylerschem Normalsieb.

Amberlite IR-112: Ein ebenso starksaures Harz wie Dowex 50W-X8 mit kleinerem Divinylbenzolgehalt. Dieses Harz wurde durch gelindes Erwärmen mit verdünnter Natronlauge und ungefähr zehnprozentiger Lösung des Wasserstoffperoxyds fast völlig entfärbt[3]. HR- sowie NaR-Form wurden benutzt. Die Korngrösse ist 20 bis 40 Maschen.

Überdies wurden ein farbloses starkbasisches Anionenaustauschharz, Dowex 1-X2 (Korngrösse: 50 bis 100 Maschen) sowie ein hellgelbes mittelstarkbasisches Harz, Amberlite XE-114 (Korngrösse: ungefähr 30 Maschen) auch gebraucht. Diese beide wurden vorher mit 2 N Salzsäure in die RCl-Form übergeführt.

Versuchsanordnung

Auf einer weissen Tüpfelplatte versetzt man einen Tropfen Schiffsches Reagens mit einigen Kationenaustauschharzkörnchen, rührt danach mit einem kleinen Glasstab um, und lässt sie einige Minuten stehen. Dann wäscht man die Harzkörnchen mit je drei Tropfen destilliertes Wassers zwei- bzw. dreimal aus, und dazu fügt man einen Tropfen der Probelösung, worin die Anwesenheit von freiem Brom erwartet wird. Einige Minuten nach der Mischung, entsteht, je nach der Brommenge in der Probelösung, vom Rande nach innen der Harzkörnchen allmählich eine klare violette Färbung, die man unter Beleuchtung mit einer Tischlampe und durch eine Zwanzigfachvergrösserungslupe wohl nachweisbar ist.

Bestimmung der Bedingungen höchster Empfindlichkeit

1. Massflüssigkeit.—Eine Reihe der Massflüssigkeiten des Broms wurde aus dem Brom-

1) Die dritte Mitteilung: M. Fujimoto, Dieses Bulletin 29, 567 (1956).

2) Von I. Guareschi (*Z. anal. Chem.* 52, 451 (1913)) wurde die Zusammensetzung dieses tief blauvioletten Farbstoffes als $C_{20}H_{17}Br_4N_3O$ bestimmt.

3) Vgl. M. Honda, H. Kakihana und Y. Yoshino „Ionenaustauschharze (Ion-kōkan Jushi)", 1. Aufl. (japanisch), Tokyo (1955), Zweites Kapitel, S. 48.

wasser dargestellt, dessen 1 ccm ungefähr 8 mg von Brom enthielt[4]. Alle folgende Vergleichungen der Experimentalbedingungen wurden mit einer Lösung ausgeführt, die durch genau einhundertfache Verdünnung des obigen Bromwassers mit destilliertem Wasser hergestellt wurde.

2. Schiffsches Reagens (Wässerige Lösung der fuchsinschwefligen Säure).—Nach der sorgsamen Vergleichung verschiedener Darstellungsweisen des Reagens, wurde folgenden Verfahren als das günstigste angewandt:

Man versetzt erstens 1 ccm der 0.2prozentigen Lösung vom Fuchsin („Merck" zur Analyse) mit 0.3 ccm der 6 N Salzsäure, verdünnt sie mit destilliertem Wasser bis zum ungefähr 5 ccm, und fügt man dazu unter Erschüttelung tropfenweise eine 30prozentige wässerige Lösung des Natriumbisulfites bis zur vollkommenen Entfärbung. Die so erhaltene farblose Lösung wird, nach dem Zusatz noch 0.1 ccm von 6 N Salzsäure, mit Wasser bis zum 10 ccm verdünnt, und in einem wohl verstöpselten Gefäss im Dunkeln aufbewahrt.

3. Die Bedingungen höchster Empfindlichkeit.—Die Ergebnisse unter verschiedenen Experimentalbedingungen ausgeführter Versuche stehen in Abb. 1 und Tabelle I. Dabei wurde zum Vergleich die schematische Darstellungsweise der scheinbaren Durchschnittsintensität der Färbung, die in der vorhergehenden Mitteilung[1] genau beschrieben ist, erfolgreich angewandt:

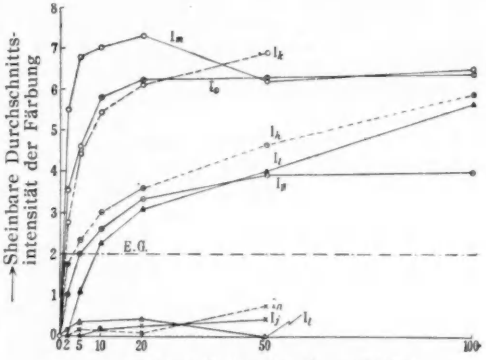

Abb. 1. Vergleichung verschiedener Bedingungen.

TABELLE I

VERSCHIEDENE REAKTIONSBEDINGUNGEN VON ABB. 1

Nr. des Experiments	Zeichen der Kurve	Inhaltsangabe des Verfahrens	Bemerkungen über Verfahren und Resultate*
I_g	—⊖—	Reagens + Dowex 50 W-X8 → (5∼6 Min**) → + Probelsg.*** (HR)	*a*
I_h	--⊖--	Reagens + Amberlite IR-112 W****(HR) → (5∼6 Min) → + Probelsg.	*a, a'*
I_i	—▲—	Reagens + Dowex 1-X2 (RCl) → (5∼6 Min) → + Probelsg.	*a, b*
I_j	—×—	Reagens + Amberlite XE-114 (RCl in 10^{-3} N HCl) → (10 Min) → + Probelsg.	*a*
I_k	--○--	Reagens + Amberlite IR-112 W (HR) → (1 Std) ----→ + Probelsg.	*c*
I_l	--△--	Reagens + Dowex 1-X2 (RCl) → (1 Std) ----→ + Probelsg.	*c*
I_m	—○—	Reagens + Dowex 50 W-X8 (HR) → (1 Std) ----→ + Probelsg.	*c*
I_n	--×--	Reagens + Amberlite XE-114 (RCl in 10^{-3} N HCl) → (1 Std) ----→ + Probelsg.	*c*
I_o	—◐—	Reagens + Dowex 50 W-X8 (HR) → (10 Min) ---→ + Probelsg.	*c*

**a*: Ohne Auswäschung der Harzkörnchen mit Wasser wird die Probelösung direkt hinzugefügt.

a': Von dem Färbungszustand der Harzphase, könnte man vermuten, dass in diesem Falle eine Art des Farbstoffsniederschlages am Rande des Harzkörnchens gebildet wird.

b: Eine violettrote Färbung, die sehr langsam in der Harzphase entsteht.

c: Die Probelösung wird in die Harzkörnchen eingetropft, die mit je drei Tropfen destilliertes Wassers dreimal ausgewaschen werden, um die Störung überschüssiges Bisulfites, das entbehren ist, völlig zu beseitigen, —— und, die dabei sehr hell himmelblau sich färben.

** Zeitdauer von Eintauchen der Harzkörnchen im Reagens.

*** Die hier benutzte Probelösung enthält 3.15 *γ* Brom (78.8 *γ*/ccm).

**** IR-112 W bedeutet „weisse" Amberlite IR-112, die vorher entfärbt wird[3].

4) Die Brommenge der Probelösung wurde jedesmals kurz vor Gebrauch folgenderweise genau bestimmt: Man versetzt ungefähr 1 g vom festen Kaliumjodid mit 2 ccm von 6 N Salzsäure in einem mit Glasstopfen versehenen Erlenmeyerkolben, und verdünnt sie mit ungefähr 30 ccm von destilliertem Wasser. Dann fügt man dazu ein bestimmtes Volumen vom Bromwasser, schüttelt sie um, und titriert das hier gebildete Jod mit einer 0.1 N-Massflüssigkeit des Natriumthiosulfates.

In Betracht dieser Resultate, wurde das Verfahren „I_m" als das am besten geeignete ausgewählt; d.h., „Etwa eine Stunde[5]) nach dem Eintauchen einiger Körnchen des Kationenaustauschharzes, Dowex 50 W-X8, von HR-Form ins Reagens, wäscht man diese mit je drei Tropfen destilliertes Wassers dreimal aus, und fügt dazu einen Tropfen der Probelösung, u.s.w."

Hier ist es vor allem bemerkenswert, dass man durch dieses Verfahren die Hinderung des im Reagens enthaltenen überschüssigen Bisulfites vollständig beseitigen kann.

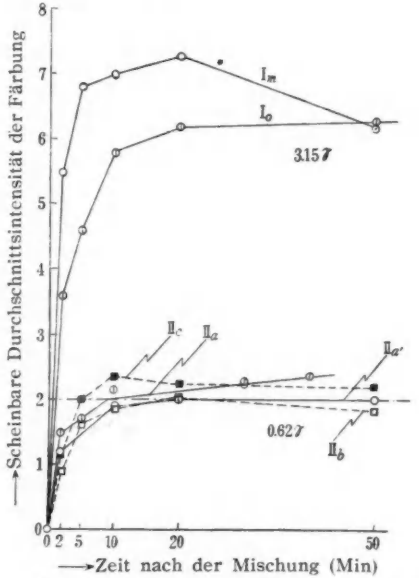

Abb. 2. Bestimmung der Erfassungsgrenze.
Kurve-II_a —◯— Reagens+HR→(10 Min) - - -→(Auswaschen)- - -→+Probelsg.,
Kurve-$II_{a'}$ —○— Reagens+HR- - -→(1 Std) - - -→(Auswaschen)- - -→+Probelsg.,
Kurve-II_b - -□- - Reagens+HR-→(5-6 Min) - - -→(Auswaschen)- - -→+Probelsg., und
Kurve-II_c - -■- - Reagens+NaR-→(5 Min) - - -→(Auswaschen)- - -→+Probelsg..

Bestimmung der Erfassungsgrenze

Vom in Abb. 2 dargestellten Resultate aus betrachtet, wurde die Erfassungsgrenze an dieser Reaktion für Brom als 0.62 γ unter Grenzkonzentration $1:6.4\times10^4$ festgestellt, wobei das Harz von NaR-Form dem von HR-Form ein wenig überlegen ist, und zwar das Eintauchen des Harzes im Reagens nur um etwa fünf Minuten wünschenswerter ist (Vgl. Fussnote 5)).

5) Wie im Falle der Erfassungsgrenzbestimmung, ist es dann noch günstiger, etwa fünf Minuten nach dem Eintauchen ins Reagens die Harzkörnchen mit Wasser auszuwaschen, falls die Bromgehalt der Versuchslösung so gering ist, dass selbst die hellhimmelblaue Färbung der Harzphase die Unterscheidung der hellviolette Färbung des Farbstoffs beträchtlich schwierig macht.

Bestimmung der Erfassungsgrenze für Bromid nach der Oxydation des Bromides zum Brom

1. Massflüssigkeit des Bromides wurde aus der wässerigen Lösung des extrareinen Kaliumbromides, deren 1 ccm 10.24 mg von Bromid (als Br) enthielt[6]), vorbereitet.

2. Entwicklung des Broms und seiner Prüfung.—Um die Bromide durch gegenwärtige Tüpfelmethode nachzuweisen, wurde ein einfacher Apparat (Abb. 3) aufgestellt:

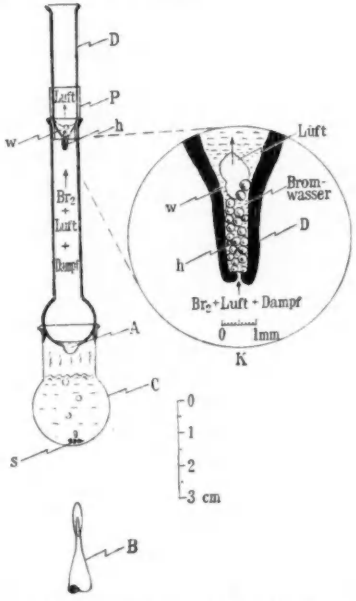

Abb. 3. Apparat zur Entwicklung und Prüfung des Broms.
A: Gefäss zur Oxydation der Probe, B: Mikrobrenner, C: Mikrowasserbad, D: Gefäss zur Aufsaugung und Prüfung des Broms, P: Vinylschlauch, h: das Reagens adsorbierte Kationenaustauschharz, w: destilliertes Wasser, s: Mikrosiedestein (Glassplitter); und K: Vergrössertes Bild des wesentlichen Teils des Apparates.

In einem Mikrokolben (A) werden alle Bromide in der Probelösung in weniger als 20 Sekunden durch Erwärmen mit einigen Tropfen eines Gemisches von 1 Teil gesättigter wässeriger Lösung des Kaliumbichromates und 1 Teil konzentrierter Schwefelsäure zu freiem Brom sehr glatt oxydiert, und hierbei erzeugter Bromdampf wird

6) Die Menge des Bromides wurde mit 0.1 N Massflüssigkeit des Silbernitrates nach Mohrschem Verfahren genau bestimmt.

7) Hierbei ist es empfehlenswert, die Entwicklungsgeschwindigkeit des durch Harzschicht durchgelassenen Dampfs bis auf alle Sekunden eine Blase einzuschränken, da sonst wegen der Temperatursteigerung des in D enthaltenen destillierten Wassers die Harzkörnchen schnell dunkelblau gefärbt werden.

mit Luft und Dampf zusammen durch die Spitze von Gefäss D in die Schicht von den in einigen Tropfen destilliertes Wassers (w) eingetauchten Harzkörnchen (h) eingeleitet[7]. Nach dem Erwärmen muss man das Gefäss D vom Mikrokolben schnell wie möglichst wegnehmen, weil anderfalls wegen Temperaturerniedrigung des Apparates destilliertes Wasser (w) in den Mikrokolben (A) rasch zurück eingezogen wird. Nach etwa 10 Min, beobachtet man die Färbung der Harzkörnchen (h) mit einer Lupe.

Die kleinste Menge auf solche Weise nachweisbares Bromides war jedoch 1.2 γ unter Grenzkonzentration $1:1\times10^5$.

Einflüsse fremder Anionen

Die Resultate der durch Oxydation mit Chromsäuregemisch ausgeführten Untersuchungen werden in Tabelle II kurz gefasst:

TABELLE II

EINFÜLSSE DER BEGLEITIONEN

Begleitionen	benutzter Verbindungstypus	Menge der Begleitionen	Nachweisbare Bromidmenge	Grenzverhältnis
F^-	KF	1.4 mg	4 γ	$1:3.5\times10^2$
Cl^-	KCl	14.2 mg	1.6 γ	$1:8.9\times10^3$
J^-	KJ	102 mg	2.4 γ	$1:4.3\times10^4$
SCN^-	NH_4SCN	2.3 mg	12 γ	$1:1.9\times10^2$
S^{2-}	Na_2S	314 γ	4 γ	$1:7.9\times10$
NO_2^-	$NaNO_2$	266 γ	12 γ	$1:2.2\times10$

Zusammenfassung

1. Durch mikroanalytische Anwendung der mit Schiffschem Reagens aufgesogenen farblosen starksauren Kationenaustauschharze wird eine empfindliche und selektive Nachweismethode für geringe Menge des Broms sowie Bromides festgestellt, wobei durch völliges Auswaschen der Harzkörnchen mit destilliertem Wasser die Reaktionsstörung von entbehrendem Überschusse im Reagens enthaltenes Bisulfites glücklicherweise vollständig beseitigt wird.

2. Zur Oxydation des Bromides zu freiem Brom wird ein einfacher Apparat aufgestellt, damit man alle Bromide in der Probelösung in der Form von Bromwasser beinahe quantitativ ansammeln und auf der Stelle mit der obengenannten Harzkörnchen direkt prüfen kann, und die Einflüsse fremder Anionen werden auch mit Hilfe dieses Apparates ausführlich untersucht.

Zum Schluss möchte der Verfasser Herrn Prof. Dr. E. Minami für seine vielen wertvollen Ratschläge bei dieser Untersuchung seinen herzlichen Dank aussprechen.

Laboratorium der analytischen Chemie,
Chemisches Institut der
wissenschaftlichen Fakultät, Tokyo
Universität, Tokyo

---

*Studies on the Graphitization. I. Changes of Crystallinity, Diamagnetic Susceptibility and Electrical Conductivity in the Process of Graphitization**

By Hideo AKAMATU, Hiroo INOKUCHI, Hiroshi TAKAHASHI and Yoshio MATSUNAGA

(Received February 21, 1956)

Introduction

Graphites are made by heat treatments of carbonaceous materials such as soots or cokes. It is widely known, however, that even under the similar conditions of heat treatment the degree of graphitization varies according to the sort of starting materials. In an extreme case, "non-graphitizable" carbons are known[1]. It is frequently said in the manufacturing process, that soots are less easy to be graphitized than pitch cokes, and among the cokes, petroleum-cokes are more facile than coal-tar-cokes. On the other hand, some questions arise when we intend to define the degree of graphitization. This is due to the fact that the graphitized materials are in multi-crystalline states and their physico-chemical properties can not be determined by their crystallinity alone, but depend upon functions of the system as a whole.

In this paper, the degree of graphitization has been studied from the viewpoints of crystallinity, magnetic susceptibility and

* The principal part of this paper was presented at the 7th annual meeting of the Chemical Society of Japan on April 1954 at Tokyo, excepting the data by X-ray. The photographic measurements were revised by a Geiger counter X-ray spectrometer.

1) R.E. Franklin, *Compt. rend.*, 232, 232 (1951).

electrical conductivity, and comparison will be made among various starting materials concerning their tendency to graphitization.

Materials and Heat Treatments

The following substances were selected as the starting materials of graphitization; they are classified into three groups.

I. Pitch cokes:
- I-1. Petroleum-coke (Great Lake Co. U.S.A.)
- I-2. Coal-tar-coke (Yahata Seitetsu Co. Japan)

II. Carbon blacks:
- II-1. "Thermax" (Thermatomic Carbon Co. U.S.A.)
- II-2. "Kosmos-15A" (United Carbon Co. U.S.A.)
- II-3. "Tokyo Gas" (Tokyo Gas Co. Japan)

III. Simple organic compounds:
- III-1. Violanthrone ($C_{34}H_{16}O_2$)
- III-2. Polyvinyl chloride

All the commercial carbonaceous products (from I-1 to II-3) were heated in vacuum at several temperatures from 1000 to 2000°C in an electric furnace of Arsem type. The duration at a peak temperature was about ten minutes. Violanthrone and polyvinyl chloride were treated preliminarily at 600°C in the ordinary atmosphere and thereafter the carbonaceous substances obtained were heated in the same way as mentioned above. The heat treatments at 2500 and 3000°C were made in an electric furnace of which the principle nearly resembles that of the industrial graphitizing furnace excepting the fact that the dimension was a laboratory scale[2]. The duration at a peak temperature was about five minutes. This procedure was made in Ohmachi manufactory of Showadenko Co., to whom our thanks are due.

X-Ray Measurements

Changes in the inter-layer spacings, $d(002)$, as the function of the heat treatment, were carefully observed. A Geiger counter X-ray spectrometer (Norelco) with copper anticathode was used. The diffraction maxima were estimated by referring to that of lead nitrate. For this purpose, (220), (211), (210) and (200) spacings of lead nitrate were used, the corresponding values of 2θ were 32.211°, 27.849°, 25.390° and 22.670° for CuK_α radiation respectively. These values had been calibrated referring to a standard quartz specimen. It has been known that in the case of low graphitized carbons, the diffraction maxima do not give directly the true inter-layer spacings[3]. Further corrections are necessary for the transformation of recorded diffraction curve into $|F|^2$ curve. This procedure was made by using the correction factors given by Ruston[4]. In the present case, however, these correction factors did not become large even in the specimens treated at lower temperatures, and they were negligibly small for the specimens treated at higher temperatures.

Following Franklin[5], in the graphitic carbons the graphite-like layers are grouped in parallel packets within which there is a random distribution of orientated and disorientated layers. In the orientated layers the inter-layer spacing is constant and equal to that of graphite 3.354 Å; in the disorientated layers the inter-layer spacing is equal to that in the non-graphitic carbons 3.44 Å, and there is a spacing of intermediate value among the first disorientated layers on either side of each orientated group.

By this formula, the apparent inter-layer spacing is in reality a mean value which depends upon the proportion of the number of disorientated layers to the total number of layers. Franklin has proposed an empirical equation which is expressed as

$$d = 3.440 - 0.086(1 - p^2),$$

where d is the mean inter-layer spacing observed and p is the fraction of the randomly disorientated layers. A similar formula has been concluded from a more theoretical point of view by Houska and Warren[6]. The value of p can be interpreted as a measure of the degree of non-graphitization, from the above point of view. The observed values of the inter-layer spacings and the p-values are shown in Table I.

TABLE I

INTER-LAYER SPACINGS AND CORRESPONDING P-VALUES OF GRAPHITIC CARBONS

Starting material	Heat-treatment temperature (°C)	Inter-layer spacing (Å)	p-value	$\frac{I(112)}{I(110)}$
Petroleum-coke	1550	3.413	0.828	0
	2040	3.385	0.600	0.40
	2500	3.365	0.358	0.62
	3000	3.351	0.000	0.73
Coal-tar-coke	1900	3.426	0.915	0.47
	2500	3.361	0.285	0.69
	3000	3.353	0.000	0.75
Thermax	1740	3.433	0.957	
	1960	3.423	0.896	
	2500	3.379	0.535	0.39
	3000	3.376	0.507	0.39
Kosmos	1960	3.428	0.900	0
	2500	3.422	0.890	0.12
	3000	3.422	0.890	0.18
		3.356	0.167	
Violanthrone	1520	3.436	0.976	
	1720	3.423	0.896	
	1960	3.420	0.876	
	2500	3.402	0.749	0.33
	3000	3.389	0.640	0.34
Polyvinyl chloride	1680	3.440	1.000	
	2020	3.428	0.925	0
	2500	3.384	0.586	0.40
	3000	3.371	0.441	0.45

2) S. Yamaguchi, T. Noguchi, S. Hatta and M. Hino, *Carbon*, **2**, 239 (1952).
3) R.E. Franklin, *Acta Cryst.*, **3**, 107 (1950).
4) W.R. Ruston, *Fuel*, **31**, 52 (1952).
5) R.E. Franklin, *Acta Cryst.*, **4**, 253 (1951).
6) C.R. Houska and B.E. Warren, *J. Appl. Phys.*, **25**, 1503 (1954).

The crystallite size determination was made from the broadening of X-ray diffraction. The X-ray spectrometer profiles were used for this purpose. In order to get the broadening β of the line due to the finite size of the crystallites, the experimentally observed width B was corrected for the instrument width b. The instrument width was obtained from the lines of reference quartz powder (10–20 micron), and the correction curve of β/B against b/B for the X-ray spectrometer line breadths was used[7].

The crystallite dimensions were calculated by the formula,

$$L = K\lambda/\beta \cos\theta ,$$

where L is the mean dimension of the crystallite perpendicular to the set of planes giving rise to the line at the glancing angle θ, λ is the wave length of the X-ray and K is a shape factor. K is nearly 0.9 for ordinary three-dimensional lattice, provided β is defined as the half-maximum line breadth, while 1.84 for two-dimensional lattice[8].

The L_c-dimension, the thickness of the parallel packets of layers, was obtained from (002) line using $K=0.9$, while the L_a-dimension, the width of the graphite-like layers was obtained from (hk0) lines. Because the low graphitized carbons have the tarbostratic structure, they give nearly the two-dimensional reflections. In such a case, the L_a-dimension was obtained from (10) line using $K=1.84$. However, when the graphitization proceeded there appears the cross lattice (101) reflection, overlapping with the (100) line on the large angle side of the latter. This makes it difficult to estimate the half-width value of (100). Therefore, for highly graphitized specimens, (110) reflection was used for the determination of the L_a-dimension. Furthermore, there occurs some question concerning the value of the shape factor.

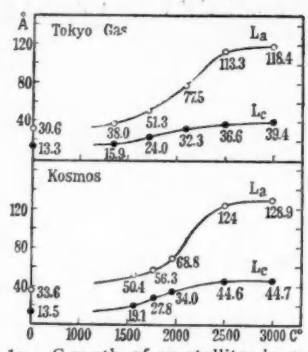

Fig. 1a. Growth of crystallites in graphitized carbon blacks.

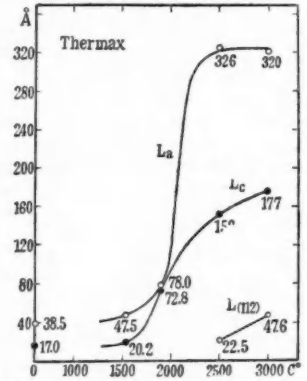

Fig. 1b. Growth of crystallites in graphitized carbon blacks.

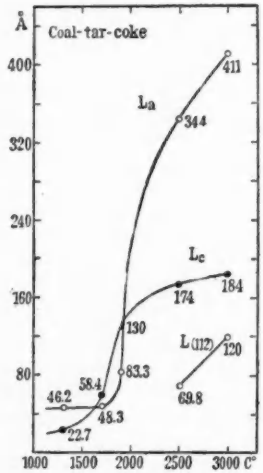

Fig. 2a. Growth of crystallites in graphitized pitch-cokes.

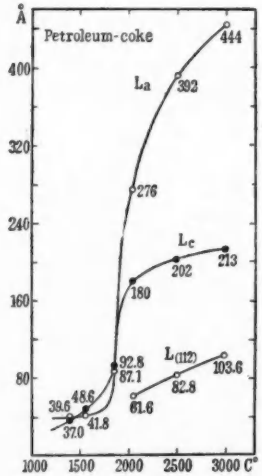

Fig. 2b. Growth of crystallites in graphitized pitch-cockes.

7) H.P. Klug and L.E. Alexander, "X-Ray Diffraction Procedures" (1954), p. 509.

8) B.E. Warren, *Phys. Rev.*, 59, 693 (1941).

When the graphitization has proceeded, and the cross lattice reflection (101) and (112) has appeared, the structure of a crystallite consists of a stack of parallel planes composed of a random mixture of groups of perfectly orientated planes and groups of completely disorientated planes; the former gives the three-dimensional reflection while the latter gives the two-dimensional reflection. In such a case, K must be some average value between 0.9 and 1.84. Concerning the shape factor, we refer the p-value in the preceding section, and used $K=0.9+(1.84-0.9)p$. Another method is obtained by referring the intensity of (112) and (110) reflection. When the graphitization has been completed, the ratio of intensity of (112) to that of (110) is 1.61. Therefore in an intermediate state,

$$K=1.84-(1.84-0.9)\left(\frac{\mathrm{I(112)/I(110)}}{1.61}\right),$$

can be used. The values of I(112)/I(110) are shown in Table I. The observed values of the crystallite dimensions are shown in Fig. 1, Fig. 2 and Fig. 3 as the function of the temperature of heat treatment.

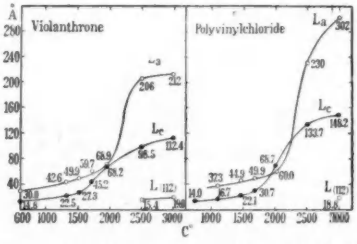

Fig. 3. Growth of crystallites in graphitized violanthrone- and polyvinyl chloride-base carbons.

Magnetic Measurements

The magnetic susceptibility at the room temperature has been measured by the Gouy method. The details of the method have been presented in a preceding paper from our laboratory[9].

To remove ash impurities which might have some effect on the magnetic susceptibility, each specimen was subjected to heating with hydrofluoric acid in a platinum crucible until the latter was evaporated up, then boiled with hydrochloric acid and finally washed with water throughly. Even after the purification, it was found in several specimens that a trace of ferromagnetic impurity still persisted, as a result the apparent susceptibility varied,depending on the magnetic field strength applied. In such a case, the ferromagnetic effect was calibrated by the formula,

$$\chi^*=\chi_\infty+2\sigma/H\,,$$

where χ^* is the apparent susceptibility observed, H is the field strength applied, σ is the saturation intensity of the ferromagnetic impurity, and χ_∞ is the susceptibility proper to the sample itself.

9) H. Akamatu and Y. Matsunaga, This Bulletin, 26, 364 (1953).

When we plot the mass susceptibility against the temperature of heat treatment, we find that the features vary widely according to the sort of starting materials, especially of the groups. However, when we plot them as a function of the L_a-dimension, it is found that all points mount on nearly one curve, irrespectively of the sort of starting materials. This is shown in Fig. 4.

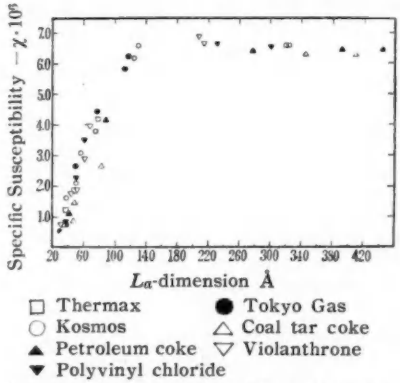

Fig. 4. Magnetic susceptibilites of graphitic carbons.

For comparison with the graphitized carbon, the magnetic susceptibility of natural graphite has been measured. Concerning the latter, there are many reports in the literature of the subject; however, they have given rather various values. The reason is presumably due to some contaminations in the graphite. In the present investigation, the purification procedure was made of two steps, e.g., in the first step specimens were subjected to alkali fusion with potassium hydroxide and carbonate at 300–400°C, and then accompanied by boiling with hydrochloric acid; in the second step the specimens which had been subjected to the above treatment were further treated with hydrofluoric acid and hydrochloric acid consecutively in the same manner as mentioned above.

The results are shown in the fourth column of Table II. The observed values are unexpectedly small; furthermore, the values for flake graphites are rather lower than those of amorphous graphites. This is due to the fact that when a graphite specimen is packed into the sample tube for magnetic measurement, the plate-like crystals take a preferred orientation with planes perpendicular to the axis of the sample tube; as a result, the measured value of susceptibility decreases, since in this direction the susceptibility has the least value. To avoid the orientation effect, the graphite powder diluted with γ-alumina was used. As an example, the mean gram susceptibility of the mixture of Korea flake graphite and alumina as a function of weight per-centage of graphite is shown in Fig. 5. A good linearity is found in the range of the lower concentration. This shows that the orientation effect of graphite crystals was almost cancelled.

The values in the last column in Table II are those which were obtained by using the mixture of graphite and alumina. Comparing those values to that in the preceding column, the difference, consequently the orientation effect, is large in the case of flake graphite, whilst in the case of amorphous graphite the effect is negligible.

TABLE II

GRAM SUSCEPTIBILITY OF NATURAL GRAPHITE

Sample	State of purification*	Ash content (%)	Gram-susceptibility in $-\chi \cdot 10^6$. From graphite alone	From mixture with alumina
Korea (flake)	Raw material	1.72		
	I-Step	0.02	5.07	6.22
	II-Step	0.07	5.38	
Korea (amorph.)	Raw material	5.47		
	I-Step	0.30	5.90	
	II-Step	0.28	5.95	6.12
	Without alkali fusion	0.36	5.77	
Ceylon (flake)	Raw material	0.74		
	I-Step	0.05	5.14	6.10
	II-Step	0.01	5.51	6.34
	Heated up to 3000°C			6.08
Madagascar (flake)	Raw material	19.85		
	I-Step	0.18	4.97	6.54
	II-Step	0.08		6.69
Mexico (amorph.)	Raw material	5.85		
	I-Step	0.14	5.57	
	II-Step	0.14	5.64	5.65

* Raw materials are commercial products which have been purified in the commercial sense.

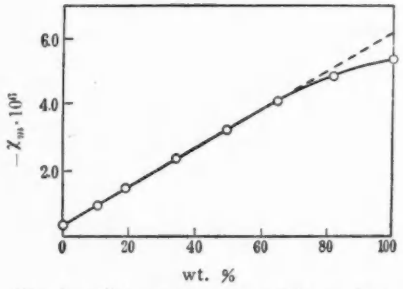

Fig. 5. The gram susceptibility of the mixture of graphite (Korea, flake) and alumina, against weight percentage of graphite.

It is seen in Table II that further purification makes increase of the diamagnetic susceptibility in every case; however, the difference is rather small. From this and the smallness of ash content, the observed value is presumably near the limiting value of the susceptibility of each specimen. In conclusion, the susceptibility of natural graphite can be assumed -6.4×10^{-6} in its good crystal form, and this agrees with the limiting values of the graphitized carbons.

Electrical Resistivity Measurements

The electrical resistivity at the room temperature has been measured by the usual potential drop method. Since the specimens are in powder form, the measurements were made under compressed states up to 200 kg/cm² in a bakelite cylinder. A nearly linear relationship was obtained between the resistivity and the reciprocal of the pressure, from which, by extrapolation, the value at the infinite compression was read as the resistivity of each specimen. The observed values are shown in Fig. 6 as the function of the L_a-dimension.

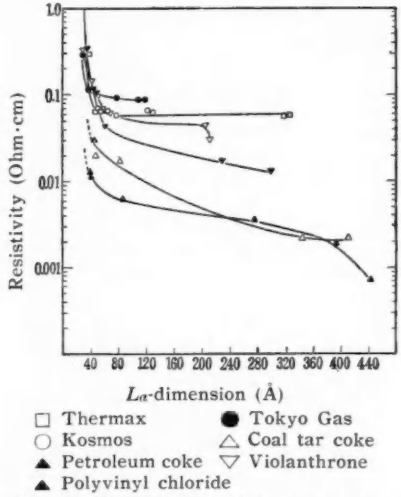

Fig. 6. Electrical resistivities of graphitic carbons.

Discussion

From the results of X-ray measurements, it has been found that the development of crystallinity by heat-treatment varies remarkably among the groups of the starting materials. This is seen from the growth of crystallites as well as the change of the inter-layer spacing or p-value.

The growth of crystallites proceeds with the most facility in pitch-cokes, and so far as this point is concerned, a large difference can not be found between petroleum-coke and coal-tar-coke. In both specimens, p-values tend to zero when they have been treated at 3000°C. This means that in this state disorientated layers have been almost entirely transformed to orientated layers. However, the intensity ratio I(112)/I(110) was yet 0.75; therefore, the perfect graphite lattice has not been completed.

In the case of carbon blacks, the growth of crystallites is slow and limited. This is due to the fact that carbon black is made

of individual particles and in each particle the growth of crystallites is limited by its particle size. The final diameters of crystallites are 118 Å, 129 Å and 320 Å in "Tokyo Gas", "Kosmos" and "Thermax" respectively, while their particle sizes estimated by electron microscopy are 400 Å, 400–500 Å and 2000-4000 Å respectively. Furthermore, the crystallinity is low; hence, the p-values were still large even in the state which was subjected to the heat-treatment at 3000°C. This might be partly due to the fact that for promoting the transformation of disorientated layers to orientated layers, the growth of crystallites in advance to a certain large size is needed. But even in the case of "Thermax" which has a pretty large dimension, the p-value is still large compared with pitch-cokes.

In the case of "Kosmos" treated at 3000°C, it was found that the (002) diffraction maximum was divided into two peaks. This is shown in Table I. It might be assumed that this carbon is made of two parts in itself in a heterogeneous manner; one is completely graphitizable and the other is less graphitizable and the graphitization proceeded suddenly in the former at this temperature.

Violanthrone is a typical polycyclic aromatic compound and polyvinyl chloride is made of linear chain molecules. No remarkable difference could be found between those materials in the general feature of graphitization. However, in the violanthrone-base carbon the growth of crystallites seems to have been attained to a saturation value already at 2500°C, while in the polyvinyl chloride-base carbon the growth is proceeding even after the heat-treatment at 3000°C. So far as this point is concerned, the former is rather like carbon black and the latter is like pitch-coke. In the case of violanthrone, all molecules themselves are stable and might become as nuclei for the aromatic condensation, and so many graphite-like layers would arise from the outset, but the development of them by the expense of nonorganized carbons, which are less in number in this case, would be rather obstructed. In order to develop each crystallite to a large one, it is desirable that there occur a small number of nuclei and a large number of nonorganized carbon atoms. This is presumably the case of polyvinyl chloride and pitch-cokes.

Since graphite is a substance having a large value of diamagnetic susceptibility, it is of interest to see how it changes the magnetic property during the process of the graphitization. The diamagnetic susceptibility increases with the size of crystallites, and this is most impressive when we plot the gram susceptibilities against the L_a-dimensions as shown in Fig. 4.

It is a noteworthy fact that all the values obtained lie on a curve irrespective of the sort of starting materials. This result agrees with the conclusion of Pinnick[10] who studied two types of carbons, while it disagrees with the result of Wynne-Jones, Blayden and Iley[11], whose curves for three types of carbons do not overlap but are shifted somewhat relative to one another along the horizontal axis. On the other hand, when we plot the gram susceptibilities against the L_c-dimensions we obtain the various curves, which do not overlap with each other, according to the sort of materials. Consequently, the present result shows that the gram susceptibility is principally determined by the value of L_a alone, and does not depend upon any other second-ordered structures in polycrystalline states. This is rather a natural conclusion when we remember the origin of the magnetism.

This result is useful to understand that the crystallite sizes obtained by the X-ray method are self-consistent with each other. The crystallite sizes estimated by the X-ray method are not necessarily in agreement with each other among the investigators. This is perhaps due to the difference in the method of calibration, apparatus and other factors. The characteristic feature of the curve of the magnetic susceptibility will be useful to make the adjustment for the differences in crystallite sizes among the investigators. Thus, in our result the rapid increment of the susceptibility begins at 30 Å and attains to the saturation value at about 130 Å, whilst in the work of Pinnick the corresponding range is 50—150 Å. Therefore, our crystallite sizes are shifted to somewhat lower values than that of Pinnick.

In a previous work[9], we have studied the diamagnetic susceptibility of polycyclic aromatic hydrocarbons. The large values of the diamagnetism of those compounds are due to the anisotropic components which are due to the closed-shell diamagnetism of the London type. This diamagnetic anisotropy increases with increasing the number of benzene rings. However, their magnetic properties are rather structure-sensitive, and even the paramagnetic contributions are found[12]. In such a case, the diamagnetic susceptibility becomes smaller than the ex-

10) H.T. Pinnick, *Phys. Rev.*, **94**, 319 (1954).
11) W.F.K. Wynne-Jones, H.E. Blayden and R. Iley. *Brennstoff-Chem.*, **33**, 268 (1952).
12) Y. Yokozawa and I. Tatsuzaki, *J. Chem. Phys.*, **22**, 2087 (1954).

pected value. Thus, $n\Delta K_b$ gives the upper limit of the molar anisotropy, where n is the number of aromatic rings and ΔK_b is the diamagnetic anisotropy of benzene (-54×10^{-6}). However, as pointed out by Mrozowski[13], the large values of graphitized carbons can not be explained by this London-type diamagnetism alone, because the susceptibility converges to -1.0×10^{-6}, when the molecule becomes a large one, and when it is expressed in the mass susceptibility per gram*.

Marchand[14] has observed the temperature dependence of the magnetism of graphitized carbons in the range of $-200-1000$°C. He found that the gram susceptibility χ, is nearly constant when the L_a-dimension is small such as 36 Å, but it becomes dependent upon the temperature when L_a becomes larger than 45 Å and when χ at the room temperature becomes above -2×10^{-6}. The susceptibility increases with decreasing the temperature and tends asymptotically to a limiting value, which is characteristic for each carbon and becomes larger with the increment in L_a. The whole behaviour is similar to that of graphite which was found by Ganguli and Krishnan[15] and interpreted as Landau diamagnetism due to the two-dimensional free electron gas having a low degeneracy temperature. The result of Marchand may be understood when we suppose the degeneracy temperatures of carbons are higher than that of graphite.

Our result, Fig. 4, corresponds to the points on Marchand's curves at the room temperature. They are in good agreement with each other. In conclusion, the large values of diamagnetic susceptibility of graphitized carbons are due to the anisotropic components, which are partly contributed from the closed-shell diamagnetism of London-type and mainly from the free electron gas diamagnetism of Landau-type. The former is related to the ground states and the latter is due to the exited states of electrons. However, a question is left how in the relatively small range of 30—130 Å of L_a the Landau diamagnetism rapidly takes place. It is of interest, at least, to see the rapid change in electronic states of graphitized carbons in this range of L_a.

However, the values of the gram susceptibility itself can not be used for the reference of the graphitization degree, as they converge so rapidly to a saturation value of graphite.

Whilst the magnetic property is determined solely by the size of the molecular plane regardless of the sort of carbon, the apparent electrical resistivity remarkably depends on the starting materials. This can be see in Fig. 6.

The general feature of the electrical resistivity of carbon at room temperature as a function of the heat-treatment has been well illustrated and discussed by Mrozowski[13]. The resistivity decreases very rapidly with increasing the temperature of heat-treatment up to about 1000°C, but above this temperature the decreasing stops and a flat plateau is generally observed. So in the present investigation, the resistivity decreases rapidly with increasing L_a in the region where L_a is small, but it comes to have a nearly constant value when L_a becomes above 40 Å. It is noteworthy that the plateau is formed at the L_a-demension where the Landau diamagnetism begins to take place. The values of resistivity at the plateau vary among the sorts of carbons. The graphitized pitch-cokes have less resistivity than the graphitized carbon blacks, and violanthrone- and polyvinyl chloride-base carbons have intermediate values. In the case of carbon blacks, each plateau is a completely flat one, while in the case of pitch cokes the resistivity gradually decreases as increase in L_a even in the range of the plateau formation. Concerning this behaviour, the polyvinyl chloride-base carbon is like pitch coke, and the violanthrone-base carbon is rather like carbon black again, as mentioned in the above discussion on the X-ray analysis. So far as the crystallite dimension is concerned, the graphitized "Thermax" at 3000°C is not different from the graphitized pitch-coke "Yahata" at 2500°C concerning both L_a and L_c, and the resitivity of the former is still twenty-five times as high as the latter.

All of those facts suggest that not only the crystallites dimension but also the higher-ordered structures of multi-crystalline states are reflected on the resistivity. Carbon black is made of particles, furthermore, in each particle the crystallite micelles aggregate in such a manner that they are independent of each other. On the other hand, pitch cokes are made of a continuous massive material in which the crystallite micelles are bridged with cross-linkages, such as C-C valence bonds, to neighbors. The difference in the mode of the aggregation between those two

13) S. Mrozowski, *Phys. Rev.*, 85, 609 (1952).

* When a molecule becomes large, the increment in number of carbon atoms is two per ring, and the limiting value of gram susceptibility is
$-x\cdot10^6=n(2\times3.36+\Delta K_b/3)+n(2\times12)=1.0$ (cf. (9)).

14) M.A. Marchand, *Compt. rend.*, 238, 1645; 239, 1609 (1954).

15) N. Ganguli and K.S. Krishnan, *Proc. Roy. Soc.*, A 177, 168 (1941).

groups has been well illustrated in the rate of wet oxidation of them[16]. This difference will persist or even be exaggerated in the graphitized state. In consequence, conserning the resistivity, the contact resistance or boundary scattering will be high in the case of carbon black, but it will be less in the case of pitch coke because of the transparent linkages between crystallites.

To explain the formation of the plateau, Mrozowski has assumed that the expected decrease of the resistivity due to growth of crystallites is compensated by a decrease in concentration of excess electrons or holes, which are responsible for the rapid decrease in the resistivity before the formation of a plateau, and the presence of which is due to the peripheral atoms which happen not to be bonded to neighbouring crystallites. This explanation may be applicable to the case of pitch cokes, in which the recombination among atoms at the peripheries of plane molecules will continue as long as the linkages remain, and the chance of occurrence of excess electrons or holes will persist. The decrease in the resistivity in a gradual manner in the region of a plateau may be understandable. But, such a flat plateau as observed in the graphitized carbon black is rather incomprehensible.

It has been found from the small angle scattering of X-ray that the fine structures are different between the graphitized carbon blacks and pitch cokes. In the graphitized carbon blacks, microporous parts arose and developed following graphitization. We are inclined to suppose that the expected decrease of the resistivity due to growth of crystallites is compensated by decrease in the number of contact points between crystallites due to the development of microporous parts. Further studies on the fine structures will be presented in the second part of this work.

16) H. Akamatu, H. Takahashi and K. Tamaru, This Bulletin, 21, 27 (1951).

Summary

Three sorts of carbon black, two sorts of pitch coke, violanthrone, and polyvinyl chloride have been subjected to heat treatment up to 3000°C. Changes in crystallinity during the graphitization have been studied by X-ray referring to inter-layer spacings and growth of crystallites. It was found that pitch cokes are graphitized with more facility than carbon blacks, and the other two substances are intermediate.

The magnetic susceptibility is determined solely by the size of plane molecules (L_a) irrespective of the sort of carbons, and tends to a limiting value -6.5×10^{-6} per gram which is coincident with the value of natural graphite, when L_a grows above 130 Å.

The electrical resistivity decreases as growth of crystallites, but there is a region when L_a becomes above 40 Å, where it tends to a nearly constant value for each carbon. Those values are different among the groups of carbons, and graphitized pitch cokes have less resistivity than graphitized carbon blacks. It was discussed that fine structures of multi-crystalline states are reflected on the resistivity.

This work is a part of the research project for carbon supported by the 117 committee in Nippon Gakujutsu Shinkokai, and the expense has been defrayed in part from a grant given by the Ministry of Education, for which the authors' thanks are due.

Department of Chemistry, Faculty of Science, The University of Tokyo
Hongo, Tokyo

Magnetochemical Study of Dianthraquinone and its Thermochromism in the Solid State

By Yoshio MATSUNAGA

(Received February 23, 1956)

Introduction

Harnik and Schmidt[1] analysed the crystal structure of dianthraquinone, and established the fact that steric limitations prevent the molecule from being planar, and the distortions within the molecule are distributed over several bonds. In the first place, with the intention of ascertaining the effect of non-coplanarity of aromatic net plane on the delocalization of π-electrons, we examined the diamagnetic susceptibility of dianthraquinone and compared it with those of some related compounds.

The reversible color change on heating (thermochromism) of a solution of dianthraquinone has been of great interest, since Meyer[2] synthesized this compound about fifty years ago. He also reported that this compound turns from lemon yellow to green, if it is heated to about 170°C in the solid state. But in this case, recrystallization or boiling with alcohol was necessary to the perfect recovery of the original color. Grubb and Kistiakowsky[3], and Theilacker and his associates[4] performed spectroscopic investigations, and concluded that the thermochromism in solution is due to the transition between isomeric forms which are in a thermal equilibrium with each other. The same absorption spectrum was also found by Hirshberg and Fischer[5], when a solution was irradiated with ultraviolet light at low temperatures. As to the nature of the colored form, Schönberg proposed a betaine-like structure[6] and in the later paper an increase of planarity of the molecule[7], while many other investigators[3,4,8,9] suggested a biradical or long-life triplet state. Only magnetic measurements will make it possible to decide whether or not the colored excited form represents a biradical. But two reports which have already appeared are unfortunately in disagreement with each other. Nielsen and Fraenkel[9] reported that paramagnetic resonance absorption can be detected in the green colored solution and solid specimen heated above 265°C; nevertheless Theilacker[10] could not find the anticipated decrease of diamagnetism by the direct susceptibility measurements. Thus, the thermochromic phenomenon in solution has been studied by many investigators, but we have few knowledge of it in the solid state. Considerable differences are found even in the temperature at which color change occurs; the values recorded include 170°C[2], 240°C[11], and 265°C[9]. To throw further light on the thermochromism in the solid state, we examined the changes of some properties accompanying the color change on heating of crystalline powder of this compound.

Experimental

Materials.—Anthracene and dianthryl were provided by Mr. T. Handa. They were sublimed in vacuo before being used for measurements. Anthrone was prepared by reduction of commercial anthraquinone with hydrochloric acid and tin, and recrystallized from the mixture of benzene and ligroin[12]. It was oxidized again to anthraquinone with chromic acid, and a repeatedly sublimed specimen was used for the magnetic measurement. Dianthrone (or dianthronyl) was prepared by oxidation of anthrone with ferric chloride in glacial acetic acid[13], and recrystallized from Solvesso-100 which was obtained from Standard Vacuum Oil Co.. It was isomerized to dianthranol by boiling with alcohol containing potassium hydroxide, and repeatedly recrystallized from ethanol, and its pyridine compound was obtained by the recrystallization of dianthrone from pyridine as described by Schönberg and Ismail[14]. Dianthrone was dissolved in pyridine

1) E. Harnik and G.M.J. Schmidt, *J. Chem. Soc.*, **1954**, 3295.
2) H. Meyer, *Monatsh. Chem.*, **30**, 165 (1909).
3) W.T. Grubb and G.B. Kistiakowsky, *J. Am. Chem. Soc.*, **72**, 419 (1950).
4) W. Theilacker, G. Kortüm and G. Friedheim, *Ber.*, **83**, 508 (1950).
5) Y. Hirshberg and E. Fischer, *J. Chem. Soc.*, **1953**, 629.
6) A. Schönberg, A. Ismail and W. Asker, ibid., **1946**, 442.
7) A. Schönberg, A. Mustafa and W. Asker, *J. Am. Chem. Soc.*, **76**, 4134 (1954).
8) S.L. Matlow, *J. Chem. Phys.*, **23**, 152 (1955).
9) W.G. Nielsen and G.K. Fraenkel, ibid., **21**, 1619 (1953).
10) W. Theilacker, G. Kortüm and H. Elliehausen, *Z. Naturforsch.*, **9**, 167 (1954).
11) R. Padova, *Ann. chim. phys.*, (8) **19**, 408 (1910).
12) "Organic Syntheses", Coll. Vol., **1** (1948) p. 60.
13) O. Dimroth, *Ber.*, **34**, 219 (1901).
14) A. Schönberg and A. Ismail, *J. Chem. Soc.*, **1944**, 307.

and oxidized with bromine to dianthraquinone[15]; it was recrystallized three times from Solvesso-100.

Heat Treatment.—About 1 g. of dianthraquinone which was put in a test tube with a thermometer inserted in it was placed in vacuo and heated by an electric furnace. The temperature of the specimen was measured from time to time, and controlled to ±3°C by means of regulating the applied voltage to the furnace. After the heat treatment, the specimen was cooled down in vacuo as quickly as possible.

Magnetic Measurement.—The susceptibility was measured using a Gouy balance as previously described[16].

X-Ray Measurement.—It was made on a North American Philips recording X-ray diffractometer, using filtered copper radiation.

TABLE I

DIAMAGNETIC SUSCEPTIBILITIES OF DIANTHRAQUINONE AND ITS RELATED COMPOUNDS

Substance	Formula	Suscept. ($-\chi$)	Molar Suscept. ($-\chi_M$) obs.	calcd.	lit.
Anthracene	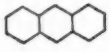	0.731	130	—	129.4[17], 134.2[18]
Dianthryl		0.707	250	254	—
Anthrone	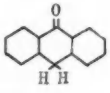	0.609	118	—	125.6[20]
Dianthrone	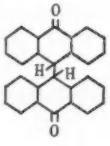	0.592	229	230	—
Anthraquinone	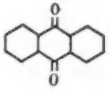	0.548	114	—	119.6[19], 113[20] 116.9[21]
Dianthraquinone	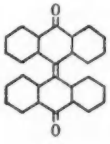	0.573	220	226	218[20]
Dianthranol	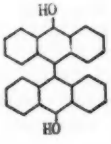	0.679	262	266	—
Dianthranol+2 pyridine	——	0.664	361	363	(pyridine 48.4[22])

15) E. B. Barnett and M. A. Matthews, ibid., **123**, 380 (1923).
16) H. Akamatu and Y. Matsunaga, This Bulletin, **26**, 364 (1953).
17) P. Pascal, *Bull. soc. chim. France*, **9**, 79 (1911).
18) A. Pacault, ibid., **1949**, D 40.
19) P. Pascal, ibid., **9**, 177 (1911).
20) E. D. Bergmann et al., *J. chim. phys.*, **49**, 474 (1952).
21) S. Banerjee, *Z. Krist.*, **A 100**, 316 (1939).
22) C. M. French, *Trans. Faraday Soc.*, **47**, 1056 (1951).

Results

The diamagnetic susceptibilities of dianthraquinone and the other compounds under consideration are given in Table I[23]. The molar susceptibilities of dianthryl, dianthrone, dianthranol and dianthraquinone have been estimated from measurements on anthracene, anthrone, and anthraquinone respectively with the aid of the Pascal's constants[24], and they also are given in Table I. In these cases, the observed values of molar susceptibility are less diamagnetic than the calculated values except dianthrone the value of which is in agreememt with the calculated one within accuracy of measurements.

The susceptibilities of dianthraquinone heated at various temperatures are given in Table II with the condition of treatment, its color, and the type of X-ray diagram. The sublimed specimen is pale green, but it possesses the identical susceptibility with the original one, and we can not find any difference in the X-ray diagram. On heating to 220°C, its color changes to deep green, susceptibility falls off to some extent, and X-ray diffraction patterns lose sharpness. (Fig. 1, curve B) On further heating to 240°C or above it, diamagnetism decreases still more, and diffraction patterns vanish almost completely (Fig. 1, Curve C). The assignment of indices in Fig. 1, curve A based on the crystallographic constants given by Harnik and Schmidt.

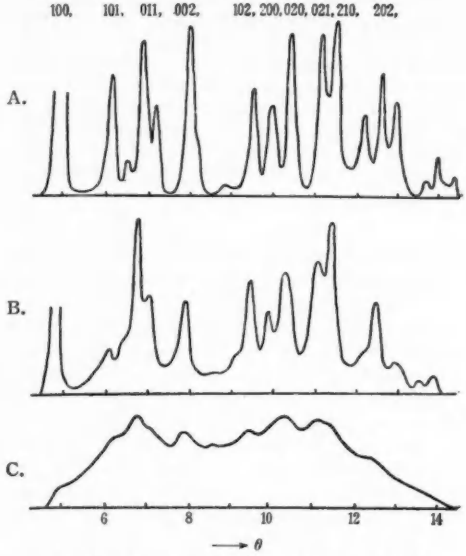

Fig. 1. Change of X-ray diagram of dianthraquinone on heating.
A. Recrystd. B. Heated to 220°C.
C. Heated to 244°C.

TABLE II

CHANGES OF SOME PROPERTIES OF DIANTHRAQUINONE ON HEATING

Conditions	Color	Suscept. ($-\chi$)	X-Ray diagram
recrystd.	yellow	0.573	cryst. (Fig. 1, Curve A)
sublimed (ca. 220°C)	pale green	0.572	cryst.
194°C, 60 min.	yellow	0.570	cryst.
220°C, 60 min.	green	0.538	cryst.+amorph. (Fig. 1, Curve B)
244°C, 60 min.	dark green	0.478	amorph. (Fig. 1, Curve C)
255°C, 80 min.	dark green	0.472	amorph.
266°C, 60 min.	dark green	0.467	amorph.
282°C, 40 min.	dark green	0.446	amorph.
297°C, 60 min.	dark green	0.418	amorph.

Discussion

Diamagnetism of Dianthraquinone.—Aromatic compounds, especially those containing large numbers of rings conjugated or condensed with each other, show the diamagnetic anisotropies which depend strikingly upon the molecular shape[25]. For such cases, it is difficult to estimate the molar susceptibilities by the direct application of the Pascal's additivity law, and we need many constitutive correction constants which are characteristic for each type of condensation of nuclei[25]. In the previous paper[27], we suggested as a compromise to assume that the molar susceptibility of an

23) Susceptibility values have been multiplied by 10^6 throughout this paper.

24) Atomic constants, −2.93 for hydrogen, −4.61 for oxygen in hydroxyl group, and +1.73 for oxygen in carbonyl group. Constitutional correction constants, +5.5 for carbon-carbon double bond and −1.29 for tertiary carbon atom in the position α to hydroxyl group.

25) Ref. (16) and references cited there.

26) A. Pacault, *Ann. chim.*, (12) **1**, 527 (1946). *Rev. sci.*, **86**, 38 (1948).

27) Y. Matsunaga, This Bulletin, **29**, 308 (1956).

aromatic compound containing conjugated rings is equal to the sum of those observed for the constitutional fragments of the molecule, and showed that this procedure gives nearly correct values for hydroxyazobenzenes. But in a few cases, the calculated values were also in serious disagreement with the experimental ones, because the effect of conjugation between the fragments of the molecule on the molar susceptibility was left out of consideration. Therefore, our calculated values in Table I by the above-mentioned procedure are nothing but the values for the imaginary cases in which the conjugations between the conjugated nuclei are absent. Then the effect of conjugation will be considered qualitatively with the aid of theoretical results given by London's method. If the theory predicts that conjugation brings about a reduction of diamagnetic anisotropy, our calculated molar susceptibilities will be the upper limits, and if the reverse effect is predicted, they will be the lower limits. McWeeny[28] established the theory that addition of rings, joined to the original system by single links, gives an increase in anisotropy less than that which will be expected in the absence of any conjugation across the bonds, so that dianthryl and dianthranol must belong to the former case. The steric hindrance completely prevents the conjugation between two anthracene nuclei, or their susceptibilities will be less than the calculated values. The observed decrease of diamagnetism suggests the imcomplete prevention of conjugation, although the planar structures of molecules as a whole are not plausible in both cases. As to dianthrone, a new conjugation does not occur by the joining of two anthrones; consequently the agreement between the observed and the calculated susceptibilities is quite natural.

For anthraquinone and dianthraquinone themselves, theoretical investigations have not yet been performed, and it seems that they would be fruitless[29]. For their isoelectronic hydrocarbons, i.e. 9. 10-anthraquinodimethane and dianthraquinodimethane, theoretical values of anisotropies were already presented by Pullman and his associates. Their results are as follows.

anthraquinodimethane, 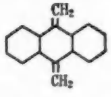 $1.941\ \Delta K_{benzene}$[30]

dianthraquinodimethane, 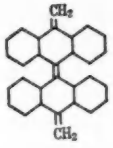 $4.033\ \Delta K_{benzene}$[30]

By analogy, it is plausible to assume that the calculated molar susceptibility for dianthraquinone is the lower limit, as the increase of anisotropy by the conjugation between two nuclei is expected in the reference compound. Theoretically, a similar relation was also predicted for *p*-benzoquinodimethane and *p*-diphenoquinodimethane[30], so that the compound containing two or more ring systems, joined to each other by double bonds, probably gives an anisotropy more than the sum of those of the original systems. Therefore the disagreement between the observed and the calculated susceptibilities for dianthraquinone must be attributed to the other cause. According to the model given by Harnik and Schmidt (Fig. 2), the length of the central ethylene linkage is 1.31 Å., owing to the angle of 40° between the planes of this double bond and the benzene rings, and the absence of the conjugation between the central double bond and four phenyl groups. In such a case, the π-electron system in dianthraquinone may be divided into three parts, namely an isolated central ethylene linkage and two identical conjugated systems. If we substitute the conjugated system of anthrone for each of the latter two, the molar susceptibility—219 will be expected from this model. The magnitude of susceptibility is consistent with the model presented by X-ray analysis. If we assume that the carbonyl groups are also completely localized, owing to the distortions distributed over the conjugated systems, further smaller value for molar susceptibility—212 will be expected. Therefore, it may be concluded that deviations of several degrees from planarity scarcely affect the delocalization of π-electrons.

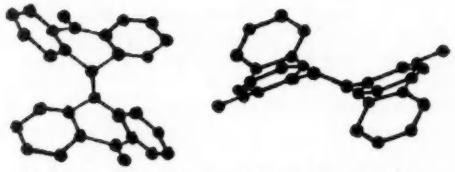

Fig. 2. Perspective view of molecular model (after Harnik and Schmidt).

Thermochromism of Dianthraquinone.—Our results show that the color change from

28) R. McWeeny, *Proc. Phys. Soc.* A 66, 714 (1953).
29) M.G. Evans, J. de Heer and J. Gergely, ibid., A62, 505 (1949).
30) G. Berthier, M. Mayot and B. Pullman, *J. phys. radium*, 12, 717 (1951).

yellow to dark green is accompanied by the decrease of diamagnetic susceptibility and the complete vanishing of sharp diffraction patterns in the X-ray diagram. This structural change does not occur suddenly at a definite temperature, but takes place gradually at an elevated temperature. The color of a specimen heated to 220°C for one hour was green; however, its change was imcomplete judging from its susceptibility and its X-ray diagram. At 240°C, the change finished within one hour. Hence, the temperature at which we can find the apparent color change must depend on the speed of elevating its temperature. The higher values recorded by Padova[1], and Nielsen and Fraenkel[2] will be due to the rapid heating of the specimen. On the other hand, Meyer's observations[2] cannot be interpreted in the same manner, since we could not succeed in recovering its color by boiling with alcohol, and their recrystallization was practically impossible, as our green specimen was scarcely dissolved in the solvent. We cannot but conclude that Meyer's green specimen is not quite the same as the other authors' including also our own. It is supposed that Meyer said green for the specimen slightly colored, so that the structural change barely occurred in his specimen. This suggestion is supported by his description; namely, he stated that the solution of dianthraquinone turns on heating to deep green and then to blackish green, but for the color of the heated solid specimen, he wrote only green.

Kortüm and his associates[31] discovered that when the deep red sulfuric acid solution of dianthraquinone is added to cold water, dianthraquinone precipitates as a dark green mass for a short period of time, and changes spontaneously to the original yellow form. The solution of the green specimen in concentrated sulfuric acid was also deep red, and we obtained a dark green precipitate similarly, when the solution was poured into water. But in this case, the precipitate did not show such a characteristic color change, and darkened somewhat on standing. For these reasons, the net change occurring in the so-called thermochromism of solid dianthraquinone from yellow to dark green may be concluded as an irreversible chemical reaction, although in its process, the same green form with that which appeared in the reversible thermochromism of solution may be supposed to be an intermediate. The large decrease of diamagnetism accompanying the color change suggests the occurrence of a paramagnetic state, and this expectation is consistent with the result given by Nielsen and Fraenkel, but we cannot discuss further its nature from our measurements.

31) G. Kortüm, W. Theilacker, H. Zeininger and H. Elliehausen, *Ber.*, **86**, 294 (1953).

Summary

The magnetic susceptibilities of dianthraquinone and its seven related compounds were measured by the Gouy method. The effect of conjugation between the constitutional fragments of the molecule was discussed with the aid of theoretical values of diamagnetic anisotropies. The depression of molar susceptibility of dianthraquinone was attributed to the localization of π-electrons in the central ethylene linkage, owing to the large distortion of the molecule. The remarkable decrease of susceptibility and the complete vanishing of sharp diffraction patterns in X-ray diagram accompanying the color change on heating of dianthraquinone were shown. The author concluded that the net change occurring in the so-called thermochromism of solid dianthraquinone is an irreversible chemical reaction.

The author wishes to express his hearty thanks to Prof. H. Akamatu for his kind direction, to Dr. M. Kobayashi for a sample of dianthraquinone used in the beginning of this study, and to Mr. T. Handa for samples of anthracene and dianthryl. The cost of this study has been defrayed from the Grant in Aid for Fundamental Scientific Research from the Ministry of Education, to which the author's thanks are also due.

Department of Chemistry, Faculty of Science, The University of Tokyo
Hongo, Tokyo

Study on Zinc Oxide-Chromium Oxide Catalyst. II. Variation of Catalytic Activity for Methanol Decomposition with Addition of Chromia and Structural Dependence of Activity

By Hiroshi UCHIDA and Yoshisada OGINO

(Received February 28, 1956)

Introduction

Zinc oxide-chromium oxide, used as a catalyst for the methanol synthesis, has been the object of intense studies made by a number of investigators since about thirty years ago. Nevertheless, most of the works have been made only on the catalytic activity of the substance in the methanol synthesis as well as in the methanol decomposition, and a knowledge sufficient for understanding the activity in relation to the structure of the catalyst is still lacking.

The present study has been made in an attempt to see as correct and comprehensive a picture of such catalysts as possible, and deals with the electrical conductivity, the surface area, the crystal structure, and the excess oxygen content, of catalysts of different chromia contents, along with their catalytic activity for methanol decomposition.

The results of the activity may be explained, to some extent, from the structural point of view.

Experimental Procedure

Catalyst Preparation.—Two series of catalysts were prepared. The catalysts of the one series, each denoted by catalyst I, were produced by the impregnation of commercial zinc oxide powder (c. p.) in chromium nitrate solutions of varied concentrations and the catalysts of the other series, each denoted by catalyst P, were by the co-precipitation of the hydroxides of zinc and chromium from solutions of zinc and chromium nitrates of different relative concentrations with aqueous ammonia. The powder of catalyst thus formed was heated at 400°C for a few hours and then pressed into a bar of 8×8 mm. square. The bar was sintered at 600°C in air for two hours and then allowed to cool to room temperature. Part of the bar was crushed into granules of 1–2 mm. diameter, to be used for the determination of activity in methanol decomposition and the surface area.

Catalytic Activity for Methanol Decomposition.—The experimental method consisted of passing methanol vapour at a constant rate of 1.98 m. mol./min. through a bed of granular catalyst in a vertical glass tube heated to temperatures from 350° to 430°C in an electric furnace. The apparatus was similar to the one described by J. R. Huffman et al.[1], but was different from it in that the constant rate was maintained, as performal by M. R. Fenske et al.[2], by immersing the methanol reservoir in a water bath at a constant temperature.

A bed of catalyst (1 g.) was reduced at 450°C in a current of hydrogen for six hours, and then methanol vapour was passed through the bed at the reaction temperature. About two hours were required for the catalyst to establish the stationary activity, and measurements were commenced thereafter. The products, gaseous and liquid, were collected and their amounts were determined. The gaseous product was analyzed, as is usually done, for carbon dioxide, carbon monoxide, and hydrogen, and the liquid product was analyzed both for methyl formate by saponification and for formaldehyde by the iodine method.

Electrical Conductivity.—As described in a previous paper[3], electrical conductivity was measured according to the method of R. H. Griffith et al.[4], by using a cube of catalyst (8×8×8 mm.) as a sample. Measurements were made first in vacuo both after the oxidation of the catalyst in oxygen at 450°C and after the reduction in hydrogen at 450°C, and second in an atmosphere of hydrogen after the measurement on the reduced catalyst.

Crystal Structure.—Information on crystal structure was furnished by the Debye-Scherrer's X-ray diagram obtained by using chromium as an anode. It was supplemented by the electron diffraction pattern of powdered catalyst.

Surface Area.—Surface area was determined from the nitrogen adsorption data plotted according to the BET theory.

Quantity of Excess Oxygen in Catalyst.—The excess oxygen content was determined according to the procedure by S. W. Weller[5]. One mole of iodine liberated from an aqueous solution of potassium iodide by the addition of a quantity of catalyst was estimated to be equivalent to 0.5 mol. excess oxygen in the catalyst. A powder of catalyst under 100 mesh was used for the determination.

1) J.R. Huffman and B.F. Dodge, *Ind. Eng. Chem.*, **21**, 1056 (1929).
2) M.R. Fenske and P.K. Frolich, ibid., **21**, 1052 (1929)
3) H. Uchida and Y. Ogino, This Bulletin, **29**, 174 (1956).
4) R.H. Grifith, P.R. Chapman et al., *Disc. Faraday Soc.*, **8**, 258 (1950).
5) S.W. Weller and S.F. Voltz, *J. Am. Chem. Soc.* **76**, 4695 (1954).

Results

Catalytic Activity for Methanol Decomposition.—Among the results of the measurement of activities of catalysts in methanol decomposition at temperatures from 350° to 430°C, the results for catalysts I at 350° and 400°C are shown in Fig. 1 and Fig. 2. In Fig. 1, the total decomposition ratio of methanol ($CH_3OH_{decomp.}/CH_3OH_{introd.}$) and the rate of evolution of carbon monoxide (mole CO/min.) are illustrated by the full and dotted lines respectively, as functions of catalyst composition. In Fig. 2, the composition of decomposition product is plotted also as such. The results for catalysts P are presented in similar manner in Figs. 3 and 4.

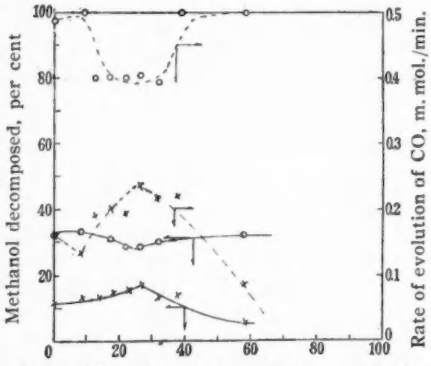

Composition of catalyst, mol. per cent Cr_2O_3

Fig. 1. Total decomposition ratio (full line) and rate of evolution of carbon monoxide (dotted line) as a function of ZnO–Cr_2O_3 composition of catalysts I.
—×—, ··×··, at 350°C. —○—, ··○··, at 400°C

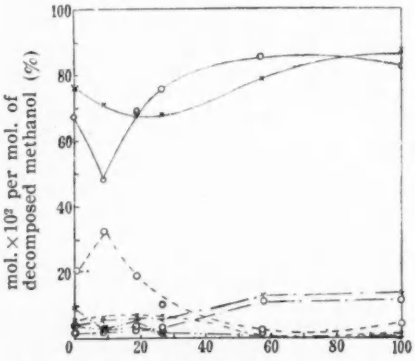

Composition of catalyst, mol. per cent Cr_2O_3

Fig. 2. Products of methanol decomposition as a function of ZnO–Cr_2O_3 composition of catalysts I.
—○— CO, at 350°C. —×— CO, at 400°C
··○·· $HCOOCH_3$, at 350°C
··×·· 〃 , at 400°C
—··—○··— HCHO, at 350°C
—··×—··— 〃 , at 400°C
—·○—·— CO_2, at 350°C
—·×—·— 〃 , at 400°C

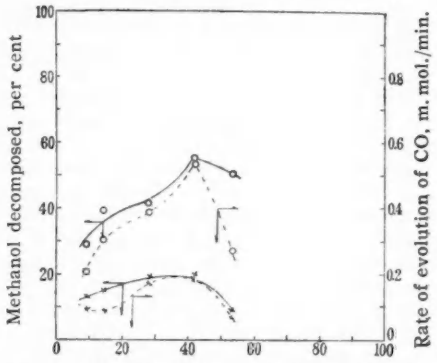

Composition of catalyst, mol. per cent Cr_2O_3

Fig. 3. Total decomposition ratio (full line) and rate of evolution of carbon monoxide (dotted line) as a function of ZnO–Cr_2O_3 composition of catalysts P.
—×—, ··×··, at 350°C. —○—, ··○··, at 400°C

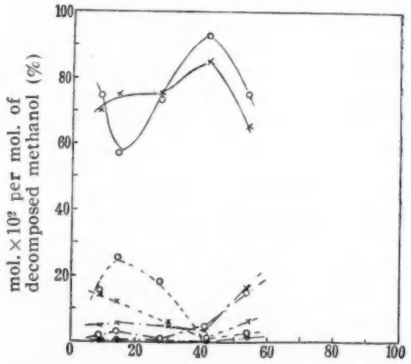

Composition of catalyst, mol. per cent Cr_2O_3

Fig. 4. Products of methanol decomposition as a function of ZnO–Cr_2O_3 composition of catalysts P.
—○— CO, at 350°C. —×— CO, at 400°C
··○·· $HCOOCH_3$, at 350°C
··○·· 〃 , at 400°C
—··●—·· HCHO, at 350°C
〃 , at 400°C
—·—○—·— CO_2, at 350°C
—·—×—·— 〃 , at 400°C

It can be seen from Figs. 1 and 3 that at 350°C a catalyst containing, for example, 26 mol.% chromia gives the highest values of the total decomposition ratio and the rate of evolution of carbon monoxide, whereas at

400°C it gives rather lower values. Fig. 5

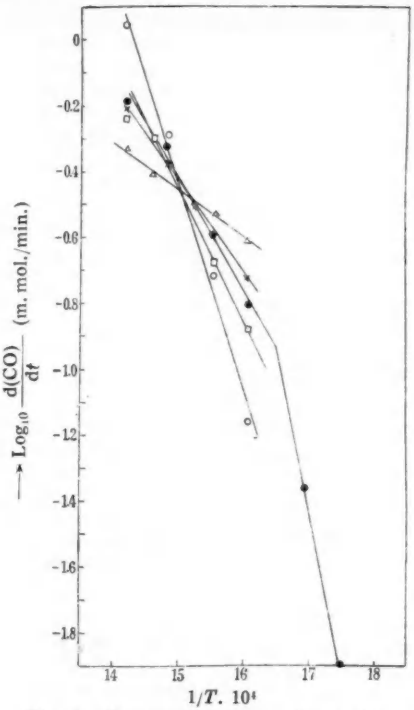

Fig. 5. Temperature dependence of rate of evolution of carbon monoxide.
—●—, zinc oxide.
—○—, catalyst I containing 58.6 mol.% chromia within.
—△—, 〃 26.3 mol.%
—□—, 〃 9.5 mol.%
—×—, 〃 14.3 mol.%

is a detailed representation of the data on the decomposition. This figure shows that the rates increase logarithmically with reciprocal absolute temperature but differently depending on the compositions of the catalysts. Therefore, catalytic activity can not be evaluated correctly unless measurements are made over a wide range of temperature.

There is a good similarity in tendency between the full line and the dotted line, both in Fig. 1 and in Fig. 3, except for the case of a catalyst containing 10 mol.% chromia. This catalyst yielded a greater amount of methyl formate particularly at a low temperature of 350°C (refer to Figs. 2 and 4)*1, but gave a lower rate of evolution of carbon monoxide despite the greater decomposition ratio.

On the basis of H. Dohse's view that the methanol decomposition follows a zeroth order reaction, the apparent activation energy of methanol decomposition by the catalysts I was given by the slope of the straight line in Fig. 5. The activation energy thus determined is lowest at a chromia content of 26 mol.%, whereas it rises with decreasing chromia content on the one side and also with increasing chromia on the other side (refer to Fig. 10 also). The more active a catalyst is at lower temperatures, the smaller is the activation energy, whereas the more active a catalyst is at a higher temperature, the greater is the activation energy.

H. Dohse[7] described that the plot of log v vs. $1/T$ for zinc oxide has a bend. Such a bend appears also at 330°C on the line constructed from the present data of experiments, and is of particular interest in view of the fact that a bend, as will be described later, appears also on the plot of electrical conductivity vs. $1/T$ for zinc oxide at the same temperature. The bend in the conductivity curve, however, shifts, with the increasing chromia content, towards so low a temperature that the corresponding bend in the activity curve can scarcely be determined accurately (refer to Fig. 7).

A comparison of the activation energy of the catalysts I with that of the catalysts P indicates that within the range of chromia content of up to 30 mol.% the energy for the latter is greater than that for the former and beyond this content the situation is reversed (refer to Fig. 10).

Electrical Conductivity.—The results of the measurements of electrical conductivity on evacuated catalysts at 350°C, which were made both after the oxidation and after the reduction of catalysts at 450°C, are shown as functions of catalyst composition in Fig. 6*2. The electrical conductivity of the oxidized, evacuated catalysts is the higher for the increasing chromia contents, whereas that of the reduced, evacuated catalysts is the lower for the increasing chromia content. In Fig. 6, the conductivity curve for oxidized, evacuated catalysts intersects that for reduced evacuated catalysts, at a certain chromia content, which is 26 mol.% for the catalysts I, and 13 mol.% for the catalysts P.

The catalyst has naturally the conductivity centres of two types, the one is the zinc

*1 This may perhaps have a close relation to the highly selective catalyst that was used in the methanol synthesis by G. Natta[6] and which contained 11 mol. % of chromia.

6) G. Natta, "Catalysis (edited by P.H. Emmett)", Rheinhold Publishing Corporation, (1955), III, P. 349.

7) H. Dohse, *Z. Physik. Chem.*, B 8, 159 (1930).

*2 The conductivity of the oxidized catalysts in oxygen atmosphere differed little from that of the oxidized, evacuated ones.

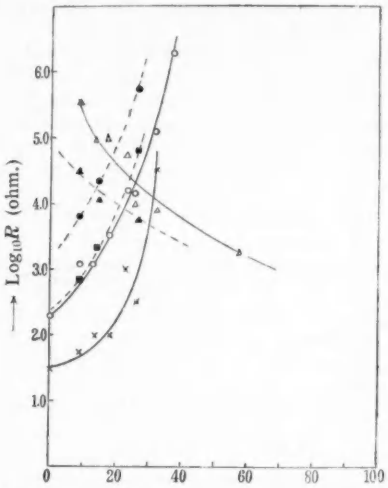

Fig. 6. Electrical conductivity of catalysts I (full line) and catalysts P (dotted line) at 350°C as a function of ZnO–Cr_2O_3 composition.
×, ■, in hydrogen after reduction
○, ●, in vacuo after reduction
△, ▲, in vacuo after oxidation

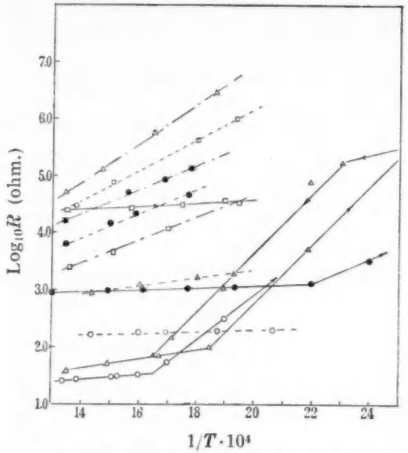

Fig. 7. Temperature dependence of electrical conductivity of catalysts I in hydrogen (full line), in vacuo after reduction (dotted line), and in vacuo after oxidation (dotted and dashed line).
○, zinc oxide. △, catalyst with 9.5 mol. % Cr_2O_3. ●, , , , 23.3 mol. %. □, , , , 33.2 mol.%

atoms (n-type) due to zinc oxide and the other the excess oxygen atoms (p-type) due to chromia. This fact implies that the n-type semi-conductivity becomes predominant in the catalysts of reduced state whereas the p-type becomes so in the catalysts of oxidized state, and that the greater amount of chromia favour the production of a larger number of p-type centres.

Logarithms of electrical resistivity determined on the catalysts in vacuo both after the oxidation and after the reduction of catalysts at 450°C, and those of catalysts in the hydrogen atmosphere after the reduction at the same temperature, are plotted against reciprocal temperatures in Fig. 7*3. As for the catalysts I in the hydrogen atmosphere, the plots for every catalyst form a pair of straight lines intersecting at a certain temperature that shifts to lower values with increasing contents. The change of the electrical conductivity with the lowering temperature was not reversible by the subsequent raise of temperature, and showed a pronounced drift.

The slope of the straight line in the high temperature range should give the activation energy of electrical conductivity in this range*4. The energy thus determined for catalysts in hydrogen depends on the chromia content of catalysts. Within the range of low chromia content (less than about 26 mol.%), the energy rises slightly with the increase of chromia content and soon reaches a maximum at about 10 mol.% chromia and thereafter takes a downward course to a minimum at 26 mol.% chromia, and this decrease is followed by a rapid rise with the further increasing chromia content (refer to Fig. 10).

In contrast, the activation energy of conductivity for catalysts evacuated after their reduction rises monotonously with increasing chromia content, whereas the energy for the catalysts evacuated after their oxidation persists almost unaffected by the increase of chromia content.

Catalyst Structure Revealed by Debye-Scherrer's X-ray Diagram and Electron Diffraction Pattern.—The catalysts I and catalysts P gave Debye-Scherr's X-ray diagrams that did not show any line corresponding to Cr_2O_3, even though the catalysts were heated at 600°C for two hours and their chromia contents were as high as 59%, but showed the lines corresponding to zinc oxide.

The diffraction lines for zinc oxide, however, become weaker with increasing chromia content. Besides these lines, the lines cor-

*3 The electrical conductivity of catalysts P at temperatures below 300°C was not determined.

*4 Considering the performance of catalysts at the practical working temperature, the energy in the low temperature range is of minor significance.

responding to neither zinc oxide nor Cr_2O_3 but to $ZnCr_2O_4$ spinel were observed. The lines due to the spinel appeared even at so small a chromia content as of 9.5 mol.% and their number increased with the chromia content increasing up to 25–30 mol.%, but above this content the lines became gradually diffused till it was difficult to distinguish the lines.

The electron diffraction patterns for catalysts I and catalyst P reveal also the lines due to the spinel. The number of these lines is far greater than the number of the diffraction lines in the X-ray diffraction diagram. The electron diffraction lines remained sharp while the chromia content increased even up to the value where the X-ray diffraction lines became rather diffused.

The results described above reveal that the catalyst comprises the oxides of zinc and chromium and the spinel of zinc chromite presumably produced by the reaction $ZnO+Cr_2O_3 \rightarrow ZnCr_2O_4$, and that the spinel in the catalyst of high chromia content exists as crystallites too small to be detected by the X-ray analysis. Accordingly, the quantity of chromia in excess of the proper amount for combination with zinc oxide seems to prevent the growth of the crystallites.

Surface Area and Quantity of Excess Oxygen in Catalyst.—The surface area of and the quantity of excess oxygen in 1 g. of catalysts are illustrated by the full and the dotted lines respectively, as functions of chromia content, in Fig. 8 for catalysts I, and in Fig. 9 for catalysts P. As is seen in these figures, every curve has a sigmoid shape and rises with increasing chromia content. The initial part (over very low chromia contents), an almost rectilinear line, shows a rather rapid rise, the middle part a very dull rise, and the last part a rise becoming very sharp. The last part begins when the chromia content attains to 35 mol.% for catalysts I, and 30 mol.% for catalysts P.

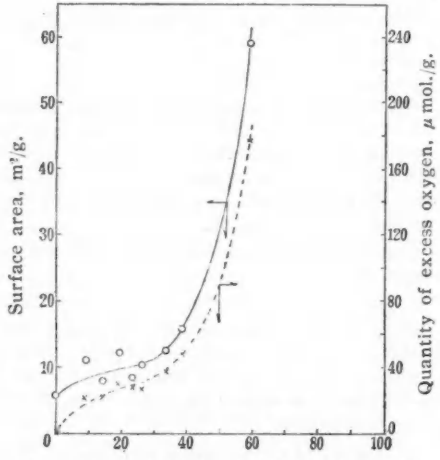

Composition of catalyst, mol. per cent Cr_2O_3

Fig. 8. Surface area (full line) of and quantity of excess oxygen (dotted line) in 1 g. of catalysts I as a function of $ZnO-Cr_2O_3$ composition.

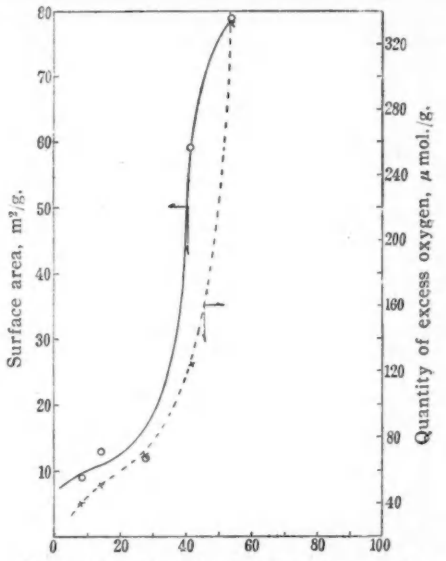

Composition of catalyst, mol. per cent Cr_2O_3

Fig. 9. Surface area (full line) of and quantity of excess oxygen (dotted line) in 1 g. of catalysts P as a function of $ZnO-Cr_2O_3$ composition.

The results described above may bring out the following picture of the surface structure of catalysts. As revealed by the trend of the surface area change, the size of the larger particles having composed granules of zinc oxide changes a little even though the chromia content attained to 30 mol.%, and any further addition of chromia results in the abrupt creation of numerous fine particles as to catalysts I, whereas it results in the sudden reduction of the particle size as to catalysts P.

For the reason that excess oxygen can exist only in the presence of the chromia which fails to combine with zinc oxide, the steep rise of the excess oxygen curve in the range of high chromia content indicates that the quantity of uncombined chromia is increasing rapidly on the surface of the catalyst. On the other hand, the deviation

of the curve from the expected rectilinear line with increasing chromia content is suggestive of the formation of crystallites between the oxides of zinc and chromium[*5]. From the results seen in the diffraction patterns, the crystallite may be the one of zinc chromite spinel. The highest concentration of the spinel crystallites in the surface, therefore, is to be found with catalysts whose excess oxygen content deviates most greatly from the quantity expressed by the expected rectilinear line[*6].

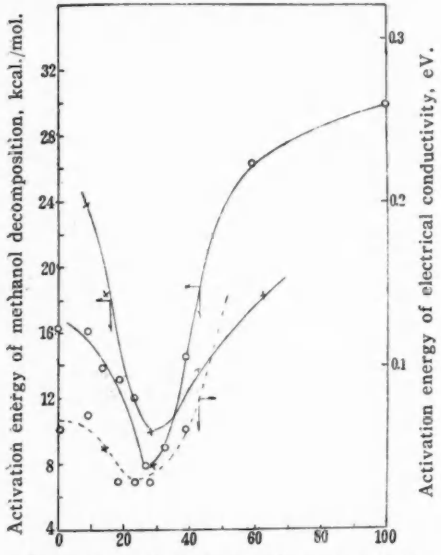
Activation energy of methanol decomposition, kcal./mol.
Activation energy of electrical conductivity, eV.
Composition of catalyst, mol. per cent Cr_2O_3

Fig. 10. Variation of activation energies for methanol decomposition (full line) and electrical conductivity (dotted line) with catalyst compositions.
○, catalysts I. ×, catalysts P.

Discussion

Methanol Decomposition.—By assuming that the rate of methanol decomposition follows the zeroth order reaction given by

$$v = Ae^{-E/kT} \tag{1}$$

where v is the rate per unit surface area of the catalyst, the logarithms of frequency factor (log A) are plotted against activation energy (E) in Fig. 11 for catalysts I and

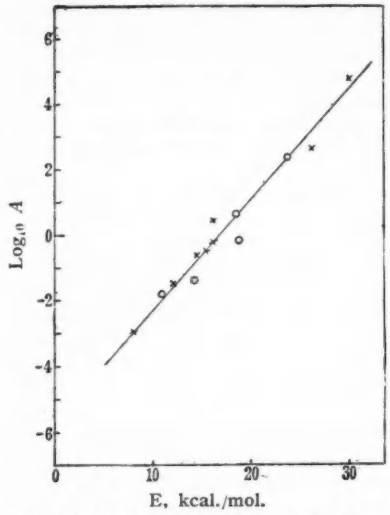

Fig. 11. Plot of logarithm of frequency factor in the rate of evolution of carbon monoxide vs. activation energy.
—×—, catalysts I. —○—, catalysts P.

catalysts P. The lines for the two kinds of catalysts are straight and approximately identical. The linear relation between log A and E has already been described by E. Cremer[8], for the rate of methanol decomposition with neodium oxides, and by G-M. Schwab[9], for the rate of the decomposition of formic acid with alloy catalysts, and some others.

The straight line can be represented by an equation,

$$A = ae^{\alpha E} \tag{2}$$

where log a is the intercept on the ordinate and α is the slope of the line. This equation is explained by assuming that active centres with high activation energy in the catalyst surface are more frequent than the ones with low activation energy[9].

The combination of Eq. (2) with Eq. (1) gives

$$v = a \cdot e^{\alpha E} \cdot e^{-E/kT} \tag{3}$$

When v is expressed in the number of moles of carbon monoxide evolved per unit surface (cm^2) per second the substitution of the values of a and α obtained from Fig. 10 in Eq. (3) results in

$$v = 1.24 \times 10^{-7} \cdot e^{0.81E} \cdot e^{-E/kT} \tag{4}$$

Eq. (4) indicates that the rate at a certain temperature, so far as the rate per unit

*5 The slow increase within the range of very low chromia content can not readily be explained. The increase is probably due to the condition that chromia is too dispersed to build up the spinel crystallite, though it is combined with zinc oxide.

*6 A greater amount of the crystallites may be produced in 1 g. of the catalyst by the further addition of chromia, but since the amount considered is based on the unit surface area it becomes rather less owing to the steep rise of surface area.

8) E. Cremer, *Z. Elektrochem.*, **53**, 269 (1949).
9) G-M. Schwab, *Disc. Faraday Soc.*, **8**, 166 (1950).

surface area is considered, is determined solely by the activation energy inherent to a catalyst, but not by any other factors.

Catalytic Activity and Electrical Conductivity.—At first sight, one may be inclined to expect the relation of the activation energy of methanol decomposition to the concentration of either the *n*-type or the *p*-type conductivity centres in the catalyst. Namely, the concentration of *n*-type conductivity centres need be only adequately low to permit electrons to transfer more readily from methanol to catalyst, and the transfer thus taking place causes the catalyst to adsorb methanol and cosequently to decompose methanol with less activation energy, if the rate of adsorption determines the rate of decomposition of methanol. However, there is a minimum of the activation energy at a catalyst (26 mol.% chromia) of *n*-type semiconductor in I series, whereas at a catalyst (30 mol.% chromia) of *p*-type semi-conductor in P series*7. Thus, no direct relation of the activation energy of methanol decomposition to the types of semiconductor can easily be found at all*8.

When both the activation energy of methanol decomposition and the activation energy of electrical conductivity are plotted as functions of the composition of catalysts I (Fig. 10), the line for the activation energy of methanol decomposition runs parallel to the line for the activation energy of electrical conductivity. Moreover, both the bend in the plot $\log R$ (in hydrogen) and the bend in the plot of $\log v$ vs. $1/T$ for zinc oxide appear at the same temperature (compare Fig. 5 with Fig. 7). A couple of these results serve as a favourable evidence for corroborating the rather direct relation between the activation energies of methanol decomposition and electrical conductivity.

In a previous paper[3] it is stated that the decrease of electrical conductivity of zinc oxide in hydrogen with the rise of temperature in the low temperature range was caused by the adsorption of hydrogen on zinc atom-pairs whereas the increase of electrical conductivity in the high temperature range was due to the adsorption on oxygen atoms. This fact in connection with the evidence just described for the relation between activation energies of methanol decomposition and electrical conductivity may lead us to expect that the rate of adsorption of a reactant (methanol or something intermediate in the decomposition) on oxygen atoms (or the electron transfer between the reactant and oxygen atoms) is determining the rate of the methanol decomposition.

Promoting Action of Chromia.—In the methanol decomposition the increase in exponential terms of the rate equation (1) is always compensated by the decrease in the frequency term. According to a recent paper by E. Cremer[10], this compensation effect may be expected at multicomponent catalysts of the same type, if different kinds of active centres act simultaneously as sites of the catalytic reaction and if the proportions of these different active centres (involving different energies) are shifted by changes in its composition. An illustration is given by E. Cremer on a reaction that takes place on two kinds (1 and 2) of active centres involving the activation energies E_1 and E_2 and frequency factor terms A_1 and A_2, respectively. In this case the overall rate constant k (or the rate v of a zeroth order reaction) becomes

$$k = A_1 \exp(-E_1/kT) + A_2 \exp(-E_2/kT),$$

and the Arrhenius plots of k for the greater values of A_2, the values of E_1, E_2 and A_1 being kept at the same, give the straight lines of decreasing slope, i. e. the decreasing activation energy, and of a common intersection point, provided that A_1 is greater than A_2 and E_1 greater than E_2.

A comparison of Fig. 10 with Fig. 8 or 9 indicates that the greater the spinel concentration in the catalyst surface the smaller is the activation energy of methanol decomposition. The fact may be explained as follows from E. Cremer's point of view. In the surface of the catalysts within the range of chromia content up to 26 per cent, zinc oxide and zinc chromite (or the oxygen atoms in zinc oxide and zinc chromite) are the two kinds (1 and 2) of the active centres for the methanol decomposition, while chromia and zinc chromite are such in the surface of the catalyst of higher chromia content. Accordingly, the catalyst with the greater concentration of zinc chromite spinel in the surface can give the smaller activation for the methanol decomposition than both the zinc oxide and chromia alone, if the activation energy of the spinel is assumed to be smaller than that of zinc oxide and of chromia.

No direct relation between the extent of the surface area and the activity for meth-

*7 According to D. J. Bevan et al. (*J. Chem. Soc.*, 1948, 1729), zinc chromite is a *p*-type semi-conductor.

*8 The influence of the concentration of *n*-type semiconductor on the catalytic activity can not completely be denied, particularly at low temperatures where the adsorption of a reactant, as will be described later, takes place on zinc atom pairs.

10) E. Cremer, "Advances in Catalysis", VII((1955), p. 85.

anol decomposition can be found. The activity at, for example, 350°C rose at first with the slow increase of surface area, but thereafter fell off despite the rapid further increase of surface area (compare Fig. 8 with Fig. 10). This result can be explained from the fact that while the surface area increases slowly the activation energy decreases, but once the surface area has begun to increase rapidly the energy turns to increase steeply. The greater amount of the chromia disintegrates the crystallites of the spinel into so extremely fine ones that it may cause the steep increase of surface area and also cover the surface to such an extent that the activation energy approaches a value as high as 30 kcal./mol. for chromia alone.

The favourable effect of chromia is thus to increase the specific activity of catalyst surface rather than to provide and stabilize the larger accessible area. This is quite contrary to G. Natta's statement[5] that the activation energy of methanol synthesis is independent of the chromia content and the promoting action of chromia is solely due to its hindering effect upon the recrystallization of zinc oxide. No decisive conclusion can as yet be made between these two different promoting actions revealed in the synthesis and in the decomposition.

Summary

From the results on the rates of methanol decomposition by the catalysts of different zinc oxide-chromium oxide compositions the rate (v) of evolution of carbon monoxide per unit surface area of catalyst has appeared to be represented by the following equation

$$v = ae^{\alpha E} \cdot e^{-E/kT}$$

where a and α are constants applicable throughout the two series of catalysts produced by different methods. The activation energy (E) of the methanol decomposition attains to a minimum value when the catalyst has a certain chromia content. It is directly related with the activation energy of electrical conductivity of the catalyst in hydrogen at high temperature but neither with the concentration of n-type conductivity centres nor with that of p-type conductivity centres. At such temperatures, the adsorption of hydrogen on the oxygen atoms in the surface was considered to participate in the electrical conductivity.

Moreover, the results on determinations of the surface area and the excess oxygen content, together with the information about the structure obtained from diffraction patterns, reveal that there is a similarity in tendency between the increase of concentration of zinc chromite spinels in the catalyst surface and the decrease of activation energy of the decomposition. This relation can be explained from the view of E. Cremer on the compensation effect.

The quantity of chromia added in excess of the proper amount for combination with zinc oxide causes both the surface area and the activation energy to increase towards those of chromia alone.

The addition of chromia has therefore a considerable influence upon the activation energy of methanol decomposition, which is quite contrary to what G. Natta described on the methanol synthesis.

Government Chemical Industrial Research Institute, Tokyo

Mikroanalyse mit Hilfe von Ionenaustauschharzen. V. Über den Nachweis spurweise vorhandenes Molybdäns mit Ammoniumrhodanid und Zinn(II)chlorid [1]

Von Masatoshi FUJIMOTO

(Eingegangen am 20. Februar 1956)

Einleitung

Wohl bekannt ist von früher her, dass eine scharlach- bzw. orangerote Färbung, die die Molybdate bei Anwesenheit von Zinn(II)-chlorid durch Einwirkung von Ammonium- oder Kaliumrhodanid liefern, als eine sehr ausgezeichnete Methode für den Nachweis sowie die Bestimmung des Molybdäns weit benutzt wird[2]. Diese rote Färbung beruht auf der Bildung von Komplexrhodanide fünfwertiges Molybdäns wie $[Mo(SCN)_5]$, $[Mo(SCN)_6]^-$ [3]. Der Nichtelektrolytkomplex ist für kolorimetrische Bestimmung des Molybdäns besonders geeignet, da dieser nicht nur mit organischem Lösungsmittel leicht ausgezogen wird, sondern auch sehr starke rote Färbung liefert. Nach Babko[3], ist es für die Bestimmung des Molybdäns nicht wünschenswert, unter den zur Bildung von Komplexanion $[Mo(SCN)_6]^-$ geeigneten Bedingungen[4] Kolorimetrie auszuführen, da dieses Anion verhältnismässig schwächer als der Nichtelektrolytkomplex gefärbt wird. Trotz diesem Nachteil wird dieses Komplexanion ins Anionenaustauschharz stark adsorbiert, und die Harzphase sich dabei deutliche und merklich beständige Orange- bzw. Orangerotfärbung liefert, welche infolgedessen als eine Tüpfelmethode mit Ionenaustauschharzen anwendbar ist. Bei gegenwärtigem Versuche, hat der Verfasser, um diese lebhaft orangerote Färbung zur Nachweismethode mit Ionenaustauschharz am zweckmässigsten zu benutzen, ausführliche Untersuchung über verschiedene Bedingungen der Färbung von der Harzphase durchgeführt, und es gelang ihm, eine neue und sehr empfindliche sowie spezifische Nachweismethode für Molybdän vollkommen festzustellen.

1) Die vierte Mitteilung: M. Fujimoto, Dieses Bulletin **29**, 571 (1956).

2) Vgl., z. B., E. B. Sandell, „Colorimetric Determination of Traces of Metals", 2. Aufl., London (1950), S. 455ff.

3) A. K. Babko, *J. Gen. Chem.* (U.S.S.R.), **17**, 642 (1947); *Chem. Abstr.*, **42**, 476*g* (1948).

4) Nach optischen Messungen Babkos wird diese Färbung dann infolge der Bildung des Komplexanions $[Mo(SCN)_6]^-$ verhältnismässig geschwächt, wenn die Konzentration der Rhodanidionen grösser als 0.2- bzw. 0.4 M ist (vgl. letztgenannte Fussnote).

Die in dieser Untersuchung benutzten Ionenaustauschharze

Dowex 1-X1: Ein aus Styrol und Divinylbenzol dargestelltes starkbasisches farbloses Anionenaustauschharz von quartärem Ammoniumtypus, dessen Divinylbenzolgehalt etwa einprozentig ist. Die Korngrösse ist ungefähr 50 Maschen von Tylerschem Normalsieb.

Dowex 1-X4: Ein ebenso starkbasisches farbloses Harz wie Dowex 1-X1, dessen Divinylbenzolgehalt jedoch etwa vierprozentig ist. Die Korngrösse ist 50 bis 100 Maschen.

Amberlite XE-114: Ein hellgelbes mittelstarkbasisches Harz. Die Korngrösse ist ungefähr 30 Maschen.

Amberlite IR-45: Ein hellbraunweisses sowie undurchsichtiges schwachbasisches Harz. Die Korngrösse ist ungefähr 30 Maschen.

Überdies wurde ein starksaures Kationenaustauschharz, Dowex 50-X8, um die fremden Matallionen, die den Nachweis stören, zu beseitigen, als eine Mikroharzsäule von NH_4R-Form angewandt. Die Korngrösse ist ungefähr 100 Maschen.

Versuchsanordnung

Auf einer weissen Tüpfelplatte versetzt man einen Tropfen der Probelösung mit einigen Körnchen des starkbasischen Anionenaustauschharzes von RCl-Form, rührt danach mit einem kleinen Glasstab völlig um, und lässt sie etwa drei Minuten stehen. Dann fügt man dazu einen Tropfen verdünnter wässeriger Lösung des Ammoniumrhodanides, und nach weiteren drei Minuten, einen Tropfen der in die Salzsäure gelösten verdünnten Lösung des Zinn(II)chlorides. Nach einigen Minuten, je nach dem Molybdängehalt von der Probelösung, entsteht über das Ganze der Harzkörnchen eine orangerote bzw. hellorange Färbung, die unter Beleuchtung mit einer Tischlampe und durch etwa zwanzigfache Vergrösserung mit einer Lupe wohl erkennbar ist.

Bestimmung der Bedingungen höchster Empfindlichkeit

1. Massflüssigkeit.—Eine Reihe der Massflüssigkeiten des Molybdäns wurde aus der gering ammoniakalischen wässerigen Lösung des extrareinen Ammoniumparamolybdates, deren 1 ccm 1.22 ± 0.003 mg von Molybdän enthielt[5], vorbereitet.

5) Die Menge des Molybdäns wurde folgenderweise einfacher bestimmt: Nach dem Verdampfen zum Trocknen bestimmtes Volumens der Probelösung, wurde der Rückstand durch Erhitzen bei ungefähr 500°C etwa eine Stunde lang ins Molybdänsäureanhydrid, MoO_3, vollkommen übergeführt und danach genau gewogen.

2. Reagenzien.—Als die Stocklösungen der Reagenzien wurden die folgenden Lösungen vorbereitet:

(1) 20prozentige wässerige Lösung des extrareinen Ammoniumrhodanids.

(2) Lösung des in die 6 N Salzsäure gelösten Zinn(II)chlorides wird in einer besonders wohl verstöpselten Flasche aufbewahrt. Diese Flasche wird gewöhnlich zur Bestimmung von ins Naturwasser gelöstem Sauerstoff nach Winklerschem Verfahren benutzt.

(3) Destillierte Salzsäure: ungefähr 6 N.

3. Bedingungen höchster Empfindlichkeit.—Die Ergebnisse unter verschiedenen Experimentalbedingungen ausgeführter Versuche werden mittels schematischer Darstellungsweise von der scheinbaren Durchschnittsintensität der Färbung, die in der dritten Mitteilung[6] genau beschrieben wurde, in Abb. 1 und Tabelle I zusammen dargestellt:

TABELLE I

VERSCHIEDENE REAKTIONSBEDINGUNGEN VON ABB. 1

Nr. des Experiments	Zeichen der Kurve	Ordnung der Versetzung von Reagenzien und Probelösung 1.	2.	3.	4.	Bemerkungen über die Resultate*
I_a	—△—	Probelsg.**	20proz. Lsg. des NH_4SCN	10proz. Lsg. (6 N HCl) des $SnCl_2$	Dowex 1-X4 (RCl)	*a*
I_b	—▽—	Dowex 1-X4 (RCl)	10proz. Lsg. (6 N HCl) des $SnCl_2$	20proz. Lsg. des NH_4SCN	Probelsg.	*a*
I_c	--○--	Dowex 1-X4 (RCl)	Probelsg.	1proz. Lsg. des NH_4SCN	0.5proz. Lsg. (6 N HCl) des $SnCl_2$	*b*
I_d	-·-○-·-	Dowex 1-X4 (RCl)	Probelsg.	20proz. Lsg. des NH_4SCN	0.5proz. Lsg. (6 N HCl) des $SnCl_2$	*c*
I_e	—○—	Dowex 1-X4 (RCl)	Probelsg.	0.2proz. Lsg. des NH_4SCN	0.5proz. Lsg. (6 N HCl) des $SnCl_2$	*b*
I_f	--△-	Probelsg.	0.2proz. Lsg. des NH_4SCN	0.5proz. Lsg. (6 N HCl) des $SnCl_2$	Dowex 1-X4 (RCl)	*d*
I_g	—□—	Dowex 1-X1 (RCl)	Probelsg.	0.2proz. Lsg. des NH_4SCN	0.5proz. Lsg. (6 N HCl) des $SnCl_2$	*b*
I_h	—×—	Amberlite XE-114 (RCl in 10^{-3} N HCl)	Probelsg.	0.2proz. Lsg. des NH_4SCN	0.5proz. Lsg. (6 N HCl) des $SnCl_2$	*b*
I_i	--×--	Amberlite IR-45 (RCl in 10^{-3} N HCl)	Probelsg.	0.2proz. Lsg. des NH_4SCN	0.5proz. Lsg. (6 N HCl) des $SnCl_2$	*b*, *e*
I_j	--◰--	Dowex 1-X1 (RCl)	Probelsg.	0.2proz. Lsg. des NH_4SCN	0.5proz. Lsg. (3 N HCl) des $SnCl_2$	*b*
I_k	-·-◪-·-	Dowex 1-X1 (RCl)	Probelsg.	0.2proz. Lsg. des NH_4SCN	10proz. Lsg. (6 N HCl) des $SnCl_2$	*b*
I_l	—◩—	Dowex 1-X1 (RCl)	Probelsg.	0.2proz. Lsg. des NH_4SCN	0.5proz. Lsg. (1 N HCl) des $SnCl_2$	*b*
I_m	—●—	Dowex 1-X1 (RCl)	Probelsg.	0.5proz. Lsg. (6 N HCl) des $SnCl_2$	0.2proz. Lsg. des NH_4SCN	*f*

**a*: Die Färbung der Harzkörnchen ist sehr schwach und unbeständig.

b: Die Harzkörnchen färben sich sehr deutlich schon nach weniger als eine Sekunde.

c: Die Harzkörnchen färben sich allmählich stärker, wobei es um die höhere Konzentration der Rhodanidionen händelt. (vgl. Abb. 3 sowie den Abschnitt „Diskussion.")

d: Die Harzkörnchen werden sehr langsam gefärbt.

e: Wegen der Undurchsichtigkeit der Harzkörnchen wird die scheinbare Intensität der Färbung beträchtlich geschwächt.

f: Die Harzkörnchen färben sich erst etwa 5 Sekunden nach der Mischung.

** Die hier benutzte Probelösung enthält 0.49 *γ* Molybdän (16.2 *γ*/ccm als MoO_3).

6) M. Fujimoto, Dieses Bulletin 29, 567 (1956).

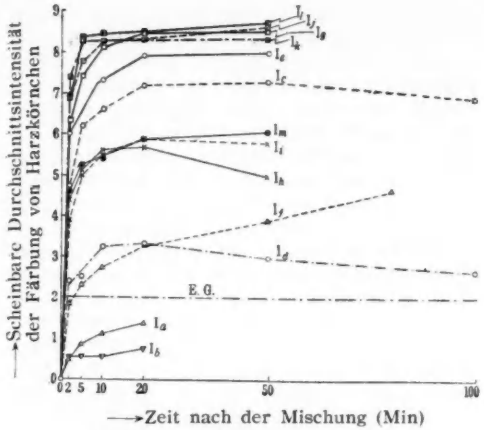

Abb. 1. Vergleichung verschiedener Experimentalbedingungen.

Von diesen Ergebnissen aus betrachtet, wurde das folgende Verfahren als das best geeignete vollkommen festgestellt:

„Man versetzt auf einer weissen Tüpfelplatte einen Tropfen der neutralen oder schwach alkalischen[7] Probelösung mit einigen Körnchen von Dowex 1-X1 (RCl-Form), rührt sie mit einem kleinen Glasstab völlig um, und lässt sie etwa drei Minuten lang stehen. Dann fügt man dazu einen Tropfen 0.2 prozentiger wässeriger Lösung des Ammoniumrhodanids, und nach weiteren drei Minuten, einen Tropfen der 0.5- bzw. 10prozentigen Lösung des in 1- bzw. 6 N Salzsäure gelösten Zinn(II)chlorides. Nach einige Minuten, beobachtet man die orange bzw. orangerote Färbung der Harzkörnchen."

Bestimmung der Erfassungsgrenze[8]

Abb. 2 stellt die Resultate durch Verfahren „I_g" von Abb. 1 durchgeführter Experimente dar:

Wie man von diesen Kurven aus klar ersieht, wurde die Erfassungsgrenze an dieser Reaktion für Molybdän, 0.024 γ unter Grenzkonzentration $1:1.6\times10^6$ festgestellt.

Einfluss der Anionenkonzentration der Probelösung auf die Empfindlichkeit der Reaktion

Gibt es eine grosse Menge von fremden Salzen in der Probelösung, wird die Empfindlichkeit der Färbungsreaktion beträchtlich beschädigt. Die Resultate der Vergleichungen der Empfindlichkeitsveränderung, die mit Natriumchlorid als ein Vertreter dieser Art von Salzen durchgeführt wurden, stehen in Abb. 3:

Wie man aus der Vergleichung dieser Kurven leicht erkennt, sinkt die Empfindlichkeit der

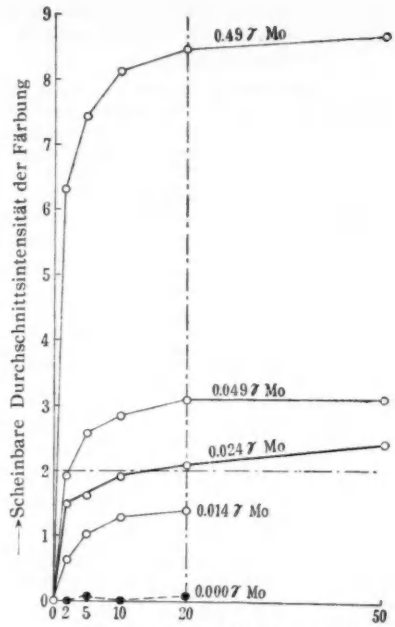

Abb. 2. Bestimmung der Erfassungsgrenze.

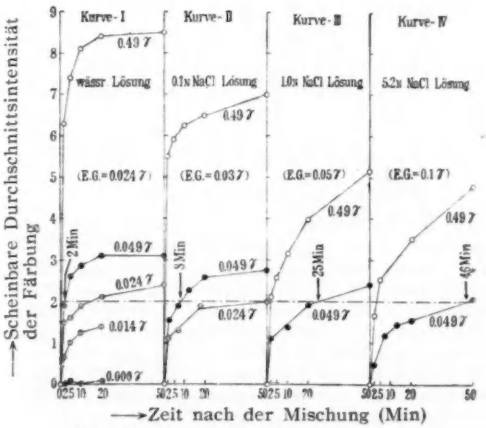

Abb. 3. Einfluss der Anionenkonzentration auf die scheinbare Färbungsintensität.

Farbenreaktion mit dem steigenden Konzentration der Chloridionen in der Probelösung allmählich herab; d. h. die Erfassungsgrenze der Nachweisreaktion verändert sich von der Menge 0.024 γ bei Abwesenheit fremder Anionen bis zu 0.05 γ im Falle der ins 1.0 N Natriumchlorid gelöster Probelösung, und noch zu 0.1 γ, wenn die Probelösung als 5.2 N Natriumchloridlösung angewandt wird. Die Ursache dieser Empfindlichkeitsabnahme wird später genau diskutiert werden[6].

7) Vgl. den Abschnitt „Diskussion" (S. 598).

8) In bezug auf die Erfassungsgrenze, vergleiche die erste Mitteilung: M. Fujimoto, Dieses Bulletin 27, 48 (1954).

Einfluss der Wasserstoffionenkonzentration der Probelösung auf die Empfindlichkeit der Reaktion

Wenn die Probelösung sauer ist, wird die Färbungsintensität der Harzphase sowieso beträchtlich schwächer, wenn auch die Konzentration fremder Anionen verhältnismässig niedrig ist.

Abb. 4 zeigt ein typisches Beispiel dafür; d. h. die Empfindlichkeitsveränderung der Reaktion,

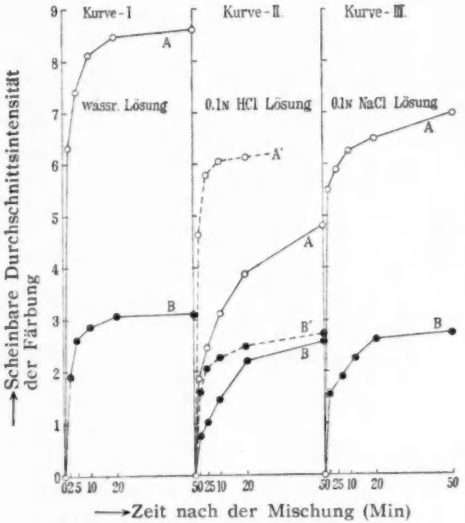

Abb. 4. Einfluss der Acidität der Probelösung auf die scheinbare Färbungsintensität.
—○—, --○-- 0.49 γ Mo in der Probelösung (0.04 ccm)
—●—, --●-- 0.049 γ Mo in der Probelösung (0.04 ccm)

wenn die Probelösung als 0.1 N-salzsaure Lösung verwandt wird. Die gestrichelten Linien stellen die Empfindlichkeitssteigerung durch gelindes Erwärmen mit ein wenig überschüssigem verdünntem Ammoniakwasser dar. Durch dieses Verfahren kann man die Reaktionsempfindlichkeit einfach zum beinahe gleichen Grade mit dieselbe des Falls, wenn die Probelösung als 0.1 N Natriumchloridlösung verwandt wird, steigern. Über diesen Verlauf der Reaktion wird der Verfasser im folgenden Abschnitt kurz erörtern.

Diskussion

Obgleich man darüber nur halbquantitativ diskutieren kann, ist der Verlauf der in Abb. III dargestellten Kurven besonders interessant. Da in der wässerigen Lösung, deren pH-Wert zwischen 14 und 6.8 liegt, die Molybdationen grösstenteils als einfache Orthomolybdationen, MoO_4^{2-}, vorhanden sind[9], könnte man vermuten, dass das Anionenaustauschgleichgewicht zwischen Chloridionen in der Harzphase und Molybdationen in der Probelösung verhältnismässig geschwind erreicht wird. Daher beruht die etwa zwei Minuten nach der Mischung beobachtete scheinbare Intensität der Färbung von der Harzphase vielleicht hauptsächlich auf die durch Reaktion der Orthomolybdationen in der Harzphase mit Rhodanidionen und Reduktionsmittel gebildeten Komplexanionen, $[Mo(SCN)_6]^-$, deren Menge, wie man in Abb. 3 deutlich ersieht, mit steigenden Chloridionenkonzentration deutlich abnimmt. Ausserdem ist es auch sehr interessant, dass, je höher die Konzentration der in der Probelösung enthaltenen Chloridionen, desto grösser ist die Zunahme der später als zwei Minuten nach der Mischung mit der Zeit entwickelten Färbung der Harzphase. Diese Steigerung der Färbungsintensität kann man als die langsame Adsorption der in der Lösungsphase gebildeten gefärbten Rhodanidkomplexanionen halbquantitativ betrachten (vgl. den Unterschied zwischen den Kurven-I_d, I_c und I_e von Abb. 1).

Abb. 4 erzeigt auch ein sehr interessantes Verhalten der in der sauren Lösung vorhandenen Molybdationen gegen das Anionenaustauschharz, wobei die Menge vorher in die Harzphase adsorbierter Molybdationen ausserordentlich kleiner als dieselbe der

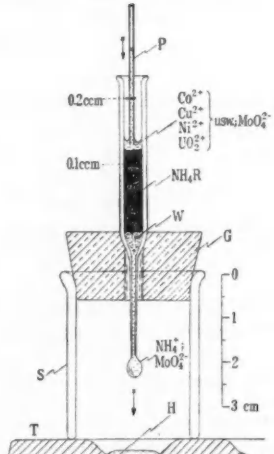

Abb. 5. Mikroharzsäule zur Trennung von Metallionen.
NH_4R: Mikrosäule des Kationenaustauschharzes von NH_4R-Form, P: Kapillarpipette (1 Tropfen = 0.02 ccm), G: Gummistopfen, S: Glasrohr (3×3.7 cm), T: Tüpfelplatte, H: Anionenaustauschharz von RCl-Form, W: Glaswolleschicht.

9) G. Jander, K. F. Jahr und W. Heuckeshoven, *Z. anorg. u. allgem. Chem.*, **194**, 383 (1930).

neutralen Probelösung mit gleicher Anionenkonzentration. Da dieser Nachteil, der von der Acidität der Probelösung herrührt, durch Neutralisation mit Ammoniakwasser beinahe vollends beseitigt wird (vgl. die bemerkenswürdige Ähnlichkeit zwischen der Gestalt von Kurve-IIA′ sowie IIB′ und der von Kurve-IIIA sowie IIIB), ist es wahrscheinlich, dass diese ungewöhnlich niedrige Färbungsintensität der Harzphase auf die Aggregation[9] der Molybdationen in der Lösung zu Riesenanionen beruht, die selbst mit Dowex 1-X1 schwierig sich adsorbieren lassen.

Einflüsse der Begleitstoffe

Wie man in Tabelle II klar ersieht, wurden die Einflüsse verschiedenartiger Begleitstoffe auf die Nachweisreaktion besonders ausführlich untersucht, und dabei wurde die Störung solcher Kationen wie Kupfer(II), Kobalt(II), Nickel(II), Uranyl(II) usw. durch einfache Anwendung einer Mikrosäule des starksauren Kationenaustauschharz von NH_4R-Form (Abb. V)[10] sehr leicht und völlig beseitigt.

Tabelle II

Einflüsse der Begleitstoffe

Begleitstoffe	benutzter Verbindungstypus	Menge von Begleitstoffen	Nachweisbare Molybdänmenge	Grenzverhältnis	Bemerkungen
Cr(VI)	K_2CrO_4	Stört völlig den Nachweis.		—	—
〃 〃	$K_2Cr_2O_7$	180 γ	0.054 γ	$1:3.3\times10^3$	*a*
W(VI)	Na_2WO_4	Stört völlig den Nachweis.		—	—
〃 〃	〃 〃	220 γ	0.12 γ	$1:1.8\times10^3$	*b*
U(VI)	$UO_2(CH_3COO)_2$	112 γ	0.098 γ	$1:1.15\times10^3$	U(VI)≦0.3proz.
〃 〃	〃 〃 〃 〃	4 mg	0.049 γ	$1:8.2\times10^4$	*c*
Mn(II)	$MnSO_4$	1.6 mg	0.049 γ	$1:3.3\times10^4$	—
Fe(III)*	$FeCl_3$	830 γ	0.098 γ	$1:8.5\times10^3$	—
Co(II)**	$CoCl_2$	230 γ	0.24 γ	$1:9.6\times10^2$	Co(II)≦0.5proz.
〃 〃	〃 〃	2.3 mg	0.12 γ	$1:1.9\times10^4$	*c*
Ni(II)	$NiCl_2$	1 mg	0.24 γ	$1:4.1\times10^2$	—
Cu(II)	$CuSO_4$	20 γ	0.24 γ	$1:8.3\times10$	Cu(II)≦0.05proz.
〃 〃	〃 〃	1.6 mg	0.06 γ	$1:2.7\times10^4$	*c*
Zn(II)	$ZnSO_4$	280 γ	0.036 γ	$1:7.8\times10^3$	—
Cd(II)	$CdCl_2$	380 γ	0.098 γ	$1:3.9\times10^3$	—
Hg(II)	$HgCl_2$	740 γ	0.024 γ	$1:3.1\times10^4$	—
$PO_4^{3-}(H_2PO_4^-)$	H_3PO_4	7.2 mg	0.048 γ	$1:1.5\times10^5$	—
NO_2^-	$NaNO_2$	44 γ	0.20 γ	$1:2.2\times10^2$	NO_2^-≦0.1proz.
NO_3^-	NH_4NO_3	7.4 mg	0.12 γ	$1:6.2\times10^4$	—
Oxalsäure	Oxalsäure	2.3 mg	0.041 γ	$1:5.6\times10^4$	—
Weinsäure	Weinsäure	3.7 mg	0.054 γ	$1:6.7\times10^4$	—
Zitronensäure	Zitronensäure	3.6 mg	0.028 γ	$1:1.3\times10^5$	—

* 10prozentige Lösung (6N HCl) des $SnCl_2$ wurde angewandt.

** Drei Tropfen der 1proz. Lösung des NH_4SCN wurde angewandt.

a: Nach der Reduktion des Chromates zum Chrom(III)salze durch gelindes Erhitzen auf einem Wasserbad mit einem Tropfen der 3proz. Lösung (1N H_2SO_4) des Wasserstoffperoxydes:

b: Nach der Trennung des Wolframates als Wolframsäureniederschlag durch Zusatz von einem Tropfen der 6- bzw. 12N Salzsäure: Es ist wahrscheinlich, dass es hier um eine Art der Siebeffekt von der Harzphase für Polymolybdate und Polywolframate sich händelt.

c: Nach der Trennung des Kations durch eine Mikroharzsäule von NH_4R-Form (Abb. 5):

10) Trennung von Metallionen mit Hilfe dieser Mikroharzsäule wird folgenderweise durchgeführt: Mit einer kleinster Mikropipette (P: ein Tropfen=0.02 ccm) fügt man zu dieser Mikrosäule einen Tropfen der Probelösung, worin verschiedenartige fremde Metallionen, die die Nachweisreaktion stören, enthalten sind, und wäscht die Säule danach mit zwei bzw. drei Tropfen destilliertes Wassers aus (1 Tropfen/Min). Man kann mit hier erhaltener metallionenfreier Lösung von Ammoniummolybdat und in der Vertiefung der Tüpfelplatte vorher vorbereiteten Anionenaustauschharzkörnchen in gewöhnlicher Weise den Nachweis des Molybdäns durchführen. Die gebrauchte Harzsäule wird durch dreimaliges Durchlaufen je dreissig Tropfen der 2 N Salzsäure, 6 N Ammoniakwassers und destilliertes Wassers leicht in die NH_4R-Form zurückgeführt.

Zusammenfassung

1. Durch einfache Anwendung farbloser starkbasischer Anionenaustauschharze zur Farbenreaktion der Molybdate mit Rhodanid und Zinn(II)chlorid wird eine neue sehr empfindliche und spezifische Methode zum Nachweis kleinster Menge des Molybdäns vollkommen festgestellt, und dabei wird das best geeignete Verfahren durch Vergleichungen verschiedener Experimentalbedingungen ausführlich untersucht.

2. Die Einflüsse der Anionen- sowie Wasserstoffionenkonzentration von der Probelösung auf die Empfindlichkeit der Nachweisreaktion werden genau untersucht, und durch genügende Überlegung über das Anionenaustauschgleichgewicht zwischen Chlorid- und Molybdationen und über die Aggregation der Molybdationen werden diese Beziehungen halbquantitativ genau diskutiert.

3. Die Einflüsse verschiedenartiger Begleitstoffe wird vollkommen studiert, wobei eine einfache Mikrosäule des Kationenaustauschharzes von NH_4R-Form zur Trennung fremder Kationen, die die Reaktion beträchtlich stören, erfolgreich angewandt wird.

Zum Schluss möchte der Verfasser Herrn Prof. Dr. E. Minami für seine vielen wertvollen Ratschläge sowie freundliche Anregungen über diese Untersuchung seinen herzlichsten Dank aussprechen.

Laboratorium der analytischen Chemie,
Chemisches Institut der
wissenschaftlichen Fakultät,
Tokyo Universität, Tokyo

Mikroanalyse mit Hilfe von Ionenaustauschharzen. VI. Über den Nachweis kleinster Menge des Nitrites mit m-Phenylendiamin[1]

Von Masatoshi FUJIMOTO

(Eingegangen am 24. März 1956)

Einleitung

Aus einer sauren wässerigen Lösung wird das *m*-Phenylendiamin in der Form von Ammoniumion in starksaures Kationenaustauschharz von HR-Form stark adsorbiert. Wirkt die salpetrige Säure oder das Nitrit bei Anwesenheit der Säuren auf das in der Lösungsphase vorhandene *m*-Phenylendiamin ein, so bildet sich intermediär ein Gemisch der Diazoniumsalze gemäss den folgenden stufenweisen Reaktionsgleichungen:

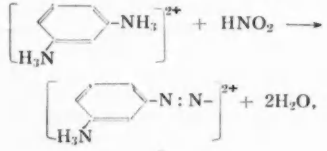

I

oder weiter

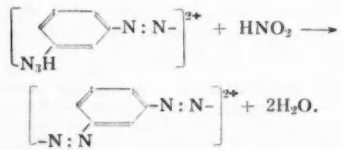

II

Sobald die letztgenannten Reaktionen stattfinden, werden die hier gebildeten Diazoniumionen (I und II) gleichfalls in obengenanntes Harz stark adsorbiert, worin diese beiden sogleich mit dem bereits in die Harzphase etwas adsorbierten *m*-Phenylendiamin koppeln und durch intramolekulare Umlagerung in ein Gemisch kationischer Azofarbstoffe (III und IV), sogenanntes Bismarckbraun[2], übergeführt werden:

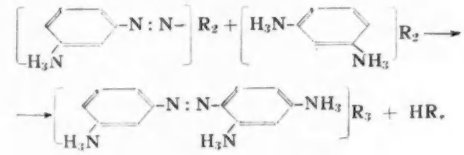

III

und auch

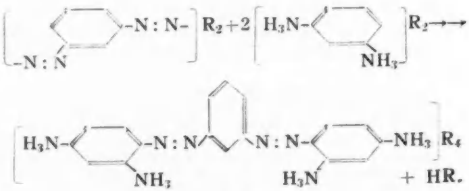

IV

1) Die fünfte Mitteilung: M. Fujimoto, Dieses Bulletin **29**, 595 (1956).

Hierbei bedeutet R einwertiges Anion vom Kationenaustauschharze.

Wegen sehr beschränktes Rauminhalts[3] der Harzkörnchen, worin die obenerwähnten Farbstoffionen unmittelbar gebildet werden, nimmt die Konzentration dieser sich färbenden Kationen durch Adsorption in die Harzphase merklich zu, und demnach verstärkt sich die Färbung der Harzphase auffallend. Auf solche Weise konnte man eine neue und sehr empfindliche sowie spezifische Nachweismethode für die Spurmenge des Nitrites mit dem Kationenaustauschharze[4] folgendermassen feststellen.

Die in dieser Untersuchung benutzten Kationenaustauschharze

Zum gegenwärtigen Zwecke wurde ein aus Styrol und Divinylbenzol dargestelltes starksaures sowie farbloses Harz von Sulfonsäuretypus hauptsächlich angewandt, dessen Divinylbenzolgehalt einprozentig ist[5]. Die Korngrösse ist ungefähr 30 Maschen von Tylerschem Normalsieb. In der vorliegenden Mitteilung wird dieses Harz als „1proz. DVB" kurz beschrieben.

Überdies wurden folgende Harze auch angewandt:

„20proz. DVB": Ein ebenso starksaures und gelbes Kationenaustauschharz wie das letztgenannte Harz, dessen Divinylbenzolgehalt jedoch zwanzigprozentig ist.[5] Die Korngrösse ist ungefähr 50 Maschen.

Dowex 50W-X8: Ein käufliches farbloses und starksaures Harz von Sulfonsäuretypus, dessen Divinylbenzolgehalt etwa achtprozentig ist. Die Korngrösse ist 50 bis 100 Maschen.

Duolite C-60: Ein hellgelbes mittelstarksaures Kationenaustauschharz von Phosphonsäuretypus, dessen Korngrösse ungefähr 20 Maschen ist.

Alle diese Harze wurden vor dem Gebrauch durch zweimaliges Durchlaufen der 2 N Salzsäure sowie destilliertes Wassers völlig in die HR-Form übergeführt.

Versuchsanordnung

Man bringt auf eine weisse Tüpfelplatte einige Körnchen des Kationenaustauschharzes und einen Tropfen verdünnter Reagenslösung, rührt danach mit einem kleinen Glasstab völlig um, und lässt sie einige Minuten lang stehen. Dann fügt man einen Tropfen der Probelösung, und nach einigen Minuten, beobachtet man unter Beleuchtung einer Tischlampe mit einer Lupe eine in der Harzphase entstandene Orange- bzw. Braunfärbung.

Bestimmung der Bedingungen höchster Empfindlichkeit

1. Massflüssigkeit.—Zum vorliegenden Zwecke wurde eine Reihe der Massflüssigkeiten des Nitrites aus der wässerigen Lösung des extrareinen Natriumnitrites vorbereitet, deren 1 ccm 9.75 mg von Nitrite (als NO_2) enthielt[6].

2. Reagenslösung.—Als die Stocklösungen des *m*-Phenylendiamins wurden folgende zwei Arten der Lösungen vorbereitet:

(1) Eine in die 0.3 N Salzsäure gelöste 0.5-prozentige Lösung.

(2) Eine in die 10prozentige Essigsäure gelöste 0.5prozentige Lösung.

3. Einfluss der Harzart[7].—Betrachtet man aus der Vergleichung verschiedenartiger Harze,

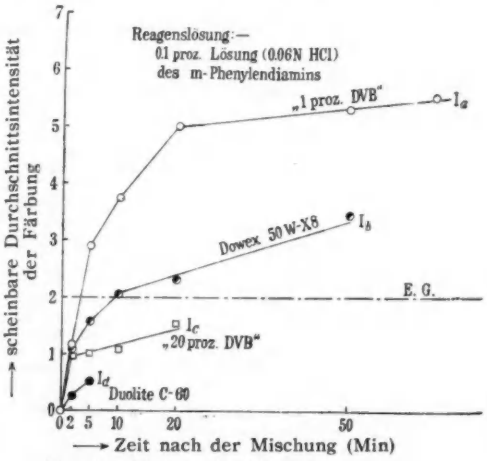

Abb. 1. Einfluss der Harzart.

2) Nur dann, wenn die obengenannten Azofarbstoffe innerhalb der Harzphase unmittelbar sich bilden, ist die gegenwärtige Nachweismethode wirksam, da die bereits in der Lösungsphase völlig gebildeten Farbstoffe wegen ihrer geringen Löslichkeit in Wasser sowie ihrer grösseren Ionenvolumen nur langsam in die Harzphase adsorbiert werden und die Färbung der Harzphase infolgedessen an ihrer Intensität geringfügig sich verstärkt (vgl. den Verlauf der Kurve-I_d von Abb. II).

3) Angenommen, dass bei der Reaktion zehn Körnchen des Harzes, dessen Korngrösse beim Eintauchen in der Lösung sechzig Maschen sei, benutzt werden, so beträgt das Volumenverhältnis zwischen der Harzphase und der Lösungsphase (0.08 ccm) etwa 1:520.

4) Starkbasisches Anionenaustauschharz adsorbiert auch diese Farbstoffe, obgleich die Ursache dafür gegenwärtig unverständlich sei. Aber die Anionenaustauschharze wurden diesmal nicht benutzt, da diese im Vergleich mit den Kationenaustauschharzen bedeutend schwächer sich färben.

5) Diese beiden Harzproben wurden von Herrn Prof. Dr. A. Kawamura an der Landwirtschaftlichen und Technischen Universität zu Tokyo nach dem Verfahren K.W. Peppers kürzlich dargestellt.

6) Die Menge in der Massflüssigkeit vorhandener Nitritionen wurde folgenderweise titrimetrisch bestimmt: 20 Min nach dem Zusatze bestimmter Menge der Massflüssigkeit des Nitrites zu einem Gemisch bestimmtes Überschusses von 0.1 N Kaliumpermanganatmassflüssigkeit und verdünnter Schwefelsäure, fügt man dazu etwa 1 g festes Kaliumjodides und titriert das hier gebildete freie Jod mit 0.1 N Massflüssigkeit des Natriumthiosulfates (vgl. S. Takagi „Teiryo-Bunseki no Jikken to Keisan (Experimente und Rechnung der quantitativen Analyse)," Band II., 5. Aufl., 1952, (japanisch), Tokyo, S. 363.

7) In bezug auf die in Abbildungen gegenwärtiger Mitteilung angewandte halbquantitative Darstellungsweise der scheinbaren Durchschnittsintensität der Färbung von der Harzphase, vergleiche III. Mitteilung: M. Fujimoto, Dieses Bulletin 29, 567 (1956).

die in Abb. 1 steht, wird das Harz, „1proz. DVB", als das best geeignete ausgewählt.

4. Vergleichung verschiedener Versuchsbedingungen.—Abb. 2 stellt die Resultate der Vergleichungen von den in Tabelle I kurzgefassten verschiedenen Experimentalbedingungen dar.

Aus der obigen Weise, werden hier zwei Verfahren, d.h., „I_n" und „I_a" als die insbesondere ausgezeichneten festgestellt; nämlich:

„Auf eine weisse Tüpfelplatte bringt man einige Körnchen des Kationenaustauschharzes, „1proz. DVB", von HR-Form sowie einen Tropfen der in die 0.06 N Salzsäure oder in die 10prozentige Essigsäure gelösten 0.1prozentigen Lösung des *m*-Phenylendiamins, rührt mit einem kleinen Glasstab um, und lässt sie etwa 10 Min stehen. Dann fügt man dazu einen Tropfen der Probelösung, und nach einigen Minuten, beobachtet man eine Braunorange- bzw. Rotorangefärbung, die über dem Ganzen der Harzkörnchen entsteht".

Hier muss man darauf besonders beachten, dass man die Salzsäure nicht im Überschuss anwendet.

TABELLE I

VERSCHIEDENE EXPERIMENTALBEDINGUNGEN VON ABB. 2

Nr. des Experiments	Zeichen der Kurve	Ordnung der Versetzung von Reagenzien und Probelösung 1.	2.	3.	4.	Bemerkungen über die Resultate*
I_a	—○—	HR**	0.1proz. Lsg.—(10 Min)***→Probelsg.**** (0.06 N HCl) des *m*-Phenylendiamins		——	*a*
I_e	—◑—	HR	0.5proz. Lsg.—(10 Min)→Probelsg. (0.3 N HCl) des *m*-Phenylendiamins		——	*a*
I_f	—△—	0.5proz. Lsg. (0.3 N HCl) des *m*-Phenylendiamins	Probelsg.—(10 Min)→HR		——	*b*
I_g	—×—	HR	6 N HCl	0.5proz. Lsg.—(10 Min)→Probelsg. (0.3 N HCl) des *m*-Phenylendiamins		*a*
I_k	—□—	HR	Probelsg.	0.1proz. Lsg. (0.06 N HCl) des *m*-Phenylendiamins	——	*a*, *c*
I_h	—▣—	HR	Probelsg.	0.5proz. Lsg. (0.3 N HCl) des *m*-Phenylendiamins	——	*a*, *c*
I_j	—◇—	HR	0.1proz. Lsg.—(5 Min)→Probelsg. (0.06 N HCl) des *m*-Phenylendiamins		——	*d*, *e*
I_i	—◈—	HR	0.5proz. Lsg.—(5 Min)→Probelsg. (0.3 N HCl) des *m*-Phenylendiamins		——	*a*, *d*
I_l	—■—	HR	0.5proz. Lsg.—(5 Min)→Probelsg. (0.3 N HCl) des *m*-Phenylendiamins		6 N HCl	*a*, *d*
I_m	--×--	HR	0.5proz. Lsg.—(5 Min)→Probelsg. (0.3 N HCl) des *m*-Phenylendiamins		6 N HCl	*f*
I_n	—⊙—	HR	0.1proz. Lsg.—(10 Min)→Probelsg. (10proz. CH_3COOH) des *m*-Phenylendiamins		——	*e*

**a*: Enthält die Probelösung kein Nitrit, so färben sich die Harzkörnchen nur schwach Purpur.

b: Die Harzkörnchen färben sich sehr langsam an ihren Rändern[2].

c: Gerade nach dem Zusatze von der Probelösung, wird die Lösung des *m*-Phenylendiamins hinzugefügt.

d: Etwa fünf Minuten nach dem Zusatze der Lösung des *m*-Phenylendiamins, werden die Harzkörnchen mit je drei Tropfen destilliertes Wassers dreimal ausgewaschen.

e: Wenn kein Nitrit in der Probelösung vorhanden ist, werden die Harzkörnchen kaum gefärbt.

f: Die Harzkörnchen sind beinahe farblos.

** HR bedeutet bei der vorliegenden Tabelle „1proz. DVB" von HR-Form.

*** Zeitdauer nach dem Eintauchen der Harzkörnchen in die Reagenslösung.

**** Die hier benutzte Probelösung enthält 0.39 γ Nitrit (9.75 γ/ccm).

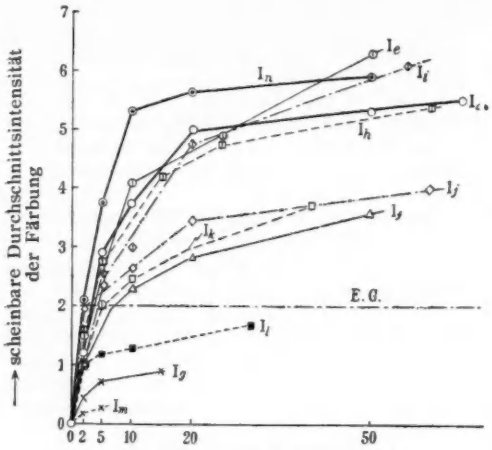

Abb. 2. Einflüsse verschiedener Experimentalbedingungen.

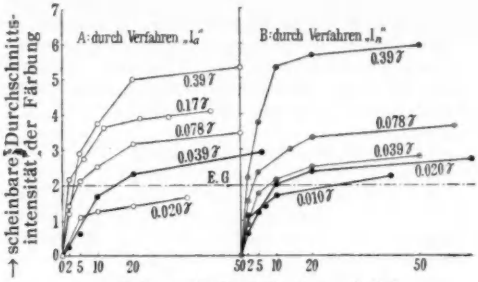

Abb. 3. Bestimmung der Erfassungsgrenze.

Bestimmung der Erfassungsgrenze

Die Ergebnisse durch Verfahren „I_n" sowie „I_a" durchgeführter Experimente werden in Abb. 3A sowie 3B zusammengestellt:

Die so bestimmte Erfassungsgrenze und die Grenzkonzentration an dieser Reaktion für Nitrit stehen in nachfolgender Tabelle:

	Durch Verfahren „I_a":	Durch Verfahren „I_n":
Erfassungsgrenze	0.039 γ NO_2	0.015 γ NO_2
Grenzkonzentration	$1:1.0\times10^6$	$1:2.7\times10^6$

Einflüsse der Begleitionen

Die Resultate durch Verfahren „I_n" durchgeführter Untersuchungen stehen in Tabelle II:

Nachweis des Nitrates nach der Reduktion zum Nitrite mit Zinkstaub

Durch Zusatz von Zinkstaub werden die Nitrate sehr glatt zu den Nitrite reduziert, und demnach werden diese mit Hilfe obengenannter Verfahren leicht nachgewiesen.

Hier wurde eine wässerige Lösung des Kaliumnitrates, deren 1 ccm 10 mg von Nitrat (als NO_3) enthielt, als die Massflüssigkeit des Nitrates vorbereitet.

Der käufliche Zinkstaub, so wie er ist, reagiert mit Nitrationen nur langsam. Daher wurde dieser, um dessen Reduktionsaktivität beträchtlich zu vergrössern, mit 1 N Essigsäure auf einem Wasserbade etwa ein Stunde lang erwärmt,

TABELLE II

EINFLÜSSE DER BEGLEITIONEN

Begleitionen	benutzter Verbindungstypus	Menge der Belgleitionen	Nachweisbare Nitritmenge	Grenzverhältnis	Bemerkungen*
F^-**	KF	Stört völlig den Nachweis.		——	*a*
Cl^-	NaCl	7.1 mg	0.03 γ	$1:2.4\times10^5$	——
Br^-	KBr	7.7 mg	0.02 γ	$1:3.8\times10^5$	——
J^-	KJ	9.2 mg	0.02 γ	$1:4.6\times10^5$	——
SCN^-	NH_4SCN	4.1 mg	0.015 γ	$1:2.7\times10^5$	——
S^{2-}	Na_2S	180 γ	0.017 γ	$1:1.1\times10^4$	*b*
SO_4^{2-}	Na_2SO_4	850 γ	0.14 γ	$1:6.1\times10^3$	——
〃	〃	2.2 mg	0.04 γ	$1:5.7\times10^4$	*c*
$Cr_2O_7^{2-}$	$K_2Cr_2O_7$	Stört völlig den Nachweis.		——	*d*
NO_3^-	KNO_3	10 mg	0.08 γ	$1:1.3\times10^5$	——
PO_4^{3-}	Na_2HPO_4	8.6 mg	0.04 γ	$1:2.2\times10^5$	——

*a: Die Lösungsphase färbt sich orangebraun und die Harzphase hellrot.

b: Infolge der Bildung von weissem Niederschlag wird die Färbung der Harzphase verhältnismässig schwierig erkennbar.

c: Nach dem Zusatze von zwei Tropfen 10 prozentiger Lösung von Bariumchlorid, wird der Nachweis durchgeführt.

d: Ein dunkelbrauner Farbstoff wird gebildet, der die Harzphase intensiv dunkelbraun färbt.

** Noch ein Tropfen 33prozentiger Essigsäure wird angewandt.

dekantiert, mit Wasser dreimal umgewaschen, und in einem Vekuumexsikkator völlig getrocknet[8].

Die kleinste Nitratmenge, die nach der Reduktion mit der Nadelspitzmenge[9] des oben behandelten Zinkstaubs nachgewiesen wurde, war jedoch 0.08 γ durch Verfahren „I_n" und 0.4 γ durch „I_a".

Zusammenfassung

1. Durch Anwendung starksaurer Kationenaustauschharze zu einem der Diazoreaktionssysteme gelingt es, starkgefärbte Azofarbstoffkationen, Bismarckbraun, unmittelbar in dem sehr beschränkten Rauminhalt des Harzkörnchens fest bilden zu lassen, und dadurch wird eine neue und sehr empfindliche Nachweismethode für kleinste Menge des Nitrites mit *m*-Phenylendiamin festgestellt.

2. Zwei Arten der Verfahren höchster Empfindlichkeit werden durch ausführliche Erforschung über verschiedene Experimentalbedingungen einwandfrei festgestellt, und durch deren Anwendung werden die Einflüsse verschiedenartiger fremder Anionen vollständig untersucht.

3. Weiterhin wird geringe Menge des Nitrates auch nach der Reduktion mit der Nadelspitzmenge des Zinkstaubs gleichermassen wie beim Nitrit nachgewiesen.

Zum Schluss möchte der Verfasser Herrn Prof. Dr. E. Minami für seine freundlichen Anregungen bei vorliegender Untersuchung seinen herzlichsten Dank aussprechen.

Für die Kationenaustauschharze, „1proz. DVB" sowie „20proz. DVB",[5] ist der Verfasser Herrn Prof. Dr. A. Kawamura an der Landwirtschaftlichen und Technischen Universität zu Tokyo zu verbindlichstem Dank verpflichtet.

Laboratorium der analytischen Chemie,
Chemisches Institut der
wissenschaftlichen Fakultät,
Tokyo Universität, Tokyo

8) Vgl. F. Feigl, „Spot Tests. I. Inorganic Applications," übersetzt von R.E. Oesper, 4. engl. Aufl., 1954, Amsterdam, S. 302.

9) Sie entspricht etwa 200 γ.

Studies on the Infrared Spectra of Ephedrine and Related Compounds. III. Infrared Spectra of Diastereoisomeric N-Methylephedrines and 1, 2-Diphenyl-2-methylaminoethanols-(1) in 3 micron Region

By Tokunosuke KANZAWA

(Received February 13, 1956)

The spectra of the diastereoisomeric N-methylephedrines and 1, 2-diphenyl-2-methylaminoethanols-(1) in 3 micron region are very like those of ephedrines as shown in the previous paper[1], but their $\Delta\nu$ values, which are differences in wave numbers of the free and the bonded OH absorption band, are somewhat different from those of ephedrines. Thus, the difference in $\Delta\nu$ values between N-methylephedrine isomers ($238-157=81\ cm^{-1}$) is much larger than that between ephedrines ($203-168=35\ cm^{-1}$). On the other hand, the two isomers of 1, 2-diphenyl-2-methylaminoethanol-(1) give smaller $\Delta\nu$ values (151 and 193 cm^{-1}) than those of ephedrines, and the erythro isomer exceptionally shows an absorption near 3600 cm^{-1} consisting of two bands by 30 cm^{-1} apart from each other, whereas the other compounds examined show only one band. Although these two pairs of compounds are similar in chemical behavior to ephedrines, the appreciable changes in $\Delta\nu$ seem to be related to the change of steric structure caused by substitution of the groups. The object of the present experiments is to obtain information on the molecular structure of these compounds and to discuss their conformations in connection with that of ephedrines as proposed previously[2].

Experimental

The spectrophotometer used, its operating conditions and the procedure for the purification of the solvents are the same as described previously[2]. N-methylephedrines were in optically active forms and 1, 2-diphenyl-2-methylaminoethanols-(1) were racemic modifications. They were supplied by Dr. K. Tanaka and Mr. T. Sugawa in this Laboratory.

1) T. Kanzawa, This Bulletin, 29, 398 (1956).

2) T. Kanzawa, This Bulletin, 29, 479 (1956).

Experimental Results

A. N-Methylephedrines.—In Fig. 1. the concentration dependence of the absorption for N-methylephedrines is shown. Over a concentration range of 0.001–0.01 mol./l. the spectra of both isomers show no appreciable change in the position and intensity of the absorption bands. On raising the concentration up to a few tenth mol./l. spectral changes are observed for both isomers, although not so marked as in the cases of ephedrines. Thus, for N-methylephedrine the intensity of a sharp band at 3617 cm^{-1} decreases and that of a broad band at 3460 cm^{-1} increases with concentration. For *l*-N-methylephedrine a band at 3613 cm^{-1} disappears already at 0.045 mol./l. (not shown in Fig. 1b) and the intensity of a broad band at 3375 cm^{-1} decreases. The shift of the broad band towards lower frequency for the concentration change from ~0.005 to ~0.1 mol./l. is about 10 cm^{-1} for both isomers.

Since N-methylephedrines have no NH group, it will be reasonable to assign the higher-frequency band to free OH stretching vibration and the lower-frequency one to bonded OH vibration (OH -N). From a behavior in concentration dependence it may be said that as long as the concentration remains small the hydrogen bond is of an intramolecular type. The possibility of the formation of the ring dimer seems to be difficult to consider from cryoscopic data for alkamines[3]. In the spectra of the dilute solution shown in Fig. 1a and 1b, it will be noticed that, when

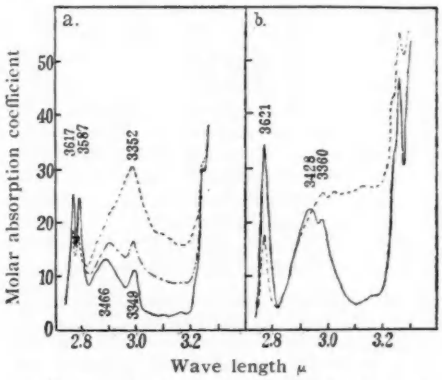

Fig. 1. Concentration dependence. N-Methylephedrine. CCl_4 solns.
a) normal. ——— 0.0046 (2 cm.), —·—· 0.097 (0.056 cm.), - - - - 0.19 mol./l. (*r*).
b) pseudo. ——— 0.0053 (2 cm.), - - - - 0.45 mol./l. (0.0195 cm.).

compared with the corresponding diastereoisomers of ephedrine, N-methylephedrine shows a smaller $\Delta\nu$ value (157 cm^{-1}) and a comparable intensity of the free OH absorption, while *l*-N-methylephedrine shows a much larger $\Delta\nu$ value (238 cm^{-1}) and a much smaller intensity.

3) E. D. Bergmann, E. Gil-Av. and S. Pincas, *J. Am. Chem. Soc.*, **75**, 68 (1953).

The shifts of the bonded OH absorptions with increasing concentration for N-methylephedrines are smaller than those for ephedrines (30 cm^{-1}) and no band appears near 3300 cm^{-1} as seen in the cases of ephedrines, where the band was assumed to be due to OH---O intermolecular hydrogen bond. For N-methylephedrine, this absence may be due to the lack of appreciable association at a concentration of 0.19 mol./l. The spectrum at a concentration higher than 0.19 mol./l. could not be taken because of the precipitation of crystallites. For *l*-N-methylephedrine the spectrum at a concentration of 0.45 mol./l. (Fig. 1b) may show one in a state containing associated molecules, because in the spectrum of liquid state only one broad band appears at 3347 cm^{-1}.

B. 1, 2-Diphenyl-2-methylaminoethanol-(1).—1) Concentration-Dependence.—In Fig. 2a the concentration dependence of the absorption of erythro (normal) 1, 2-diphenyl-2-methylaminoethanol-(1) is shown. Since this compound has the hydroxyl and methylamino groups like ephedrine, it is expected that spectra similar to that of ephedrine should be obtained. However, as seen in Fig. 2a the spectra are quite different. Thus, the absorption near 3600 cm^{-1} is a doublet composed of two sharp bands (3617 and 3587 cm^{-1}) of about the same intensity, and a broad absorption at 3466 cm^{-1} is weaker than the bands near 3600 cm^{-1} and also a well-defined band appears at 3349 cm^{-1}.

On raising the concentration, the intensities of the two bands near 3600 cm^{-1} decrease in the same degree and at a concentration of 0.063 mol./l. a single absorption appears at 3352 cm^{-1}. Since, as in the cases of ephedrines and N-methylephedrines, the intensities and the positions of the absorption bands remain unchanged in a concentration range 0.001–0.01 mol./l., the presence of the intramolecular hydrogen bond will be expected in a dilute

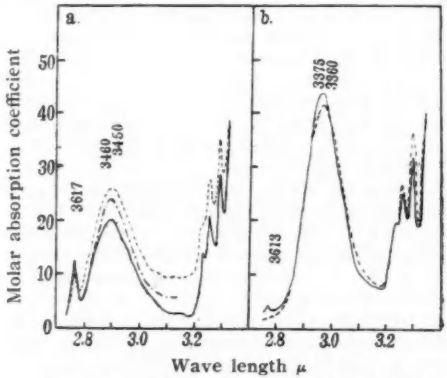

Fig. 2. Concentration dependence. 1,2-Diphenyl-2-methylamino-ethanol-(1). CCl_4 solns.
a) erythro (normal). ——— 0.0062 (2 cm.), —·—· 0.046 (0.3 cm.), - - - - 0.068 mol./l. (*r*).
b) threo (pseudo). ——— 0.0031 (2 cm.), - - - - 0.068 mol./l. (0.3 cm.).

solution. The spectrum at 0.063 mol/l. shows an interaction between molecules and thus the association occurs at a lower concentration than in the cases of ephedrines (0.1–0.2 mol./l.). As for the doublet structure of the bands near 3600 cm^{-1}, it seems that some kind of resonance splitting occurs as will be discussed later.

The band at 3466 cm^{-1}, which becomes stronger and shifts to 3448 cm^{-1} with concentration increase may be due to OH vibration perturbed by an intramolecular OH---N hydrogen bond in the same way as in the cases of ephedrines. The band at 3349 cm^{-1}, which may be assigned to NH vibration, is more intense than the NH absorption for ephedrines. This increase in the intensity of the NH absorption may be attributed to a change of structure from methylethylamine type of ephedrines to methylbenzylamine type*.

An intense peak at 3352 cm^{-1} at a higher concentration may be the superposition of the bonded OH absorption shifted by an intermolecular OH---O hydrogen bond and the NH absorption. It will be noticed that $\Delta\nu$ (151 cm^{-1}) between the higher-frequency component of the free OH vibration and the broad band at 3466 cm^{-1} is smaller than that of ephedrine (168 cm^{-1}) and the intensity ratio of the sharp component to the broad one is much larger than that for ephedrine and N-methylephedrine.

Threo 1, 2-diphenyl-2-methylaminoethanol-(1) (Fig. 2b) shows only one band near 3600 cm^{-1} unlike erythro isomer and a similar absorption in a range 2.7–3.3 μ to that of γ-ephedrine and γ-N-methylephedrine. The change in the absorption with concentration proceeds in the same manner as the other compounds. Therefore, a band at 3621 cm^{-1} can be assigned to free OH vibration, and a band at 3428 cm^{-1} to bonded OH vibration and further a peak at 3360 cm^{-1} to NH vibration. Here again, the NH absorption is more intense than that of γ-ephedrine. At a concentration of 0.068 mol./l. association is appreciable. As in the case of the erythro isomer, at the lower concentration, the free OH absorption is stronger than the bonded one and, at the higher concentration, the bonded OH absorption at 3428 cm^{-1} is covered by a slope of a peak at 3348 cm^{-1}. In this case a continuous absorption over a range 3.0–3.2 μ appears unlike the erythro isomer.

2) Solvent Effect and Interaction with Triethylamine.—The solvent effect and the interaction with triethylamine were studied in order to obtain information on the nature of the doublet band shown by erythro 1, 2-diphenyl-2-methylaminoethanol-(1) (Fig. 3).

In carbon disulfide solution the doublet bands shift towards lower frequency, compared with those in carbon tetrachloride solution, and the lower frequency component (3571 cm^{-1}) is much more intense than the higher-frequency one (3592 cm^{-1}). At a lower concentration, the bonded OH absorption (3442 cm^{-1}) and NH absorption (3338 cm^{-1}) are well-defined. At a higher concentration, association seems to occur and the NH absorption still remains. The tendency of association of the erythro compound in carbon disulfide solution is weaker than that of ephedrine.

In chloroform solution the shift of the doublet is to about the same degree as in carbon disulfide solution and the intensities of the components are about the same. The NH absorption at 3344 cm^{-1} is stronger than the bonded OH absorption. A weak absorption seems to appear in the region with longer wave length than NH absorption, but no appreciable association occurs.

In benzene solution the free OH absorption is not a doublet, but a single band at 3571 cm^{-1}. The bonded OH absorption is weak and the NH absorption is well-defined.

In Fig. 3b the interaction of the erythro compound with triethylamine in carbon tetrachloride solution is shown. By addition of triethylamine, the higher-frequency component of the doublet becomes weaker than the lower-frequency one and a continuous absorption appears in 3.1–3.3 μ region. At a concentration of 0.5 mol./l. of triethylamine the bonded OH absorption still remains and the NH absorption at 3345 cm^{-1} shifts to 3339 cm^{-1} and new bands appear at 3185 and 3143 cm^{-1}. These spectral bahaviors may be explained as in the cases of ephedrines[2]. By the interaction of free molecules with triethylamine an intermolecular OH---N hydrogen bond is formed and gives rise to an absorption at 3143 cm^{-1}. At the same time $NHCH_3$ group bridged by an intramolecular OH---N bond may interact with triethylamine and causes an absorption (NH---N) at 3185 cm^{-1}. It is seen that the intramolecularly bonded OH absorption and the NH absorption still remains at higher concentrations of triethylamine.

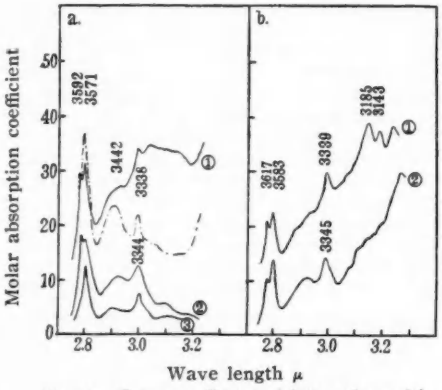

Fig. 3. Solvent effect and interation with triethylamine. Erythro 1, 2-diphenyl-2-methylaminoethanol-(1).
a). 1. CS_2 ——— 0.03 (2 cm.), —·—· 0.0044 mol./l. (0.3 cm.) 2. $CHCl_3$, 0.16 mol./l. (0.056 cm.) 3. Benzene, 0.16 mol./l. (ν).
b). 1. 0.02 mol./l. + $(C_2H_5)_3N$ 0.26 mol./l. 2. +0.5 mol./l. (0.3 cm.) in CCl_4.

* According to the results obtained by Russell and Thompson (*J. Chem. Soc.*, **1955**, 483) absorption of ν(NH) in dibenzylamine is stronger than that in dialkylamine.

Discussion

The above results may be explained in the same manner as described for ephedrines[2]. The conformations capable of forming an intramolecular OH---N hydrogen bond are illustrated in Fig. 4 for diastereoisomers of N-methylephedrine and 1, 2-diphenyl-2-methylaminoethanol-(1). The appearance of the free OH absorption in the spectra for these two diastereoisomers will mean that all the compounds examined may be mixtures of rotational isomers, in one of which the OH and NR_1CH_3 groups are *trans* and in the others of which they are *gauche*.

$\Delta\nu$ of N-methylephedrine (151 cm^{-1}) is somewhat smaller than that of ephedrine (168 cm^{-1}). This may be explained qualitatively as follows. $N(CH_3)_2$ group will exert a stronger repulsive force from its bulkiness and, on the other hand, in a favorable steric position, a stronger attraction because of the stronger proton accepting power than $NHCH_3$ group in ephedrine. Since a repulsion between the methyl and phenyl groups may be the same in both compounds, the repulsion between the OH and $N(CH_3)_2$ groups may contribute more to the $\Delta\nu$ value of N-methylephedrine than the attraction between them. The equilibrium ratio of the rotational isomers may be about the same as that for ephedrine.

On the other hand, for ψ-N-methylephedrine $\Delta\nu$ (238 cm^{-1}) is much larger than that for N-methylephedrine and ψ-ephedrine (203cm^{-1}). In this case the repulsion between the methyl and phenyl groups will give rise to a closer approach and accordingly a smaller $\Delta\nu$ than that of N-methylephedrine. However, considering the above-mentioned repulsion between the OH and $N(CH_3)_2$ groups $\Delta\nu$ of ψ-N-methylephedrine should be about the same as or smaller than that of ψ-ephedrine. Accordingly, the observed larger value of ψ-N-methylephedrine may be explained by the predominance of the other gauche type isomer than that shown in Fig. 4, in which the repulsion between the phenyl and $N(CH_3)_2$ groups will be larger than that between the phenyl and $NHCH_3$ groups in ephedrine. A possible explanation as regards the very weak intensity of the free OH vibration will be that the trans isomer may be fairly unstable because of the repulsion between bulky groups crowded together.

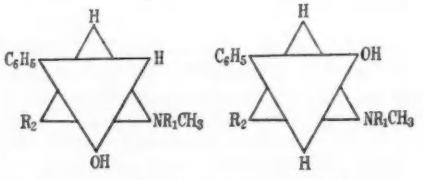

erythro (normal) threo (pseudo)

Fig. 4.

R_1	R_2	
H	CH_3	Ephedrine
CH_3	CH_3	N-Methylephedrine
H	C_6H_5	1, 2-Diphenyl-2-methylaminoethanol-(1)

For 1, 2-diphenyl-2-methylaminoethanol-(1) the origin of the doublet bands near 3600 cm^{-1} found for the erythro isomer should be discussed first. From the behavior of the doublet under various conditions described hitherto it will be noticed that the solvent effect seems to be different for each component. Such a tendency would suggest that the lower-frequency component might be caused by a sort of bonding of the OH group. Considering the smallness of $\Delta\nu$ (30 cm^{-1}) between the components, this bonding is not so strong as the ordinary OH---N hydrogen bonding. From this point of view proton acceptor other than $NHCH_3$ group should be considered. As an acceptor as such, the phenyl group attached to the asymmetric carbon atom adjacent to the other one having OH group might be considered. To confirm such an assumption a spectrum of benzylphenyl carbinol was taken in a dilute carbon tetrachloride solution. Only one sharp band was observed at 3610 cm^{-1} and therefore it may be said that the doublet is not caused by such an interaction. On the other hand, a spectrum of erythro 1, 2-diphenyl-2-aminoethanol-(1) showed also a doublet composed of bands at 3617 and 3590 cm^{-1}, a broad band at 3482 cm^{-1}, NH absorption at 3399 cm^{-1} and one more band near 3μ. The wave numbers of all the absorptions except one at 3617 cm^{-1} are larger than those of corresponding bands of erythro 1, 2-diphenyl-2-methylaminoethanol-(1). Those shifts are probably caused by a difference in nature of amino and methylamino groups. From these observations, it will be more reasonable to consider that the doublet is caused by some resonance effect or other.

It will be noticed from the spectra that the intensity of the free OH absorption at 3617 cm^{-1} for the threo isomer is stronger than the bonded OH absorption, and the intensities of the doublet for the erythro isomer are also stronger than that of the bonded one. Moreover, assuming the sum of the intensities of the components of the doublet as that of the free OH absorption subjected to no perturbation, an intensity ratio of the free OH absorption to the

bonded one is much larger for the erythro isomer than for the threo isomer. Accordingly this will mean that a rotational isomer having the OH and $NHCH_3$ groups in trans position is more stable in the erythro isomer than in the threo one. In addition it may be said from the comparison of the intensity ratios that the trans isomer is more aboundant in 1,2-diphenyl-2-methylaminoethanols than in ephedrines. These considerations on the equilibrium ratio of the rotational isomers can also be obtained by taking account of the repulsion between the larger phenyl groups in the conformation of the erythro compound shown in Fig. 4, although the presence of the stable trans isomer in the threo compound seems to be difficult to explain.

$\Delta\nu$ for the erythro isomer ($151\,cm^{-1}$) and the threo isomer ($193\,cm^{-1}$) are smaller than the corresponding isomers of ephedrine (168 and $203\,cm^{-1}$) and N-methylephedrine (157 and $238\,cm^{-1}$). This may be explained as follows. For the erythro isomer a larger repulsion between the phenyl groups of the gauche type molecule (Fig. 4) than that between the methyl and phenyl groups in ephedrine will give rise to a longer O-N distance and a smaller $\Delta\nu$ value than those in ephedrine. For the threo isomer, it can be expected that the repulsion between the phenyl groups will make $\Delta\nu$ larger than that of ephedrine. However, the experimental result is the reverse. Considering this fact another gauche isomer which has two phenyl groups in trans position may be more stable than that shown in Fig. 4 and show the smaller $\Delta\nu$ value as observed.

From the results obtained through this series of experiments, it can be concluded that the values of $\Delta\nu$ due to OH---N intramolecular hydrogen bond are more or less dependent on the kind and the nature of substituents attached to the asymmetric carbon atoms in ephedrine-like molecules. It has been observed, however, that $\Delta\nu$'s of the erythro (normal) isomers are always smaller than those of the threo (pseudo) isomers. The present finding of the presence of the intramolecular OH---N hydrogen bond in the erythro isomers as well as in the threo isomers may be related to the chemical fact that a crystalline ephedrine-copper complex can be prepared, although it is much less stable than ψ-ephedrine complex in aqueous organic solvent[4].

The author wishes to express his sincere thanks to Professor I. Nitta of Osaka University for his kind guidance and Dr. T. Shimanouchi of Tokyo University for his valuable advice. The Author's thanks are also due to Dr. S. Kuwada and Dr. A. Watanabe in this Laboratory for their continued encouragement.

Research Laboratory Takeda Pharmaceutical Industries, Ltd., Osaka

4) *Z.* Földi, T. Földi and A. Földi, *Chemistry and Industry*, 1297 (1955).

Introduction of Side Chains into Polyglycine Dispersed on Solid Surface. I

By Shiro AKABORI, Kenji OKAWA and Mikio SATO

(Received February 22, 1956)

In 1953, Snell[1] reported a reversible catalytic cleavage of β-hydroxy amino acids in the presence of pyridoxal and certain metal ions in aqueous solutions of pH 3–12. Th. Wieland[2] observed recently, the conversion of glycyl-residue into seryl- or threonyl residue by Snell's method.

$$\underset{\substack{|\\OH}}{\overset{|}{R\text{-}CH}}\text{-}\underset{\substack{|\\NH_2}}{\overset{|}{CH}}\text{-}COOH \rightleftharpoons R\text{-}CHO + \underset{\substack{|\\NH_2}}{\overset{|}{CH_2}}\text{-}COOH$$

In 1954, one of the authors (S. Akabori) postulated[3] a hypothesis that the "foreproteine" should have been produced by the following reactions in three steps.

1. Formation of amino-acetonitrile from formaldehyde, ammonia and hydrogen cyanide.

$$CH_2O + NH_3 + HCN \longrightarrow H_2N\text{-}CH_2\text{-}CN + H_2O$$

2. Polymerization of amino-acetonitrile on a solid surface, followed by the hydrolysis to polyglycine and ammonia.

1) E. Snell, D. Metzler and J. Longenecker, *J. Am. Chem. Soc.*, **75**, 2786 (1953).

2) Th. Wieland and K. Dose, *Angew. Chem.*, **66**, 781 (1954).

3) S. Akabori, *Science* (Japan), **Vol. 25**, 54 (1955).

$$x(NH_2\text{-}CH_2\text{-}CN) \longrightarrow \text{-(-NH-}CH_2\text{-}\underset{\underset{NH}{\|}}{C}\text{-)}_x\text{-} \xrightarrow{H_2O}$$

$$\text{-(-NH-}CH_2\text{-CO-)}_x\text{-} + x\cdot NH_3$$

3. Introduction of side chains into polyglycine.

Akabori pointed out, further, that the asymmetric formation of amino acid residues could be explained, at least in one single peptide chain, by his hypothesis, assuming that the configuration of polyglycine absorbed on the solid surface is *cis*-form, as shown in the following scheme.

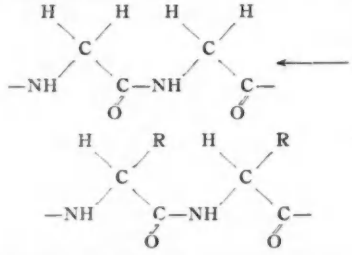

Experimental studies on the first and second reactions are now in progress in the author's laboratory. The present work deals with studies in regard to the reaction of the last step.

By the treatment of polyglycine spread on kaolinite with formaldehyde or acetaldehyde in the presence of a basic catalyst, glycyl residues are partly converted to seryl- or threonyl residues. By treating powdered polyglycine without solid bearer, with formaldehyde or acetaldehyde in the same way, practically no introduction of side chains was observed.

Experimental

Outline of Experiments.—Polyglycine was prepared, on one hand, through glycine N-carboxylic anhydride (G.C.A.) according to Leuchs[4] and on the other hand, by the polycondensation of glycine ester according to Kurtius[5]. Bulk preparations of polyglycine were obtained from G.C.A. by keeping its solution in dioxane, with a small quantity of pyridine, at room temperature for several days.

Materials.—Glycine N-Carboxylic Anhydride.[6]—Five grams of carbobenzyloxy glycine and 2.3 ml. of thionylchloride were dissolved in 5 ml. of acetic anhydride and heated to boiling for five minutes. On cooling the solution, fine crystals of G.C.A. were deposited. Yield 1.9 g.

Polyglycine in Bulk (without Bearer).—Two grams of G.C.A. were dissolved in 20 ml. of dry dioxane, 4 ml. of dry pyridine was added to it and the solution was kept in a sealed tube at room temperature. After four to five days, a mixture of ether and petroleumether was added to the reaction mixture, polyglycine precipitated in amorphous state was filtered, washed with ether and dried. The yield was 0.8 g. Polyglycine thus obtained was soluble in water with great difficulty, and gave positive biulet reaction.

Polyglycine Dispersed on Kaolinite.—a) From G.C.A.—Two grams of G.C.A. were dissolved, in 20 ml. of dry dioxane with 4 ml. of dry pyridine 15 g. of kaolinite were added to it and the whole mixture was placed in a sealed tube and allowed to stand at room temperature for eighteen hours under occasional shaking. The gelatinized reaction mixture was finally heated to 70°C for two hours. After cooling, the mixture was taken out from the tube and washed with ether, then with water. The dried polyglycine kaolinite weighed 16.5 g.

b) From Glycine Ester.—Glycine ethyl ester dissolved in ether was mixed with kaolinite, ether was distilled off and the remaining mixture was heated to 130°C for five hours. The product was washed with ether, then three times with hot water, and dried.

Several preparation of polyglycine kaolinite prepared in almost the same ways were analysed for their N contents. The results are shown in Table I.

TABLE I

Sample	Material Glycine ester	Kaolinite	Reaction Temp.	Reaction Time	N Contents %
P.G.K.1	5.9 g.	20.0 g.	130°C	5.0 hrs.	1.58
P.G.K.2	4.9	15.0	130	5.0	1.26
P.G.K.3	4.9	15.0	130	5.9	1.38
P.G.K.4	4.9	15.0	130	5.9	1.34

Degree of Polymerization of Polyglycine Kaolinite.—One hundred and fifty mg. of polyglycine kaolinite (Sample P.G.K. 3) were suspended in 10 ml of 4% aq. sodium bicarbonate solution mixed with 0.3 ml. of dinitrofluorobenzene dissolved in 10 ml. of ethyl alcohol and shaken for seven hours at room temperature. After the alcohol was distilled off, 10 ml. of 12 N hydrochloric acid were added and boiled for three hours. Dinitrophenyl-glycine formed was extracted with ether, purified by a silica gel column and determined by a photoelectric colorimeter. Terminal-N % 0.0098. Degree of polymerization; Total.N %/Term.-N % =140.

A determination of terminal. N% by van Slyke's method gave 0.008%, Total-N %/Term.-N % =172.

4) H. Leuchs, *Ber.*, **39**, 857 (1906).
5) T. Kurtius, *Ber.*, **16**, 755 (1833).
6) A. Farthing, *J. Chem. Soc.*, **1950**, 3213.

Condensation of Formaldehyde or Acetaldehyde with Polyglycine Kaolinite.—Powdered polyglycine kaolinite was mixed with aq. formaldehyde or acetaldehyde and small quantity of various basic catalysts and kept at 60°C–100°C. After various reaction times, the solid matter was filtered, washed with alcohol and dried. An aliquot of the reaction products was boiled with 6 N hydrochloric acid for five hours. Kaolinite was filtered and filtrate was concentrated in vacuo. A small quantity of alcohol was added to the residue and evaporated again to removed hydrochloric acid. The remaining solution was diluted with water, neutralized to pH 7 and brought to 10 or 20 ml. A measured volume of the solution was pipetted out, dinitrophenylated by the usual method and the resulted DNP-amino acids were separated by a silica gel chromatography as shown in Fig. 1–2. The yellow bands corresponding to DNP-

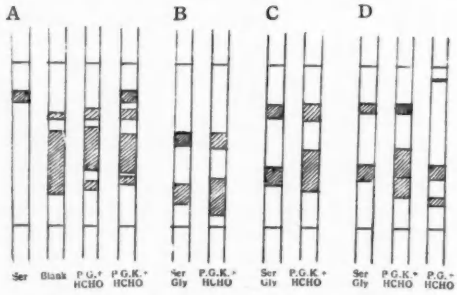

Fig. 1. D.N.P.-amino acids' column chromatograph of P.G.K.+HCHO.

Column.	Solvent
A. Silica Gel-W.	AcOH−6.5 Phosph. Etp. Buff.
B. Silica Gel-I.	20 ml. BuOH+80 ml. $CHCl_3$ −20% AcOH.
C. Silica Gel-10	20 ml. BuOH+80 ml. $CHCl_3$ −20% AcOH.
D. Celite	50 ml BuOH+100 ml. $CHCl_3$ −pH. 4.6 Acetate Buff.

glycine and DNP-serine or DNP-threonine were cut out, eluted by methyl alcohol and determined by a photoelectric colorimeter. The results of experiments under various conditions are listed in Table II.

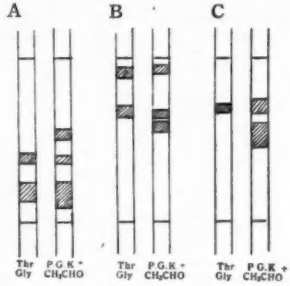

Fig. 2. D.N.P.-amino acids' column chromatograph of P.G.K.+CH_3CHO.

Column	Solvent
A. Silica Gel-I.	20 ml. BuOH+80 ml. $CHCl_3$ −20% AcOH.
B. Silica Gel-I.	5 ml. sec. BuOH+95 ml. $CHCl_3$ −2% AcOH.
C. Silica Gel-X.	50 ml. BuOH+100 ml. $CHCl_3$ −pH. 4.6 Acet. Buff.

Discussion

From the results described above, it could be concluded that the methylene group of polyglycine adsorbed on kaolinite is quite susceptible as compared with polyglycine without bearer, to the condensation reaction with aldehyde giving rise to β-hydroxy amino acids residues. It is also clear from the results of end group determination of the polyglycine and molar ratio of serine/glycine in the reaction products, that the condensation occurred not only at amino terminal glycyl residues but also at methylene groups of non-terminal glycyl residues.

Summary

1) Polyglycine dispersed on the surface of kaolinite was prepared by the polycondensation of N-carboxylic anhydride or glycine ester on kaolinite.

2) It was concluded that a part of glycyl residues in polyglycine dispersed on kaolinite

TABLE II

Sample	Weight	Catalyst	Aldehyde	Solutions	Reaction Temp.	Reaction Time	Mol. ratio of Oxy amino acids/Gly.
PGK*	1.0 g.	K_2CO_3	HCHO	10 ml.	80°C	7 hrs.	0.031
PGK*	1.0	$NaHCO_3$	HCHO	10	80	7	0.030
PGK*	1.0	T. E. A.	HCHO	10	100	2.5	0.004
PGK3	1.0	K_2CO_3	HCHO	10	80	7	0.02–0.03
PGK*	0.5	K_2CO_3	CH_3CHO	10	60	50	0.015
PGK*	0.5	$NaHCO_3$	CH_3CHO	10	60	50	0.014
PG	25 mg.	T. E. A.	HCHO	3	100	3	−
PG	100 mg.	K_2CO_3	HCHO	10	80	7	+

PGK*, Polyglycine kaolinite which was prepared by N carboxylic anhydride method.
PG, Polyglycine without kaolinite. T. E. A., Triethylamine.
HCHO, 35% aq. solution. CH_3CHO, 20% aq. solution.

was easily converted to seryl or threonyl residues by the condensation with formaldehyde or acetaldehyde.

3) The condensation occurred not only at amino terminal glycyl residues but also at non-terminal glycyl residues.

Department of Chemistry, Faculty of Science, Osaka University, Osaka

---

*Kinetic Studies on Hydrogenation of Fat. An Effect of Poison Formed in Catalysis on the Rate of Hydrogenation**

By Ryoichi MIYAKE and Yoshizo SHIMAMURA

(Received January 10, 1956)

Despite the considerable experimental studies conducted during these fifty years, there is still much remaining to be cleared up as to the facts regarding the hydrogenation rate, and no satisfactory method has been obtained so far of analyzing the reaction rate mathematically, since hydrogenation has several peculiarities which render mathematical analysis of it difficult. For instance, even the reaction order[1] of an unsaturated molecule, a fundamental problem in kinetics has not yet been clarified. The present discussion is based upon the results of experiments using copper catalysts and whale oil. The conclusions obtained in this study are applicable not only to a specific catalyst and oil, but also to the common reaction of hydrogenation of fat. Further reports confirming these points in greater detail will be issued in the near future. Throughout this experiment, the pressure of hydrogen is kept constant, so the kinetic behavior of the hydrogen molecule is left out of consideration.

Experimental and Results

The hydrogenation of finback whale oil was carried out throughout this series of experiments under atmospheric pressure of hydrogen and at 180°C by using somewhat modified H. Adkin's[2] Cu-Cr-O catalysts.

The experimental technique is outlined here which is practically identical with those employed previously[3]. A static method was employed. The whole glass apparatus was used, which consists of a reaction bulb (a 25 mm. height and a 45 mm. in diameter) connected through a flexible spiral glass tube to a gas burett. The reaction bulb was immersed in an oil bath and was given a horizontal rotation of R.P.M. 200 by a piston of 3 cm. in diameter. The reaction periods from start to end of the motion were recorded.

Two types of slightly modified H. Adkin's Cu-Cr-O catalyst[4] were used.

Type (a): Without barium chromate. Copper content amounting to 43% as a metal on an average.

Type (b): With barium chromate. The amount of barium chromate was adjusted so as to contain 10% of metallic copper in the catalyst.

The activity of those catalysts is satisfactorily uniform when the decomposition temperature of copper ammonium chromate is strictly controlled at about 350°C. Their characteristic features will be briefly described.

The Cu-Cr-O catalyst readily reduced accompanying initial induction period to an active metallic copper and to chromium oxide (Cr_2O_3) at above 120°C consuming about 18 cc. (N.T.P.) of hydrogen per 0.1 g. of type (a) catalyst about 8 cc. per 0.1 g. of the type (b) catalyst in hydrogen atmosphere, and somewhat less volume of hydrogen is consumed in the wet reducing process at the same temperature in each case. In hydrogenation of whale oil with this catalyst under low pressure of hydrogen, highly unsaturated acids are partly saturated while those of oleic acid series are not hydrogenated. The selection is perfect[3,5]. The catalyst is usually added to oil after it is reduced, but sometimes it may be used without reduction. In the latter case reduction of the catalyst takes place within thirty minutes at 180°C accompanying simultaneous hydrogenation of oil.

The results[6] of the analysis using finback whale oil indicate that when selective hydrogenation goes on completely, unsaturated acids ($|\overline{3}$-acids) higher than acids of linoleic acid series ($|\overline{2}$-acid) are converted to those of linoleic acid series ($|\overline{2}$-acid) at iodine value (I.V. in short) 90, and that acids of linoleic acid series which are unsaturated

* A principal part of the present work was presented at the Monthly Meeting of the Pharmaceutical Society of Japan held on March 17th, 1951 in Tokyo Univ.

1) F.L. Morritz, E. Lieber and R.B. Bernstein, *J. Am. Chem. Soc.*, 75, 3116 (1953).

2) H. Adkins, R. Connor and K. Folkers, *J. Am. Chem. Soc.*, 54, 1138 (1932).

3) R. Miyake, *J. Pharm. Soc. Japan*, 68, 9 (1948).

4) ibid., 68, 18-31 (1948).

5) Mr. T. Namba kindly informed us about the result of his observation several years ago, that in the hydrogenation of soybean oil by a hydrogen bubbling method some acids in oleic acid series are saturated in the presence of Cu-Cr-O catalyst under the same conditions as in this experiment.

6) R. Miyake, *J. Pharm. Soc. Japan*, 68, 2 (1948).

in middle grade are reduced to those of oleic acids series at I. V. 70.

Experiment No. 1.—A case in which velocity of hydrogenation apparently obeys unimolecular law.

In the run V. 317 a sintered catalyst reduced at rather high temperature was used. 0.1252 g. of catalyst (a) was completely reduced in the reaction bulb in hydrogen at 270°C for twenty minutes absorbing 14.9 cc. of hydrogen (N. T. P.); then the reduced catalyst was covered by 0.9572 g. of whale oil (I. V. 98.6) to avoid exposure to the air before it was used for hydrogenation. The I. V. of hydrogenated oil was 74.4. The hydrogen adsorption rate is shown in Fig. 1 and the experimental formula obtained by the method of least square from the data of Fig. 2 is as follows:

$$2.303 \log (23.07 - x) = -0.008475t + 3.914.$$

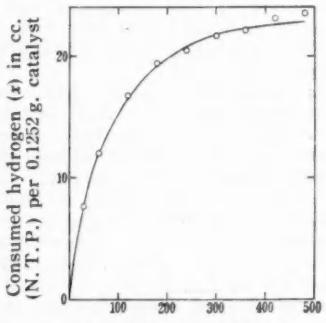

Fig. 1. Run V 317. 0.1252 g. of catalyst was used after reduction at 270°C. The curve is the calculated one from the formula V 317.3 and V 317.4.

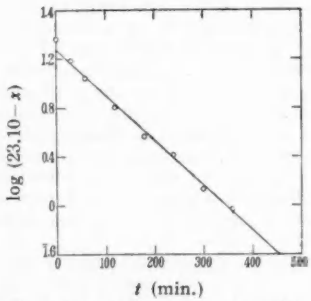

Fig. 2. Run V 317. The logarithum of concentration of highly unsaturated compounds in cc. is plotted against time. The reaction is seemingly of the first order.

Experiment No. 2.—This experiment was carried out to show that the velocity of hydrogenation was independent of the concentrations of highly unsaturated acids in oil. The unreduced catalyst (a) was used. Within the range of the experiment the velocity may be regarded as equal regardless of the change of the concentration. Results are summarized in Table I and in Fig. 3.

TABLE I

Run no.	Catalyst (g.)	Whale oil (g.)	Refined hydrogenated whale oil (g.)	Highly unsaturated compounds (%)
V 321	0.1023	0.8894	1.9570	4.5
V 322	0.1200	1.0759	3.006	3.8
V 323	0.1040	0.8970	—	14.3

Whale oil: I. V. 110, n_d^{40} 1.4655; content of highly unsaturated compounds, weight % 14.3. Refined hydrogenated whale oil: I. V. 70.6, n_d^{40} 1.4603.

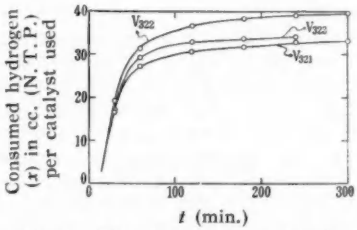

Fig. 3. The independence of the rate upon the concentration of acceptor. In run V 323 whale oil and in run V 321 and V 322 mixtures if whale oil and refined hydrogenated whale oil are hydrogenated with unreduced catalysts listed in Table I.

Experiment No. 3.—An experiment was undertaken to discover the cause of the fall of catalyst activity. With 0.1 g. of unreduced catalyst 1 g. of whale oil was hydrogenated (V 283 (1)). Then 1 g. of whale oil was added and hydrogenated (V 283 (2)), and once again 1 g. of whale oil was added and hydrogenated (V 283 (3)). The catalyst thus deactivated was thoroughly washed with ether in Soxhlet apparatus and then used again as a catalyst of hydrogenation of fresh whale oil (V 285). In experiments V 283 (2) and (3), catalyst was evidently in reduced state. In V 285 catalyst was slightly oxidized due to exposure to the air during washing by either. The data are shown in Table II and in Fig. 4. In Fig. 5 to show more clearly the reactivation of catalyst, the net amount of hydrogen absorbed per one g. of whale oil, i.e. a corrected value obtained by substrating from the total absorbed hydrogen the volume of hydrogen consumed for the reduction of catalyst which are calculated from the drop of iodine value, are plotted against the reaction time.

TABLE II

Run no.	Catalyst (g.)	Whale oil (g.)	Iodine value of hydrogenated oil
283 (1)	0.1192	1.0265	69.2 (calculated)
283 (2)	0.1192	0.1192	
283 (3)	0.1192	0.9826	
285	0.0508	0.5099	70.2 (experimental)

Iodine value of whale oil: 107

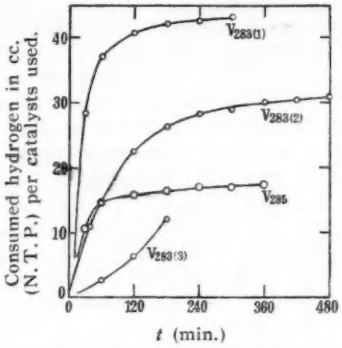

Fig. 4. The deactivation feature of catalyst in hydrogenation with succesive addition of 1 g. oil and reactivation of waste catalyst by washing with ether.

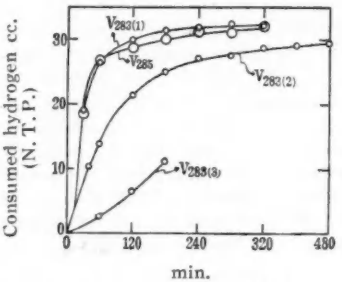

Fig. 5. The net amount of hydrogen absorbed per one g. of oil, calculated from Fig. 4 and Table II.

Experiment No. 4.—The fact that the reaction rate was increased when the amount of catalyst increased in a certain range is illustrated here using the unreduced catalyst type (a). The hydrogenation conditions were similar to those of the foregoing experiments. 1-2 g. of whale oil was used. The results are summarized in Fig. 6., in which the maximum rate (cc./min.) of hydrogenation of the higher unsaturated acids ($\frac{1}{3}$-acid) are plotted against the amounts of catalyst used. The rate is proportional to the amounts of catalysts used, when too much catalyst is not applied. If sufficient catalyst is used, the rate of reaction becomes nearly constant, being independent of the amount of catalyst. This fact might induce an opinion that the diffusion rate of hydrogen into an oil phase may be the limiting factor[7] in this case. Discussion on this follows. The diffusion theory, however, is not tenable in this case, because faster consumption of hydrogen can be observed in the same apparatus by using a more effective catalyst such as nickel. A study on this phenomenon is now being undertaken by Yajima. It will suffice here to state that oil is saturated with hydrogen under the conditions of this experiment.

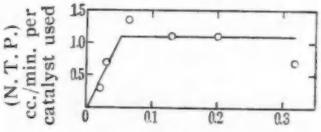

Fig. 6. The dependance of rate upon the amount of catalyst. Differing from the circumstance employing the dry-reduced catalyst, the wet-reduced catalyst becomes partially inactivated by the irreversible poisonous substances, presumably formed from the fat by the accompanying oxidizing action of the oxide catalyst in the reduction period. The injurious effect, however, do not become pronounced until not too much unreduced catalyst (about 0.2 g. in this case) is used.

Kinetic Consideration

The consideration are principally inferred from the behavior of unsaturated oil molecules in the reaction system, quite apart from the behaviour of hydrogen molecule, since the hydrogen pressure was maintained constant throughout this series of experiments, and further, as mentioned in Experiment No. 4, the oil was evidently saturated with hydrogen. The fact that hydrogenation rate is independent of the concentration of the highly unsaturated molecules indicates the rate determining step is the hydrogenation process on the surface of catalyst, that the diffusion of oil molecules to the catalyst surface is fast enough to establish the adsorption equilibrium of oil molecules between the catalyst and the liquid phase, and that the highly unsaturated molecules are strongly adsorbed, although the reaction is sometimes apparently first-order kinetics as shown in Experiment 1.

The decrease in rate of reaction with time is necessarily ascribed to successive deactivation of catalyst, by possible two principal factors, poisoning and sintering. The results of Experiment No. 3 indicate that the effect of the latter can be ignored.

In conclusion, as the equilibrium in the reaction system is established, the rate of hydrogenation is directly proportional to the amount of catalyst, i. e., the decrease in the rate is directly corresponding to the decrease in the number of active centers caused by a catalytic poison in a first approximation.

In order to interpret the change in rate in view of this conclusion, an assumption is made induced from the suggestive results obtained in Experiment No. 1 that the num-

7) V. I. Gol'danski and S. Yu. Elovich, *C.A.*, **41**, 2973 (1948).

ber of active centers is reduced by the quantity of poison formed in the process of catalysis in proportion to the amount of hydrogenated molecules. Thus, if x cc. of hydrogen reacts at time t min. the rate is assumed

$$dx/dt = K_1(N_o - K_2x),$$

where

K_1 = the hydrogenation rate constant (cc./min.) per unit active center,

N_o = the original number of active centers, which is supposed here to be capable of combining an unsaturated compound and hydrogen together,

K_2 = this term consists principally of the proportional constant of catalytic poison formation reaction, absorption coefficient of poison and proportionality constant so as to make K_2x correspond to the number of active centers deactivated.

This equation, however, has a linear expression with respect to x similar to the first order formula; it involves two reaction rate constants, K_1 and K_2. Although N_o/K_2 corresponds to the initial concentration of reactant in the first order kinetics, it can be determined only from experimental data.

The analysis of Run No. V 317 with the applification of this equation is shown in Fig. 7, wherein an abrupt change in rate at point (b). Hence it is expressed by the following two equations.

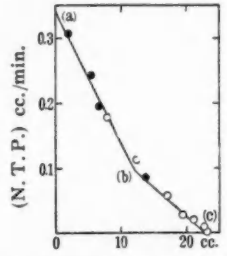

Fig. 7. $dx/dt - x$ relation from V 317.
○ experimental
● interpolated

$$dx/dt = 0.3430 - 0.02021x \quad \text{(V 317.1)}$$

$$dx/dt = 0.2047 - 0.00889x \quad \text{(V 317.2)}$$

These equations are dissolved and calculated integral constants by adopting suitable experimental points on Fig. 7. The result is

$$2.303 \log (16.97 - x) = -0.0202t + 2.826 \quad \text{(V 317.3)}$$

$$2.303 \log (23.06 - x) = -0.00889t + 2.935 \quad \text{(V 317.4)}$$

From these four equations, the following figures for the point (b) are obtained: 0.0967 cc./min., 12.18 cc. and sixty two minutes respectively for dx/dt, x and t. The iodine value at (b) is estimated as 88. This is in good agreement with the calculated iodine value 90, at which $\overline{\overline{3}}$-acids will disappear. Thus, the equation (V 317.3) can be used for the former stage of hydrogenation of $\overline{\overline{3}}$-acids before sixty-two minutes and thereafter the equation (V 317.4). Therefore K_1N_o for $\overline{\overline{2}}$-acids must be taken 0.0967 cc./min. (at point b). The slopes of the pair of straight lines in Fig. 7 are shown respectively in terms of K_1K_2 for $\overline{\overline{3}}$-acids and K_1K_2 for $\overline{\overline{2}}$-acids in the equations (V 317.3 and V 317.4) and the ratio of these $K_1(\overline{\overline{3}})/K_1(\overline{\overline{2}})$ can be calculated from the ratio of the value of these slopes if the value of $K_2(\overline{\overline{3}})/K_2(\overline{\overline{2}})$ is known. If an assumption is made that $K_2(\overline{\overline{3}})/K_2(\overline{\overline{2}})$ is unity, then $K_1(\overline{\overline{3}})/K_1(\overline{\overline{2}}) = 0.0202/0.00899 = 2.25$, which is comparably consistent with the value obtained from instances in which $K_2(\overline{\overline{3}})$ and $K_2(\overline{\overline{2}})$ happen to be negligible compared with the change in K_1 terms as will be reported in the next work. The appearance of the breaking point (b) in Fig. 7 indicates the occurrence of good selectivity which is also consistent with being indifferent to the reaction rate with the concentration of the highly unsaturated molecules.

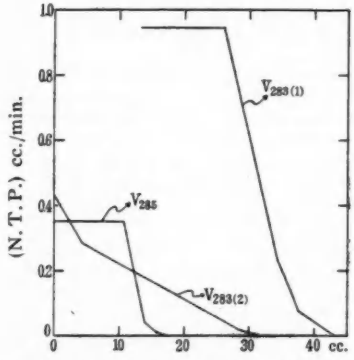

Fig. 8. $dx/dt - x$ relation from Experiment No. 3 (Fig. 4). The graph of V 283 (1) will proceed same in shape from this position to the left through decreasing values of 9.9 cc. to x, provided correction is made on it by substracting the required hydrogen for the reduction of catalyst in Fig. 4.

Reviewing Fig. 8, it deserves special notice here for the arising of different types of active center in the hydrogenation range of $\overline{\overline{2}}$-acids, their slopes being respectively 0.0861 and 0.0476. An assumption being made

of the equality of both K_2 again here concerning both types of active center, the ratio of slope is nearly 2** which corresponds to the ratio of K_1 term in two types of active center, catalyzing the same substance in this case.

The reaction rate after passing over the point of about I. V. 75 changes to the very slow one in this catalyst indicating the possibility of the appearanse of some special constitution of fatty molecule ($\overline{\overline{2}}'$) (Table III).

is not expressed in explicit form for the present.

The features under the above consideration, however, are shown in very few instances; they hold true also for many examples we have tested. On the other hand, the occurrence of induction period incidentally which appeared in Experiment No. V 283 (3) in the reduced state catalyst is not so rare but is not reproducible, and of course quite different from that which was experienced with the unreduced catalyst as noticed before.

TABLE III

THE STRAIGHT LINES IN FIG. 8 ARE EXPRESSED BY TWO TYPES OF FORMULAS EITHER $dx/dt=a$ OR $2.303 \log(b-x)=-ct+d$. THE ESTIMATED VALUE OF THESE TERMS ARE TABULATED. $(dx/dt)_i$, $(x)_i$ AND $(I.V.)_i$ ARE THE RESPECTIVELY THE CALCULATED VALUES AT THE POINT OF INTERSECTION OF CROSSING TWO LINES

Run no.	a	b	c	d	$(dx/dt)_i$	$(x)_i$	$(I.V.)_i$	Acids range being hydrogenated
V 283 (1)	0.944							$\overline{\overline{3}}$-acids
					0.944	26.2	89	
		37.1	0.0861	4.76				$\overline{2}$-acids
					0.229	34.5	79	
		39.2	0.0476	3.66				2-acids
					0.080	37.6	76	
		43.4	0.0138	2.64				2′-acids
V 283 (2)		13.0	0.0331	2.56				$\overline{3}$-acids
					0.288	4.32	103	
		30.3	0.0111	3.42				$\overline{3}$-, $\overline{2}$-acids
					0.0195	28.6	77	
		31.6	0.00641	2.78				$\overline{2}$′-acids
V 285	0.3505							$\overline{\overline{3}}$-acids
					0.350	10.6	85	
		14.4	0.0946	4.355				$\overline{2}$-acids
					0.0425	13.9	78	
		16.8	0.0159	1.881				$\overline{2}$′-acids
					0.0162	15.7	74	
		17.5	0.00921	1.653				$\overline{2}$′-acids

The occurrence of linear sector of rate in the early stage is evidently the direct proof of zero order reaction with unsaturated molecules, but it is of interest in view of the point of poison formation. It is suggested that the solubility of poison must be taken into account. In fact, the hydrogenated whale oil contains poisonous substance in it, so hydrogenized oil must be re-refined by alkali and bleaching clay before applying it in Experiment No. 2. Some reactivation of activity accompanied by adding a fresh oil as will be seen in V 283 (2) and (3) might be attributed to, apart from the change in constitution of oil by adding new whale oil, the desorption of poison from catalyst and this concept is introduced into K_2, although it

Some other criteria will be afforded here as regards to the phenomena which are encountered in the hydrogenation of fat aside from the one as discussed above. The inherent impurities present in oil are irreversible poison, leading to permanent inactivation of the catalyst, and bearlittle relation to the change in rate under the condition wherein the absorption equilibrium is established.

The gaseous poisons which happen to occur as impurities in hydrogen may damage a catalyst in the very similar manner proportional to the consumed hydrogen. There is evidence, however, against this in the experiments using the same hydrogen in a gas bubbling hydrogenation method, in which the extent of volume of hydrogen passed had no effect on the activity of catalyst. Another

** This figure will be shown as a characteristic one of this catalyst in the next report.

effect might be raised from the pyrolysis of oil. It can be left out of consideration in view of kinetics also because time effects were not observed in the above analytical treatments. All these factors can be left out of consideration in the first approximation.

The present criterion appears to be in general accord with the view originally set forth by Armstrong and Hilditch[8], which unfortunately has not been developed to further kinetic treatments. The present authors in writing this report are feeling utmost reverence toward their foresight. In addition it will be pertinent here to recall the Ubbelohde's observations[9], whose data are seemingly all responsible for the present conception, although he did not interpret his results from the viewpoint of catalytic poison.

Summary

Estimation of the volume of hydrogen consumed by a static method with Cu-Cr-O under atmospheric pressure of hydrogen at 180°C by hydrogenation of whale oil was studied kinetically.

It was observed that the reaction is zero order to the concentration of the molecule to be hydrogenized, and, in spite of it, the reaction velocity gradually decreases due to the reversible poisoning of catalyst. An assumption was made that a poisonous substance is formed in the process of catalysis, and that its amount is proportional to the degree of hydrogenation. The following formula is presented.

$$dx/dt = K_1(N_0 - K_2x)$$

The authors wish to express their condial thanks to Dr. G. Fujinaga, Ex-Director, and Dr. H. Fujii, Director, of Nippon Marine Company for their kind offer of aid.

A part of the expense of this research has been defrayed from the Scientific Research Grant of the Ministry of Education.

The Pharmaceutical Institute of Chiba University, Chiba

8) E.F. Armstrong and T.P. Hilditch, *Proc. Roy. Soc. London*, A 96, 137 (1919).
9) L. Ubbelohde and R. Schönfeld, *Z. angew. Chem.*, 44, 184 (1931).

---

*Studies on the Oxy-acid Phosphors. V. Stannate Phosphors (Part I)**

By Yoshihide KOTERA, Tadao SEKINE and Michiko YONEMURA

(Received January 7, 1956)

Introduction

The stannate phosphors were investigated for the first time by E. Tiede and E. Villain, who reported magnesium stannate activated by manganese showing green emission under cathode rays excitation[1]. F. A. Kroeger[2] studied the alkali-earth and zinc stannates activated by titanium and calcium stannate activated by manganese, but the details of their preparation, characteristics, etc. are yet unknown. We have prepared various stannate phosphors and found some remarkable results.

Experimental and its Results

(1) Purification of Sodium Stannate and Metallic Salts.—In the preparation of stannate phosphors, a commercially available chemically pure grade of stannic chloride was used as one of the starting materials and purified as follows. The stannic chloride was dissolved in water and filtered. The sodium stannate solution was obtained by the reaction of the stannic chloride solution with solution of caustic soda in excess and by filtering off the resulting sediment. The precipitate, which was obtained by neutralization of this solution with conc. hydrochloric acid was filtered and dissolved again by addition of caustic soda solution. The filtrate was used as the purified sodium stannate solution.

The other starting materials were respective metallic salts, which were purified by the process described in a previous paper[3].

Each metallic salt solution was added to the sodium stannate solution, and respective metastannate salts were precipitated, their purity being established spectrographically.

(2) Mixing and Firing.—Each metastannate salt, respective metallic oxide or carbonate, flux

* Read before the Sixth Annual Meeting of the Chemical Society of Japan 1953. Report IV was published in This Bulletin, 28, 132 (1955).
1) E. Tiede and E. Villain, *Ber.*, 73, 274 (1940).
2) F.A. Kroeger, "Some Aspects of the Luminescence of Solids", Elsevier Publishing Co. (1948), p. 158.
3) Y. Kotera and T. Sekine, This Bulletin, 27, 13 (1948).

TABLE I

THE COLOURS OF EMISSIONS OF STANNATE PHOSPHORS

Host Lattice	Activator	3650Å		2537Å		Cathode Rays	
Mg_2SnO_4	Mn	none		green	ff	green	m
〃	Mn*1	none		none		blue	m
〃	Ti	none		bluish white	s	bluish white	s
〃	Ti*1	none		blue	s	blue	s
〃	Bi	blue	m	blue	ff	bluish violet	f
〃	Pb	none		green	ff	bluish violet	f
Ca_2SnO_4	Mn	none		none		orange	m
〃	Ti	none		blue	s	blue	s
〃	Bi	violet	m	violet	ff	bluish violet	m
〃	Pb	yellowish orange	m	none		yellow	m
〃	Ce	bluish white	f	red	ff	blue	m
Sr_2SnO_4	Ti	none		blue	m	blue	m
〃	Pb	none		orange	ff	orange	f
〃	Bi	none		none		yellowish orange	f
〃	Bi*2	none		none		red	f
Ba_2SnO_4	Ti	yellow	ff	yellowish orange	m	blue	m
〃	Pb	none		yellow	m	yellow	m
Zn_2SnO_4	Mn	yellowish white	f	none		yellowish white	f

s: strong, m: medium, f: faint, ff: very faint

*1. $Na_2B_4O_7 \cdot 10H_2O$ as a flux, other, NaF.

*2. SrO: SnO_2=1:1, others, see Table II.

TABLE II

THE OPTIMUM MIXING RATIO FOR THE PREPARATION OF STANNATE PHOSPHORS

Host Littice	SnO_2: MO or MCO_3	Flux	Activator
Mg_2SnO_4	1: 2.2 (MgO)	NaF or $Na_2B_4O_7 \cdot 10H_2O$ 0.1 mol.	Mn 1 mol. %
Ca_2SnO_4	1: 2–3* (CaO)		Ti 1–10 mol. %
Sr_2SnO_4	1: 2 ($SrCO_3$)		Bi 1 mol. %
Ba_2SnO_4	1: 2 ($BaCO_3$)		Pb 5 mol. %
Zn_2SnO_4	1: 6 (ZnO)		Ce 1 mol. %

* There is a difference between the optimum ratio for ultraviolet excitation and that for cathode rays.

and activator were mixed in an agate mortar. Sodium fluoride, borax or some other salt was used as a flux. The solution of flux salt was purified by the addition of ammonium sulfide and, after filtration, the filtrate was added to the batch. As for activator, commercially available chemically pure manganese sulfate, ceric oxide, lead oxide, bismuth nitrate or titanium oxides were used. If necessary, they were purified by the process previously reported[3].

The batch was fired for two hours at 1100°C in air by an electric furnace.

(3) Properties.—The properties of some stannate phosphors and the optimum mixing ratios for their preparation were shown in Tables I and II respectively.

In the case of magnesium stannate activated by titanium, the change of flux caused the spectral shift of emission, as shown in Figs. 1 and 2 for 2537Å and cathode rays excitations respectively. In Fig. 1, the radiant energy curves were drawn in the same energy scale by arbitrary adjustment of the heights of the individual curves, to show relative spectral locations, while, in Fig. 2, the full lines were drawn relative to the value

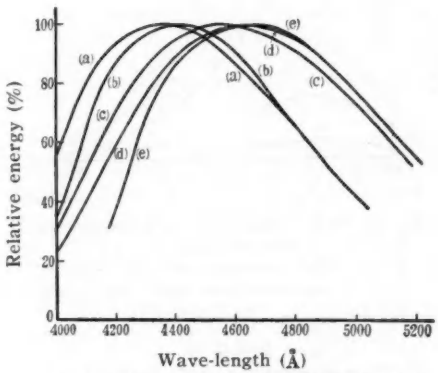

Fig. 1. The variation of emission spectra with different fluxes in Mg_2SnO_4: Ti (ultraviolet light).
(a) $Na_2B_4O_7$ (b) H_3BO_3 (c) $Na_2B_4O_7$ (Ti 1%) (d) NaF, MgF_2 or Al_2O_3 (e) KH_2PO_4 (Ti 10 mol.% (except (c)), 1100°C ×2 hrs. MgO: SnO_2=2.2)

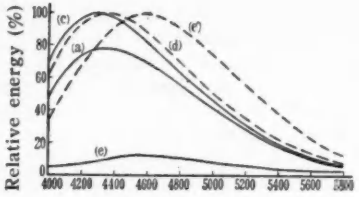

Fig. 2. The variation of emission spectra with different fluxes in Mg_2SnO_4: Ti (cathode rays)
(a) $Na_2B_4O_7$ (c) $Na_2B_4O_7$ (Ti 1%) (e) KH_2PO_4 (8 kV, 200 μA)

of 100 for the highest energy of sample (a) and the dotted lines were drawn in the manner analogous to Fig. 2. Both flux and activator amounted to 0.1 mol. per 1 mol. of the host crystal, and the other conditions were the same as the previous ones. Although lithium, sodium or potassium halides was used as a flux, the emission spectrum was found to be identical with that of sodium fluoride. Magnesium stannate showed itself to be a weak bluish emission when borax was employed as a flux, but it was difficult to determine the emission spectrum.

The emission spectra and the brightness of calcium stannate activated by titanium under cathode rays excitation were shown in Fig. 3 and Table III. In these measurements, the ratio of

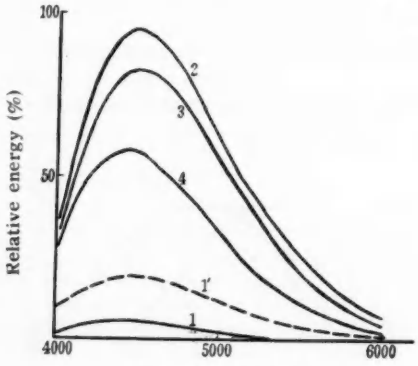

Fig. 3. The variation of emission spectra with CaO: SnO_2 in Ca_2SnO_4: Ti
(5 kV, 50 μA, current density, $5\cdot10^{-5}$A/cm², 1': measured with higher sensitivity for sample 1. See Table III).

TABLE III

THE BRIGHTNESS OF Ca_2SnO_4: Ti

No. of samples	CaO: SnO_2	Brightness
1	1: 1	4.8
2	2: 1	24.1
3	3: 1	16.7
4	6: 1	14.7

CaO to SnO_2 was varied from 1: 1 to 6: 1, and the generation of cathode rays was made at 5 kV., 50 μamp., the current density being $5\cdot10^{-5}$amp./cm². Taking a zinc silicate activated by manganese as the standard sample for the measurements of brightness, commercial calcium magnesium silicate activated by titanium had the value of 35.0. The same measurements were carried out on calcium stannate activated by cerium, in which case the amount of cerium was varied from 0.001 to 0.05 mol. per mol. of the host crystal. The results were shown in Fig. 4 and Table IV,

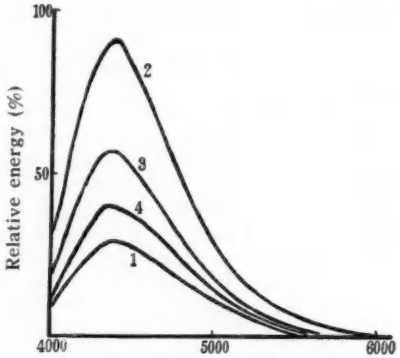

Fig. 4. The variation of emission spectra with Ce concentration in Ca_2SnO_4: Ce
(5kV, 50 μA, current density 10^{-5}A/cm². See Table IV)

TABLE IV

THE BRIGHTNESS AND RADIANT ENERGY AT 4350Å OF Ca_2SnO_4: Ce

No of Samples	Ce Concentration mol./1 mol. Ca_2SnO_4	Brightness	Relative energy
1	0.001	4.4	30
2	0.01	8.8	90
3	0.02	7.7	58.5
4	0.05	4.4	39

See Fig. 4.

the fourth column of the latter expressing the relative value of radiant energy at the wavelength 4350Å.

These measurements were carried out by means of an automatic recording spectroradiometer[4].

Discussion

The stannate phosphors activated by titanium were investigated by F. A. Kroeger[2]. He studied the function of titanium as an activator in the matrix of silicate, stannate or zirconate, and discussed the properties of stannate phosphors activated by titanium in detail. He found that titanium acts in the above-mentioned matrixes as an activator

4) Y. Kotera, *Rept. Gov. Chem. Ind. Research Institute, Tokyo*, **50**, 398 (1955).

only when the preparation was made under oxidizing condition and it does not act as an activator in compounds of aluminium, phosphorus, or boron. From these facts he concluded that the luminescence effect correlated with titanium is attributed to tetravalent Ti^{4+} ions and the activator is built in isomorphously. Further he found that the amounts of titanium are considerably higher than is usual for activation; there is a certain relation between the spectral distributions of absorption and emission due to titanium and orthostannates and metastannates of Ca, Sr, and Ba present examples of the systematic change of the temperature quenching.

We found that some stannates, particularly orthostannates, show considerably strong emission when activated by several heavy metals including titanium. As may be seen in Table I, manganese acts as an activator in the matrix of zinc stannate, in addition to magnesium and calcium stannates[1,2] and the emission is also ascertained when activated by cerium, bismuth and lead. The optimum mixing ratio in Table II corresponds roughly to the highest value of brightness. It is remarkable that zinc stannate shows the strongest emission when prepared by employing zinc oxide in much excess, such result not being obtained in other matrixes. Probably this matrix is not composed of the compound which contains zinc oxide in much excess, but the formation of the matrix would proceed rather slowly and incompletely. Further it is noteworthy that the various emissions are observed for the preparations of magnesium stannate activated by titanium or manganese with different fluxes. In the case of magnesium stannates activated by titanium the emission changes are confirmed from the results shown in Fig. 1. These might be explained by an assumption that there are two kinds of centers, one is that of tin and the other that of titanium, each emission being intensified by different fluxes. It is expected that a longer wave-length emission might be caused by tin and a shorter one by titanium from the comparison of emission spectra of (a) and (c), but it is difficult to draw an accurate conclusion. Hoffmann[5] found that SnO_2 or glass containing SnO_2 luminesceses under excitation of ultraviolet light, but the colors of their emissions are mostly brown, and probably tin does not always act as an activator; it seems to be difficult to compare his results with ours. In the case of manganese activation, the blue emission is found under excitation of cathode rays when borax is used as a flux, and this result supports the above explanation. Kroeger[2] found that two different emissions occur, depending on the wave-length of the exciting radiation, and this fact might be explained by assuming the existence of two kinds of luminescence centers. The emission spectra under excitation of cathode rays for magnesium stannates with different fluxes look somewhat varied (Fig. 2), and such a phenomenon has not yet been observed.

From the practical viewpoint, it is important that calcium stannate activated by titanium with flux of borax shows the emission, the intensity of which is about 75% of that of $CaWO_4$. Furthermore, calcium stannate activated by titanium or cerium shows emission as indicated in Figs. 3, 4, Tables III and IV, and might be used as a blue component of color television.

5) J. Hoffman, *Sprechsaal*, **65**, I, 82 (1932).

Summary

Various stannate phosphors were prepared and some of their emissions were determined. Stannate phosphors emit green, blue or yellowish white light when activated by manganese, blue, violet or red by bismuth, orange, green or blue by lead, while those activated by cerium show blue or red emission. It is expected that the activation by tin also occurs in some cases. This is supported by the fact that the emission of magnesium stannate activated by titanium changes by the variation of flux. For different specimens of calcium stannate activated by titanium or cerium, emission spectra under excitation of cathode rays were measured.

The authors wish to thank Mr. Masami Yamada and Mr. Koji Mitsuhashi for the measurements of spectral distribution of cathode rays emission, and Dr. Shoji Makishima and Mr. Kenji Tanaka for the general discussion on the subject and the experimental work they have done.

Government Chemical Industrial Research Institute, Tokyo

*A Method for Determination of Thermodynamic Dissociation Constants from Absorption Spectra with Applications to ortho- and para-Phenylenediamines**

By Tosinobu ANNO and Akira SADÔ

(Received January 18, 1956)

Introduction

The dissociation constants of the mono-acidic bases or the mono-basic acids can be determined fairly well from the absorption curves of the substances in solution at different pH values[1], while with the dibasic acids and diacidic bases the spectroscopic determination of dissociation constants becomes more complicated[2]. Thamer and Voigt[2] have described a method for determining the dissociation constants in these cases. They measured the optical density of solutions of constant ionic strength at different pH values for a fixed wave length. The apparent dissociation constants are determined from these optical density data, and corrected to the true ones, using the Debye-Hückel equation.

We present here another method using the optical density data of solutions at only five different pH values. As an application of the present method, *ortho-* and *para-*phenylenediamines are chosen. There are a good many prior determinations of dissociation constants for the latter compound while the value of the second dissociation constant of the former compound is not found in the literature on the subject. The advantages and the disadvantages of the present method will also be discussed.

Method

We shall describe the method only for the diacidic bases, the application to acids or amphoteric electrolytes being obvious. The following equation can be shown to hold[2]:

$$D=\frac{Lc\left[\epsilon_1+\frac{k_{1b}}{a_{OH}}\epsilon_2+\frac{k_{1b}k_{2b}}{a^2_{OH}}\epsilon_3\right]}{1+\frac{k_{1b}}{a_{OH}}+\frac{k_{1b}k_{2b}}{a^2_{OH}}} \quad (1)$$

where ϵ_1, ϵ_2, and ϵ_3 represent the molar extinction coefficients of undissociated diacidic base B, its singly and doubly dissociated ions BH^+ and BH_2^{++}, respectively. D denotes the optical density of the solution of hydroxyl-ion activity a_{OH} and of analytical concentration c of the base in all its forms measured with an absorption cell of the length L. k_{1b} and k_{2b} are the apparent basic dissociation constants defined by

$$k_{1b}=\frac{a_{OH}[BH^+]}{[B]}, \qquad k_{2b}=\frac{a_{OH}[BH_2^{++}]}{[BH^+]}, \quad (1a)$$

where brackets indicate concentrations. According to Thamer and Voigt "If k_1 and k_2 overlap and k_1/k_2 is therefore small, one can use optical density data and pH data with equation 4 (our equation 1) to obtain ϵ_2, k_1, and k_2 by successive approximations. However, the calculations are very laborious". It is the purpose of this paper to show that using Eq. (1) the dissociation constants can be calculated *without* successive approximations. From Eq. (1) the following equation can easily be derived:

$$D'x-y+(D'-\epsilon_3)z/a_{OH}=(\epsilon_1-D')a_{OH}, \quad (2)$$

where $D'=D/Lc$, $x=k_{1b}$, $y=k_{1b}\epsilon_2$, and $z=k_{1b}k_{2b}$. ϵ_1 and ϵ_3 are measurable as D' in alkaline ($pOH \ll pk_{1b}$) and acidic ($pOH \gg pk_{2b}$) solution, respectively. If the measurements are made of D' at three different medium pH values and constant ionic strength, Eq. (2) gives a set of linear simultaneous equations, in which x, y and z are unknowns, for a fixed wave length. No iterative process is involved in solving these equations for x, y and z, from which k_{1b}, k_{2b}, and ϵ_2 can be determined. Although what values of pH are appropriate as "three different medium pH values" depends on the substance, the following general rule may be given:

If $k_{1b}/k_{2b} \gg 1$, (usually >10), these pH values are chosen such that $a_{OH} \cong \sqrt{k_{1b}k_{2b}}$, $a_{OH} \cong k_{1b}$ and $a_{OH} \cong k_{2b}$.

If $k_{1b}/k_{2b} \cong 1$, they are all chosen such that $p_{OH} \cong pk_{1b}$ ($\cong pk_{2b}$), usually with intervals of 0.3–0.5 pH units.

* Presented at the Meeting of the Kyushu Branch of the Chemical Society of Japan, Fukuoka, November 7, 1953.

1) For example see, Hughes, Jellinek, and Ambrose, *J. Phys. Colloid Chem.*, **53**, 410 (1949).

2) B.J. Thamer and A.F. Voigt, *J. Phys. Chem.*, **56**, 225 (1952).

Experimental Results

The samples of *o*- and *p*-phenylenediamines used were commercial ones. Absorption curves were determined with a Beckman DU spectrophotometer with a fixed slit-width for each substance at a given wavelength. Values of pH were determined using a pH-meter supplied by Shimadzu Seisakusho with a Beckman glass electrode. They were converted into the hydroxyl-ion activity using the ionization constant of water K_w[3]. The optical density data are listed in Tables I and II for *o*- and *p*-phenylenediamines, respectively. They are limited to those corresponding to 10–90 percent transmittance. Since it is impossible to obtain the optical density data satisfying the above criterion with one concentration value of the solution, we must use two different concentration values for each substance and for each pH value. In acidic and alkaline extremes dilution by the solvent does not bring about the change of the hydrogen-ion concentration, since in such cases the buffer action of the solvent is strong. For intermediate pH values McIlvaine's[4] Na_2HPO_4-citric acid buffer solutions with appropriate pH values were first prepared and then diluted to low ionic strength so that the Debye-Hückel equation can be applied. In this way, the buffer action was weakened and the pH value of the solution came to depend slightly upon the analytial concentration of the substance. Therefore, the optical density data of solutions with different concentrations are listed separately in the table. This supplied additional equations for the calculation of the dissociation constants and, as far as possible, two sets of equations were selected and used for calculation for a fixed wave length. The agreement between the values of the dissociation constants calculated from different sets of equations for a fixed wave length represents a measure of the experimental accuracy, particularly, of pH measurements. A preliminary investigation shows the dissociation constants of these substances to be: *o*-, $k_{1b} \geqq 10^{-10}$, $k_{2b} = 10^{-14}$; *p*-, $k_{1b} \geqq 10^{-8}$, $k_{2b} \geqq 10^{-11}$. From these figures appropriate values of pH are selected according to the criterion stated above. All measurements were made at room temperature. The control of the ionic strength was made with KCl. In the case of *o*-compound, where the relatively high ionic strength was necessary, dilution of the buffer solutions as prepared according to the indication in the literature was unnecessary. In this case the pH value does not depend on the concentration of the substance, since the buffer action of the solvent is strong. This is the reason why Table I for *o*-compound contains only one column for each intermediate pH value. The extinction coefficient ϵ_2 of singly charged ion BH^+ can in principle be calculated, but the error included will be great compared with k_{1b} and k_{2b}, because, contrary to them, ϵ_2 cannot be determined as an average value, since ϵ_2 assumes, in

3) The values used for calculations are obtained by interpolation of the values reported by Harned and Hamer, *J. Am. Chem. Soc.*, 55, 2194 (1933).

4) T.C. McIlvaine, *J. Biol. Chem.*, 49, 183 (1921).

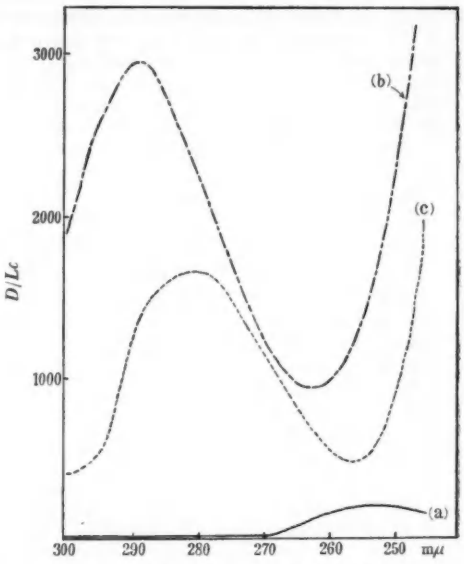

Fig. 1. Absorption curves of *o*-phenylenediamine in 6 N-HCl (a), 0.2 N-Na_2CO_3 (b), and pH 2.10 (c) solutions.

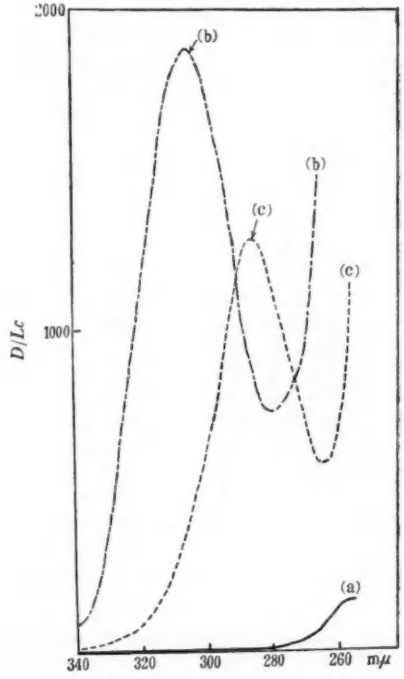

Fig. 2. Absorption curves of *p*-phenylenediamine in 1 N-HCl (a), 0.2 N-Na_2CO_3 (b), and pH 4.95 (c) solutions.

TABLE I

THE VALUES OF D', AND DISSOCIATION CONSTANTS OF *o*-PHENYLENEDIAMINE

Temp.: 14°C, μ: 1.0 mol./l.

Wavelength in mμ	D' Values					k_{1b} ×10¹⁰	k_{2b} ×10¹⁴
	6 N HCl	1.00 N HCl pH 0.00[a]	Na_2HPO_4-citric acid buffer solutions pH 2.10	Na_2HPO_4-citric acid buffer solutions pH 4.60	0.2 N Na_2CO_3		
290	9.5	125	1210	1640	2930	4.77	4.43
285	9.2	162	1550	1940	2800	4.11	4.21
280	12.0	175	1650	1940	2280	2.80	4.22
275	12.0	160	1490	1710	1690		5.44
270	16.0	131	1170	1340	1230		4.21
265	61.2	131	840	1000	970		4.78
260	130	166	560	710	950	2.84	5.20
255	172	192	475	700	1280	4.01	6.88
250	160	216	810	1200	2100	3.54	4.99
					Mean	3.68 ±0.32	4.93 ±0.30

a) The value of the mean activity coefficient of 1.00 N-HCl is given in B. E. Conway, Electrochemical Data (Elsevier Publishing Company, Amsterdam, 1952), p. 75, to be 0.809 at 25°C which amounts to pH=0.10.

TABLE II

THE VALUES OF D', AND DISSOCIATION CONSTANTS OF *p*-PHENYLENEDIAMINE

Temp.: 14.5°C, μ: 0.049 mol./l.

Wavelength in mμ	D' Values								k_{1b} ×10⁸	k_{2b} ×10¹²	Columns[a] used for calc.	k_{1b} ×10⁸	k_{2b} ×10¹²	Columns[a] used for calc.
	1 N HCl	Na_2HPO_4-citric acid buffer solutions pH 3.13	pH 3.00	pH 5.20	pH 4.95	pH 6.75	pH 6.70	0.2 N Na_2CO_3						
340	3	4		7		61	60	87	1.10		3, 5, 7	1.02		3, 5, 8
335	3	4		14		127	122	180	1.08		3, 5, 7	1.09		3, 5, 8
330	3.3	6		21		248	247	355	1.07		3, 5, 7	0.97		3, 5, 8
325	3.7	7		43		447	454	645	1.06		3, 5, 7	0.93		3, 5, 8
320	4.0	16		82		721	714	1034	1.12		3, 5, 7	1.03		3, 5, 8
315	4.3	34		144	109		1000	1432	1.02		3, 5, 8	1.12		3, 6, 8
310	4.7	71		250	213		1240	1760	1.07	7.56	3, 5, 8	1.08	8.19	3, 6, 8
305	5.0	130		407	375		1390	1880	1.02	8.67	3, 5, 8	1.02	9.38	3, 6, 8
300	5.3	217	170		606		1430	1820	0.99	10.05	3, 6, 8	0.95	10.86	4, 6, 8
295	5.6	335	280		906		1395	1590	0.89	10.50	3, 6, 8	0.87	9.60	4, 6, 8
290	6.1	437	378		1177		1292	1300		10.50	3, 6, 8		10.15	4, 6, 8
285	6.6	480	408		1283		1137	1015	1.46	10.68	3, 6, 8	1.47	10.13	4, 6, 8
280	7.4	455	388		1200		961	815	1.15	10.22	3, 6, 8	1.16	10.59	4, 6, 8
275	8.3	381	316		989		827	773	0.63	10.45	3, 6, 8	0.65	10.28	4, 6, 8
270	13.5	297	237		767		814	1035		10.37	3, 6, 8		10.93	4, 6, 8
265	53	256	199		592		1058	1600	2.49	11.34	3, 6, 8	2.57	12.01	4, 6, 8
260	114	297	243		628		1738	2620	1.73	9.87	3, 6, 8	1.73	12.37	4, 6, 8
255	150	490	443		1138		3120	4400	1.46	8.95	3, 6, 8	1.45	9.56	4, 6, 8
						Mean			1.21 ±0.11	9.93 ±0.30		1.19 ±0.11	10.34 ±0.33	

a) The set of numbers in column 12 shows that for each wave length the set of D' values corresponding to the column indicated by these numbers is substituted in Eq. (2) and the values of k_{1b} and k_{2b} found in column 10 and 11, respectively, are calculated from the resulting set of three equations. Column 15 relates to columns 13 and 14 as column 12 does to columns 10 and 11.

general, different values at different wave lengths. For this reason, the calculated ϵ_2 values are not given in the tables. The observed D'-values of a solution whose pH value lies in the middle of pk_{1b} and pk_{2b} is a fairly good measure of the absorption by the species BH^+ only, provided pk_{1b} and pk_{2b} are separated with each other by 3 or 4 as in phenylenediamines. The influence of the other species can be neglected at this value of pH. Figs. 1 and 2 show the absorption curves of *o*- and *p*-phenylenediamines, respectively, in acidic (a), alkaline (b), and medium pH (c) solutions. As was mentioned above, the curves (a), (b) and (c) are mainly due to species BH_2^{++}, B and BH^+, respectively. If at a given wave length the extinction coefficients of species B and BH^+ are alike, the calculated value of k_{1b} at this wave length is prboably in error. In the same way, if the extinction coefficients of species BH^+ and BH_2^{++} are alike, k_{2b} calculated at this wave length is probably in error. Furthermore, the D' values corresponding to too high transmittance are likely to be in error. In fact, anomalous values are obtained from these data and these values are not given in the tables.

Thus the mean values of the apparent dissociation constants are:

o-, $k_{1b}=(3.68\pm0.32)\times10^{-10}$, $k_{2b}=(4.93\pm0.30)\times10^{-14}$:

p-, $k_{1b}=(1.20\pm0.08)\times10^{-8}$, $k_{2b}=(1.01\pm0.03)\times10^{-11}$.

For the apparent dissociation constants obtained above, activity corrections were made, using the Debye-Hückel equation of the following form[5]:

$$-\log\gamma_i=\frac{Az_i^2\sqrt{\mu}}{1+Ba_i\sqrt{\mu}},$$

$$A=\frac{1}{2.303}\frac{N^2e^3}{(DRT)^{3/2}}\left(\frac{2\pi}{1000}\right)^{1/2},$$

$$B=\left(\frac{8\pi N^2e^2}{1000DRT}\right)^{1/2}$$

where e is the electronic charge, R is the gas constants, D is the dielectric constant of water at the absolute temperasure T, N is the Avogadro's number, and μ is the ionic strength of the solution[6]. z_i and a_i are the charge and the radius of ion i. a_i is assumed to be 5 Å for both phenylenediamines in all their forms. The activity coefficients thus calculated for each experimental condition are collected in Table III.

TABLE III

ACTIVITY COEFFICIENTS OF *o*- AND *p*-PHENYLENEDIAMINES CALCULATED BY DEBYE-HÜCKEL EQUATION

Isomers	*ortho*	*para*
Temp., °C	14	14.5
μ (mol./l)	1.0	0.049
γ_B	1.00	1.00
γ_{BH^+}	0.646	0.830
$\gamma_{BH_2^{++}}$	0.174	0.474

Then the final dissociation constants are calculated to be:

o-, $K_{1b}=(2.4\pm0.3)\times10^{-10}$,
$K_{2b}=(1.3\pm0.1)\times10^{-14}$ at 14°C;

p-, $K_{1b}=(1.0\pm0.1)\times10^{-8}$,
$K_{2b}=(5.8\pm0.1)\times10^{-12}$ at 14.5°C,

where the errors due to the Debye-Hückel equation are neglected. It is interesting to compare these results with the values obtained by other methods. They are listed in Table IV taken from Landolt-Börnstein Tables[7]. It can be seen that the present method yields reasonable values of dissociation constants. Moreover, the present work adds the value of the second dissociation constants of *o*-phenylenediamine to the literature. Of course the precise value of K_{2b} of this compound is still uncertain since we were forced to make this determination at rather high ionic strength.

TABLE IV

DISSOCIATION CONSTANTS OF PHENYLENEDIAMINES[a]

Isomers	Step	Temp., °C	Constant	Method	Author
o-	1st	21	$2.3_5\times10^{-10}$	Potentiometric	Kuhn & Wassermann Kuhn & Zumstein
o-	1st	25	3.3×10^{-10}	Hydrolysis, partial extraction	Farmer & Warth
p-	1st	18	1.3×10^{-8}	Conductmetric	Walden & Ulich
p-	1st	18	1.1×10^{-8}	Potentiometric	Kolthoff & Bosch
p-	1st	ca. 20	1.0×10^{-9}	Potentiometric & colorimetric	Pring
p-	1st	21	9.5×10^{-9}	Potentiometric	Kuhn & Wassermann
p-	2nd	18	3.5×10^{-12}	Potentiometric	Kolthoff & Bosch
p-	2nd	21	1.5×10^{-11}	Potentiometric	Kuhn & Zumstein

a) Taken from ref. (7) in text.

5) For example see, D. A. McInnes, "The Principles of the Electrochemistry", Reinhold, New York (1939), Chap. 7.

6) The values of physical constants used in the calculation are taken from DuMond and Cohen, *Revs. Modern Phys.*, **25**, 691 (1953), except for the dielectric constant of water, for which the values are obtained by the interpolation of the values listed in S. Kaneko, *J. Electrochem. Soc. Japan*, **20**, 273 (1952).

7) Landolt-Börnstein, "Physikalisch-Chemische Tabellen" Springer, Berlin (1931), 2te Ergänzungsband, p. 1094.

Comparison with Thamer-Voigt's Method[8,9]

As an application of the present method to the case where k_1 and k_2 are not separate from each other as for phenylenediamines, and also as a comparison of the present method with Thamer-Voigt's we have calculated the dissociation constants for isophthalic acid from the data presented by these authors[2]. The results are given in Table V. The mean values of the dissociation constants calculated by both methods agree very well.

TABLE V

OPTICAL DENSITIES[a] AND DISSOCIATION CONSTANTS OF ISOPHTHALIC ACID

Wave length in Å	Optical densities					$k_1 \times 10^4$	$k_2 \times 10^5$
	1.58	3.56	pH 4.18	5.095	8.72		
2476.0	0.987	1.134	1.152	1.036	0.982	3.21	3.62
2460.0	1.298	1.435	1.421	1.233	1.146	3.45	3.29
Wave length in Å	Optical densities					$k_1 \times 10^4$	$k_2 \times 10^5$
	1.58	3.37	pH 3.96	4.91	8.72		
2476.0	0.987	1.109	1.164	1.056	0.982	3.02	3.96
2460.0	1.298	1.410	1.446	1.256	1.146	2.71	4.52
					Mean[b]	3.10	3.85
					Mean (Thamer-Voigt)[c]	2.78	4.00

a) Optical density data are taken from ref. (2) in text.
b) Mean over four calculated values using the present method.
c) See ref. (2) in text.

In Thamer-Voigt's method it is ture that the optical density measurements of many kinds of solution of different pH values reduce the errors due to optical density or pH measurements included in the final values of k_1 and k_2, but the preparation of many kinds of solution is laborious especially for substances unstable in solution. Besides, it is necessary in their method that the optical density versus pH curve should show a decided maximum or minimum. In most cases a suitable wave length may be chosen so that the curve has a maximum or minimum. In the present method, the number of solutions to be prepared is considerably reduced. In addition, the above mentioned maximum or minimum are unnecessary. These are the advantages of the present method. While the error due to the optical density measurement becomes less by taking the mean over many values determined at different wave lengths, the error due to pH measurement cannot be reduced, which is the disadvantage of the present method.

In conclusion, the present method is experimentally easier to carry out especially for substances unstable in solution. For stable substances, the dissociation constants

8) It should be noted that k_1 and k_2 used in this section should be read as k_{1b} and k_{2b}, respectively, for diacidic bases such as phenylenediamines. For dibasic acids such as isophthalic acid k_1 and k_2 should be read as k_{1a} and k_{2a}, respectively, and defined by

$$k_{1a}=\frac{a_H[AH^-]}{[AH_2]},\quad k_{2a}=\frac{a_H[A^{--}]}{[AH^-]}$$

where a_H is the H-ion activity and AH_2, AH^- and A^{--} denote undissociated, singly and doubly dissociated dibasic acid, respectively.

9) After the preparation of this manuscript had been completed, a paper by B. J. Thamer (*J. Phys. Chem.*, 59, 450 (1955)) came to our attention. This method is essentially identical with ours excepting that ε_1 and ε_3 (in our notation) are not assumed to be the molar extinction coefficient at alkaline and acidic extremes. In diacidic bases (for example) having very small values of dissociation constants, his method may be particularly useful, since the direct determination of ε_3 necessitates the high value of ionic strength of the solution. If the optical density of the solution as acidic as possible (comforming to the requirement of low ionic strength) is practically equal to ε_3, Thamer's method has no advantages because in his method a set of five equations containing five unknowns must be solved for a fixed wave length instead of a set of three equations in our method. If the optical density of the solution as acidic as possible is considerably different from ε_3, his method may not give the precise value of the k_{2b}, because in such a solution rather a small fraction of the base exists in the form BH_2^{++} and even a small error in the optical density measurement results in a rather considerable error in k_{2b}. Therefore, for most practical purposes, our method involving the solution of a set of three equations for a fixed wave length may be sufficient.

may be determined by Thamer-Voigt's method a little more accurately.

The extension, of our method to polyelectrolytes appears possible, provided that each dissociated species has a different extinction coefficient in a proper wave-length region, although the number of simultaneous equations to be solved increases. For example, a tribasic acid requires a set of five equations.

The authors express their hearty thanks to Professor S. Imanishi who read the manuscript and made many suggestions. Thanks are also due to Professor R. Matuura for permission to use a pH meter and for making valuable suggestions.

Departments of Chemistry, Faculty of Science, Kyushu University, Fukuoka

---

The Action of Hydrogen Bromide and Oxygen on Various Ethenoid Compounds. I

By Makoto TAKAHASI*

(Received January 12, 1956)

The mechanism of the hydrocarbon oxidation by means of molecular oxygen at room or higher temperature is very complicated and its study has been an object of many investigations for many years. Although the mechanism has not yet been completely elucidated, the recent progress of the free radical chemistry has made clear that the oxidation by molecular oxygen involves free radical intermediates in the course of the reaction. The research of the oxidation at room temperature is very interesting and important, but the relatively slow velocity of the reaction at room temperature makes difficult such an investigation. It has been found that many materials such as catechol and hydroquinone which can serve as hydrogen donors retard the oxidation. However, hydrogen bromide which is also one of the hydrogen donors is known to be a distinguished accelerator of the oxidation of hydrocarbons by molecular oxygen, as described by F.F. Rust and W.E. Vaughan[1]. They carried out an extensive investigation of the oxidation of aliphatic and aromatic hydrocarbons catalysed by hydrogen bromide, and they proposed the following mechanism for the reaction,

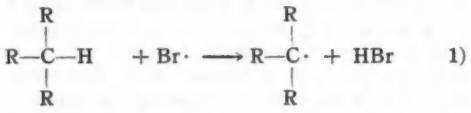

1)

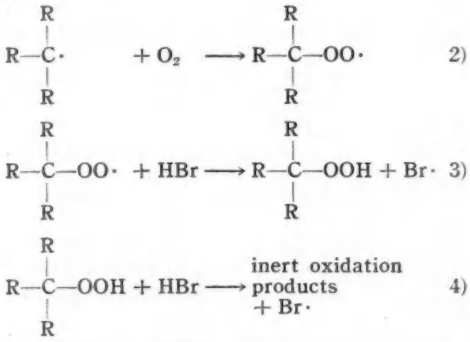

2)

3)

4)

Y. Urushibara and O. Simamura[2] extended their study of oxygen effect in the addition of hydrogen bromide to ethenoid compounds to the action of the mixture of oxygen and hydrogen bromide on allyl bromide, crotonic acid, and several other compounds. O. Simamura and the present author[3] studied the joint action of hydrogen bromide and oxygen on cinnamic acid and determined the orientation of the bromine atom when it adds to the double bond of cinnamic acid. Namely, the free radical 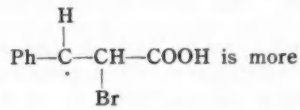 is more likely formed as the intermediate rather than

* Present address: Department of Chemistry, College of General Education, The University of Tokyo.

1) F.F. Rust and W.E. Vaughan, *Ind. Eng. Chem.*, **41**, 2595 (1949).

2) Y. Urushibara and O. Simamura, This Bulletin, **14**, 323 (1939).

3) O. Simamura and M. Takahasi, ibid., **22**, 60 (1949).

the alternative 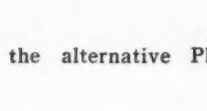 , because

ω-bromoacetophenone and carbon dioxide are obtained as the oxidation products and it can be supposed that they are derived from

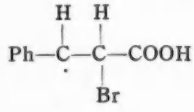

through the hydroperoxide

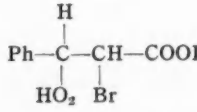

In order to compare the relative stability of these radicals theoretically, the author carried out a computation of the delocalization energies of the odd electron of the free radicals, Ph—$\dot{C}H_2$ and $\dot{C}H_2$—COOH, according to the same method as that which was adopted by G. W. Wheland[4], and obtained 15.3 kcal./mol. for the former and 16.7 kcal./mol. for the latter, assuming $S=0.25$, $\delta=0.8$, $\delta'=0$ and $\eta=0.8$. It may be impossible to conclude from these values that the latter is more stable than the former, for the calculation is of the zeroth order approximation. The values of bond dissociation energies of benzyl bromide and bromoacetic acid measured by the pyrolytic method of M. Szwarc[5] or that of toluene by the substitution reaction of bromine according to E. R. VanArtsdalen[6] will supply useful knowledge concerning this problem.

In this series of our papers the general scheme of the oxidation of various olefinic compounds in the presence of hydrogen bromide is discussed on the ground of the experimental data. This first paper deals with α,β-disubstituted ethenoid compounds, such as cinnamic acid, *m*-nitrocinnamic acid, *p*-methoxycinnamic acid, maleic acid, citraconic acid, crotonic acid, stilbene, and ω-nitrostyrene. The two substituted cinnamic acids, *p*-methoxycinnamic acid with an electron donative methoxyl group, and *m*-nitrocinnamic acid with an electron attractive nitro group, are both unreactive to the mixture of hydrogen bromide and oxygen at room temperature. The former has been found to have an antioxidant action by itself. When *p*-methoxycinnamic acid was added to the solution of cinnamic acid in carbon tetrachloride, it suppressed the reaction of cinnamic acid with the mixture of hydrogen bromide and oxygen to some extent. This may be attributed to the fact that the substitution reaction of *p*-methoxycinnamic acid with bromine atom may take place rapidly, stopping the chain reaction by bromine atom.

The general scheme of the action of hydrogen bromide and oxygen on ethenoid compounds has been discussed by Y. Urushibara[7a] and O. Simamura[7b] and by F. F. Rust and W. E. Vaughan[8], and is supposed to be as follows.

1) olefin + oxygen + hydrogen bromide $\longrightarrow$ Br· (initiations)

2) 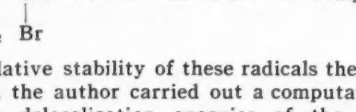 (propagation)

3) 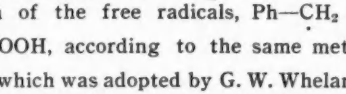 (propagation)

4) 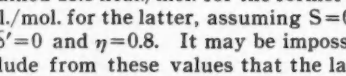 (propagation)

5) 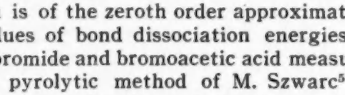 $+H_2O$ (overall reaction for the formation of bromohydrin)

6) 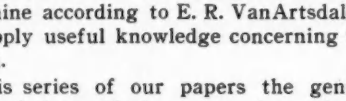 (formation of bromoketone)

7) 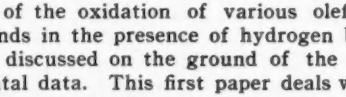 (formation of dibromide, termination)

8) 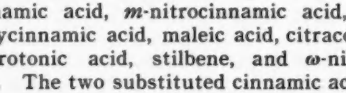 (formation of dibromide, propagation)

9) $Br\cdot + Br\cdot \longrightarrow Br_2$ (termination)

However, this scheme, applied to the reaction of cinnamic acid with hydrogen bromide and oxygen, may not give a satisfactory explanation of our experimental results. If it is assumed that all cinnamic acid dibromide is produced as a chain termination product

4) G. W. Wheland, *J. Am. Chem. Soc.*, **64**, 900 (1942).
5) M. Szwarc, *Chem. Revs.*, **47**, 75 (1950).
6) M. R. Anderson, Jr., H. A. Scheraga and Erwin R. VanArtsdalen, *J. Chem. Phys.* **21**, 1258 (1953).
7a) Y. Urushibara, *Kagakusoko*, Vol. 6, (1944).
7b) O. Simamura, This Bulletin, **17**, 326 (1942).
8) F. F. Rust and W. E. Vaughan, *J. Org. Chem.*, **7**, 491 (1942).

as in the above mechanism, one mole of bromine would be required to produce one mole of cinnamic acid dibromide, and in order to obtain one mole of bromine, at least one mole of cinnamic acid would be consumed by the reaction with one mole of oxygen molecule giving some oxidized product of cinnamic acid. That is, according to the above mechanism, one cycle of propagation reaction would involve only the reaction of one mole of cinnamic acid with one mole of oxygen molecule giving one mole of bromine as cinnamic acid bibromide or as free bromine molecule. Furthermore, in order to obtain one mole of ω-bromoacetophenone, one mole of cinnamic acid and one mole of oxygen molecule would be consumed giving no excess bromine.

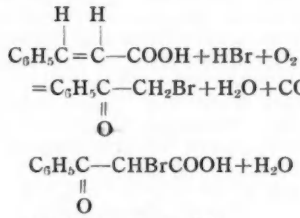

(stoichiometrically)

Our semi-quantitative experiment on the reaction of cinnamic acid with the mixture of hydrogen bromide and oxygen gives some evidence suggesting that the above scheme is not sufficient. The amount of cinnamic acid dibromide produced from 0.0187 mol. of cinnamic acid was 0.0101 mol. (53.4 mol. percent) and that of ω-bromoacetophenone was 0.0048 mol. (25.6 mol. percent for cinnamic acid used). The amount of carbon dioxide evolved was 0.0006 mol. It is noted that the amount of carbon dioxide in mole was not the same as that of ω-bromoacetophenone. This fact suggests the presence of the unstable compound $C_6H_5CCHBrCOOH$ in the

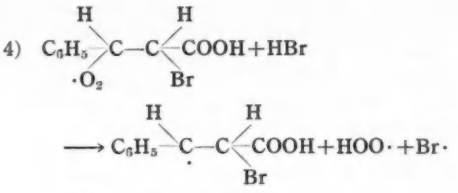

reaction product. Although the fate of the residual cinnamic acid of about 20% is not ascertained now, neither bromohydroxycinnamic acid nor dihydrocinnamic acid were found in any detectable amount in the reaction products. These compounds, if they existed, would suggest some other process of the formation of bromine from hydrogen bromide. Here, in order to give a reasonable explanation on the experimental result that cinnamic acid dibromide is produced in the yield of more than fifty percent, the following process is proposed in addition to the above ones:

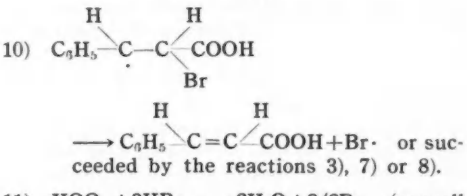

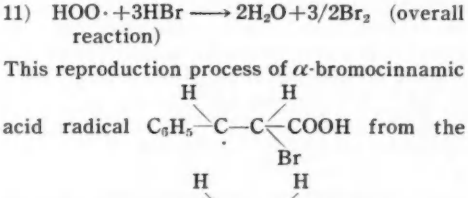

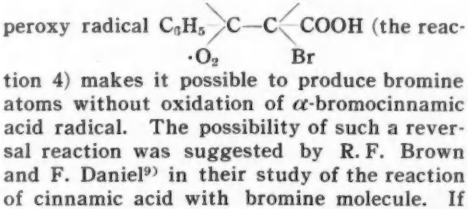

succeeded by the reactions 3), 7) or 8).

11) $HOO\cdot+3HBr \longrightarrow 2H_2O+3/2Br_2$ (overall reaction)

This reproduction process of α-bromocinnamic acid radical from the peroxy radical 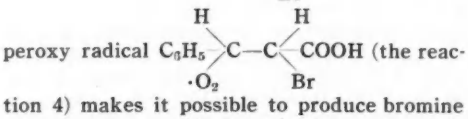 (the reaction 4) makes it possible to produce bromine atoms without oxidation of α-bromocinnamic acid radical. The possibility of such a reversal reaction was suggested by R. F. Brown and F. Daniel[9] in their study of the reaction of cinnamic acid with bromine molecule. If it is assumed that such a process takes place actually, this may be an example of sensitization of oxygen by free radical process.

While the mechanism of the initiation reaction is not yet clear, the author will give some fuller suggestion in a later paper. Here it is to be remembered that catechol suppresses the reaction of cinnamic acid with oxygen and hydrogen bromide incompletely. This incompleteness of the antioxidant action of catechol in the presence of an excess of oxygen suggests that catechol cannot inhibit the initiation reaction. Nitrobenzene was found to have no action as an antioxidant in the reaction of cinnamic acid with hydrogen bromide and oxygen, while it is known that it has an inhibiting action in the polymerization reaction. This may be explained by the fact that nitrobenzene does not react with bromine atoms very rapidly.

In the reaction products of crotonic acid with the mixture of hydrogen bromide and oxygen, carbon dioxide and an irritating aldehyde are found in addition to β-bromobutyric acid, α,β-dibromobutyric acid, α-

9) R. F. Brown and F. Daniels, *J. Am. Chem. Soc.*, **62**, 2820 (1940).

hydroxy-β-bromobutyric acid which were already described by O. Simamura[1]. The aldehyde gave 2,4-dinitrophenylhydrazone containing bromine and was not identified with the supposedly probable aldehyde, α-bromopropionaldehyde, which gave a 2,4-dinitrophenylhydrazine derivative containing no bromine. At present, the quantitative estimation of these compounds is difficult, so that the material balance in the reaction is not discussed here.

The reaction of maleic acid with hydrogen bromide and oxygen was confusing. The reaction gave a small amount of carbon dioxide. The author at first considered that carbon dioxide was an oxidation product of maleic acid produced in nearly the same way as from cinnamic acid. However, the acid gave carbon dioxide in the reaction with hydrogen bromide in the absence of oxygen, so that it is considered that the acid was decarboxylated through the ionic or any molecular process. It is known that maleic acid adds almost no bromine molecule at room temperature. Citraconic acid gave no reaction product except citraconic anhydride with the mixture of hydrogen bromide and oxygen. These experiments with maleic acid and citraconic acid show that ethenoid α,β-dicarboxylic acids do not react with the mixture of hydrogen bromide and oxygen, due to the stabilization of the ethylenoid double bond by two carboxyl groups.

The reaction of hydrogen bromide and oxygen with stilbene was already studied by O. Simamura[2], and he decribed the formation of stilbene dibromide and an oily product. The present author found a bromophenol and a carbonyl compound in the oily product in addition to a very small amount of carbon dioxide, but the identification of the phenol and the carbonyl compound has not yet been successful. The yield of stilbene dibromide was about 25 mol. percent of the stilbene used. The mechanism of the formation of a phenol from stilbene will be discussed in a later paper concerning the mechanism of the reaction of diphenylethylene with the mixture of hydrogen bromide and oxygen.

The reaction of ω-nitrostyrene with hydrogen bromide appears to be remarkably different from those of the other olefinic compounds. It gave a bromine atom by the action of hydrogen bromide in the absence of oxygen. No influence of oxygen was observed here. M. Takebayashi[10] described a similar action of nitroethylene on hydrogen bromide. ω-Nitrostyrene gave hydroxylamine, ammonia, ω-nitrostyrene dibromide, and an oily substance which was not identified until the present. The reaction mechanism will be discussed in future, when the reaction products have been analysed completely.

10) M. Takebayashi, *J. Chem. Soc. Japan*, 64. 192 (1942).

Experimental

Materials.—Hydrogen bromide was prepared by the three following methods. a) Bromine was dropped from a dropping funnel into tetralin with gentle heating, and the produced hydrogen bromide was passed through tetralin, anthracene, and phosphorus pentoxide. This method was adopted at first, but hydrogen bromide thus prepared was found to contain a small amount of carbon dioxide, which was presumably produced by the decomposition of some impurities such as tetralin hydroperoxide. b) Bromine was dropped on wet red phosphorus, and the produced hydrogen bromide was purified as in (a). The hydrogen bromide thus produced contained no carbon dioxide, but the production of hydrogen bromide was not smooth enough and the yield was small. c) Hydrogen and bromine were combined directly according to "Org. Synth"[11]. The tank hydrogen dried with phosphorus pentoxide was mixed with bromine, and the mixture was heated by a gentle flame. The hydrogen bromide was passed through copper turnings under a slightly reduced pressure applied to the outlet of the reaction vessel by a Mariot bottle.

Oxygen was obtained from a tank, and passed through aqueous alkali and over phosphorus pentoxide.

Benzene and carbon tetrachloride were purified and dried according to "Org. Solvents,"[12] and distilled.

Cinnamic acid obtained from a commercial source was recrystallized from ethyl alcohol, and kept for a time in an evacuated desiccator, m.p. 133°C.

p-Methoxycinnamic acid was synthesized from anisaldehyde and malonic acid in the presence of ammonia, m.p. 173–4°C.

m-Nitrocinnamic acid was synthesized from *m*-nitrobenzaldehyde according to "Org. Synth."[13], m.p. 196–7°C. Crotonic acid and maleic acid were commerical products. Maleic acid was recrystallized from a mixture of ether and acetone, m.p. 130°C.

Citraconic acid was obtained by pyrolytic distillation of citric acid through citraconic anhydride. ω-Nitrostyrene was synthesized from benzaldehyde and nitromethane, m.p. 58°C.

Stilbene was synthesized by the reduction of benzoin according to "Org. Synth."[14] and recrystallized from ethyl alcohol, m.p. 120°C.

Reactions.—Reaction of Cinnamic Acid with Hydrogen Bromide and Oxygen.—Cinnamic

11) "Organic Syntheses", Collective Vol. 2, John Wiley & Sons, Inc., p. 339.
12) A. Weissberger and E. Proskauer, "Organic Solvents", Oxford University Press, pp. 105, 156.
13) "Organic Syntheses", Collective Vol. 1, John Wiley & Sons, Inc., p. 398.
14) ibid., Vol. 23, p. 86.

acid (0.0187 mol.) was weighed and put together with 30 ml. of carbon tetrachloride, and the dry mixed gas of hydrogen bromide and oxygen was passed through the suspension at room temperature for about 230 minutes. The reaction gas was passed through a calcium chloride tube, over water to absorb hydrogen bromide, and through a barium hydroxide solution. The precipitated barium carbonate was collected on a glass filter, and weighed. About 0.0006 mol. of carbon dioxide was produced from 0.0187 mol. of cinnamic acid. In the reaction vessel about 2.953 g. of a solid matter were deposited, and this matter was proved to be almost pure cinnamic acid dibromide by melting point measurement and analysis of bromine. The carbon tetrachloride solution gave 3.8 g. of a mixture of oil and solid mattter on evaporation at atmospheric pressure. The oil and solid matter were separated on a glass filter. The solid, weighing 0.146 g., melted at 195°C. without recrystallization and was identified with cinnamic acid dibromide. The light-greenish oil weighed 2.23 g. and had an irritating smell. 0.318 g. of the oil was added to a solution of 0.4 g. of 2, 4-dinitrophenylhydrazine prepared according to R. L. Shriner[15]. Rapid formation of a dinitrophenylhydrazone was observed but the mixture was left overnight. The collected 2, 4-dinitrophenylhydrazone weighed 0.257 g., which corresponded to 1.8 g. (0.0048 mol.) of the hydrazone to the total amount of the oil. The 2, 4-dinitrophenylhydrazone melted at 214–5°C and contained 21.1% of bromine (Calcd. for $C_{14}H_{11}O_4N_4Br_2$: Br, 21.1 %). It was identified with the 2, 4-dinitrophenylhydrazone of ω-bromoacetophenone by a mixed melting point with an authentic specimen. In addition to cinnamic acid dibromide and ω-bromoacetophenone, a small amount of an unidentified substance was obtained, but no dihydrocinnamic acid (m.p. 47°C), bromohydroxycinnamic acid (m.p. 120°, 156°, 164°C) nor any other acidic substance were found in the reaction mixture. The total amount of cinnamic acid dibromide was 3.099 g. (0.0101 mol.) which corresponded to 53.4 mol. percent of cinnamic acid used. The substance was dried in a desiccator to constant weight. Two more experiments on the reaction of cinnamic acid with hydrogen bromide and oxygen under the same conditions gave similar results. The amounts of cinnamic acid dibromide produced did not differ by more than 0.3 g.

The Reaction of Cinnamic Acid with Hydrogen Bromide and Oxygen in the Presence of Catechol.—Two solutions of cinnamic acid (3.0 g.) in 40 ml. of carbon tetrachloride were prepared, 0.1 g. of catechol being added to one. Both the solutions were subjected to the action of hydrogen bromide and oxygen at the same time. For the solution containing catechol, carbon dioxide was not evolved, and cinnamic acid was recovered, and no 2, 4-dinitrophenylhydrazone was precipitated with the 2, 4-dinitrophenylhydrazine. From the other solution, carbon dioxide was evolved, and cinnamic acid dibromide was obtained.

15) R.L. Schriner and R.C. Fuson, "The Systematic Identification of Organic Compounds", John Wiley & Sons, Inc., p. 171.

Effect of Nitrobenzene.—In 40 ml. of carbon tetrachloride containing 1 ml. of nitrobenzene, 2.01 g. of cinnamic acid were added and the mixture of hydrogen bromide and oxygen was passed through the solution for 535 minutes. Carbon dioxide and cinnamic acid dibromide were obtained and no antioxidant effect of nitrobenzene was observed.

Reactions of *p*-Methoxycinnamic Acid and of *m*-Nitrocinnamic Acid with Hydrogen Bromide and Oxygen.—Hydrogen bromide and oxygen were pased through a solution of *p*-methoxycinnamic acid (3.0 g.) in 40 ml of carbon tetrachloride for 310 minutes. Evolution of carbon dioxide did not take place, and *p*-methoxycinnamic acid was recovered. When hydrogen bromide and oxygen were passed through a solution of 2 g. cinnamic acid and 0.021 g. of *p*-methoxycinnamic acid in 30 ml. of carbon tetrachloride for 265 minutes, a small amount of carbon dioxide was produced, and the reaction product consisted mainly of cinnamic acid dibromide. When 2 g. of cinnamic acid and 2 g. of *p*-methoxycinnamic acid dissolved in 30 ml. of carbon tetrachloride were subjected to the action of hydrogen bromide and oxygen for 405 minutes, a very small amount of carbon dioxide was produced during the passage of the mixed gas, but almost all cinnamic acid and *p*-methoxycinnamic acid were recovered from the carbon tetrachloride solution as a mixture.

Hydrogen bromide and oxygen were passed through a suspension of 2.0 g. of *m*-nitrocinnamic acid in 30 ml. of benzen for 310 minutes at room temperature. *m*-Nitrocinnamic acid was recovered completely without evolution of carbon dioxide.

Reaction of Crotonic Acid with Hydrogen Bromide and Oxygen.—In 50 ml. of carbon tetrachloride 10 g. of crotonic acid was added and the mixture of hydrogen bromide and oxygen was passed through the solution at room temperature for 265 minutes. The carbon dioxide formed was caught as barium carbonate, which weighed 0.215 g. (0.001 mol.). On the bottom of the vessel an oily product deposited from the carbon tetrachloride solution, and, on being kept in a refrigerator, gave a crystalline mass which melted at 95°C. and was identified with α-hydroxy-β-bromobutyric acid. The oil separated from the crystalline mass reduced Fehling's solution at room temperature and gave a small amount of 2, 4-dinitrophenylhydrazone, m.p. 180–200°C. The purification of the hydrazone by either recrystallization or chromatography was unsuccessful. The carbon tetrachloride solution gave about 15 g. of an oil on evaporation. The oil was distilled under a reduced pressure of 20 mmHg. The first fraction which boiled at 48–100°C under that pressure was crotonic acid, the second fraction (1.5 g.) which boiled at 125–130°C was β-bromobutyric acid, and the third fraction (6.5 g.) which passed over at 135–148°C solidified for the most part and the solid melted at 86–88°C. In the flask remained some residue, which melted at 86–88°C. It was identified with crotonic acid dibromide. The velocity of hydrolysis of the second fraction was compared with those of α-bromo- and β-bromobutyric acids. Each compound was weighed into

a flask, and 2.0 ml. of a 5.9 N NaOH solution was added. After standing for one hour at room temperature the mixture was neutralized with nitric acid, silver nitrate was added, and the precipitated silver bromide was weighed. α-Bromo- and β-bromobutyric acids liberated 2.6 and 70% of bromine, respectively. The second fraction of the distillation was hydrolysed under the same condition to the extent of 68% and was thus proved to be composed of β-bromobutyric acid. Every fraction gave a positive reaction with Fehling's reagents, and gave a small amount of a 2,4-dinitrophenylhydrazone suggesting a contamination with some aldehyde, the identification of which was not successful.

Reaction of Maleic Acid with Hydrogen bromide and Oxygen.—Hydrogen bromide and oxygen were passed through a solution of 3.000 g. (0.026 mol.) of maleic acid in 50 ml. of carbon tetrachloride for 315 minutes at room temperature, and 0.0008 mol. of carbon dioxide and 3.199 g. of a precipitate were obtained. The carbon tetrachloride solution gave almost no residue on evaporation. The precipitate showed a large range of melting points. From the precipitate 1.00 g. was sampled and 20 ml. of distilled water was added to it. The water-insoluble part was very small in quantity and it was found to be fumaric acid by a melting point measurement. The water-soluble part was extracted with 20 ml. of ether twice, but both the ethereal extract and the aqueous solution contained maleic acid contaminated with some unidentified compound containing bromine. Formerly the author considered that the carbon dioxide was produced by the free radical mechanism, but, the recent experiment on the reaction of maleic acid with hydrogen bromide in the absence of oxygen showed that carbon dioxide was formed in nearly the same order of amount as in the presence of oxygen. Namely a carbon tetrachloride solution containing 3.00 g. of maleic acid gave about 0.0004 mol. of carbon dioxide on passing hydrogen bromide for 270 minutes at room temperature. Furthermore, when 3 g. of maleic acid with 0.05 g. of catechol was dissolved in 40 ml. of benzene, and hydrogen bromide and oxygen were passed for 165 minutes, 0.0005 mol. of carbon dioxide as barium carbonate was formed.

Reaction of Citraconic Acid with Hydrogen Bromide and Oxygen.—In 60 ml. of benzene 5.0 g. of citraconic acid was dissolved, and the mixture of hydrogen bromide and oxygen was passed through the solution for 360 minutes at room temperature. During the reaction no evolution of carbon dioxide was observed. After evaporation of the reaction mixture, the residual oil was distilled under a reduced pressure of 18 mmHg. and nearly the whole distilled at 98–100°C. The distillate contained no bromine and was identified with citraconic anhydride.

Reaction of Stilbene with Hydrogen Bromide and Oxygen.—To 70 ml. of carbon tetrachloride 5.0 g. (0.028 mol.) of stilbene was added and the mixture of hydrogen bromide and oxygen was passed through the solution for 330 minutes at 19.0°C. Carbon dioxide produced from stilbene was caught in the form of barium carbonate which weighed 0.092 g. (0.00047 mol.). In the reaction vessel a colorless precipitate was deposited from the carbon tetrachloride solution of red color. The deposit weighed 2.73 g. and was found to be composed of stilbene dibromide, m.p. 237°C. It corresponds to 25 mol. percent of the stibene used. The carbon tetrachloride solution was divided into two parts, 44 ml. and 20 ml. The former was shaken with 50 ml. of a 1 N sodium hydroxide solution twice. The sodium hydroxide solution was saturated with carbon dioxide and the separated oil was extracted with ether. The ethereal extract gave a small amount of a phenolic substance on evaporation which gave a positive test for a phenol with ceric ammonium nitrate, the color being brown. It melted at 75°C, and contained bromine, although its amount was very small and its analysis was not successful. It was presumed to be crude tribromophenol, m.p. 96°C. The aqueous solution, saturated with carbon dioxide and shaken with ether, was acidified with sulfuric acid and extracted with ether, but the extract gave practically no appreciable amount of a residue on evaporation. From the carbon tetrachloride solution, shaken with aqueous sodium hydroxide, an oily matter was obtained on evaporation and was distilled under a reduced pressure. A fraction boiling at 112–118°C under 0.9 mmHg gave a crystalline matter. It was separated from the oily part, and recrystallized from alcohol. The substance melted at about 100°C and contained only 8.6% of bromine. Probably it was not pure enough, but the amount was so small that no further recrystallization was attempted. It was supposedly unchanged stilbene, b.p. 166–7°C under 12 mmHg, m.p. 124°C.

Summary

(1) The reaction of α,β-substituted ethenoid compounds with the mixture of hydrogen bromide and oxygen were studied. In the case of cinnamic acid, a reaction mechanism has been tentatively proposed on the basis of the identfied products and their semi-quantitative estimation. The quantitative study of the reaction of cinnamic acid suggests the possibility that oxygen is sensitized by the presence of some free radical if it is relatively stable.

(2) Some experimental data with crotonic acid, sitlbene, and other compounds were presented. Unfortunately, the analysis of the reaction products has not yet been completed up to the present, so that no detailed discussion on these compounds was attempted. A general discussion on the reactions of ethenoid compounds with the mixture of hydrogen bromide and oxygen will be made in a later paper.

The author wishes to express his hearty thanks to Prof. Y. Urushibara and Prof. O. Simamura for their kind guidance and encouragement throughout this work.

Department of Chemistry,
Faculty of Science,
The University of Tokyo,
Komaba, Tokyo

Studies on Seven-membered Heterocyclic Compounds Containing Nitrogen. I. Synthesis of 1-Azacycloheptan-4-one Hydrochloride

By Akira Yokoo and Shiro Morosawa

(Received March 28, 1956)

As to azacycloheptanones, syntheses of 1-methyl-1-azacycloheptan-3-one[1], 1-methyl-2-ethyl-1-azacycloheptan-3-one[2], 1,2-dimethyl-1-azacycloheptan-3-one[3], and 1-alkyl-5-phenyl-1-azacycloheptan-4-ones[4] have been reported, but no such compound as one that has no side-chain is obtained except a lactam-type 1-azacycloheptan-2-one.

The present authors obtained 1-benzyl-1-azacycloheptan-4-one (II) (b.p. 137–139°C/2 mmHg.; hydrochloride, m.p. 186–187°C (decomp.); 2,4-dinitrophenylhydrazone hydrochloride, m.p. 206°C (decomp.)) by the Dieckmann condensation of ethyl N-benzyl-γ-(β-carbethoxyethylamino) butyrate[5] (I), using the methods of Prill and McElvain[1], and of Leonard and Barthel[2]. Reduction of II hydrochloride by palladous oxide as a catalyst afforded 1-azacycloheptan-4-one hydrochloride (III), m.p. 171°C (decomp.). 2,4-Dinitrophenylhydrazone hydrocholoride of III was formed in two kinds of crystal; one melted at 155°C (decomp.) and the other at 211°C (decomp.). The formed could be converted into the latter.

The action of diazomethane on 1-benzoyl-1-azacyclohexan-4-one yielded an oil, b.p. 172–179°C/0.01 mmHg. likely to be 1-benzoyl-1-azacycloheptan-4-one from the analytical value and also from that of 2,4-dinitrophenylhydrazone, m.p. 175–6°C. An attempt was made to obtain III by hydrolysis of the oil with hydrochloric acid, but the resultant oily substance did not crystallize. 2,4-Dinitrophenylhydrazone derived from the oily substance, however, was, though in poor yield, found to be identical with the one, m.p. 155°C (decomp.) from III by mixed fusion. Further detailed study on these experiments will be described in subsequent papers.

The Dieckmann condensation of ethyl N-benzoyl-γ-(β-carbethoxyethylamino) butyrate[5] was unsuccessful.

The present study was carried out as a part of the general research on the azulenoid compounds (the representative, Prof. Tetsuo Nozoe). The authors take this opportunity to extend their deep gratitude to the members of the Department of Organic Chemistry of Tokyo Institute of Technology for their carrying out the carbon and hydrogen microanalyses and also to Mr. Kameji Yamane (this laboratory) for his cooperation in the present experiments.

Experimental

1-Benzyl-1-azacycloheptan-4-one (II).—In a 1 l. three-necked, round-bottomed flask fitted with a Hershberg stirrer, a dropping funnel and a fractionating column which had a thermometer on its head and a side arm attached to a condenser set for downward distillation, were placed sodium ethoxide, prepared from 2.3 g. of sodium[6] and 400 cc. of dry xylene. The reaction flask was heated under stirring in an oil-bath sufficiently to cause gentle refluxing from the column, and a solution of 32.1 g. of ethyl N-benzyl-γ-(β-carbethoxyethylamino) butyrate in 200 cc. of dry xylene was added dropwise during sixteen hours. The heating was then continued until the mixture of alcohol and xylene distilled out and the thermometer registered the boiling point of xylene. The reaction mixture was extracted with four 30 cc. portions of water and three 40 cc. portions 2N hydrochloric acid. The extracts were united and refluxed with 240 cc. of concentrated hydrochloric acid for five hours. The hydrochloric acid was expelled by heating on a water-bath under reduced pressure as completely as possible and 50% potassium hydroxide solution was added to the residue to make pH 8 and extracted with five 50 cc. portions of ether. The aqueous solution was then made strongly alkaline and further extracted with seven 30 cc. portions of ether. These ether extracts were all combined and dried over magnesium sulfate. Dry hydrogen chloride was passed through to give hydrochloride of II as a precipitate. The precipitate was dried in a desiccator and dissolved in 12 cc. of methanol

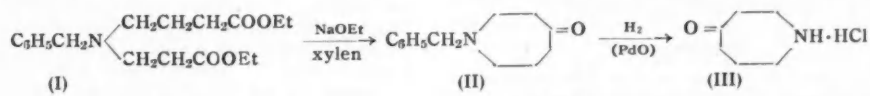

(I) (II) (III)

1) E.A. Prill and S.M. McElvain, *J. Am. Chem. Soc.*, 55, 1233 (1933).
2) N.J. Leonard and E. Barthel, ibid., 71, 3098 (1949).
3) N.J. Leonard and S. Gelfand, ibid., 77, 3269 (1955).
4) R.E. Lyle and G.G. Lyle, *C.A.*, 49, 9047 (1955).
5) A. Yokoo and S. Morosawa, *J. Chem. Soc. Japan*, 77, 599 (1956).
6) "Organic Reaction", Vol. I, p. 278.

and crystallized by adding ether. This crystal was recrystallized from methanol-ether solution as white needles, m.p. 186–187°C (decomp.), yield 5.2 g. (Found: N, 5.74. Calcd. for $C_{13}H_{17}ON \cdot HCl$: N, 5.85%).

2, 4-Dinitrophenylhydrazone Hydrochloride.—The mixture of II hydrochloride (0.1 g.), 2, 4-dinitrophenylhydrazine (0.2 g.), alcohol (10 cc.) and concentrated hydrochloric acid (0.2 cc.) was heated for two minutes. The crystals formed were recrystallized from water to yield 0.2 g. of yellow crystals, m.p. 206°C (decomp.). (Found: N, 16.87. Calcd. for $C_{19}H_{21}O_4N_5 \cdot HCl$: N, 16.65%).

The above-mentioned hydrochloride was made alkaline by adding 50% potassium hydroxide solution and taken up in ether. After drying over magnesium sulfate, the ether was removed and vacuum distillation of the residue gave II, b.p. 115–118°C/0.01 mm. (Found: N, 7.17. Calcd. for $C_{13}H_{17}ON$: N, 6.89%).

1-Azacycloheptan-4-one Hydrochloride (III).—A solution of 4 g. of II hydrochloride in 150 cc. water was shaken with 0.3 g. of PdO under hydrogen atomosphere at room temperature until the theoretical amount of hydrogen had been absorbed. After separation of the catalyst by filteration, water was removed under reduced pressure and the residue was crystallized from alcohol and ether to yield 2.1 g. (84%) of colorless needles, m.p. 171°C (decomp.).

Anal. Found: C, 48.51; H, 7.98; N, 9.29. Calcd. for $C_6H_{11}ON \cdot HCl$: C, 48.83; H, 8.08; N, 9.36%.

2, 4-Dinitrophenylhydrazone hydrochloride was obtained in yellow needles, m.p. 212°C (decomp.) (Found: N, 21.61. Calcd. for $C_{12}H_{15}O_4N_5 \cdot HCl$: N, 21.24%). Another kind of crystal was also obtained in orange scales, m.p. 152–155°C (decomp.), which was not depressed on admixture with the specimen derived from 1-benzoyl-1-azacycloheptan-4-one by hydrolysis and was also able to be converted into the modification in yellow needles by boiling with hydrochloric acid in methanol.

Chemical Institute, Faculty of Science, Okayama University

Raman Spectrum of Hinokitiol (m-Isopropyltropolone)

By Sunao IMANISHI and Mitsuo ITO

(Received April 6, 1956)

Introduction

In a previous paper[1] the Raman spectrum of tropolone in benzene solution was studied, and the more important vibrational frequencies there found were compared with infrared and vapor ultra-violet absorption data[2], together with known facts about benzene, and the types of vibrational modes in the tropolone molecule having these frequencies were discussed qualitatively. Up to the present no complete theoretical calculation of normal vibrational modes of any cycloheptatriene derivatives has been attempted, preventing unambiguous interpretation of all the vibrational frequencies found in the Raman spectrum to be given. In this paper the Raman effect for hinokitiol was studied in order to obtain further experimental information regarding the characteristic frequencies common to "tropolonoid" molecules.

Experimental

The hinokitiol sample used in this experiment was prepared in the Medical Department of Kumamoto University, and was kindly placed at our disposal by Prof. K. Sebe. The sample was expected to be sufficiently pure, so no further purification was attempted. Five grams of the sample was dissolved in 20 cc. of pure benzene, and with this solution a Wood's tube of 1 cm. bore and 15 cm. length was filled. The Wood's tube has an outer jacket through which a saturated solution of sodium nitrite was circulated to cut off ultra-violet radiations of wave-lengths below 4047Å completely, and the Hg 4047Å line partially.

Filtering the mercury radiations with sodium nitrite solution appeared to help suppress photochemical coloring of hinokitiol markedly. However, after a prolonged irradiation with two quartz mercury lamps, burning at 10 amp. each, the sample ultimately turned red-brown as in the case of tropolone, and the effective time of exposure must have been much shorter than the twenty hours' used in the experiment.

The spectrograph employed had two dense flint glass prisms each of 13 cm. height and 22 cm. side length. The camera lens was of 60 cm. focal length, giving an effective aperture of F/5 and a linear dispersion of about 20Å/mm. at 4359Å. Kodak "Plus X" panchromatic film was used to record the scattered spectrum. The microphotometer trace of the spectrum is reproduced in Fig. 1, together with those of tropolone and the solvent (benzene). The Raman lines due to benzene are marked with arrows. The original

1) S. Imanishi and M. Ito. This Bulletin, 28, 75 (1955).
2) S. Imanishi and M. Ito, to appear in *J. Chem. Phys.*, 1956.

traces were made with a recording microphotometer supplied by the former Institute of Physical and Chemical Research, Tokyo. It is seen in this figure that in the hinokitiol spectrum the long wave end is superposed by a strong background, making eye observation of weak Raman lines not

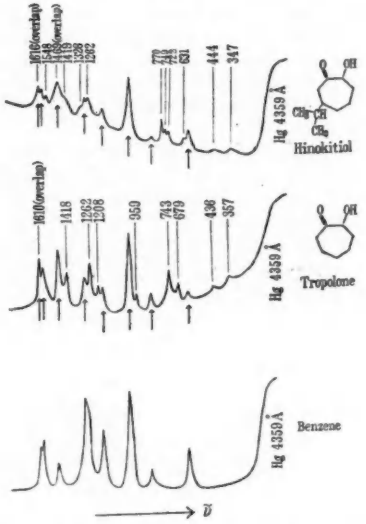

easy. Wave-lengths of Raman lines were determined against those of Fe comparison lines. Their wave-number shifts from the exciting Hg line 4359Å, as well as estimates of their relative intensities, are given in Table I.

TABLE I

VIBRATIONAL FREQUENCIES IN HINOKITIOL (cm^{-1})

Hinokitiol Raman C_6H_6 Solution	Infra-red Absorption* Liquid	Tropolone[1] Raman C_6H_6 Solution
347 (2)		357 (2)
444 (1)		436 (1)
631 (2)		679 (2)
722 (2)	730 (m)	
749 (2)		
770 (3)	770 (w)	743 (3)
	820 (m)	
	890 (w)=2×444	
	910 (w)	
	940 (m)	959 (1)
	990 (w)=347+631	
	1050 (w)=347+722	
	1100 (w)=347+749	
		1208 (2)
1264 (4)	1250 (s)	1262 (4)
1326 (3)	1350 (w)	
1419 (4)	1410 (m)	1418 (5)
1469 (5)	1470 (s)	
1548 (4)	1560 (m)	
1616 (5)	1600 (s)	1610 (5)

* The frequencies and intensities in this column are those estimated from the published absorption curve of ref. (3).

Discussion

The only data pertaining to the vibrational spectrum of hinokitiol so far published and available for comparison are those we owe to Shimanouchi et al[3] which deal with the infra-red absorption. Approximate positions and relative intensities of absorption maxima observed by these authors are listed in column 2 of Table I. In the Raman spectrum of hinokitiol three new bands are found in the low frequency region below 650 cm^{-1}, which were not found infra-red absorption. In the high frequency region above 1200 cm^{-1} agreement with infra-red data is very good. As any Raman frequency associated with a considerable intensity must be regarded as a fundamental, all of the twelve Raman shifts given in the Table are here taken as such. On the basis of this assumption, in fact, many of the weak maxima measured in the infra-red in the intermediate frequency region can be interpreted as overtones and combinations as indicated in the Table.

The two low frequencies 357 cm^{-1} (2) and 436 cm^{-1} (1) in tropolone (Table I) are preserved in hinokitiol [347 cm^{-1} (2) and 447 cm^{-1} (1)], almost unaffected by the substitution with the isopropyl group. From their magnitudes these frequencies are very probably of outplane torsional vibrations of the tropolone ring. The strong Raman shifts of 1262, 1419 and 1616 cm^{-1} in hinokitiol coincide exactly with the 1262, 1418 and 1610 cm^{-1} shifts in tropolone, allowing for errors in measurement. As absorption bands of almost the same frequencies as these three are invariably found in infrared absorption of many tropolone derivatives it is apparent that these also belong to vibrations characteristic of the tropolone skeleton. Among them the strongest 1616 cm^{-1} is attributed to the C=O stretching vibration[4], although the value is considerably lowered from that of the ordinary C=O frequency ($\gtrsim$1700 cm^{-1}). On the other hand the frequencies between 1262 and 1548 cm^{-1}, which are considered to be of C—C stretching vibrations of the ring, are as a whole higher than the corresponding frequencies in benzene compounds. These facts support Koch's[5] view that in molecules with the heptatriene ring C=O bond forces are weaker and C—C bond forces are stronger than those in benzenoids. These changes in bond forces may have been

3) K. Kuratani, M. Tsuboi and T. Shimanouchi, This Bulletin, 25. 250 (1952).

4) Scot and Tarbel, *J. Am. Chem. Soc.*, 72, 240 (1950). Doering and Knox, ibid., 73, 828 (1951).

5) Koch, ibid., 73, 512 (1951); Bellamy, "The Infrared Spectra of Complex Molecules", Methuen, London (1954), p. 75.

caused on the one hand by resonance, or what amounts to the same thing, by the electron migration from the carbonyl O atom into the ring, and on the other by the formation of intramolecular hydrogen bonding between the two O atoms of the tropolone molecule. Furthermore these facts seem to suggest that the heptatriene ring in tropolone owes its stability to the attachment of the carbonyl group.

The comparatively strongly observed Raman shift 770 cm^{-1} corresponds to the strong 743 cm^{-1} in tropolone. This frequency is also found in infra-red absorption, but there it was found as a shoulder to the strong absorption peak at 730 cm^{-1}. By analogy with tropolone the vibrational mode with this frequency is assumed to be the totally symmetric breathing vibration of the molecule, to which in-plane ring deformation contributes considerably. This conclusion is supported by the hinokitiol vapor ultra-violet absorption[6], in which three strong and board bands form a progression with ~600 cm^{-1} interval, starting from the O, O band on its shorter wave side. Then this ~600 cm^{-1} frequency must represent the excited (electonic) state value of the 770 cm^{-1} fundamental of the ground state. In tropolone the excited state value of the corresponding 743 cm^{-1} breathing vibration is 643 cm^{-1}. Apart from the above evidence from ultra-violet absorption, we have calculated the two totally symmetric vibration frequencies of the cycloheptatrienyl (tropylium) ion $(CH)_7^+$ with D_{7h} symmetry, using force constants borrowed from benzene, in order to check the magnitudes of these vibration frequencies in a seven-membered ring compound. They came out to be 863 cm^{-1} (C and H in phase) and 3038 cm^{-1} (C and H in reversed phase), showing that the in-plane breathing frequency is considerably lowered from 992 cm^{-1} in benzene (D_{6h}). These vibrations should be strictly infra-red inactive and the most Raman-active. In fact, in the infra-red data reported by Doering and Knox[7] there is no absorption near the calculated 863 cm^{-1} region, just as expected.

Now, it can be seen in analogy with benzenoids that this type of vibration will gain intensity in infra-red absorption with still lowered frequency by the substitution of H atoms with heavy radicals as in tropolonoids, with the consequent loss of the D_{7h} symmetry. These arguments also support our assignment regarding the breathing vibrations in tropolone and hinokitiol, and make understandable their intensity relation in infra-red and Raman spectra.

The ramaining Raman frequencies 722 and 749 cm^{-1} in hinokitiol have no corresponding shifts in tropolone, so that they may be attributed to internal vibrations of the isopropyl radical.

The authors thank Professor K. Sebe of Kumamoto University for the supply of the hinokitiol samples. The cost of the experiment was defrayed from the Science Research Expenditures of the Education Board.

Chemical Laboratory, Faculty of Science, Kyushu University, Fukuoka

6) S. Imanishi and M. Ito, Orally communicated to the Chem. Soc. Japan Meetings, 1952.

7) Doering and Knox, *J. Am. Chem. Soc.*, **76**, 3203 (1954).

Studies on Organic Reagents for the Colorimetric Analysis of Germanium. I. Reactions between Germanium and Some Organic Compounds

By Kenjiro KIMURA, Kazuo SAITO and Masako ASADA

(Received January 24, 1956)

Recently germanium, one of the less-common elements, found its special usefulness in electronics. This fact makes it very important for scientist to explore even the very poor resource of germanium in nature. The study on the distribution and migration of germanium in the earth's crust is also important from the standpoint of geochemistry.

For these reasons an excellent method for the quantitative analysis of germanium is urgently needed. Up to the present time a variety of analytical methods for germanium have been proposed, which covered gravimetric, volumetric, colorimetric, spectrographic and polarographic methods[1]. For a trace amount of germanium, however, the colorimetric method seems to be most excellent. In the colorimetric analysis choice of a reagent is always important. So far the use of many reagents such as ammonium molybdate[2], oxidized hematoxyline[3], phenylfluorone[4] quercetin[5], and quinalizarine acetate[6] has been proposed. But none of them was found to be entirely satisfactory. The difficulty lies in the complicated procedure required to remove interfering ions, as well as in the adjustment of hydrogen ion concentration within a narrow range. Moreover, for some reagents, the reagent itself or the compound between the reagent and germanium is not stable. Some other reagents form sparingly soluble precipitates with germanium. In such a case the colorimetric measurement has to be made on a colloidal solution.

In this report the authors tried to confirm the functional groups which combine with germanium. Special attention was paid to correlate the structure of the reagent to its reactivity with germanium. A search was made for a reagent which combines with germanium in a strongly acidic solution without forming any precipitates, its absorption spectrum being changed. In addition, the reaction should not be interfered with by foreign ions. A. Tchakirian and P. Bevillard studied the functional groups* which are supposed to combine with germanium. In their earlier studies[7a-e] they concluded as follows. (1) In order to react with germanium the organic molecule under consideration must have two hydroxyl groups on ortho positions and also a carbonyl- or quinoimine-group; the latter is able to bring about a tautomery between hydroxyl- and carbonyl-groups. (2) *Ortho* diamine groups, that are analogous to ortho dihydroxyl groups fail to react with germanium. (3) The larger the molecule, the more sensitive the reaction with germanium. A larger molecule reacts with germanium even at a low pH. Reaction at such a low pH excludes the interference by other elements. On the other hand, the molecule tends to be sparingly soluble in solvents. To increase the solubility of such a compound it is desirable to introduce an acidic group such as sulphonate into the compound. In their late studies[7f-g], they stated that the function of the carbonyl group was not clear and that a salt was formed by the combination of the quinoimine group with the dihydroxyl germanic acid which was preliminarily formed. They also stated that the ortho dihydroxyl groups react with germanium even in a compound without carbonyl- or quinoimine group. In order to confirm their results, the present authors examined the reaction between germanium and flurone-, naphthoquinone-, and cumarin derivatives. This study appears to give an orientaion to find a new reagent for the colorimetric analysis of germanium.

1) H.H. Krause and O.H. Johnson, *Anal. Chem.*, **25**, 134 (1953).

2) N.A. Filippona and L.I. Kusentzowa, *Zavodskaya Lab.*, **16**, 536 (1950) (C.Z., **2**, 2503 (1951)). E.B. Sandell, "Colorimetric Determination of Trace of Metals", New York (1953), pp. 134, 333. L. Erdey and E. Boder, *Z. Anal. Chem.*, **134**, 81 (1951).

3) H. Newcombe, W.A.E. Mcbryde, J. Bortlett and F.W. Beamish, *Anal. Chem.*, **23**, 1023 (1951).

4) H.J. Cluley, *Analyst*, **76**, 523 (1951). Y. Oka, T. Kanno and K. Shiba, *Japan Analyst*, **3**, 389 (1954).

5) Y. Oka and S. Matsuo, *J. Chem. Soc. Japan*, **76**, 610 (1955).

6) C.K.N. Nair and J. Gupta, *J. Sci. Ind. Research*, **10B**, 300 (1951); ibid., **11B**, 274 (1952).

* On the nomenclature of functional group, A. Tchakirian et al. had used "phenol-" and "quinon-". In the present paper, they are called "hydroxyl-" and "carbonyl-", respectively.

7) A. Tchakirian and P. Bevillard, a) *Compt. rend.*, **233**, 256 (1951); b) ibid., 1003; c) ibid., 1112; d) P. Bevillard, ibid., **234**, 216 (1952); e) *Mikrochem.*, **39**, 209 (1952). f) *Compt. rend.*, **235**, 880 (1952). g) *Bull., Soc. Chim. France*, **1954**, 304.

Experiment

The following experiments were carried out to examine whether or not the presence of hydroxyl groups on ortho positions be essential for the compound to react with germanium.

The Reaction between Fluorone Derivatives and Germanium

The following compounds were used in this experiment.

2, 6, 7-Trihydroxy-9-methylfluorone[8]
6-Hydroxy-2, 7-dimethoxy-9-phenylfluorone[9]
2, 6, 7-Trimethoxy-9-phenylfluorone[10]
4, 5, 6-Trihydroxy-9-phenylfluorone[11]

In the first place, the authors synthesized these compounds by conventional method. After the syntheses, the absorption spectra, the reactivity with germanium and the shift of the maximum of the absorption band, resulting from the addition of germanium, were examined for each compound. For the measurement of absorption spectrum the solution was prepared in the following way. A 10^{-4}mol. of each compound was dissolved in a mixture of about 80 ml. of ethanol (94%) and 5 ml. of 6 N sulphuric acid. The resulting solution was transferred into a measuring flask and its volume adjusted to 100 ml. A 2 ml. portion was diluted to 50 ml. with either pure water or water containing 13 ml. of ethanol and 10 ml. of 6 N hydrochloric acid. The concentration of each compound in the solution was 4×10^{-6} mol. per ml. The reactivity of these compounds with germanium was studied over a wide range of pH. The results are summarized in Table I; the absorption curves are shown in Fig. 1.

TABLE I

PROPERTIES OF FLUORONE DERIVATIVES

Name	Structure	M. p.	Colour of crystals	Colour of aq. and/or ethanolic soln.	Change in colour of an acidic soln. on the addition of germanium solution
(1) 2,6,7-Trihydroxy-9-phenylfluorone	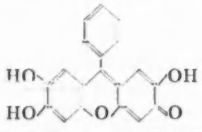	350°C	Reddish orange	Dark red (b.) Orange (n.) Yellow (a.)	Change to reddish (similar to that in a neutral solution) Precipitate formed
(2) 2,6,7-Trihydroxy-9-methylfluorone	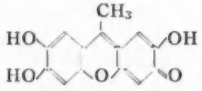	Decomp. at 279°C	Yellowish orange	Dark red (b.) Orange (n.) Yellow (a.)	Change to reddish (similar to that in a neutral solution) Precipitate formed
(3) 6-Hydroxy-2,7-dimethoxy-9-phenylfluorone	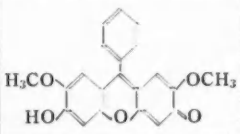	282°C	Dark red	Light orange (n.) Yellow (a.)	None
(4) 2,6,7-Trimethoxy-9-phenylfluorone	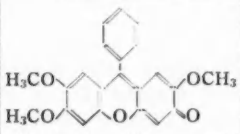	174°C	Orangish yellow	Insoluble (b.) Light orange (n.) Yellow (a.)	None
(5) 4,5,6-Trihydroxy-9-phenylfluorone	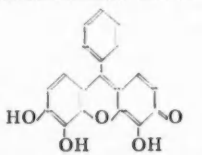	Decomp. at ca. 200°C	Dark purple	Violet blue (b.) Dark purple (n.) From red to yellow (a.)	Change to more reddish (similar to that in a neutral solution) Precipitate appeared after one day

b.: basic solution n.: neutral solution a.: acidic solution

8) C. Lieberman and S. Lindenbaum, *Ber.*, **37**, 1171 (1904); ibid., 2728.
9) F. Kehrmann and M. Gunther, *Ber.*, **45**, 2884 (1923).
10) F. Kehrmann and M. Gunther, *Ber.*, **45**, 2884 (1923).
11) W. R. Orndorff and C. Wang, *J. Amer. Chem. Soc.*, **47**, 290 (1925); ibid., **49**, 1284 (1927); R. N. Sen and N. N. Sarkar, ibid., **47**, 1079 (1925).

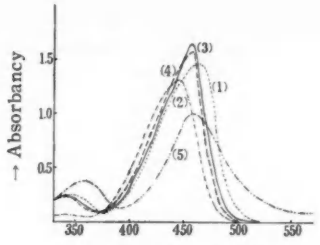

Fig. 1–(1). Absorption curve of fluorone derivatives.
(1) 2, 6, 7-trihydroxy-9-phenylfluorone
(2) 2, 6, 7-trihydroxy-9-methylfluorone
(3) 6-hydroxy-2, 7-methoxy-9-phenylfluorone
(4) 2, 6, 7-trimethoxy-9-phenylfluorone
(5) 4, 5, 6-trihydroxy-9-phenylfluorone

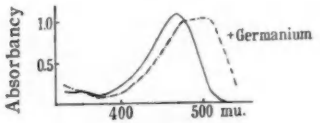

Fig. 1–(2). The absorption curve of 2,6,7-trihydroxy-9-phenylfluorone, (3×10^{-5} mol. per ml.) in acetone and that of the solution containing both germanium (6.94 μg. per ml.) and the reagent. (These are true solutions almost without water.)

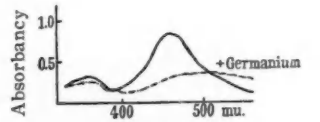

Fig. 1–(3). The absorption curve of 4,5,6-trihydroxy-9-phenylflourone (4×10^{-5} mol. per ml.) in ethanol and that of the soln. containing both germanium (13.9 μg. per ml.) and the reagent.

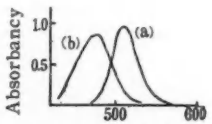

Fig. 1–(4). Absorption curves of complexes between germanium and 2, 6, 7-trihydroxy-9-phenylfluorone[a] and 2, 6, 7-trihydroxy-9-methylfluorone[b]. These solutions contain germanium (8.33 μg. per ml.) and a large amount of reagent. Here reference soln. is an ethanolic solution of the reagent.

The synthesis of a new compound, 2-hydroxy-6, 7-dimethoxy-9-phenylflurone, was tried in vain by methylation of 2, 6, 7 trihydroxy-9-phenylfluorone with diazomethane. If this compound could have been synthesized, it would have been possible to decide whether the functional group which directly combines with germanium is only hydroxyl group. Since it is possible that not only hydroxyl but also carbonyl-group can combine with germanium such an experiment would be very important.

The Reaction between Naphthoquinone Derivatives and Germanium

In order to examine the relation between two hydroxyl groups and a carbonyl group with respect to the reaction with germanium, naphthoquinone derivatives were chosen. For these derivatives the reactivity and the change in the absorption band resulting from the complex formation were studied. The compounds used in the experiment are summarized in Table II.

About 5 mg. of each compound were dissolved in 10 ml. of ethanol (94%). To 1 ml. of this solution was added 1 ml. of ethanol and the volume adjusted to 10 ml. with water. One ml. of first solution was added to the mixture of 1 ml. of ethanol and 4 ml. of germanium standard solution (6.9 μg. per ml.). This solution was made up to 10 ml. with water and its absorption measured. The results are shown in Fig. 2. As was expected, neither the compounds without two hydroxyl groups (e. g. the compound No. 1.) nor those in which two hydroxyl groups are not located on ortho positions (e. g. the compounds No. 2 and 3) showed any significant reaction with germanium.

The reactions between germanium and those compounds which have a carbonyl group adjacent to a hydroxyl group were also negative. According to these results it was clear that one hydroxyl group is not one of the functional groups which directly combine with germanium.

The solutions of these compounds were true solutions and did not show any appreciable precipitate on the addition of germanium. The reaction of these compounds with germanium brings about a change in colour of the solution, from orange or red to purple or dark red. The extinction of the solution was slightly increased, whilst the absorption spectrum remained almost unchanged in each case. Since it is possible that they have a low tendency to react with germanium, further experiments were carried out by use of a larger quantity of germanium (70 μg. per ml.). As shown in Fig. 2–(4), however, the absorption spctra changed only very slightly.

The Reaction between Cumarin Derivatives and Germanium

Compared with naphthoquinone derivatives, fluorone derivatives have many advantages in their reactivity with germanium. The syntheses of these compounds are easier; they react not only with a trace amount of germanium but also selectively in an acidic solution. Apart from the

TABLE II
NAPHTHOQUINONE DERIVATIVES

	Conventional Name	Structure	Reaction with Germanium
(1)	2-Hydroxynaphthoquinone	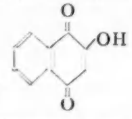	Negative
(2)	2-Hydroxynaphthazarine	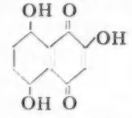	Nagative
(3)	Shikonin	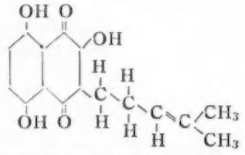	Negative
(4)	Spinazarin	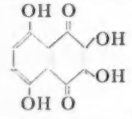	The colour of ethanolic solution changes from orange to reddish orange
(5)	Spinochrome Bl	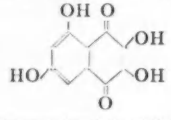	The colour of ethanolic solution changes from yellow to yellowish orange
(6)	Spinochrome F	?	The colour of ethanolic solution changes from red to purple
(7)	Spinochrome Aka	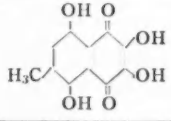	The colour of ethanolic solution changes from pale red to dark red
(8)	Spinochrome Ml	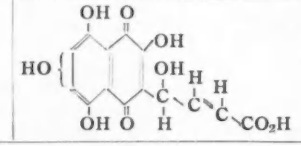	The colour of ethanolic solution changes from pale red to dark red

number of benzene rings, the greatest difference in the structure of these two kinds of compound lies in the fact that the fluorone derivatives are heterocyclic and contain an oxygen atom in the ring, whilst the naphthoquinone derivatives are not. In order to find whether the difference in the structure of those compounds has any effect upon the reactivity with germanium, the reaction between germanium and the following two cumarin derivatives was similarly studied.

cumarin diol[12] 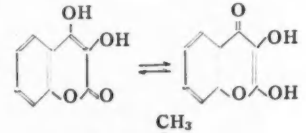

4-methyl-esculetin[13] 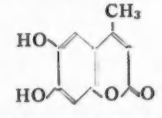

12) F. Arndt, L. Löwe, R. Un and E. Ayca, *Ber.*, 84, 319 (1951).

13) "Organic Syntheses", Collective Volume I, New York (1932), p. 352.

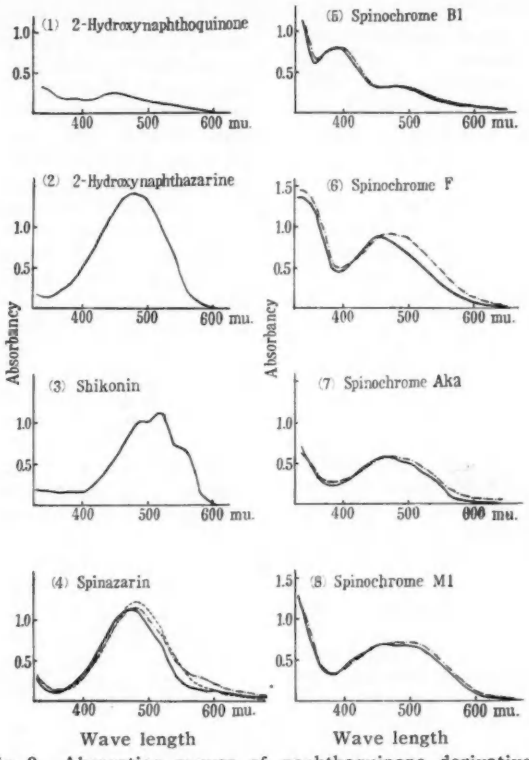

Fig. 2. Absorption curves of naphthoquinone derivatives containg 5.5 μg. of germanium per ml.
(1) (2) and (3) do not change by the addition of germanium.

The compounds were synthesized by the conventional methods. Their colour ranges from colorless to yellow. The absorption spectrum of the solution of each compound as well as of a mixed solution with germanium was studied, both in neutral and 1 N-hydrochloric acid solutions. It was disclosed that cumarindiol fails to react with germanium, whereas 4-methyl esculetin shifts the absorption band from ultra violet to visible. This seems to arise from the formation of germano-complex in a neutral solution. The red shift was more remarkable than in the cases of naphthoquinone derivatives. The results are shown in Fig. 3.

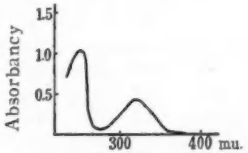

Fig. 3-(1). Absorption curve of cumarindiol. This curve does not change by the addition of germanium.

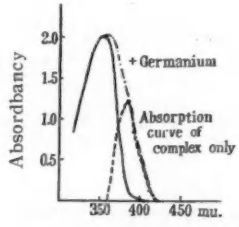

Fig. 3-(2). Absorption curve of 4-methyl-esculetin.

This compound appears, however, not very suitable for the colorimeteric analysis of germanium. In the presence of sodium- or ammonium chloride, the above-mentioned red shift does not take place. Moreover, these compounds are less sensitive for the detection than fluorone derivatives. The wave length of the absorption maximum lies in the boundary between ultraviolet and visible regions.

Conclusion

In order to find an organic compound which is suitable for the colorimetric analysis of germanium, several compounds including fluorone-, naphthoquinone- and cumarin derivatives were studied. The relation between the structure of these compounds and the reactivity with germanium, as well as the shift of the maximum of the absorption spectrum on reaction with germanium, were closely studied. The results confirmed one of the conclusions previously presented by A. Tchakirian and his co-loborators. That is, the presence of two hydroxyl groups on ortho positions is essential for the reaction with germanium. The larger the molecule, the more marked the reaction with germanium. The reactivity with germanium at a low pH is increased with increase in moleculer weight. A compound such as spinazarine, shikonin and 2-hydroxy-naphthoquinone in which one of the two hydroxyl groups on ortho positions is replaced by a carbonyl oxygen, fails to show any reaction with germanium. Cumarindiol has two hydroxyl groups on ortho positions, but in this compound there is a tautomery between the hydroxyl group and the carbonyl oxygen. This could be the reason why this compound does not show any appreciable reaction with germanium, although it has two hydroxyl groups on ortho positions. Accordingly, it is clear that the functional groups which combine directly with germanium are ortho hydroxyl groups. Carbonyl group provides negative results even when it is situated ortho to the hydroxyl group. Present results also indicate that heterocyclic compounds such as fluorone- and cumarin derivatives are more advantageous than homocyclic ones such as naphthoquinons as a reagent which selectively combines with germanium at a low pH. The former compounds are also superior in the fact that their absorption spectra are much more affected by the addition of germanium. Concerning the structures of the compound between germanium and these organic compounds, no diffinite conclusion can be drawn from this study. Further studies are in progress.

The authors wish to express their sincere thanks to Dr. Chika Kuroda for supplying precious samples of naphthoquinone derivatives, and to the late Dr. Fujiro Iimura of Tokyo University for helpful advice in this study. The expenses were defrayed from a grant given by the Ministry of Education to which the authors' thanks are due.

Department of Chemistry, Faculty of Science, The University of Tokyo, Hongo, Tokyo

---

Studies on Organic Reagents for the Colorimetric Analysis of Germanium. II. Synthesis of a New Reagent and its Reaction with Germanium

By Kenjiro KIMURA, Hirotoshi SANO and Masako ASADA

(Received January 24, 1956)

In the previous report[1] it was observed that the absorption band of the solution of heterocyclic compounds such as fluorone and cumarine derivatives shows red shift in the presence of germanium. The authors examined many organic reagents for germanium which have been reported so far by other workers[2,3,4,5]. The results of the experiments showed that among these reagents phenylfluorone is the best because it has high sensitivity for germanium. In addition, the analytical procedure using this reagent is simple, and the reaction is obstructed by few ions. On the other hand, it forms slightly soluble compound with germanium. This makes colorimetric determination very difficult. Moreover, the absorbancy of the colored solution varies with the time elapsed since the solution was prepared. In this study, therefore, the present authors tried

1) K. Kimura, K. Saito and M. Asada, This Bulletin **29**, 635 (1956).
2) Hanna Newcombe, W. A. E. McBryde, John Borthlett and F. E. Beamish, *Anal. Chem.*, **23**, 1023 (1951).
3) H. J. Cluley, *Analyst*, **76**, 523 (1951).
4) C. K. N. Nair and J. Gupta, *J. Sci. Ind. Research*, **10 B**, 300 (1951); ibid., **11 B**, 274 (1952).
5) Y. Oka and S. Matsuo, *J. Chem. Soc. Japan*, **74**, 931 (1953).

to synthesize a new reagent which is similar to phenylfluorone but has none of such defects as described above.

Since it is very difficult to find out a specific reagent for germanium, germanium has to be separated from other elements before it is subjected to quantitative determination. The best procedure for the separation of a trace of germanium seems to be the distillation of germanium tetrachloride from a fairly concentrated hydrochloric acid solution. If we could determine germanium in the distillate with or without simple pretreatment, the procedure would be very convenient for analysis. For this reason it is desirable to find out a new reagent which reacts specifically with germanium, forming a soluble complex in a strongly hydrochloric acid solution. The authors considered that one of the phenylfluorone derivatives, 2, 6, 7-trihydroxy-9-(4'-dimethylaminophenyl)-fluorone, is a reagent suitable for such purpose. Hereafter we call this reagent dimethylaminophenyl-fluorone. Since such a compound has never been described in the literature of the subject, the authors tried to synthesize this reagent by similar procedure which was widely used for the synthesis of phenylfluorone and its analogous compounds[6].

Experiment

The Synthesis of the New Compound

Reagents Used.—*p-Dimethylaminobenzaldehyde*: First-grade reagent prepared by Tokyo Kasei Ind., Co. Japan, was used without any purification.

Hydroxyhydroquinone triacetate: The reagent was synthesized[7] from commercial *p*-benzoquinone, anhydrous acetic acid and concentrated sulfuric acid. Recrystallized twice from 95% ethanol solution.

Ethanol: Commercial 95% ethanol.

The Procedure for Synthesis.—To a mixture of 160 ml. of ethanol, 160 ml. of water and 16 ml. of concentrated sulfuric acid in a round-bottomed flask was added 37 g. of hydroxyhydroquinone triacetate and 11 g. of dimethylaminobenzaldehyde*. Under a reflux condenser the solution was heated in a water bath for twenty hours. Then the solution was allowed to cool until the precipitation of orange crystalline substance was completed. The precipitate was filtered and washed with water until the red color of the washing solution almost disappeared. The crystals seemed to be hydrolyzed easily and the colour of crystals was changed after washing. The precipitate on the filter paper was mixed with a larger amount of water and the system was heated until the hydrolysis was complete. The hydrolyzed precipitate was filtered under suction, washed thoroughly with water and dried in a vacuum desiccator. To 1 to 2 g. of the product was added a mixture of 50 ml. of ethanol, 50 ml. of water and 5 ml. of concentrated sulfuric acid. The resulting system was heated on a water bath to dissolve the precipitate. The small amount of active charcoal was added to the resulting solution. The charcoal adsorbed a dark-reddish brown substance which was supposed to be a polimerized product. The suprenatant solution was filtered through a hot funnel. The cooling of filtrate resulted in the formation of yellowish orange crystalline precipitate. The precipitate was filtered, washed thoroughly with a small amount of the mixture of ethanol and water. And then it was mixed with a large amount of water. The hydrolysis of the precipitate was performed by heating. The filtration, washing and drying up of the precipitate was repeated several times for the purpose of recrystallization. The authors are of the opinion that the followtng reactions occurred in this procedure.

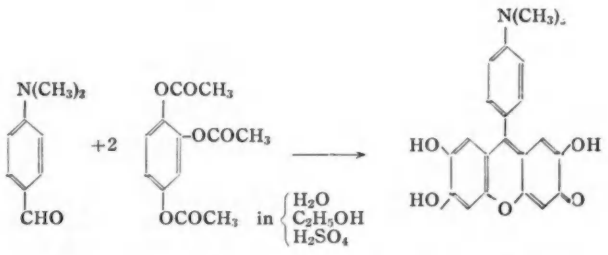

Anal. Found: C, 68.10; H, 4.75; N, 4.07. Calcd.: C, 69.30; H, 4.69; N, 3.83%.

Properties of the Product.—M. p. >250°C. Colour: Red, Green fluorecence. Form: While the sulfate forms plate-like crystals, its hydrolyzed product is powder. Solubility: Insoluble in water. Slightly soluble in ethanol, giving an orange solution.

6) C. Lieberman and S. Lindenbarum, *Ber.*, **37**, 1171 (1904); ibid., 2728; F. Kehrmann and M. Gunther, *Ber.*, **45**, 2884 (1923); W.R. Orndorff and C. Wang, *J. Am. Chem. Soc.*, **47**, 290 (1925); ibid., **49**, 1284 (1927); Rajendra Nath Sen and Nripendra Nath Sarkar, ibid., **45**, 2984 (1923); ibid., **47**, 1079 (1925).

7) "Organic Syntheses, Collective Volume I", John Wiley & Sons Inc., New York (1948), p. 317.

* Two mol. of hydroxyhydroquinone triacetate and one mol. of dimethylaminobenzaldehyde are used to prepare the reagent. A mixture of ethanol, water and concentrated sulfuric acid in the proportion of 10:10:1 was used as a solvent to dissolve the above compounds. The proportion of each compound in the solvent and the amount of the solvent are fixed at such values that the compounds were completely dissolved and the yield of the resulting product was maximum.

The addition of acid to the ethanol solution of the compound increased its solubility and the colour of solution became deep red. When the addition of acid was continued further, the red colour of solution was diminished and changed from orange to yellow. At the same time, the solubility was decreased. The concentration of acid which was necessary to change the colour of the solution was dependent on the amount of the reagent in the solution.

Absorption Curves of the Reagent Solution.—The following samples were used to measure absorption curves. The original solution was prepared by dissolving 1 mg. of new compound in 50 ml. of ethanol.

Sample 1: 5 ml. of the original solution was diluted with ethanol to 25 ml.

Sample 2: The original solution was mixed with 2 ml. of 0.2 N -HCl and diluted with ethanol to 25 ml. The concentration of acid in the resultant solution was 0.016 N.

Sample 3: The original solution was mixed with 2 ml. of 2 N-HCl and diluted with ethanol to 25 ml. The final acid concentration was 0.16 N.

Sample 4: The original solution was mixed with 2 ml. of 6 N HCl and diluted with ethanol to 25 ml. The final acid concentration was 0.48 N.

Sample 5: The original solution was mixed with 5 ml. of 6 N-HCl and diluted with ethanol to 25 ml. The final acid concentration was 1.2 N. The results are shown in Fig. 1.

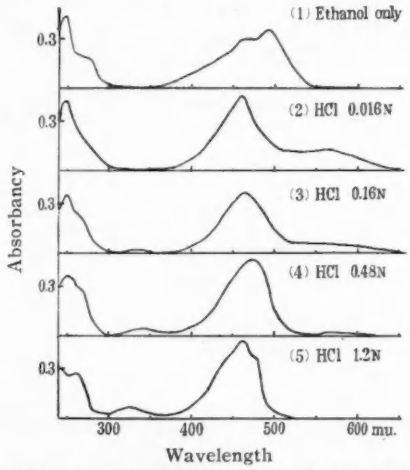

Fig. 1. Absorption curves of dimethylaminophenylfluorone.

In strongly acidic solution in which the effect of amino group is almost negligible, the absorption curve of this compound is very similar to that of phenylfluorone. Considering the above-mentioned properties as well as the procedure for synthesis, there is little doubt that the compound is a reagent suitable for our purpose. For the measurement of absorption spectra, the commerical 95% ethanol was purified until the substance such as aldehyde showing the absorption bands at the near ultraviolet region was completely eliminated.

Reaction of the New Compound with Germanium

Reagents Used.—Germanium standard solution: The germanium dioxide used in this experiment was prepared by Tokyo Gas Co.. The standard solution was made by dissolving 1.00 g. of water-soluble powder (99.9% GeO_2) in hot water. Then the volume of the resulting solution was adjusted to 1 liter.

Two ml. of this solution was taken in 200 ml. volumetric flask and diluted up to 200 ml. The final solution contained 10.0 μg. of GeO_2 [6.94 μg. of Ge) per ml. The solution could not be preserved for a long time without the change of concentration.

0.05% solution of dimethylaminophenylfluorone: 0.050 g. of dimethylaminophenylfluorone was dissolved by heating in a mixture of approximately 80 ml. of ethanol and 5 ml. of 6 N-hydrochloric acid. After cooling, the solution was diluted with ethanol until the volume of solution became 100 ml. The final solution was deep red and contained 0.05 per cent of dimethylaminophenylfluorone by weight.

Hydrochloric acid: Commercial first-grade reagent (sp. gr. 1.2) was diluted with water.

Procedure.—Two ml. aliquots of standard GeO_2 solution were taken in four 25 ml. volumetric flasks. Then 1.3 ml., 6.3 ml. and 12.5 ml. of 2 N-HCl were added to the first three volumetric

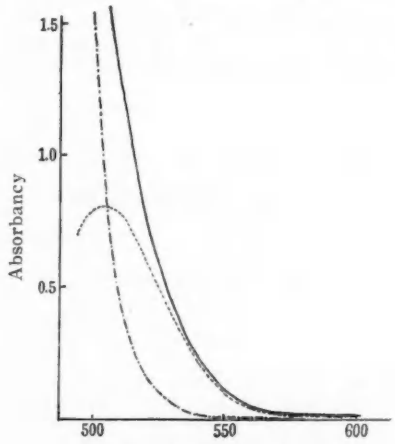

—·—·— 0.01% Dimethylaminophylfluorone soln. only (reference soln.: distilled water)

——— Germanium added (")

------ Complex between Ge and dimethylaminophenylfluorone (reference soln.: 0.01% dimethylaminophenylfluorone soln)

Fig. 2. Absorption curves of the complex between germanium and dimethylaminophenylfluorone.

flasks respectively and 8.3 ml. of 6 N-HCl was added to the last volumetric flask. The volume of each solution was made up to approximately 15 ml. To the resulting solutions were added 5 ml. aliquots of 0.05% dimethylaminophenylfluorone solution and the final volume of the solutions were adjusted to 25 ml. The final concentration of hydrochloric acid in the solutions obtained are 0.1 N, 0.5 N, 1 N and 2 N, respectively. Four reference solutions were prepared without adding germanium. These solutions were compared with those containing germaium. The results are summarized in Table I.

TABLE I

Concentration of HCl	Reaction with Germanium
0.1 N	Red orange colour appeared immediately after the addition of reagent.
0.5 N	Same as above.
1 N	Orange colour appeared 5 minutes after the addition of reagent.
2 N	No change was observed.

After the addition of reagent, the solution contained 0.01% dimethylaminophenylfluorone by weight and 0.56 μg. of germanium per ml. Even when these solutions were kept standing for about fifty hours, no precipitate appeared. The absorption spectrum of the obtained complex is shown in Fig. 2. The figure shows the absorption spectrum of the complex in 0.5 N-HCl.

Conclusion

An attempt was made to synthesize a new colorimetric reagent for germanium which has no such defects as was observed in the other reagents. Using a comparatively simple procedure, a crystalline substance was obtained, which was found to be suitable for our purpose. The authors call this reagent dimethylaminophenylfluorone. The compound reacts with germanium in an acid solution and forms a soluble complex. The present experiments led us to the conclusion that this compound is an excellent reagent for the colorimetric analysis of germanium.

Department of Chemistry, Faculty of Science, The University of Tokyo
Hongo, Tokyo

SHORT COMMUNICATION

Splitting of the First Band of [Co^{III}(X)(edtaH)]-type Complexes

By Yoichi SHIMURA and Ryutaro TSUCHIDA

(Received March 20, 1956)

Recently it was reported[1] that the absorption band of rare-earth cation split into several bands by interacting with EDTA in solution. The main purpose of the present communication is to report that somewhat similar splitting occurred with a cobaltic EDTA complex anion.

The visible and ultraviolet absorption spectra of $[Co^{III}(edta)]Na\cdot 4H_2O$, $[Co^{III}(NO_2)(edtaH)]\ Na\cdot H_2O$ and $[Co^{III}(Br)(edtaH)]Na\cdot 3H_2O$* were examined. The salts were prepared by the method of Schwarzenbach[2]. Measurements were made by a Beckman DU spectrophotometer. The spectra of the bromo complex was measured in 60% perchloric acid solutions to prevent its aquation, and the other two salts in aqueous solutions. The absorption curves obtained and their analyses are shown in Figs. 1 and 2. The curve analyses were made by use of the same method as described in a previous paper[3].

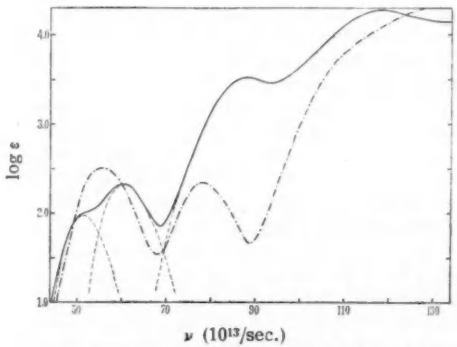

Fig. 1. Absorption curve of the nitro complex.
——— $[Co^{III}(NO_2)(edtaH)]\ Na\cdot H_2O$: Ia band, ν_{max}=60.4 ($\log \varepsilon_{max}$=2.32); Ib band, 51.4 (1.97); nitro specific band, 88.6 (3.52); third band, 118.5 (4.27).
–·–·–·– $[Co^{III}(edta)]Na\cdot 4H_2O$: first band, 55.9 (2.51); second band, 78.1 (2.36).

As is seen in Fig. 1, the first absorption band of $[Co(NO_2)(edtaH)]^-$ distinctly split

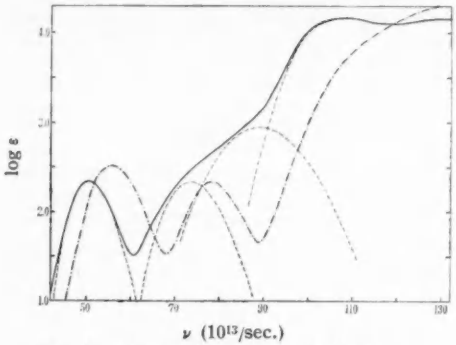

Fig. 2. Absorption curve of the bromo complex.
——— $[Co^{III}(Br)(edtaH)]Na\cdot 3H_2O$: first band, $\nu_{max}=50.6$ ($\log \varepsilon_{max}=2.34$); second band, ca. 73.5** (ca. 2.34); bromo specific band, 89.0 (2.95); third band, ca. 108 (4.16).
-·-·-·- $[Co^{III}(edta)]Na\cdot 4H_2O$.

into two components. This is the first example of such splitting in connection with the complexes containing one or more nitro ligands. The Ia-component is in the region of shorter wave lengths as compared with the first band of $[Co(edta)]^-$. This is in agreement with what is expected from the higher position of the nitro-group on the spectro-chemical series. The sub-component Ib is in the long wave length side of the first band of $[Co(edta)]^-$. Contrary to the nitro complex, no splitting is observed in $[Co(Br)(edtaH)]^-$ (Fig. 2). Since distinct splittings were reported[4,5] for $[Co(NH_3)_5(Br)]^{2+}$ and *trans*-$[Co(en)_2(Br)_2]^+$, the present result is rather unexpected. The reason for this is unknown. To solve the problem it will be necessary to collect more extensive data for the spectra of the complexes belonging to several different structural types.

The occurrence of a nitro or bromo specific band in these nitro or bromo complexes confirms the opinion that these complexes contain the EDTA anion as quinquedentate ligand. The third absorption bands due to co-ordination of the nitro and bromo anions are also observed. The specific and the third bands are equally shifted towards longer wave lengths than those of the corresponding nitro- or bromo-pentammine cobaltic complexes, as follows:

	Specific band	Third band
$[Co(NO_2)(edtaH)]^-$	88.6×10^{13}/sec.	118.5×10^{13}/sec.
$[Co(NO_2)(NH_3)_5]^{2+}$	92.4[6]	125.7[6]
$[Co(Br)(edtaH)]^-$	89.0	ca 108
$[Co(Br)(NH_3)_5]^{2+}$	95.4[4]	118.4[4]

Further work is in progress on the analogous EDTA complexs of Cr(III) and V(III).

Department of Chemistry, Faculty of Science, Osaka University, Osaka

* edta represents a quadrivalent ethylenediaminetetraacetate anion $C_{10}H_{12}N_2O_8^{4-}$ and edtaH a tervalent anion $C_{10}H_{13}N_2O_8^{3-}$.

** This value was estimated by Sone's formula, $\nu_2=1.189\,\nu_1+13.31$ (see ref. (3)).

1) a) T. Moeller and J.C. Brantley, *J. Am. Chem. Soc.*, **72**, 5447 (1950). b) R.C. Vickery, *J. Chem. Soc.*, **1952**, 421. c) L. Holleck and D. Eckhardt, *Naturwiss.*, **40**, 409 (1953); *Z. Naturforsch.*, **8** a, 660 (1953); ibid., **9** a, 347 (1954); ibid., **9** b, 274 (1954).
2) G. Schwarzenbach, *Helv. Chim. Acta*, **32**, 839 (1949).
3) Y. Shimura and R. Tsuchida, This Bulletin, **28**, 572 (1955).
4) M. Linhard and M. Weigel, *Z. anorg. Chem.*, **266**, 49 (1951).
5) M. Linhard and M. Weigel, ibid., **271**, 101 (1952).
6) M. Linhard and M. Weigel, ibid., **267**, 113 (1951).

An X-ray Diffraction Line Observed in Acid-treated Carbonized Coals and Paramagnetic Absorption

By Katsuya INOUYE

(Received April 18, 1956)

During our extensive examinations of carbonization mechanism of various coals by means of X-ray diffraction[1], it has been experienced for several samples that a new diffraction line appears other than the usually observed carbon patterns which are indexed as (002) and (100). The characteristics of the line and its occurence are as follows:

(1) The lattice constant is 4.18 ±0.10Å, the line existing just inside (002) band. The line is fairly intense and sharp. (See Fig. 1).

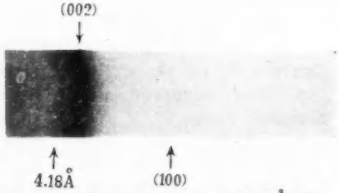

Fig. 1. The position of 4.18Å line

No other pattern than this and carbon patterns has been observed on the film, using Kodak No-screen X-ray film in 45 mm. radius powder camera covering 5–80° Bragg angle and Ni-filtered CuKα ray operated at 35 kV. and 20 mA. No low-angle band was recognized by a Geiger-counter goniometer recording up to 1° of Bragg angle.

(2) The line has been observed in the samples produced from the following bituminous coals (single or blended) and carbonized up to the following maximum temperatures: American coking coal, 520 and 620°C; Yatake coking coal, 500°C; blended coal slack of 25 parts American coking coal and 75 parts Yubari weakly coking coal, 600°C; blended coal slack of 6 kinds of bituminous coals in order to obtain a coherent coke, 200, 300 and 400°C. The volatile matter content (dry ash-free basis) of the single or blended coals prior to carbonization was approximately 34 to 43%. The carbonization was carried out in an experimental electric furnace at a rate of elevation of temperature of 3.3°C/min. in nitrogen atmosphere. At other carbonization temperatures, the similar coals did not show the line by similar treatments.

(3) The line appears only after the carbonized samples are boiled with 20% HCl for approximately forty hours or more, with reflux and frequent renewing, followed by alternative wetting and gentle evaporating with 40% HF in Pt crucible over fifteen times.

(4) The line is stable at room temperature for over one year, but disappears by heating the sample at 600°C for ten minutes in nitrogen atmosphere.

The probable mistakes in X-ray techniques, e.g., diffraction by CuKβ ray or WLα_2 ray, diffraction caused by camera body or sample amount, etc. have all been denied by careful experiments. The cause of the line is unlikely in the inorganic impurities, because the treatments with acids result naturally in gradual diminishing of inorganic components and, in particular, because no accompanying lines exist and the line disappears by heating the sample at 600°C. The lattice parameter is not consistent with any carbon halide patterns so far reported.

This phenomenon may be at fault but is interesting if it is remembered that the distinct paramagnetic resonance absorption has been reported recently for coals carbonized especially up to 500–600°C[2], and the absorption has been ascribed to the existence of some broken carbon bonds. The paramagnetic resonance absorption of one of the series which showed the line (cf. Table I) was measured by Mr. I Miyashita using a microwave of 3.2 cm. wave-length[3].

These results may imply that a correlation is expected to be found between the appearance of the 4.18Å line and the structural disturbance during a certain stage of carbonization before the carbon cluster commences to grow up to more rigid hexagonal lamellae in coke. To show a rather sharp

TABLE I

PARAMAGNETIC RESONANCE ABSORPTION OF CARBONIZED COALS

Coal slack carbonized: 25 American coking coal and 75 Yubari weakly coking coal.

Sample No.	Carbonization Temperature °C	4.18Å Line	χ_g
1	400	–	2.6×10^{-8}
2	600	–	$10.\times10^{-8}$
3*	600	+	8.5×10^{-8}
4	800	–	No absorption

* Sample 3, which shows the 4.18Å line, was prepared by treating Sample 2 with acids as described above.

diffraction pattern, the formation of a crystallographic lattice by means of acid treatments is expected, for example in the peripheries of cluster. The pre-existence of some broken bonds may be advantageous for further lattice development. According to Miyashita[4], the decrease of the absorption from 10×10^{-8} to 8.5×10^{-8} in accordance with the appearance of the line after acid treatments coincides with the general rule that the value of absorption decreases with the development of crystalline state, though he holds the view that the absorption may be due to a state of triplet and not necessarily to the broken bonds.

The author's thanks are due to M. Abiko and A. Roppongi, with whose assistance in the X-ray studies of carbonization of coals this fact has been revealed and to Mr. I. Miyashita (Hokkaido Univ.) for measuring the paramagnetic resonance absorption. Financial support has been provided by the Hirohata Iron Works of Fuji Iron and Steel Ind. Co. Ltd.

Resources Research Institute
Saitama-Kawaguchi

1) K. Inouye, H. Tani and M. Abiko, *J. Fuel Soc. Japan*, **32**, 292 (1953); K. Inouye and M. Abiko, ibid., **32**, 386 (1953); K. Inouye and M. Abiko, *J. Chem. Soc. Japan (Ind. Chem. Sect.)*, **59**, 37 (1956).

2) J. Uebersfeld, A. Etienne and J. Combrisson, *Nature*, **174**, 614 (1954); A. Etienne and J. Uebersfeld, *J. Chim. Phys.*, **51**, 328 (1954); D.J.E. Ingram, J.G. Tapley, R. Jackson, R.L. Bond and A.R. Murnachan, *Nature*, **174**, 740 (1954); J.E. Bennett, D.J.E. Ingram and J.G. Tapley, *J. Chem. Phys.*, **23**, 215 (1955).

3) Y. Yokozawa, I. Miyashita, M. Kugo and K. Higashi, This Bulletin, **28**, 536 (1955).

4) Private communication.

Über die Erhöhung der Empfindlichkeit von den Niederschlagbildungsreaktionen durch Anwendung der Ionenaustauschharze

Von Masatoshi FUJIMOTO

(Eingegangen am 17. Februar, 1956)

In einer Reihe der Untersuchungen über die mikroanalytischen Anwendungen der Ionenaustauschharze zum Nachweis geringer Substanzmenge[1] werden lediglich solche Reaktionen, die die in die Harzphase selektiv adsorbierenden und stark sich färbenden Ionen bilden, deshalb gern verwandt, weil die Färbung dieser Ionen, die sich hauptsächlich in den *beschränkten Rauminhalt* der Harzkörnchen adsorbieren lassen, bemerkenswerterweise verstärkt wird.

Dagegen wurde hier eine Art der Niederschlagbildungsreaktionen zur Tüpfelanalyse mit Ionenaustauschharze angewandt, wobei die Empfindlichkeit von der Reaktion durch Beschränkung der Fällungsstelle an der *Grenzfläche* zwischen Harz-und Lösungsphase beträchtlich vergrössert wurde.

Als ein geeignetes Beispiel dafür wurde folgende Reaktion ausgewählt:

$Ag^+ + Cl^- \longrightarrow [AgCl]\downarrow$[2] (weisser Niederschlag).

Wenn eine Lösung von Silbernitrat mit einem Anionenaustauschharze von RCl-Form sich berührt, werden die Nitrationen in der Lösung zuerst mit den Chloridionen von Harzphase ausgetauscht, welche sofort an der Oberfläche der Harzkörnchen mit Silberionen in der Lösung gemäss den Gleichungen

$[RCl] + NO_3^- \rightleftarrows [RNO_3] + Cl^-$, und

$Cl^- + Ag^+ \longrightarrow [AgCl]\downarrow$ (weisse Niederschlagmembran)

reagieren. Der so gebildete Silberchloridniederschlag wird als eine weisse dichte Schicht an der Oberfläche der Harzkörnchen angesammelt, und gegen schwarzen Hintergrund deutlich nachgewiesen.

Die Ergebnisse mit einem durchsichtigen[3] und farblosen starkbasischen Anionenaustauschharze, Dowex 1-Xl (RCl-Form) unter verschiedenen Bedingungen ausgeführter Untersuchung stehen in Tabelle I:

TABELLE I

VERGLEICHUNG VERSCHIEDENER BEDINGUNGEN VON NIEDERSCHLAGBILDUNG

		Zeit nach der Mischung (Min) 2				5				10				20			
Mit 4.3γ Ag^+ (108 γ/ccm)	A:	+	+	+	+	(+)	(+)	(+)	(+)	(+)	(+)	(+)	(+)	(+)	(+)	(+)	(+)
	B:	+	+	±	∓	+	±	±	∓	+	±	∓	∓	+	±	±	±
	C:	±	±	±	±	±	±	±	±	±	±	±	±	∓	∓	∓	∓
Mit 0.43γ Ag^+ (10.8 γ/ccm)	A:	−	−	−	−	−	−	−	−	−	−	−	−	−	−	−	−
	B:	±	(+)	±	±	±	(+)	±	(+)	±	(+)	±	(+)	(+)	(+)	(+)	(+)
	C:	+	+	+	+	+	+	+	+	+	+	+	+	+	+	+	+

−: kein Niederschlag; ±: unsicher, (+): schwach, +: sicher, und ±, ∓, usw.: intensiv getrübt.

Inhaltsangabe des Verfahrens:—

A: 2N NaCl (1 Tropfen) + $AgNO_3$ (1 Tropfen) + H_2O (1 Tropfen),
B: RCl (einige Körnchen) + $AgNO_3$ (1 Tropfen) + H_2O (1 Tropfen),
C: RCl (einige Körnchen) + $AgNO_3$ (1 Tropfen) + 4M NH_4NO_3 (1 Tropfen).

Ionenaustauschharz: Dowex 1-Xl (RCl-Form).

Abb. 1 ist eine Skizze des Zustandes von den mit 4.3γ Silberionen 20 Min nach der Mischung erhaltenen Harzkörnchen (nach Verfahren „B"), worin man eine am Rande der Harzkörnchen sich entstehende weisse Trübung gegen schwarzen Hintergrund der Tüpfelplatte entschieden deutlich erkennen kann.

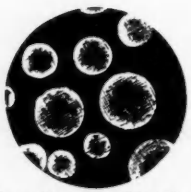

Abb. 1. Vergrössertes Bild der getrübten Harzkörnchen.

Wie man im obengenannten Beispiel klar ersieht, lässt sich diese Methode zur Niederschlagbildung durch Ionenaustausch an der Grenzfläche zweier Phasen künftig als eine sehr geeignete empfindliche Tüpfelmethode auf die verschiedenartigen Niederschlagbildungsreaktionen umfangreich erweitern.

Laboratorium der analytischen Chemie, Chemisches Institut der wissenschaftlichen Fakultät, Tokyo Universität, Tokyo

1) Vgl. M. Fujimoto, „Mikroanalyse mit Hilfe von Ionenaustauschharzen. I, II, III, IV, V und VI", Dieses Bulletin, **27**, 48, 347 (1954) sowie **29**, 567, 571, 595, 600 (1956).

2) Das Zeichen, [ ], bedeutet die feste Phase, und, ↓, die Niederschlagbildung.

3) Obwohl hinsichtlich der Löslichkeit schlechthin die Anwendung des Harzes von RJ-Form günstiger als die des Harzes von RCl-Form ist, ist es nicht zweckmässig, das Harz von RJ-Form zu hier erwähntem Zweck zu verwenden, da dieses beträchtlich undurchsichtig ist.